This item was submitted to Loughborough's Research Repository by the author.
Items in Figshare are protected by copyright, with all rights reserved, unless otherwise indicated.

Rising damp in buildings : a theoretical study of likely factors and experiments on leaching, wall suction gradients

PLEASE CITE THE PUBLISHED VERSION

PUBLISHER

© P.B. Lee

LICENCE

CC BY-NC-ND 4.0

REPOSITORY RECORD

Lee, P.B.. 2013. “Rising Damp in Buildings : A Theoretical Study of Likely Factors and Experiments on Leaching, Wall Suction Gradients”. figshare. https://hdl.handle.net/2134/13112.

Loughborough University

This item was submitted to Loughborough University as a PhD thesis by the author and is made available in the Institutional Repository (https://dspace.lboro.ac.uk/) under the following Creative Commons Licence conditions.

creative commons

COMMONS DEED

Attribution-NonCommercial-NoDerivs 2.5

You are free:

- to copy, distribute, display, and perform the work

Under the following conditions:

Attribution. You must attribute the work in the manner specified by the author or licensor.

Noncommercial. You may not use this work for commercial purposes.

No Derivative Works. You may not alter, transform, or build upon this work.

- For any reuse or distribution, you must make clear to others the license terms of this work.
- Any of these conditions can be waived if you get permission from the copyright holder.

Your fair use and other rights are in no way affected by the above.

This is a human-readable summary of the Legal Code (the full license).

Disclaimer

For the full text of this licence, please go to:
http://creativecommons.org/licenses/by-nc-nd/2.5/

BLL ID NO: — D37144/81

LOUGHBOROUGH
UNIVERSITY OF TECHNOLOGY
LIBRARY

AUTHOR/FILING TITLE
LEE, P

ACCESSION/COPY NO.
189312/02

VOL. NO.

CLASS MARK

LOAN COPY

05. NOV
04. DEC
17. MAR 82
10. JUN
07. NOV
28. NOV 83
23. MAR 84

26. FEB 84
1 84

018 9312 02

RISING DAMP IN BUILDINGS:

A THEORETICAL STUDY OF LIKELY FACTORS; AND EXPERIMENTS ON LEACHING, WALL SUCTION GRADIENTS, AND A PILOT METHOD OF SIMULTANEOUSLY MEASURING ALL CAPILLARY-HYDRAULIC PROPERTIES.

by

P.B. LEE

(B.Sc., D.I.S.)

A Doctoral thesis submitted in

partial fulfilment of the requirements

for the award of

Doctor of Philosophy

of Loughborough University of Technology

September 1980

Supervisor; Dr. G. Mason

Department of Chemical Engineering

© by P.B. Lee 1980

Loughborough University
of Technology Library
Date May 81
Class
Acc. No. 185312/02

MEMORANDUM

The work described in this thesis was carried out by me in the Department of Chemical Engineering at Loughborough University of Technology between October, 1974 and September, 1977 under the supervision of Dr. G. Mason (Lecturer, Department of Chemical Engineering).

No part of this thesis has previously been submitted by me for any other higher degree, and the work described herein is original and unaided except where specific reference has been made.

14 August, 1980

DEDICATION

I dedicate this thesis to my mother and father for the help and support they have given to me.

ACKNOWLEDGEMENTS

I wish to thank Dr. G. Mason (then at Loughborough University of Technology), for his help and guidance during the course of this work.

I am further indebted to the technical staff of the Department of Chemical Engineering and to the information services staff of the University Library for the help they have also given me.

SUMMARY

This thesis is concerned with the phenomenon of Rising Damp, which is a complex example of the simultaneous flows of volume (water), heat, solutes and electricity within a porous material.

The physical complexity of this natural occurrence has required that the phenomenon be reduced into a series of scientific areas or related topics, which are presented as separate chapters. A full account of the structure of the thesis can be found in the introduction section.

The common areas covered in this work are mathematical description of the loss of moisture by damp porous materials (i.e. evaporation) and of the movement of moisture within unsaturated porous materials both in terms of non linear "Diffusivity" type expressions (Chapter Three) or more usefully in terms of non linear "free energy" type expressions (Chapter Eight); capillary suction developed in damp walls.

Other less common topics investigated are leaching of soluble materials from the porous matrix and prediction of the consequent increase in matrix permeability to fluid; electro kinetic aspects of Rising Damp; coupling of transport processes within porous materials.

Several of the topics discussed in this work are common to several scientific disciplines giving rise to a 'looseness' and 'multiplicity' of nomenclature. To overcome this problem, particular care and space has been devoted to explaining the terminology used in this work, which is especially useful to readers who are unfamiliar with this area of study.

To conclude, the thesis covers the essential aspects of Rising Damp and, as such, it may be used as a platform from which the phenomenon can be investigated more comprehensively.

CONTENTS

		Page
Introduction		1
Chapter One	Assessment of the problem and phenomenon of Rising Damp	6
1.	Defining Rising Damp	6
2.	Origins of wall moisture	6
3.	Problems caused by damp walls	7
4.	Forces and potential gradients causing moisture movement	8
5.	Coupling of flow potentials and forces	9
6.	Extent of dampness within a wall	12
References		13
Appendix I		19
Chapter Two	Porous material terminology	21
1.	Introduction	21
2.1	Surface tension	21
2.2	Contact angle	22
2.3	Surface tension, spreading and contact angle	25
2.4	Surface tension and free energy	30
3.1	Porosity	36
3.2	Darcys law	38
3.3	Saturation	40
3.4	Saturation states	40
3.5	Saturation and capillary pressure	44
4.1	Hysteresis in porous materials	47
4.2	Hysteresis terminology	49
4.3	Domain concept	49
List of symbols and units		55
References		57
Chapter Three	Equation of motion of moisture in an unsaturated porous material	62
1.	Introduction	62
2.	The Navier-Stokes equation	62
3.	Poiseuille's law	63
4.	Darcy's law	64
5.	Principles of moisture movement in unsaturated porous materials	66

Page

6. Free energy per unit mass of moisture in an unsaturated porous material 70
6.1 Effect of pressure on free energy 72
6.2 Effect of solutes on free energy 74
6.3 Effect of a force field on free energy 76
6.4 Effect of electrical potential upon free energy 77
6.5 Effect of temperature on free energy 79
7. Factors affecting the diffusivity coefficients 80
7.1 Moisture liquid diffusivity 81
7.2 Moisture vapour diffusivity 85
7.3 Thermal vapour diffusivity 89
7.4 Thermal liquid diffusivity 89
7.5 Solute vapour diffusivity 90
7.6 Solute liquid diffusivity 91
7.7 Electro osmotic coefficient 97
List of symbols and units 101
References 105

Chapter Four Electro kinetic phenomena 111
1. Introduction 111
2. Electro osmosis 113
3. Calculation of the electro osmotic effect 113
4. Electro osmosis in porous materials and electro osmotic coefficient 119
5. Coupled flow of water and electricity through porous materials 120
6. Discussion of some electro kinetic phenomena 121
7. Electrical conductivity of the porous matrix system 124
List of symbols and units 126
References 128
Appendix I 130
Appendix II 131

		Page
Chapter Five	Evaporation	132
1.	Introduction	132
2.	Terminology	133
2.1	Water vapour pressure	133
2.2	Saturated vapour pressure	133
2.3	Saturation deficit	134
2.4	Relative humidity	134
2.5	Absolute humidity or vapour density	134
2.6	Specific humidity	134
2.7	Humidity	134
2.8	Dew point temperature	135
2.9	Wet bulb temperature	137
3.	The drying process	137
3.1	Description of the drying process. External observations	137
3.2	Constant rate period	138
3.3	First falling rate period	140
3.4	Second falling rate period	140
3.5	Description of the drying process. Internal considerations	141
4.	Methods of estimating evaporation	144
4.1	Requirements for evaporation	145
4.2	Dalton method	145
4.3	Turbulent aerodynamic methods	146
4.4	Energy balance approach	151
4.5	Discussion and evaluation of Rn	151
4.6	Discussion of the soil heat flux	155
4.7	Bowen ratio	157
4.8	Evaporation into still air	160
4.9	Summary	162
List of symbols and units		165
References		168
Chapter Six	Leaching of porous materials	177
1.	Introduction	177
2.	Acidisation models	178
2.1	Capillaric models	178
2.2	Dimensionless model	182

Page

3. Moving boundary models 188
3.1 Muskat model 188
4. Discussion of the models predicting the change of permeability 204
List of symbols and units 214
References 217

Chapter Seven Experimental work 220
1. Introduction 220
2. Experimental study number one. Leaching 220
2.1 Introduction 220
2.2 Experimental procedure 232
2.3 Discussion 238
3. Experimental study number two. Investigation of the seasonal variation of suction developed by a wall suffering from Rising Damp 263
3.1 Introduction 263
3.2 Experimental procedure 265
3.2.1 Design of a mercury-water tensiometer 265
3.2.2 Design of the porous cup 266
3.3 Sensitivity of the tensiometer instrument 268
3.4 Cup conductance 269
3.5 Time constant 273
3.6 Air trap 274
3.7 Experimental method 274
3.8 Experimental results 277
3.9 Experimental errors 277
3.9.1 Tensiometer errors 277
3.9.2 Moisture content errors 284
3.10. Discussion 286
3.10.1 Tensiometer curves and tensiometer design 286
3.10.2 Cup conductance via the in-situ method 289
3.10.3 Moisture content profiles 291

Page

4.	Experimental study number three. An experimental study to investigate the feasibility of a method to simultaneously measure the hydraulic properties of unsaturated permeability, moisture content and evaporation rate with respect to the capillary suction developed by a moist porous material	293
4.1	Introduction	293
4.2	Experimental procedure	296
4.2.1	Preparation of samples	296
4.2.2	Experimental apparatus and method	297
4.3	Experimental computations and results	303
4.3.1	Calculation of porosity	303
4.3.2	Calculation of evaporation rate	303
4.3.3	Calculation of suction developed by the core	306
4.3.4	Calculation of the pressure potential between the pressure tapping points and the base of the core	307
4.3.5	Calculation of the weight lost by the plaster core	307
4.3.6	Calculation of the percent saturation of the core	307
4.3.7	Unsaturated permeability of the core	308
4.3.8	Dry bulb temperature and relative humidity	308
4.4	Experimental errors	308
4.4.1	Manometer errors	308
4.4.2	Temperature errors	314
4.4.3	Evaporation rate error	314
4.4.4	Moisture content (percent saturation) error	314
4.4.5	Porosity error	315
4.5	Discussion	315
4.5.1	Unsaturated permeability experiment	315
4.5.2	Moisture content experiment	318
4.5.3	Evaporation experiment	322

Page

4.6 Summary of the feasibility investigation 329
List of symbols and units 330
References 331
Appendix I 333
Appendix II 335
Appendix III 338
Appendix IV 342
Appendix V 344
Appendix VI 345
Appendix VII 346

Chapter Eight Discussion of the phenomenon of Rising Damp 348
1. Introduction 348
2. Equation of motion. Free energy expressions 349
2.1 Moisture liquid diffusivity 350
2.2 Thermal liquid diffusivity 351
2.3 Solute liquid diffusivity 352
2.4 Electro osmotic diffusivity 354
2.5 Vapour moisture diffusion 355
2.6 Moisture vapour diffusivity 356
2.7 Thermal vapour diffusivity 357
2.8 Osmotic vapour diffusivity 360
2.9 Vapour diffusion supplement 360
3. Moisture fluxes in soils under natural conditions 361
3.1 Net moisture flux 363
3.2 Thermal and moisture gradients 363
3.3 Thermal moisture fluxes 363
3.4 Moisture fluxes induced by moisture content gradients 365
3.5 Solute-induced moisture flow 369
3.6 Electrically induced moisture flow 372
3.7 Summary of natural moisture fluxes 373
4. Cures and cures of symptoms of dampness 375
4.1 Cures of Rising Damp 375
4.1.1 Electro osmotic methods 375

Page

4.1.2 Chemical injection 392
4.1.3 Traditional methods of treating dampness 395
4.2 Alleviating or hiding dampness 396
4.2.1 Methods of increasing the evaporation flux 396
4.2.2 Wall linings 397
4.3 Summary of treatments of Rising Damp 398
5. Review of the phenomenon of Rising Damp 400
6. Suggestions for further work 410
7. Conclusions 413
List of symbols and units 415
References 419

INTRODUCTION

The work presented in this thesis is an examination of the phenomenon of Rising Damp in walls of buildings and other structures. Superficially the name of the phenomenon suggests that it is merely a natural occurrence characterised by an excess of moisture within the porous building material, and as such the presence and movement of moisture could simply be explained in terms of surface physics (e.g. surface tension, contact angle, capillary pressure, etc.).

Detailed inspection of the phenomenon reveals it to be in fact a much more complicated process involving the simultaneous flows of moisture, heat, solutes and electricity. The flow process is complicated further owing to the coupling or interaction between the various potentials and flows, *e.g.* a pressure potential not only produces volume flow of solution but may also produce flows of heat, electricity and solutes, and consequently generate their corresponding potential gradients.

The complexity of the phenomenon means that work is spread over a wide range of subjects. Consequently the usual thesis format has been modified to accommodate the large number of topics to be discussed. The phenomenon has been reduced into a number of major topics, or groups of related topics, which have been presented as separate chapters. References are included at the rear of each chapter, together with a list of symbols.

To understand the phenomenon more clearly it is necessary to develop mathematical expressions to describe the moisture cycle through all its flow stages, when in contact with porous building materials. In other words expressions are required to predict the movement of salt, moisture, electricity and heat between the limits of the water table (or source of moisture), the soil, the wall, and finally the atmosphere.

Much of the theory required to describe the flow processes connected with Rising Damp has been developed, previously, in other fields which also involve moisture flow through porous materials (e.g. soil science, physics, agricultural, civil and chemical engineering). The aim of the present work is to bring together the existing theories and knowledge to provide a foundation from which the phenomenon can be evaluated.

This broad source of information has resulted in two special problems. The first which is only a minor one, is the 'looseness' of nomenclature and symbols which have been used to represent some physical properties. This problem is usually encountered when comparing material from different academic disciplines although it can occasionally be observed within the same field of study. The slackness of nomenclature can lead to confusion or even worse to misleading ideas and results particularly where information is gleaned from figures. It is for this reason that particular care and space has been used to define the symbols and nomenclature used throughout this work.

The second problem which was more important was the choice of a suitable system of units. Science is generally moving towards the S.I. system of units. However for the work presented in this thesis, the c.g.s. system of units has been adopted.

The reasons for this choice are that for the most part, the c.g.s. system appears to be the one that is most common to all the disciplines in this field of study and that much of the published literature has used the c.g.s. system. Furthermore it is more convenient to use the (frequently required) conversion of moisture flux (mass flow of moisture per unit area of porous material per unit time) to a velocity of moisture in the c.g.s. system than in the S.I. system, although as emphasised below the conversion factor between the two systems is often a multiple of ten.

The c.g.s. system in common with the S.I. system, is a system of 'absolute' units and for the most part the difference between the c.g.s. and S.I. values are merely multiples of ten. There is however, in this work, one area where other differences occur both between the magnitude (other than multiples of ten) and theoretical description of physical coefficients in the two systems. The special area is that of electro-kinetics. Even so there is no great difficulty involved since the differences between the two systems have been specifically noted, together with the conversion(s) from one system to the other.

The presentation of both systems of units does have the advantage that it clarifies the position of both systems with regard to each other which is useful for readers who are unfamiliar with electro-kinetic theory and the different unitary systems.

The preceding paragraphs provide some hint of the layout that has been adopted, in this work, to describe the phenomenon of Rising Damp. The following is an outline of the structure of this thesis.

Chapter One provides an outline of the scope of the problems caused by excess dampness. Also included are brief discussions of damage caused by excess dampness and its origins; the forces that can induce moisture to move and their interactions with each other.

Chapter Two is a collection of 'porous material' terminology, descriptions and definitions. It was intended that this chapter should provide a background knowledge to readers who are not acquainted with the field of moisture movement through unsaturated porous materials.

The chapter consists of three separate parts. The first part is devoted to surface physics (surface tension, contact angle, etc.). The second section is concerned with the macroscopic effects of the interaction of the fluid and the porous material. The chapter is concluded by a discussion of hysteresis in porous materials.

The equation of motion of moisture has been derived in Chapter Three. It was developed from the Navier-Stokes expression. The basic expression was then expanded into a series of Diffusivity type expressions. The flow coefficients and potential gradients of the Diffusivity expressions were individually discussed together with the factors which affect the flow coefficients.

Chapter Four is concerned with the electro-kinetic aspects of Rising Damp. The mechanism inducing moisture movement within a porous material when subject to an electrical potential gradient was examined. The electro osmotic flow coefficient was derived from basic principles and the factors which affect the flow coefficient were also discussed.

The 'moisture cycle' was completed in Chapter Five in that the topic of evaporation was discussed. Several methods of estimating evaporation were examined.

In Chapter Six the more complex topic of leaching was covered. Leaching of porous materials is peculiar since it appears to be both a consequence and a cause of Rising Damp. It is a consequence of rising dampness because the upward movement of moisture leaches soluble salts from within the porous building materials. It is a cause of dampness since an unleached building material may exhibit a low permeability to moisture, whilst a leached building material might offer little resistance to moisture flow and consequently allow a greater volume of moisture to enter into the wall.

The emphasis of the chapter was concerned with the prediction of the rate of change of moisture permeability with respect to the volume of fluid injected through the porous material. In essence leaching is a problem of predicting the relative motion and stability of a moving interface.

The experimental work conducted for this project has been presented in Chapter Seven. The chapter was devoted, mainly, to the effects of

leaching upon the saturated permeability to moisture of plaster of Paris cores, to complement the theoretical aspects developed in Chapter Six.

Other experimental topics included a long term survey of the capillary suction developed by a wall suffering from Rising Damp, and a feasibility study to determine whether the hydraulic properties of unsaturated permeability, moisture content and evaporation rate (into still air) could be measured simultaneously and correlated against capillary suction.

Chapter Eight is a discussion of several, more general aspects of Rising Damp. The equation of motion of moisture was re-expressed in terms of Energy equations rather than Diffusivity type expressions (c.f. Chapter Three). Also included in the chapter is an analysis of the relative magnitude of the various modes of moisture movement through soils; a discussion of the cures and treatments of dampness; a physical description of Rising Damp. The chapter is concluded with suggestions for further work and conclusions.

CHAPTER ONE

ASSESSMENT OF THE PROBLEM AND PHENOMENON OF RISING DAMP

1. Defining Rising Damp

Buildings can suffer wall moisture problems for a variety of reasons and in several cases the occurrence of damp is mistakenly attributed to Rising Damp. Strictly Rising Damp is the movement of moisture from the ground into the wall because of failure or lack of a damp proof course. Rising Damp should not be confused with other wall moisture problems caused by faulty piping or guttering, or because of structural failures of building materials, e.g. fractured lintels and walls[(1)-(5)].

2. Origins of wall moisture

Moisture from the ground can infiltrate into a wall because of the following reasons:- (i) originally no damp proof course was installed in the wall. (ii) the damp proof course was installed inadequately or subsequently the damp proof course failed. (iii) the damp proof course was bridged by conducting porous materials[(1)(4)(5)].

Wall moisture problems caused by (i) and (ii) above are difficult to cure. The degree of difficulty of curing moisture problems caused by (iii) is determined by the nature of the "bridge". Examples of bridges are (a) earth piled up against a wall above the damp proof course. (b) raised paths straddling the damp proof course. (c) rendering the wall surface across the damp proof course. (d) mortar droppings in the cavity between the walls. (e) solid porous floors which are higher than the wall damp proof course, and have no damp proof layer themselves.

The "bridges" associated with (a), (b), (c) can be easily removed, thus curing the rising damp whereas removal of the "bridges" type (d), (e) is more difficult.

3. Problems caused by damp walls

The presence of excess moisture in a wall leads to building problems in itself, but additional problems are caused by soluble salts present in the wall moisture. The major problem is damage both to the wall and surrounding materials. The following list represents a brief summary of some of the common damp problems:-

(1) Frost action. Spalling of building materials due to "frost cycle"[2][3][13].

(2) Efflorescence.[6]-[16][28] The frost cycle damage is exacerbated by the damage caused by efflorescence and vice versa. Additional problems associated with efflorescence are those of loss of evaporative area because of pore clogging and reduced evaporation because of dissolved salts[14]; chemical damage to cement mortar (Sulphate attack)[17][18] and plaster (spalling and bubbling); and staining of wall paper.

(3) Leaching. Leaching of soluble salts from the wall, particularly from cement or mortar, which causes an increase in moisture permeability of the structure. In addition this soluble material adds to the problem of efflorescence.

(4) Osmotic gradient. The salt gradient developed in the wall may cause additional moisture flow particularly if the wall acts as a semi permeable membrane[7][19].

(5) Rotting and corrosion. Corrosion of metal will occur. Wet and dry rot of timber, furniture and household goods[3][5][18][20] and also mould and fungi growth.

(6) Fuel consumption. Increased fuel consumption because of continual evaporative cooling resulting in a low room temperature[2].

(7) Health and comfort.[21-22] Damp cold rooms are uncomfortable, and sometimes they may be a contributory factor to ill health (bronchitis, arthritis and hypothermia).

Particular examples of buildings suffering from excess moisture conditions are discussed by Seiffert[23], whilst a more general discussion of the problem of moisture and its effect upon building materials is discussed by Handisyde[24], Simpson and Horrobin[25] and Benster[5].

Further literature published by the Building Research Establishment relating to the damage caused by dampness, the treatment of dampness and corresponding choice of building materials can be found in Appendix I.

4. Forces or potential gradients causing moisture movement

There are four groups of potential fields or forces which can move moisture in porous materials. These are:-

(1) Pressure potential. This potential is developed from the surface tension forces acting at the curved fluid interfaces, producing a difference in pressure across the meniscus. In addition hydrostatic pressure forces are also included in this category.

(2) Temperature gradient. Flow caused by a temperature gradient can either occur solely in the vapour phase or solely in the liquid phase or simultaneously in both phases. Liquid phase flow is attributed to density differences (thermosyphon effect). Flow in the gaseous phase is attributed to vapour diffusion, arising from the difference in vapour pressure between the hot and cold liquid.

Water is evaporated from the warm areas and is condensed at the cold areas. Where the hot and cold areas are connected, bulk (pressure induced) flow of liquid may occur from the cold to the hot areas. The cyclical flow of fluid is often called the "capillary-distillation cycle"[26][27].

Thermal flow is often induced by the effect of temperature gradient upon surface tension and/or contact angle at the solid-liquid-gas interface.

(3) Concentration gradient. Flow of water caused by a solute concentration gradient is normally associated with that of osmosis through a semi-permeable membrane or partial ("leaky") semi-permeable membrane. It is a consequence of efflorescence from building materials that salt concentration gradients are developed, but whether the building materials act as semi-permeable membranes is difficult to assess; although slight reference to this point has been published[7][19].

(4) Electrical potential. The interaction of electric fields upon porous media and aqueous solutions permeating the porous media gives rise to several electro-kinetic phenomena[29]. The two phenomena most relevant to Rising Damp are Electro osmosis - movement of salt solution with respect to the porous media because of an externally applied electric field - and Streaming Potential - generation of an electrical potential gradient across a porous material because of bulk solution flow within the porous material.

5. Coupling of flow potentials and forces

Quantitative description of movement of moisture through porous materials or membranes is complicated by the fact that the different flows, forces and potential fields interact with each other.

A simple example of this interaction is Streaming Potential. The primary force is that of pressure, inducing movement of fluid within the pores of the permeable substance. A consequence of this fluid flow is the development of an electrical potential (streaming potential) across the porous medium acting to drive fluid back through the porous material and opposing the pressure potential. In addition it is not unreasonable to assume that

other potential fields are developed which tend to produce moisture movement.

Any of the potential fields may be chosen as the primary force with the other potentials being developed because of the coupling action. More than one primary force may be applied simultaneously in such a fashion that the desired bulk liquid flow is all in the same direction.

The interaction or coupling of the forces can be represented as a matrix

$$J_1 = L_{11}X_1 + L_{12}X_2 + L_{13}X_3 + L_{14}X_4$$
$$J_2 = L_{21}X_1 + L_{22}X_2 + L_{23}X_3 + L_{24}X_4$$
$$J_3 = L_{31}X_1 + L_{32}X_2 + L_{33}X_3 + L_{34}X_4$$
$$J_4 = L_{41}X_1 + L_{42}X_2 + L_{43}X_3 + L_{44}X_4$$

$$J_i = \sum_{i}^{n} L_{ij} X_j$$

J_i represents the net flux of a particular variable i.e. volume (water), 1; salt, 2; heat, 3; and electrical current, 4. The respective forces, either primary or secondary, are represented by X_j. The L_{ij} terms represent the flow coefficients which relate the flow to the corresponding potential. Generally where $i = j$, the coefficients describe the direct (primary) effect whereas for $i \neq j$, they describe the cross-effect from interference by other fluxes and, therefore, they are sometimes described as coupling coefficients.

Usually flow through porous membranes occurs at constant temperature, hence the temperature terms will become zero, leaving electric, solute and pressure terms. Coupled flow of these variables have been discussed in the literature[(30)-(43)]. Usually, the relationships governing the flow equations are assumed to be

linear, which together with the Onsager law means that the overall flows can be characterised by six phenomenological coefficients.

Although the fluxes of volume, salt and electricity are fully described by these expressions, their usefulness is very limited since there can be considerable variation of the magnitude of several of the coefficients. As an example consider the flow coefficient which is directly related to the pressure potential. This coefficient is normally known as the hydraulic conductivity (or filtration coefficient), and is the proportionality coefficient in Darcy's relationship.

For saturated porous materials, this coefficient is normally regarded as a constant, but for unsaturated porous materials the coefficient is a function of the suction or moisture content of the porous material and its magnitude may vary by a factor of one million. Because the Darcy coefficient is now a variable, flow of fluid through the same porous material at different moisture contents may be regarded as flow through different porous media each with its own particular value of the Darcy coefficient and corresponding phenomenological coefficients. Determination of the values of all the coefficients at different moisture contents is a very tedious process, if not an impossible one.

In view of the above stated difficulty of application of the phenomenalistic equations, flow relationship will only be developed for the 'direct' coefficients and forces, with special reference to coupled coefficients where the coupled phenomena are important. In addition Kedem and Katchalsky[34] stated that for very coarse membranes volume flow and exchange flow are independent. Each of the flows are determined only by its conjugate force.

6. Extent of dampness within a wall

The extent of the damp area within a wall is essentially determined by the relative net flows of moisture into and out of the wall. Changes in either flow will change the area (volume) of wall affected by excess dampness. In section 4, the four potentials causing moisture movement within the porous material were mentioned and generally it is changes in these potentials which produce moisture movement in the wall.

Normally variations of these potential fields are governed by environmental factors, although additional factors may affect the magnitude of the various fluxes and potentials.

Usually moisture flow into the wall is by infiltration from the ground, although when the air humidity is high water can be extracted from the air by hygroscopic salts in the wall, and by capillary condensation. Also when the high humidity is accompanied by a temperature drop, water may condense on the wall surface because the dew point temperature of the air has been exceeded.

Flow of water from the wall is by evaporation and sometimes by drainage. The evaporative flux can be positive (loss of moisture from wall) or negative as described above. Drainage of moisture from the wall is associated with a falling water table in the ground upon which the wall is situated.

The most obvious environmental factor that affects the two flows is the weather, in particular its seasonal variations. In the winter months the ground is wetter, rain more prevalent, and the water table higher, all of which lead to higher moisture levels in the wall. The humidity of the air is higher which means a lowering of the evaporation rate. The problem of efflorescence also becomes more prevalent in the winter months, which may lead

to clogging of pores and extraction of moisture from the atmosphere with a consequent increase in the wall moisture level. During the summer months the situation is reversed and the wall tends to dry out.

Another seasonal (and also diurnal) variable is that of wall temperature. Edlefsen and Anderson[44] have shown that increasing wall temperatures will cause water to drain from the wall into the ground causing a consequent increase in the height of the water table. The seasonal temperature variation tending to reinforce the drying conditions described above.

An additional factor which affects the degree of dampness in a wall is "leaching". It is different from the other factors inasmuch that it is not directly dependent upon the weather. Soluble salts are 'leached out' of the mortar by moisture passing through it, making the mortar more permeable to water. Also the salts are concentrated at the evaporative surface, with the possibility that concentration potentials become established which can then act as an additional moisture driving force.

A superficial analysis of the effects of the flow factors indicates that the extent of dampness in a wall will progressively increase (leaching and salt pore clogging) but superimposed upon this increase will be a cyclical variation (seasonal fluctuations).

References Chapter One

(1) "Rising Damp in Walls", Building Research Station Digest No. 27, 2nd Series, 6 pages.

(2) "Suggested unified method of building diagnosis for determining the origin of wall moisture", M. Zador, Int. Cons. Int du Batim pour la Rech (CIB) - RILEM, Symp. on Moist. Probl. in Build., 2nd Programme, Rotterdam, Neth. Sept. 10-12 1974, Pap 5.2.4, 12 pages.

(3) "Effects of water and moisture on a building", R.M. McNeal, Construction Sepcifier, 27 No. 11 pp. 24-29, 1974.

(4) "The causes of dampness in buildings", Building Research Station Digest, No. 33, 1st Series, 7 pages, August, 1951.

(5) "A study and assessment of water penetration and rapid deterioration in existing dwellings - Developed as a guide to future building design, production and maintenance management", N.A. Benster, A thesis submitted to the University of Manchester Institute of Science and Technology, 1970.

(6) "Contributions to the study of florescence", L.F. Cooling, Trans. Brit. Ceram Soc., 29 No. 2, pp.39-52, 1930.

(7) "Some effects of soluble salts in clay products", B. Butterworth, Trans. Brit. Ceram Soc., 36 pp.233-242, 1937.

(8) "Efflorescence", R.K. Robertson, Jnl. Canad. Ceram Soc., 13, pp.40-43, 1944.

(9) "Developing a test method for efflorescence of masonry mortar", P.L. Rogers, Am. Soc. Testing Matls., Tech. paper 190, part 200, pp.64-66, 1954

(10) "Contributions to the study of efflorescence, Part VIII", B. Butterworth, Trans. Brit. Ceram Soc., 53, pp.563-607, 1954.

(11) "Study of efflorescence on experimental brickwork piers", T. Ritchie, Jnl. Am. Ceram Soc. 38, No. 10, pp.357-361, 1955.

(12) "Study of efflorescence produced on ceramic wicks by masonry mortars", T. Ritchie, Jnl. Am. Ceram Soc., 38, No. 10, pp.362-366, 1955.

(13) "The effect of weathering on certain mortars exposed in brick masonry with and without caps and flashings", J.W. McBurney, Proc. Am. Soc. Testing Matls., 56, pp.1273-1287, 1956.

(14) "Surface growth of salt crystals as a contributory cause of frost damage to bricks", A. Watson, Trans. Brit. Ceram Soc. 56, No. 7, pp.366-368, 1957.

(15) "Efflorescence on brickwork", A.F. Greaves-Walker, Jnl. of Ind. and Eng. Chem., 2, No. 9, pp.373-375, 1910.

(16) "Contributions to the study of Efflorescence, Part I", W.A. McIntyre and R.J. Schaffer, Trans. Ceram Soc., 28, pp.363-380, 1929.

(17) "The deterioration of buildings", H.D. Searles-Wood, The Power Engineer (London), 24, No. 280, pp.266-267, 1929.

(18) "The Chemistry of building materials", R.M.E. Diamant, Business Books Ltd., London, 1970.

(19) "Injury to plaster due to osmosis", F.L. Brady, Nature, 126 p.684, 1930.

(20) "A field study of a house destroyed by fungus attack resulting from uncontrolled moisture", F.H. Hedden, P. Labosky, R.A. Spray. Am. Soc. of Agric. Eng., Paper No. 75 - 4007, 8 pages, 1975.

(21) "The influence of humidity on human thermal comfort", N. Biswas, Int. Cons. Int. du Batim pour la Rech (CIB)/RILEM, Symp. on Moist Probl. in Build., 2nd Programme, Rotterdam, Neth. Sept. 10-12, 1974, paper 3.1, 15 pages.

(22) "Comfort in damp cold air with spot radiant heating", A. Moisan, J. Lebrun, Int. Cons. Int. du Batim pour la Rech (CIB)/RILEM, Symp. on Moist Probl. in Build., 2nd Programme, Rotterdam, Neth. Sept. 10-12, 1974, paper 3.2, 12 pages.

(23) "Damp diffusion and buildings", K. Seiffert, Elsevier Publ. Co. Ltd., 1970.

(24) "Building Materials. Science and practice", C.C. Hanisyde, The Architectual Press, London, 4th Ed. 1961.

(25) "The weathering and performance of building materials", J.W. Simpson and P.J. Horrobin, Medical and Technical Publ. Co. Ltd., 1970.

(26) "Moisture flow induced by thermal gradients within unsaturated solids", W.L. Hutcheon, Highway Research Board Special Report, 40, pp.113-133, 1958.

(27) "On the mechanism by which water moves through a porous material subjected to a temperature gradient", J.M. Kuzmak, P.J. Sereda, Highway Research Board Special Report, 40, pp.134-146.

(28) "Recent disintegration of mortar in brick walls", C.C. Connor, W.E. Okerson, Proc. Am. Soc. Testing Matls., pp.1170-1194, 1957.

(29) "Physical surfaces", J.J. Bikerman, Academic Press, 1970, p.404.

(30) "Reciprocal relations in irreversible processes. I", L. Onsager, Physical review, 37, pp.405-426, 1931.

(31) "Reciprocal relations in irreversible processes. II". L. Onsager, Physical review, 38, pp.2265-2279, 1931.

(32) "Non-equilibrium thermodynamics of membrane processes", A.J. Staverman, Transactions of the Faraday Soc., 48, pp.176-185, 1952.

(33) "Transport processes in ion-selective membranes", J.W. Lorimer, E.I. Boterenbrood, J.J. Hermans. Discussions of the Faraday Society, No. 21, pp.141-149, 1956.

(34) "Thermodynamic analysis of the permeability of biological membranes to non-electrolytes", O. Kedem, A. Katchalsky. Biochimica et biophysica acta, 27, pp.229-246, 1958.

(35) "Description of the transport of solvent and ions through membranes in terms of differential coefficients", I. Michaeli, O. Kedem. Trans. of Faraday Society, 57, pp.1185-1190, 1961.

(36) "Permeability of composite membranes", O. Kedem, A. Katchalsky. Trans. of Faraday Soc., 59, part 1, pp.1918-1930; part 2, pp.1931-1940; part 3, pp.1941-1953, 1963

(37) "Prevention of moisture rise in capillary by electrical short circuiting", D.H. Gray. Nature, 223, pp.371-374, 1969.

(38) "Coupling phenomena as a possible cause of 'Non-Darcian' behaviour of water in soil", G.H. Bolt, P.H. Groenevelt. Bull. Int. Assoc. of Scientific Hydrology, 14, No. 2, pp.17-26, 1969.

(39) "Some aspects of non-equilibrium thermodynamics in flow through porous media", S.K. Baijal, A.N. Sriramulu. Indian Jnl. of Tech., 13, pp.480-483, 1975.

(40) "Coupled flow phenomena in thin free-surface films", C.H. Gartside, J.F. Osterle. Applied Science Research (The Hague), 30, No. 6, pp.453-468, 1975.

(41) "Movement of water through soil as influenced by osmotic pressure and temperature gradients", J. Letey. Hilgardia, 39, No. 14, pp.405-418, 1968.

(42) "Coupling phenomena in synthetic membranes", S.R. Caplan. U.S. Office of Saline Water, Research and Devel. progress report No. 413, 1969, 121 pages.

(43) "Thermodynamics of irreversible processes", D.G. Miller. Chemical Review, 60, pp.15-37, 1960.

(44) "Thermodynamics of soil moisture", N.E. Edlefsen, A.B.C. Anderson. Hilgardia, 15, No. 2, 298 pages, 1943.

Appendix I

Summary of Building Research Establishment Digests relating to the topic of moisture in buildings.

First Series

No.	Title	Year
11	No title, but paper concerned with damp proof courses in walls	1963
20,21	The weathering, preservation and maintenance of natural stone.parts I and II	1950
23	Condensation problems in buildings	1950
31	Concrete in sulphate-bearing clays and ground waters	1951
33	The causes of dampness in buildings	1951
41	The treatment of damp walls	1952
47	The control of lichens, moulds and similar growths on building materials	1963
68	Damp-proof courses	1954
86	Damp-proof treatments for solid floors	1956
90	Colourless water proofing treatments for damp walls	1956
123	Sulphate attack on brickwork	1959

Second Series

No.	Title	1st publ.	Latest ed.
27	Rising Damp in walls	1962	1969
54	Damp-proofing solid floors	1965	1968
55,56,57	Painting walls I, II, II	1965	1969,1967,1968
65,66	Selection of clay building bricks	1965,1966	1968
75	Cracking in buildings	1966	1970
77	Damp proof course	1966	1969

No.	Title	1st publ.	Latest ed.
89	Sulphate attack on brickwork	1968	1971
90	Concrete in sulphate-bearing soils and ground waters	1968	1970
125	Colourless treatments for masonry	1971	
139	Control of lichens, moulds and similar growths	1977	
174	Concrete in sulphate-bearing soils and ground waters	1975	
176	Failure patterns and implications	1975	
177	Decay and conservation of stone masonry	1975	
197,198	Painting Walls		
	I. Choice of paint	1977	
	II. Failures and remedies	1977	
200	Repairing brickwork	1977	
201	Wood preservatives, application methods	1977	

CHAPTER TWO

POROUS MATERIAL TERMINOLOGY

1. Introduction

Rising Damp is a natural example, albeit a complicated one, of the flow of fluid through a porous material. The study of this phenomenon covers a wide variety of scientific subjects extending from the fundamental aspects of surface physics to the engineering description of the macroscopic flow of moisture. The purpose of this chapter is to summarise the more common and useful subjects that are required to describe Rising Damp.

Because of the wide variety and "general" nature of the subjects, it is more convenient to group the references in terms of related topics in keeping with the layout of the chapter, although where necessary specific references will be cited. Both the specific references and grouped (general) references can be found at the end of this chapter.

The first group of references is concerned with the physics of surfaces, the individual topics being surface tension, contact angle, contact angle hysteresis and finally spreading of fluids on surfaces. The second group is related to the macroscopic effects of the interaction of the fluid and the porous material. The individual topics are porosity, permeability, saturation and saturation states, and finally saturation, capillary pressure and the pF scale. The third group is a brief discussion of the topic of hysteresis in porous materials.

2.1 Surface tension

Consider a drop of liquid surrounded by its vapour. A molecule in the interior of the liquid experiences the attraction of all molecules surrounding it. Because of the symmetry of attraction, there is no resultant force on the molecules in the bulk. In the surface the molecules are attracted more strongly by the dense liquid than by the rare vapour. This difference in

attraction causes the liquid to behave as though enclosed in a stretched skin. Because of the difference in attraction work must be performed to raise the molecule to the boundary. When the surface is extended more molecules are raised and the work done against the molecular forces during this process is called the work required against surface tension. The dimensions of surface tension are force per unit length or energy per unit area, these units are dimensionally identical.

Strictly surface tension is a measure of the free energy of a material in contact with own vapour. When the liquid is in contact with another substance (either an immiscible liquid or solid) the free (interfacial) energy is called interfacial tension. The relationship between the interfacial tension and the corresponding surface tensions was stated by Dupré, which for a liquid(1)-liquid(2)-gas system is

$$W_{L1L2} = \gamma_{L1G} + \gamma_{L2G} - \gamma_{L1L2} \qquad (1)$$

where W_{L1L2} is the amount of work required to separate a unit area of interface between the two liquids L_1 and L_2. γ_{L1L2} is the interfacial tension between the two liquids and γ_{L1G}, γ_{L2G} are the corresponding surface tensions. A sign convention is adopted such that when work is done on the system it is positive and when work is performed by the system it is negative. Similarly when new surface is created, energy is consumed and when the surface interface is decreased energy is released.

2.2 Contact angle

When a liquid is placed upon a flat solid, the liquid will spread until equilibrium is attained. The angle measured through the liquid is called the contact angle as indicated in Fig. 1. By convention the contact angle is measured through the more dense fluid.

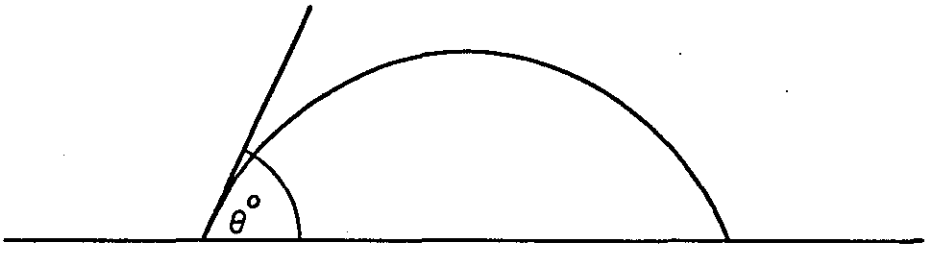

Fig. 1. The contact angle θ^{o}. A sessile drop on a plate.

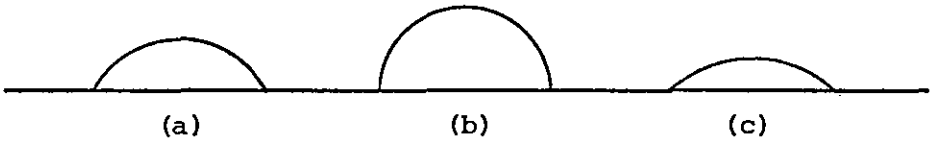

Fig. 2. Hysteresis of wetting. The base of the drop does not change when the volume increases from (a) to (b) or decreases from (a) to (c).

The angle can vary between 0° and 180°. When the angle is 0°, the liquid is said to wet the solid and as the contact angle θ° increases the liquid wets the solid less and less. Contact angles are also observed between liquid-liquid-solid and liquid-liquid-gas systems.

The contact angle, θ°, is important as is capillary pressure, P_c, and surface tension, γ, since together they determine the relative motion between solids and liquids. Unfortunately knowledge of contact angles is much less satisfactory than that of surface tension. In addition the theory relating to contact angles and surface tension is controversial. Further problems are incurred since the experimental values of surface tension and especially contact angle are subject to variability.

Experiments designed to measure contact angle may be arranged into two groups, those which involve surface tension to estimate contact angle and those that do not. However both groups indicate that contact angle is subject to hysteresis[1].

Hysteresis may be simply demonstrated by considering the following example. A drop of liquid is placed on a horizontal plane surface (Fig. 2a). When equilibrium is attained a contact angle or narrow range of contact angles will be established. If a small volume of liquid is added, the drop will become taller, but the area of the base will not change (Fig. 2b). The contact angle will be greater for the drop in (2b) than in (2a). Alternatively liquid may be removed such that the drop becomes shorter, once again without changing the base area (Fig. 2c). This will result in a smaller contact angle.

Eventually a situation is reached where addition or subtraction of liquid causes a sudden change in the base area of the drop. The two extremes of contact angle, measured just before

rapid movement of the drop occurs, are called the advancing contact angle, θ_A^o, when the base expands and the receding contact angle, θ_R^o, when the base contracts. Both the advancing and receding angles may be observed on a single drop when the support is tilted (Fig. 3).

A summary of the more common explanations of contact angle hysteresis are given below:-

(1) The jerky motion of the drop (Fig. 2) involves the whole volume of liquid and hence the bulk viscosity of the liquid may determine the contact angles.

(2) Surface roughness would cause hysteresis even if a contact angle θ_o^o remained constant (Fig. 4). Although θ_o^o remains constant, two apparent contact angles θ_1^o , θ_2^o can be observed.

(3) When a liquid is moving over a solid, the advancing contact angle is between vapour, liquid and dry solid whilst the receding angle is associated with vapour, liquid and wet solid surface.

(4) There may be some interpenetration of solid and liquid which may cause swelling. In this case the advancing angle meets an unaltered solid whilst the rear of the drop recedes from a swollen surface.

(5) When the solid is soft a ridge may be formed along the three phase line. This may cause hysteresis as in (b) above.

2.3 Surface tension, spreading and contact angle

Consider a three phase system consisting of two immiscible liquids L_1 , L_2 and a gaseous phase. γ_{L1G} , γ_{L2G} and γ_{L2L2} are the respective surface tensions of liquid 1 and the gaseous phase, liquid 2 and the gaseous phase and the interfacial tension between the two liquids.

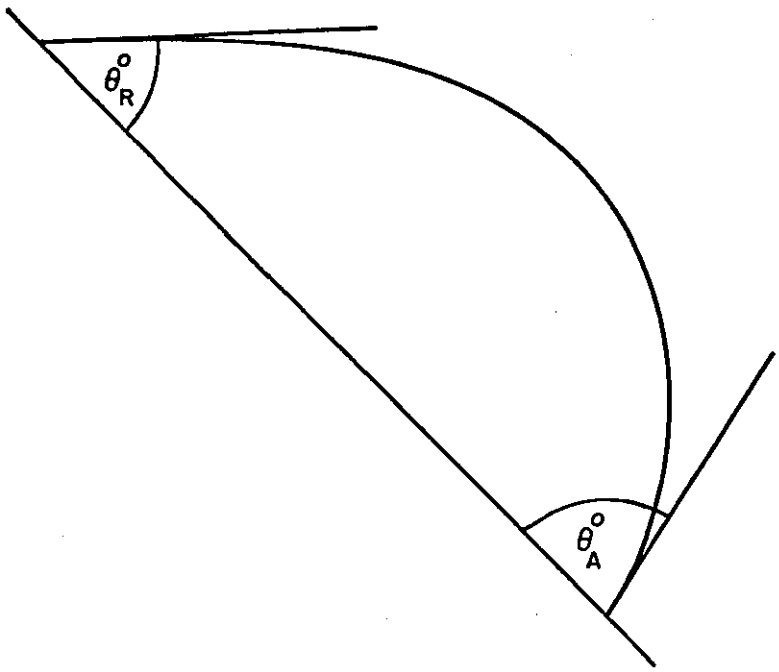

Fig. 3. Drop on a sloping plate showing advancing (θ_A^o) and receding (θ_R^o) contact angles.

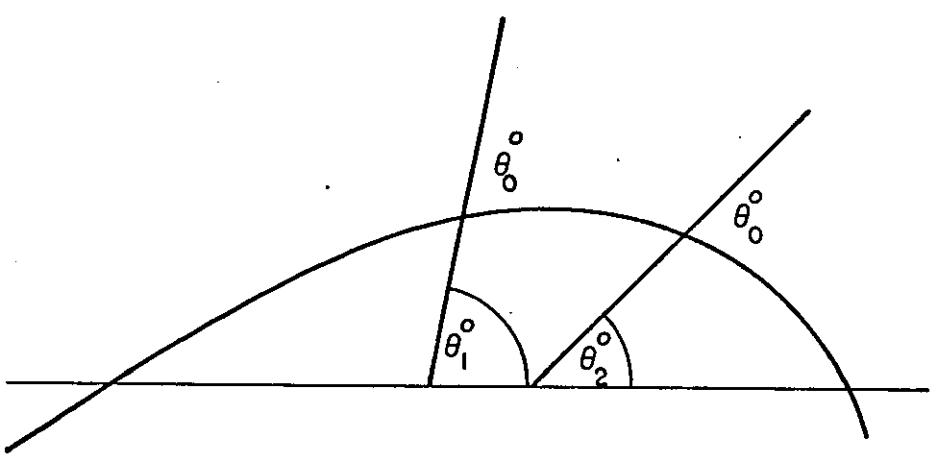

Fig. 4. Hysteresis of contact angle caused by surface roughness. The true contact angle θ^o remains constant when the three phase line moves, but the apparent angle changes from θ_1^o to θ_2^o.

The oldest relationship between the above surface (and interfacial) tensions was proposed by Young in 1805, which, for the system above is expressed as

$$\gamma_{L1L2} = \gamma_{L1G} - \gamma_{L2G} \quad (2)$$

where $\gamma_{L1G} > \gamma_{L2G}$.

Antonoff in 1907 proposed a more generalised form of Young's equation which dealt with miscible systems, i.e.

$$\gamma'_{L1L2} = \gamma'_{L1G} - \gamma'_{L2G} \quad (3)$$

where γ'_{L1G} , γ'_{L2G} are the respective surface tensions of the two liquids when mutually saturated with each other, and γ'_{L1L2} is the interfacial tension between the two liquids. For a completely miscible system, there will be no interface and obviously $'_{L1L2}$ will be zero.

Another fundamental formula relating to surface tension was also proposed by Dupré (1866) which for a liquid-liquid-gas system can be expressed as

$$W_{L1L2} = \gamma_{L1G} + \gamma_{L2G} - \gamma_{L1L2} \quad (4)$$

where W_{L1L2} is called the work of adhesion between the two different liquids. It is the amount of work required to separate unit area of the liquid-liquid interface. Dupré's equation (4) may be applied to either miscible or immiscible liquid-liquid systems.

When equation (4) is applied to a single liquid, L, it yields

$$W_{LL} = 2\,\gamma_{LG} \quad (5)$$

where W_{LL} is called the work of cohesion of the liquid and it is the work required to separate unit area of liquid to create new liquid-gas interfaces.

Combining equations (2) and (4) yields

$$W_{L1L2} = 2\,\gamma_{L2G} \quad (6)$$

Equation (6) states that the work of adhesion between the two liquids is equal to the work of cohesion of the liquid of lower surface tension (L2). An equation similar to equation (6) can also be derived for miscible liquid systems.

When applied to a solid-liquid-gas system equation (4) is expressed as

$$W_{SL} = \gamma_{SG} + \gamma_{LG} - \gamma_{SL} \tag{7}$$

where W_{SL} is called the work of adhesion between the solid and liquid. It is the amount of work required to separate unit area of solid and liquid in contact with each other.

If Young's relationship (Eq.(2)) is applied to the solid-liquid-gas system and furthermore if the liquid exhibits a contact angle, θ^{o}, with the solid (Fig. 5), the expression relating the surface tension is

$$\gamma_{SG} = \gamma_{SL} + \gamma_{LG} \cos \theta^{o} \tag{8}$$

Combining equation (8) with (7) yields

$$W_{SL} = \gamma_{LG} (1 + \cos \theta^{o}) \tag{9}$$

This equation expresses the fundamental relationship between the adhesion of the liquid to the solid, and the contact angle.

The necessary condition for spreading to be possible is that the process shall involve a reduction in the free energy of the system. Consider a drop of liquid resting on a solid. If the liquid spreads to cover an additional square centimetre of solid surface, then there is an increase of both the liquid-gas and liquid-solid interfacial areas and a corresponding reduction of the solid-gas interfacial area.

The change in free surface energy associated with the change in area described above must be negative, i.e. energy is lost by the system. Mathematically the energy change is expressed thus

$$\Delta f_{A} = \gamma_{LG} + \gamma_{SL} - \gamma_{SG} \tag{10}$$

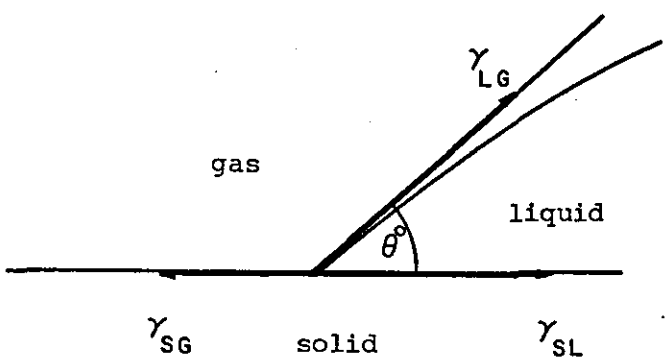

Fig. 5. Alleged equilibrium of a drop on a horizontal solid. Tension γ_{SG} balances the sum of the tensions γ_{SL} and γ_{LG} Cos θ^o.

where Δf represents the free energy change. Equation (8) can be combined with eqn. (10) to eliminate γ_{SG} to yield

$$\Delta f_A = \gamma_{LG} (1 - \cos \theta^o)$$

The same free energy change can be obtained by subtracting the work of adhesion between the solid and liquid (eqn.(9)) from the work of cohesion of the liquid phase (eqn.(5))

$$\Delta f_A = W_{LL} - W_{SL}$$

$$= \gamma_{LG} (1 - \cos \theta^o) \qquad (11)$$

Equations (7), (8) used to derive the free energy relationships, eqns. (10), (11) are of only limited use and validity. Equation (7) may only be used when there is no additional energy consumed through change in the principal radii of curvature of the liquid (c.f. section 2.4). Another implicit assumption associated with the derivation of equation (7) is that the changes in area for each of the three interfaces are the same, this assumption is not always the case[2]. This assumption is also necessary to validate eqn. (8). Further treatment of the applicability and validity of equations (7) and (8) is discussed by Bikerman[31], and Davies and Rideal[32].

2.4 Surface tension and free energy

The free energy of a system can be expressed by

$$\Delta f = \upsilon \Delta P - \Delta W_m - s \Delta T$$

where Δf, the free energy difference; ΔP, the pressure difference; ΔW_m, is the mechanical work performed, excluding that of expansion of a gas against a pressure, P; ΔT, the temperature difference; υ, specific volume of the fluid; s, the entropy of the fluid. In the present work, the physical properties are related to a gram of fluid unless stated otherwise.

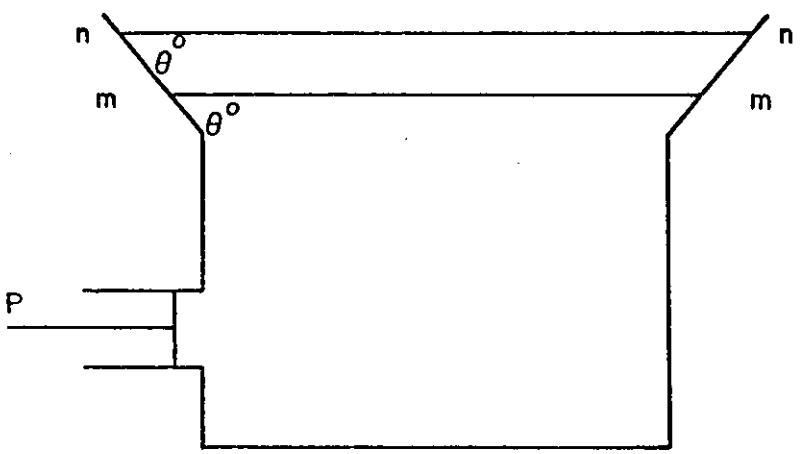

Fig. 6a. A system in which the area of the vapour-liquid interface can be varied without changing the curvature. P is the piston which can raise the liquid level from mm to nn.

For a reversible isothermal change and assuming that the volume also remains constant, the free energy change can be expressed as

$$\Delta f = \upsilon \Delta P - \Delta W_m \qquad (12)$$

Equation (12) states that the free energy change consists of two components, one associated with a pressure change in the liquid, which is caused by a change in the radius of curvature; the other component is the work associated with creation of new liquid surface.

Consider the following example which elucidates the different free energy changes when a liquid spreads over a surface. Fig.6a is an example of a system in which no change of liquid curvature occurs. When the piston, P, is pushed into the vessel, the liquid rises in the funnel from level mm to nn.

The liquid surface remains horizontal because the angle of the funnel has been chosen such that the angle between the funnel wall and the liquid surface is equal to the contact angle θ^o.

Neglecting hydrostatic pressure changes due to the difference in height of levels mm and nn, and the surface energy changes associated with the changes in area between the solid and gas, and solid and liquid, the free energy change is proportional to the increase in area of the gas-liquid interface

$$(\Delta f)_{net} = \gamma_{LG} (\Delta A)_{net} \qquad (13)$$

where $(\Delta f)_{net}$ is the total free energy change of the system; $(\Delta A)_{net}$ is the total change in area of the liquid-gas interface: γ_{LG} is the surface tension between the liquid and the gas.

A similar system can be found in Fig. 6b except that the angle of the funnel has been altered such that the liquid surface is no longer horizontal but curved. When the piston is moved inwards, the meniscus not only rises but also increases in radius when it moves from level mm to nn.

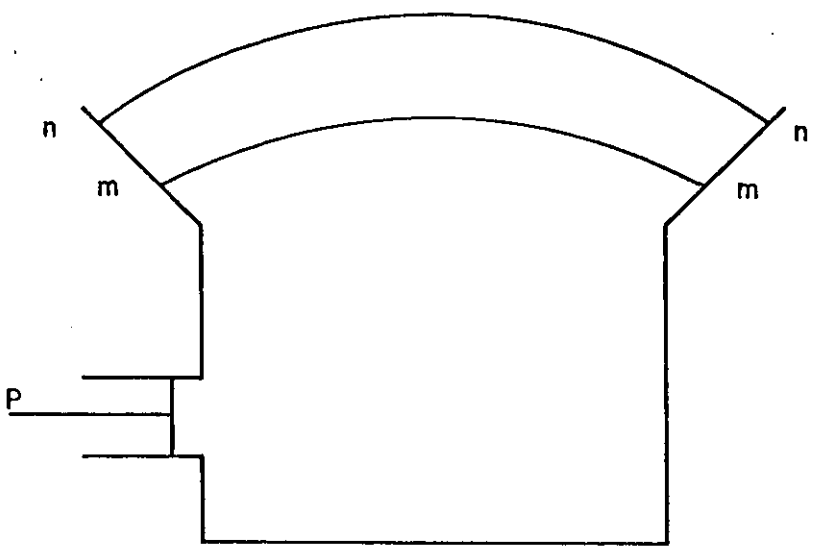

Fig. 6b. A system in which the area and the curvature of the vapour-liquid interface are varies simultaneously. Curve nn has a greater radius of curvature then curve mm.

Once again, neglecting the hydrostatic energy component and the surface energy components associated with the solid-liquid and solid-gas interfacial areas, energy is used to create liquid-gas surface and in addition further energy changes are involved because of the change of radius of liquid curvature. The change of liquid curvature is simultaneously accompanied by a pressure change throughout the bulk liquid.

The pressure difference across a curved liquid-gas interface, where R_1 , R_2 are the principal radii of curvature measured at right angles to each other is given by

$$\Delta P_c = \gamma_{LG} \left(\frac{1}{R_1} + \frac{1}{R_2}\right) = \gamma_{LG}\, \omega \qquad (14)$$

where ΔP_c, the pressure difference across the interface; ω, $\left(\frac{1}{R_1} + \frac{1}{R_2}\right)$. Schematic representation of the principal radii of curvature can be found in Figs. 7a, 7b.

Where the radii of curvature are the same, equation (14) is reduced to

$$\Delta P_c = \frac{2\,\gamma_{LG}}{R} \qquad (15)$$

where R is the common principal radius of curvature.

Equation (15) is normally associated with menisci in small cylindrical capillaries in which the principal radii are the same. Note where the <u>liquid</u> meniscus is concave towards the vapour, the pressure in the liquid just below the interface, is less than the pressure in the vapour phase.

Returning to the example found in Fig. 6b, the total free energy change, ignoring the hydrostatic, solid-liquid and solid-gas changes when the level rises from mm to nn, is given by

$$(\Delta f)_{net} = \gamma_{LG}\, (\Delta A)_{net} + \Omega\, d\, \omega \qquad (16)$$

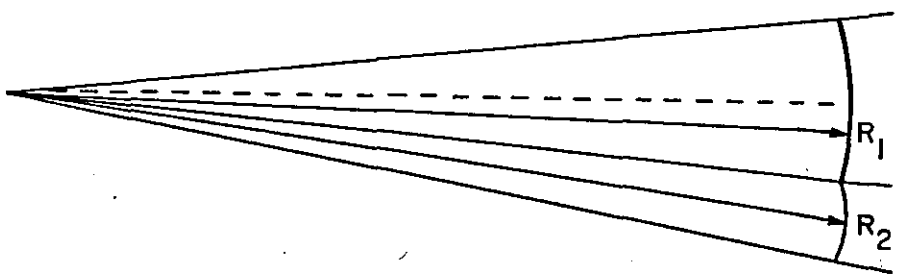

Fig. 7a. Principal radii of curvature, R_1, R_2 of a fluid interface.

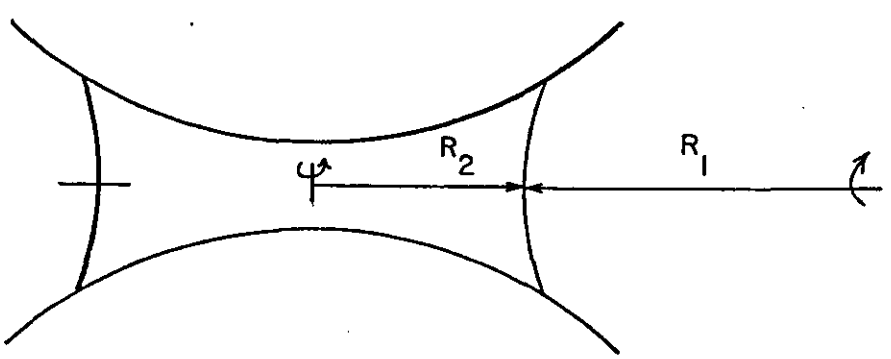

Fig. 7b. Pendular ring of fluid between two solid surfaces. R_1, R_2 the principal radii of curvature in the vertical and horizontal planes respectively.

where Ω is a coefficient whose magnitude depends upon the number of processes occurring during the motion. For example, if the liquid contains a solid sediment, this may dissolve (or more may be precipitated) when the piston moves, provided the solubility of the sediment is a function of pressure. If the liquid in Fig. 6b is pure and incompressible and the volume of the vessel is denoted by $(V)_{net}$ then the free energy change of equation (16) can be expressed as

$$(\Delta f)_{net} = \gamma_{LG} (\Delta A)_{net} + (V)_{net} \gamma_{LG} d\omega \qquad (17)$$

Note the neglection of hydrostatic pressure and solid-liquid, solid gas surface energy terms means that Ω is equal to $(V)_{net} \gamma_{LG}$.

The expression relating the pressure drop across a phase interface and its principal radii of curvature (c.f. equation (14)) is commonly known as Laplaces equation. For a curved interface in a circular capillary ($R_1 = R_2 = R$) and zero contact angle, the pressure difference across the interface is given by

$$\Delta P = \gamma_{LG} \left(\frac{2}{R}\right) = \gamma_{LG} \left(\frac{2}{r}\right) \qquad (18)$$

where r, radius of the capillary and R, the common principal radius of curvature.

When the contact angle between the liquid and solid is θ^o (Fig. 8), the pressure difference is expressed by

$$\Delta P = \gamma_{LG} \cos \theta^o \left(\frac{2}{r}\right) \qquad (19)$$

i.e. R equals $r(\cos \theta^o)^{-1}$.

3.1 Porosity ϕ

Porosity of a material is defined as the fraction of the bulk volume of the material that is not occupied by the solid skeleton of the material. One may distinguish two types of porosity, namely absolute or effective. Absolute porosity is a measure of the total void space with respect to the bulk volume regardless of

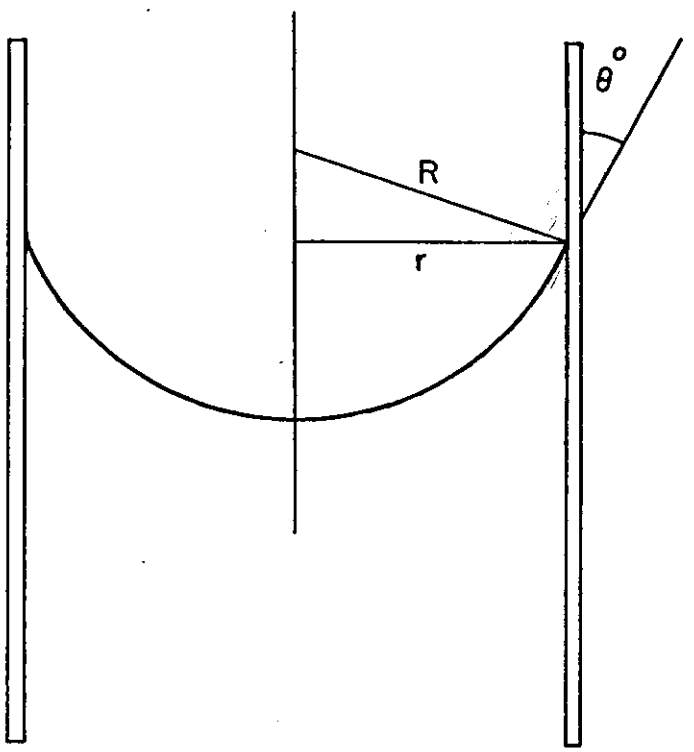

Fig. 8. Fluid meniscus in a capillary tube of radius r, exhibiting a contact angle θ^{o}. R is the common principal radius of curvature.

the interconnection of the pore voids. Effective porosity is the percentage of interconnected void space with respect to the bulk volume. It is an indication of conductivity to fluid but not necessarily a measure of it.

3.2 Darcy's Law

Permeability is that property of a porous material which characterises the ease with which a fluid may be made to flow through the material by an applied potential gradient. The equation which defines permeability in terms of measurable quantities is called Darcy's Law.

If steady horizontal flow of an incompressible fluid is established through a porous material of length, ℓ, in the direction of flow and constant cross-sectional flow area, A, then Darcy's Law is defined as

$$J_v = \frac{Q}{A} = K' \nabla \Phi \qquad (20)$$

where Q is the volumetric flow rate ($cm^3\ sec^{-1}$); J_v, the macroscopic fluid velocity ($cm\ sec^{-1}$); $\nabla \Phi$, the applied pressure potential, which is assumed to be linear; K', a coefficient of proportionality.

Unfortunately, Darcy's Law is used in many different disciplines (soil science; physics; civil, chemical and agricultural engineering). Consequently a wide variety of different systems of units have arisen. Also there is considerable looseness in the usage of the definitions of permeability and hydraulic conductivity, often one becoming synonymous with the other. The following is a brief attempt to clarify some of the common systems of units into a systematic pattern.

The potential, Φ, (eqn. (20)) can be expressed as either energy per unit volume of fluid or energy per unit mass of fluid or as energy per unit weight of fluid. The dimensions of the

proportionality coefficient K' will vary accordingly. The coefficient K' is often referred to as the Darcy coefficient.

(1) Energy per unit volume of fluid (g cm^{-1} sec^{-2})

The potential, Φ, has the same dimensions as those of pressure (force over area). The pressure potential can be expressed in terms of height of fluid i.e. ρ_L g h_w where ρ_L, the fluid density; g, the gravitational acceleration and h_w, the height of fluid. The dimensions of the potential gradient, $\nabla\Phi$ (force over volume) expressed in the c.g.s. system of units are gm cm^{-2} sec^{-2}. The dimensions of the coefficient k' are cm^3 sec gm^{-1}. Furthermore the coefficient K' can be expressed as

$$K' = \frac{k}{\mu}$$

where k is the specific permeability of the porous material (cm^2); μ, the viscosity of the fluid (g cm^{-1} sec^{-1}).

Sometimes the units of specific permeability, k, are expressed in terms of their pioneer as darcys, d, or millidarcys, md (1 md = 0.001 d) where

$$1 \text{ darcy} = \frac{1\ (cm^3\ sec^{-1}) \cdot 1\ (c.p)}{1\ (cm^2) \cdot 1\ (ats.\ cm^{-1})} = 9.87 \times 10^{-9}\ cm$$

Note c.p , centipoise and ats. , atmosphere (of pressure).

(2) Energy per unit mass (cm^2 sec^{-2})

To convert a potential with dimensions of ergs cm^{-3} to one of ergs gm^{-1} one divides the former by the fluid density, ρ_L. The dimensions of the potential gradient are cm sec^{-2} i.e. the dimensions of acceleration. The dimension of the proportionality coefficient is time i.e. sec.

(3) Energy per unit weight. (cm)

To convert a potential from ergs cm^{-3} to a potential expressed as ergs per unit weight, one divides by $\rho_L g$. The potential has the dimensions of length and is often called hydraulic head, h_w.

The gradient of this potential is called hydraulic gradient and is dimensionless. The coefficient, K', is called hydraulic conductivity, K, and obviously has the dimensions of cm sec^{-1} i.e. velocity. Expressed in terms of the specific permeability and fluid properties, the hydraulic conductivity coefficient is expressed by

$$K = \frac{k \rho_L g}{\mu}$$

3.3 Saturation

The saturation of a porous medium with respect to a particular fluid is defined as the fraction of the void volume of the medium filled by the fluid. If the fluid is denoted by the subscipt w, then the fractional saturation with respect to this fluid is defined thus

$$S_w = \frac{\text{volume of fluid in the medium}}{\text{total volume of voids in the medium}}$$

Another method of expressing saturation with respect to water, is moisture content. It is usually defined upon a dry weight basis i.e. grams of moisture per gramm of dry solid. Alternatively moisture content can be expressed volumetrically i.e.

$$\theta = \frac{\text{c.c. of moisture}}{\text{c.c. of porous material}}$$

Fractional saturation can obviously vary between 0 and 1 or 0 to 100% on a percentage basis. Zero saturation corresponds to a moisture content of zero, whilst a saturation of one (or 100%) corresponds to the highest moisture content value.

3.4 Saturation states

When the percentage saturation of a fluid passes from 0% to 100%, one may distinguish three types of fluid saturation states, namely pendular, funicular and insular (Fig. 9). For simplicity consider a simple air-water system where the porous material is

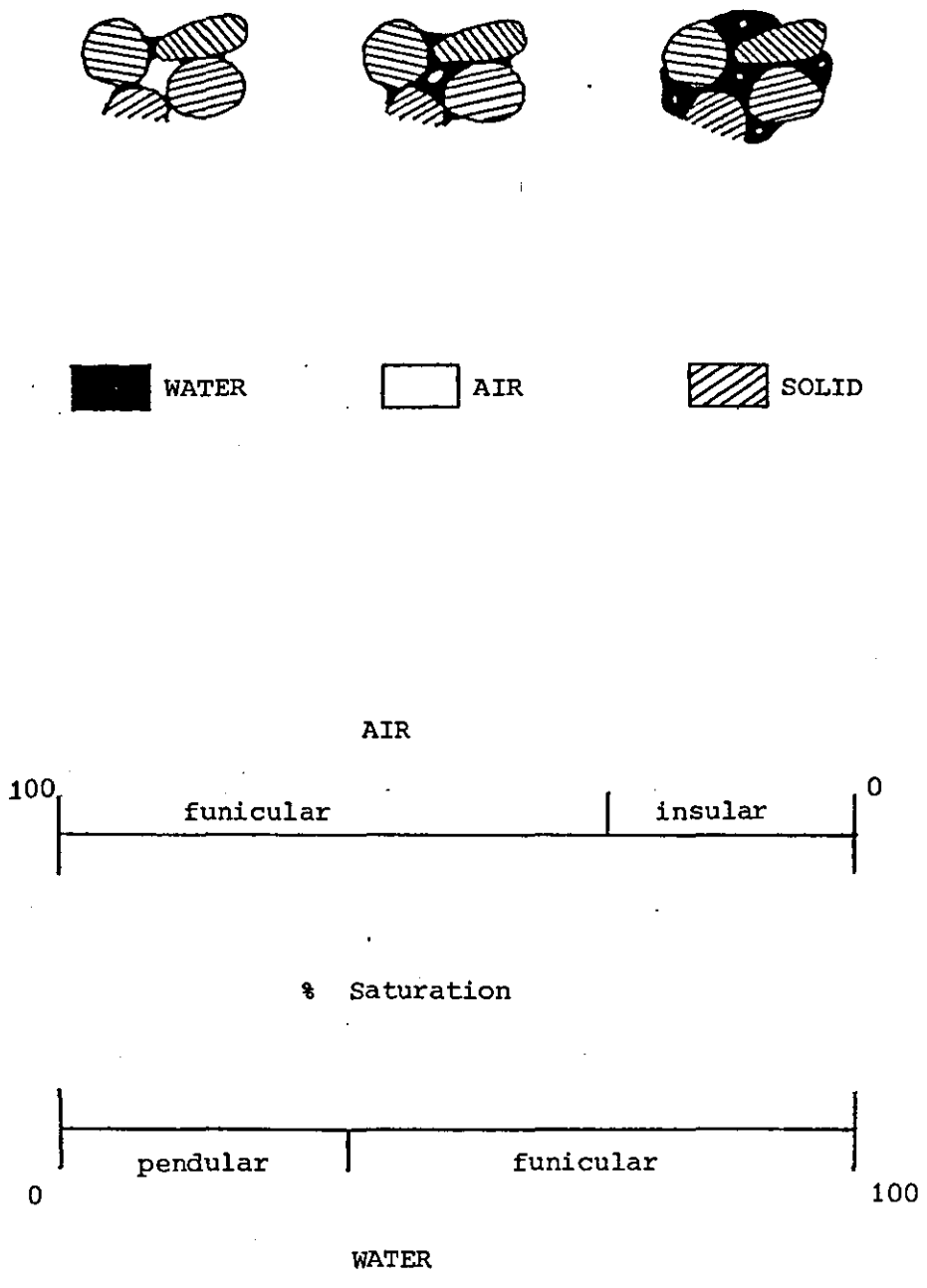

Fig. 9. Water-air saturation states.

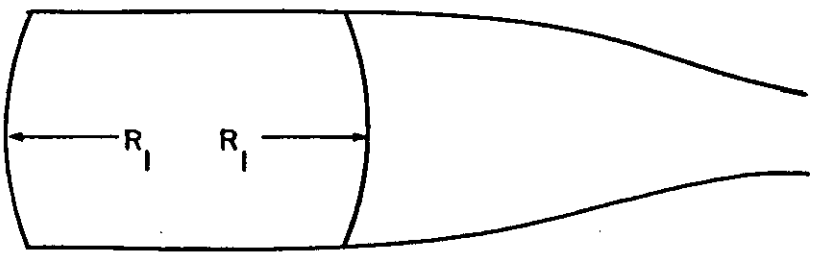

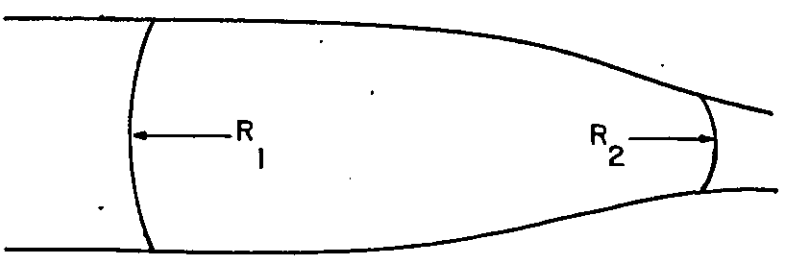

Fig. 10. Change in principal radii of curvature of a moving drop of fluid in a capillary tube of varying radius.

initially dry. At very low water saturations (Fig. 9a) the water forms immobile rings around the grain contact points; these rings are called pendular rings and have a doughnut shape, so to speak. If the saturation is very low, these rings do not touch one another nor do they communicate with each other, except perhaps through very thin films of water on the solid surface. As the water saturation is increased the size of the pendular rings also increases and finally at a sufficiently high fluid saturation they touch to form a continuous mesh of fluid. The saturation at which this transition takes place is termed the equilibrium to the wetting phase, i.e. the phase which preferentially adheres to the solid surface (Fig. 9b). Above the critical saturation, the wetting phase (water) offers a continuous but tortuous path to its movement under the application of a pressure gradient. This saturation state is called the funicular state.

As the saturation of the wetting fluid is increased further a situation develops when the non-wetting fluid (air) can no longer exist as a continuous phase, and it breaks into individual globules or bubbles. The transition is called the equilibrium saturation to the non-wetting phase. The non-wetting phase is now dispersed and said to be in a state of insular saturation. An insular globule of non-wetting fluid moves only by virtue of the differential pressure applied across it within a moving wetting fluid. These moving globules often become lodged in the necks of pores. In order for the globule to be displaced, the pressure difference across it must be sufficient to squeeze it through the capillary restriction, but such squeezing offers a large resistance, the so called Jamin effect.

For a circular capillary, the pressure change observed when the principal radius of curvature changes from R_1 to R_2 (Fig. 10) can be expressed as

$$\Delta P = 2\,\gamma_{LG}\left(\frac{1}{R_2} - \frac{1}{R_1}\right) \tag{21}$$

3.5 Saturation and capillary pressure

The void space of a porous material contains many sharp recesses. If the liquid saturation is increased, water preferentially collects in the recesses to form menisci. Further increases in liquid saturation cause the radii of curvature of the gas-liquid interfaces to alter, which consequently changes the pressure difference across the interface in accordance with equation (14).

Generally liquid menisci are concave towards the vapour phase in porous materials, hence the pressure in the liquid phase, just below the interface, is lower than the pressure in the gaseous phase. Assuming that the gaseous phase is at atmospheric pressure, the pressure in the liquid will always be less than atmospheric pressure until the material becomes fully saturated. The pressure in the liquid phase will steadily become less negative as the liquid saturation increases since the radii of curvature R_1, R_2 increase with liquid saturation (c.f. eqn. (14)).

The negative pressure difference is often called capillary suction, capillary tension, capillary potential or capillary pressure. The magnitude of the pressure difference is often related to the height to which a column of fluid will rise up a circular capillary.

Consider a capillary of radius, r, with the base of the capillary immersed in fluid (Fig. 11). The liquid meniscus is assumed to be concave to the vapour and consequently fluid is drawn up into the capillary. The equilibrium height, h_w, of the column of fluid is measured from the free water surface denoted by Q which is used as a datum. If the pressure at Q is P_0 and the pressure in the liquid just below the meniscus is P_1 the pressure

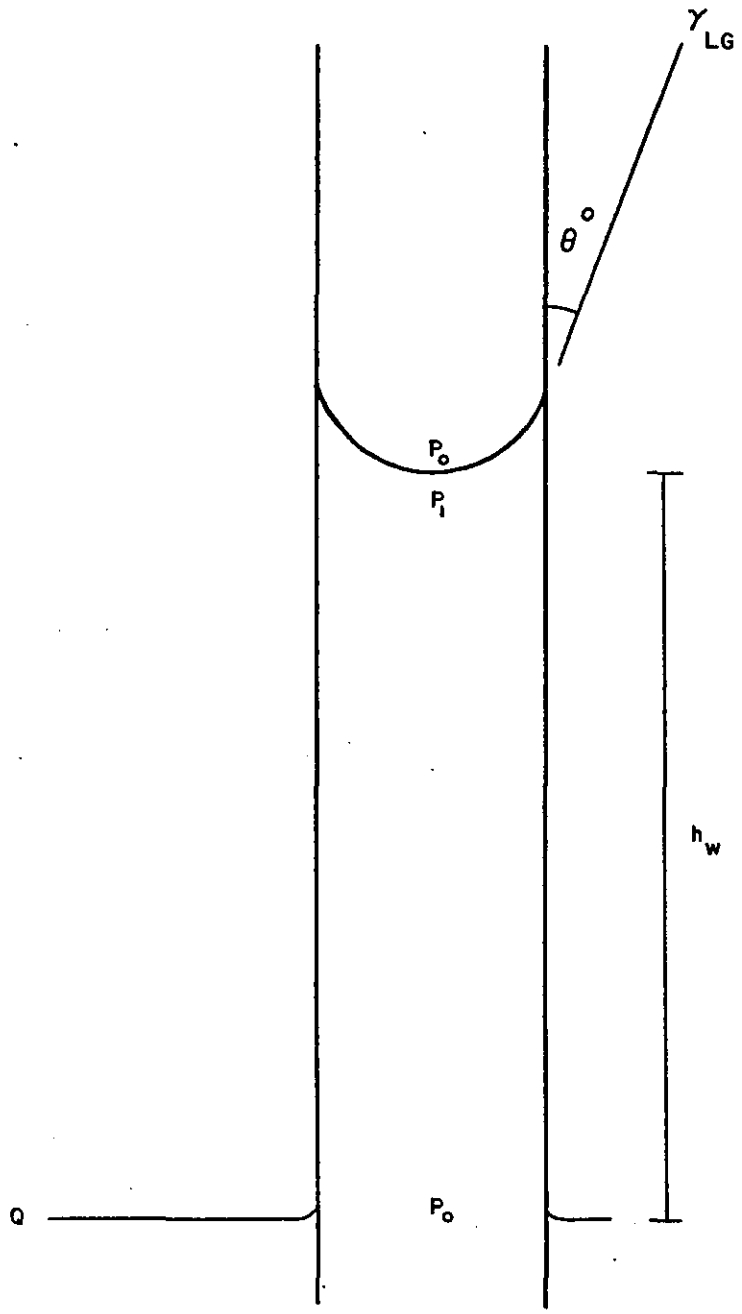

Fig. 11. Rise of fluid in a capillary tube. P_o is the atmospheric pressure; P_1, the pressure under the fluid meniscus; h_w, the height of the capillary rise; θ^o, the contact angle; and γ_{LG} the interfacial tension between the fluid and gaseous phase.

difference can be expressed by

$$\Delta P = P_0 - P_1 = \rho_L g h_w \tag{22}$$

Neglecting the small variation of the fluid vapour pressure and air pressure over the height, h_w, the total pressure above the meniscus can be taken as P_0 also. Using Laplace's equation (eqn.(14)), the pressure across the interface is given by

$$P_0 - P_1 = \frac{2 \gamma_{LG} \cos \theta^o}{r} \tag{23}$$

and combining eqns. (22) and (23) yields

$$\rho_L g h_w = \frac{2 \gamma_{LG} \cos \theta^o}{r} \tag{24}$$

The sign convention adopted in this work is that r is positive when concave to the vapour and increasing h_w is measured in an upward direction.

If the contact angle θ^o is less than 90° fluid will rise up the capillary and if θ^o is greater than 90° fluid will be depressed in the capillary. For θ^o exactly equal to 90° there is no difference in height between fluid in the capillary and the free water surface.

It is obviously apparent, although it has not been stated directly, that saturation (or moisture content) vs. capillary pressure curves may be determined for different porous materials. Similarly, because permeability of a given fluid phase is dependent upon the saturation of that phase (i.e. increasing the saturation provides a greater area for flow and a consequent increase in permeability) curves of permeability vs. capillary pressure can also be determined.

The fact capillary curves of many porous materials have several features in common has lead to attempts to devise some general equation to describe all such curves. Leverett[3] approached the problem from the standpoint of dimensional

analysis. Reasoning that the capillary pressure should depend upon porosity, ϕ; interfacial tension, γ_{SG} and on some sort of mean pore radius Leverett defined a dimensionless function which he called the j-function

$$j(S_w) = \frac{P_c}{\gamma_{SG}} \sqrt{\frac{k}{\phi}}$$

In the equation above the ratio of the permeability, k, to the porosity, ϕ, was taken as being representative of a mean pore radius.

Similarly the capillary pressure (or capillary potential), like the applied potential in Darcy's Law can either be expressed as energy per unit volume, unit mass or unit weight of fluid. The most common unit used to express the capillary potential is the height of a column of water (ergs per unit weight). It should be noted that the dimensions of capillary pressure in the Leverett j-function are energy per unit volume.

Between the limits of saturation, the capillary potential can change by a factor of more than 1 million (x 10^6) therefore the potential is commonly plotted on a logarithmic scale.

Schofield[4] was the first to express the capillary potential in terms of a logarithmic scale which he called the pF scale (analogous to the pH scale for expressing acidity or alkalinity of liquid solutions). The pF is defined as

$$pF = \log_{10} h_w \qquad (25)$$

where h_w is the height of a liquid column of unit density (usually water) which is equivalent to the capillary suction or capillary potential.

4.1 Hysteresis in porous materials

Another phenomenon associated with the interaction of fluids and porous materials is hysteresis. A process is said to exhibit

hysteresis if, when the direction of change of an independent variable x is reversed a dependent variable Y fails to retrace the values through which it passed in the forward process. An example of hysteresis is the absorption and desorption of a gas a porous material. The partial pressure of the gas is usually chosen as the independent variable (x) and the amount of material absorbed as the dependent variable (Y).

The absorption and desorption processes are normally brought about by altering the partial pressure of the gas, directly in the gaseous phase, or indirectly through the liquid phase. The two processes with liquid phase changes are imbibition (wetting, infiltration) and drainage (drying).

The partial pressure of the gas can be equated to the reduced vapour pressure of the gas above a curved phase interface (c.f. eqn.(14)), and hence the independent variable can be expressed in terms of the pF scale (eqns. (22)-(25)). Similarly the amount of material absorbed (dependent variable) can be expressed in terms of saturation (or moisture content).

Hysteresis of the hydraulic functions of porous materials has been attributed to a number of possible causes[5] including (i) contact angle dependence on whether the porous material is wetting or drying (ii) the geometry of the pore space and the associated possibility of multiple stable positions of a gas-liquid interface in such pores (iii) the effects of air (gas) entrapment and (iv) particle rearrangement in unconsolidated porous media.

The hydraulic functions of interest are hydraulic conductivity - moisture content, ($K(\theta)$); hydraulic conductivity - pressure head, ($K(h_w)$); and moisture content - pressure head, ($\theta(h_w)$). There is little doubt of the hysteretic nature of the

$\theta(h_w)$ function[(4)-(8)(10)(12)-(22)]; with further references in cited papers. The $K(h_w)$ function will also exhibit hysteresis[(9)(11)(14)(16)(17)] because of the interdependence of the $K(\theta)$ and $\theta(h_w)$ functions. The $K(\theta)$ function appears to be single valued[(17)(21)(22)] or exhibit very slight hysteresis[(11)(14)(18)].

4.2 Hysteresis terminology[(12)(13)(23)(24)]

The hysteresis envelope consists of a primary ascending curve, (or alternatively, a primary wetting curve) and a primary descending curve (sometimes called a primary drying curve) which together define the main loop (or boundary loop) (Fig. 12a). The boundary loop represents the extreme range of values over which hysteresis can occur. If the ascending or descending path along the boundary curve is reversed before the limit of the loop is reached, a new path is traversed. This new path is called a primary scanning curve (Fig. 12b,c). Similarly, if the path along the scanning curve is reversed before the limit of the boundary curve is reached, more new paths are traversed. These new paths are known as secondary scanning curves (Fig. 12d).

4.3 Domain concept

From a macroscopic viewpoint hysteresis curves are found to be smooth and continuous, although from a microscopic viewpoint the curves exhibit a series of discrete jumps, i.e. Haines Jumps. Normally hysteresis curves can be regarded as representing the macroscopic behaviour of the system. Thus it is reasonable to assume that the mechanism responsible for the hysteresis must occur at a microscopic level. The net behaviour of the whole system being governed by the average behaviour of a set of micro-systems (domains)[(24)-(29)].

In a porous material the interconnected pore space may be regarded as being sub divided into a series of voids which are connected to each other by smaller openings, usually called

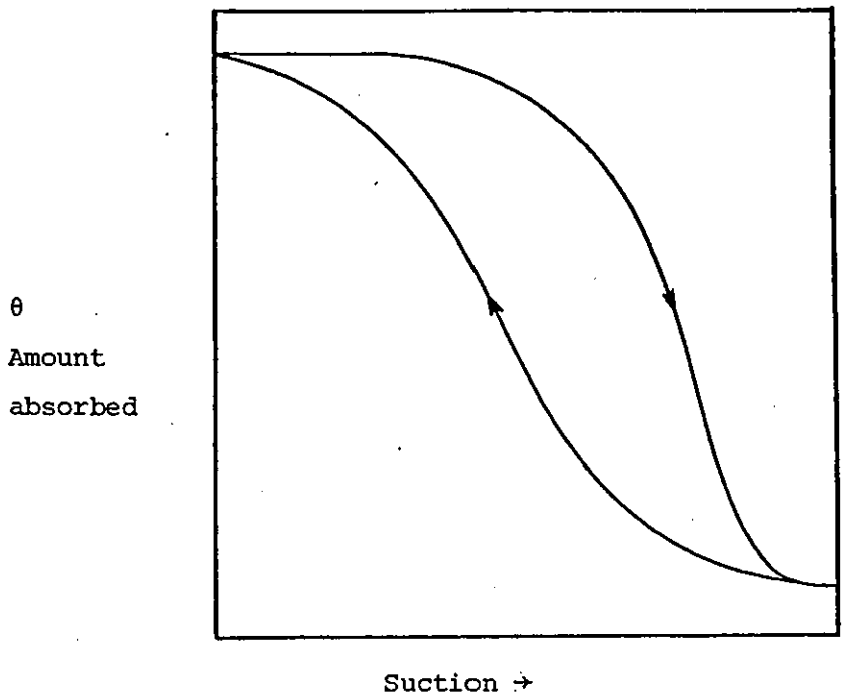

Fig. 12a. Primary ascending and descending curves.

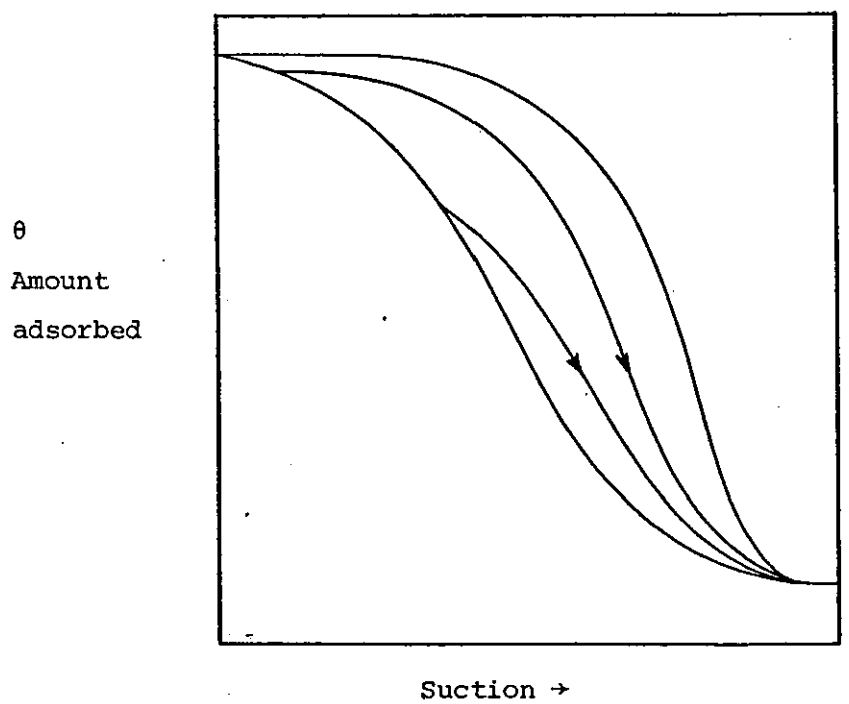

Fig. 12b. Primary descending scanning curves.

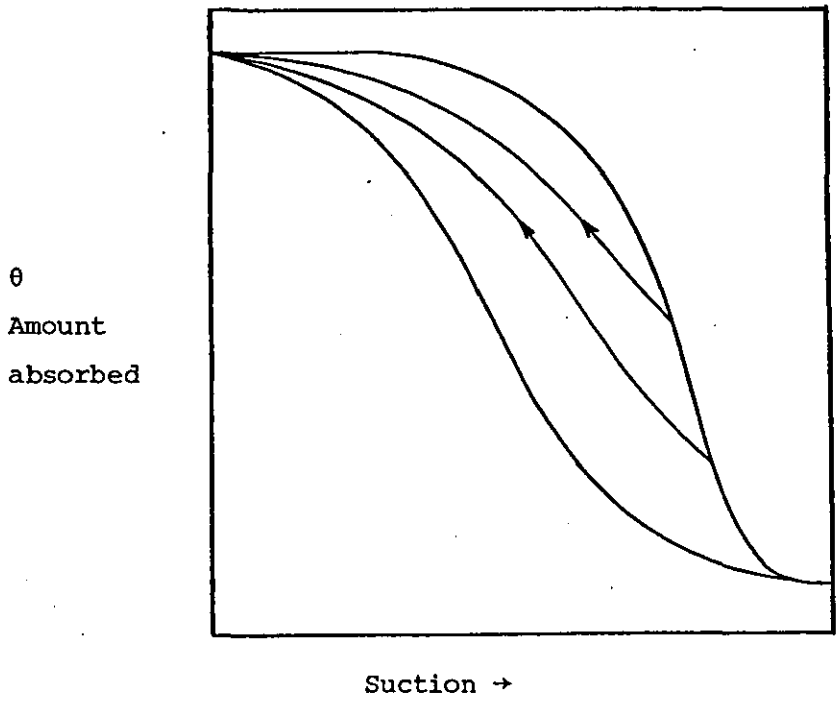

Fig. 12c. Primary ascending scanning curves.

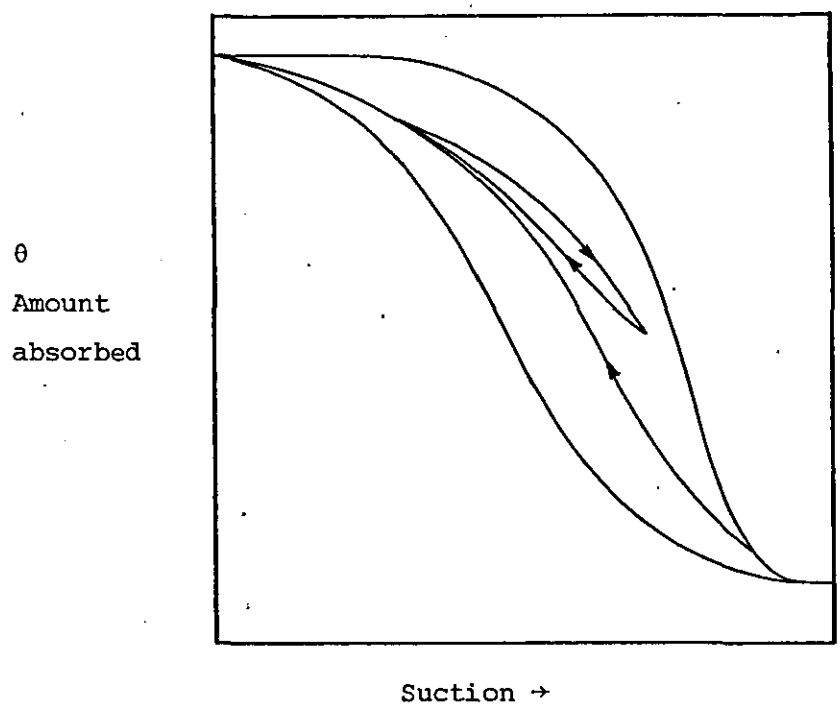

Fig. 12d. Secondary ascending and descending scanning curves.

windows. If the voids and windows vary in size, then for a small change in capillary potential only a small number of voids will empty or will fill up, with the result that the macroscopic response of the system to a change in capillary potential will appear to be smooth and continuous. In other words the overall behaviour of the system will be related to the size and number of both the voids and the interconnecting windows.

It is important to determine whether the domains act dependently or independently of each other. A typical example of independent domain behaviour is that of absorption of a vapour. The vapour is able to penetrate into every connected void, thus enabling each void to act independently of its neighbours, as the process of absorption proceeds.

The process related to absorption which occurs solely in the liquid phase is imbibition. The behaviour of the system is now critically dependent upon the movement of the vapour-liquid interface through the voids as liquid has to flow from one void to another. Obviously this process will be an example of dependent domain behaviour. Similarly desaturation via the liquid phase (drainage) will also exhibit dependent domain behaviour.

Desaturation through the gaseous phase is more complicated. Initially when the porous material is fully saturated, loss via the vapour phase can only occur at the periphery of the porous material. Increasing the capillary suction will cause some of the outer menisci to collapse and retract into the porous material. Further increases in capillary suction will cause more menisci to collapse, until the gaseous phase has access to all the voids. Thus the initial behaviour of the system is of the dependent kind, whereas the latter behaviour of the system can be

said to be of the independent kind.

The concept of independent domains developed to account for hysteresis generally has been shown by Poulovassilis[12] to be applicable to the hysteresis displayed by porous materials. However Topp and Miller[14] and Topp[17] stated that the independent domain model was inadequate to explain porous material hysteresis. Furthermore Poulovassilis and Childs[20] and Topp[19] indicated that the independent domain model was applicable to some porous materials but not to others.

The problem of whether hysteresis in porous building materials can be explained in terms of the independent domain model is of little consequence in comparison to the problem that arises from the fact that hysteresis is observed in the hydraulic functions. The great problem that arises is that hydraulic conductivity, K, which is a function of the fluid properties and fluid saturation, becomes dependent upon the previous wetting and drying history of the porous material. Also the moisture diffusivity, D_θ, will likewise be dependent upon the moisture history, since D_θ is proportional to K. For natural problems, i.e. Rising Damp, the previous wetting and drying history is not known. In addition when large areas of damp porous materials are considered, some regions may be drying whilst others may be becoming more saturated, which makes the accurate prediction of the moisture flows very difficult if not impossible.

Furthermore in the application of the domain concept it is assumed that there are no permanent intrinsic changes within the porous material. With respect to Rising Damp, changes in intrinsic permeability can occur because of salt crystallisation, i.e. either by simple precipitation of salts blocking the pores, or by

salt pressure (or ice pressure as caused by frost action) bursting the framework of the porous matrix. Alternatively intrinsic changes may occur because of dissolution of soluble constituents of the matrix through leaching. Both efflorescence and leaching will restrict the application and use of the domain concept.

List of symbols and units of Chapter Two

A	area for flow (cm^2)
$(\Delta A)_{net}$	total change of area (cm^2)
D_θ	moisture diffusivity of a porous material ($cm^2\ sec^{-1}$)
Δf_A	free energy change per unit area of surface ($g\ sec^{-2}$)
$(\Delta f)_{net}$	total free energy change ($g\ cm^2\ sec^{-2}$)
Δf	free energy change per gram of fluid ($cm^2\ sec^{-2}$)
g	gravitational acceleration ($cm\ sec^{-2}$)
h_w	height of a column of fluid; pressure head of a column of fluid (cm)
J_v	macroscopic velocity of fluid ($cm\ sec^{-1}$)
K	Hydraulic conductivity; Darcy coefficient of a porous material ($cm\ sec^{-1}$)
k	permeability to fluid of a porous material (cm^2)
P	pressure ($g\ cm^{-1}\ sec^{-2}$)
P_c	capillary pressure ($g\ cm^{-1}\ sec^{-2}$)
Q	volumetric flowrate of fluid ($cm^3\ sec^{-1}$)
R	principal radius of curvature of a fluid meniscus (cm)
R_1, R_2	principal radii of curvature of a fluid, measured perpendicularly to each other (cm)
r	radius of a capillary (cm)
S_w	fractional or percentage saturation of fluid W
s	entropy per gram of fluid ($cm^2\ sec^{-2}\ {}^oK^{-1}$)
T	temperature (^oC, ^oK)
W_m	all mechanical work per gram of fluid excluding that of expansion of a gas against a pressure P
W_{LL}	work of cohesion, defined as the amount of work required to separate unit area of surface of the same liquid, L, to create new fluid interfaces ($g\ sec^{-2}$)

W_{L1L2} work of adhesion, defined as the amount of work required to separate unit area of interface between two liquids L1, L2 to create new fluid interfaces (g sec^{-2})

W_{SL} work of adhesion between a solid, S, and liquid, L,. It isdefined as the amount of work required to separate unit area of interface between a solid and a liquid to create new fluid interfaces (g sec^{-2})

γ interfacial or surface tension, where subscripts S, L, G refer to the solid, liquid and gaseous phases respectively comprising the fluid interface (g sec^{-2})

γ' interfacial or surface tension of miscible systems where the subscripts S, L, G refer to the solid, liquid, and gaseous phases respectively comprising the fluid interface (g sec^{-2})

θ moisture content of a porous material

θ^o fluid contact angle

θ_A^o, θ_R^o advancing and receding fluid contact angles respectively

μ fluid viscosity (g cm^{-1} sec^{-1})

ρ_L density of the fluid in the liquid phase (g cm^{-3})

υ specific volume of the fluid (cm^3 g^{-1})

Φ generalised pressure potential

ϕ porosity of a porous material

ω a factor defined as the sum of the reciprocals of the principal radii of curvature, i.e.

$$\omega = \left(\frac{1}{R_1} + \frac{1}{R_2}\right) \quad (cm^{-1})$$

References Chapter Two

cited references

(1) "Physical surfaces", J.J. Bikerman, Academic Press N.Y., 1970, p.253

(2) "Physical surfaces", J.J. Bikerman, Academic Press N.Y., 1970, p.240

(3) "Flow of fluids through porous materials", R.E. Collins, Rheinhold Publ. Co. N.Y., 1961, p.31

(4) "The pF of water in soils", R.K. Schofield, Trans. of the 3rd Int. Congr. Soil Sci., No. 2, pp.37-48, 1935

(5) "Soil water theory and its application in field situations", A. Klute, Soil. Sci. Soc. Am. Special Publ., No. 5, pp.9-35, 1973

(6) "Capillary conduction of liquids through porous mediums", L.A. Richards, Physics, 1, pp.318-333, 1931

(7) "Water conduction from shallow water tables", R.E. Moore, Hilgardia, 12, No. 6, pp.383-426, 1939

(8) "Uptake and retention of water by soil as determined by distance to a water table", L.A. Richards, Jnl. of Am. Soc. of Agronomy, 33, pp.778-786, 1941

(9) "Permeability-capillary potential curves for three prairie soils", H.R. Christensen, Soil Sci., 57, pp.381-390, 1944

(10) "Movement and distribution of water in soil in relation to highway design and performance", D. Croney, J.D. Coleman, W.P.M. Black, Highway Research Board, Special report No. 40, pp.226-252, 1958

(11) "Measuring capillary conductivity", D.R. Nielsen, J.W. Biggar, Soil Sci., 92, pp.192-193, 1961

(12) "Hysteresis of pore water, an application of the concept of independent domains", A. Poulovassilis, Soil Sci., 93 No. 6, pp.405-412, 1962

(13) "Capillary equilibrium in porous materials", N.R. Morrow, C.C. Harris, Jnl. of Soc. Pet. Eng., 5, pp.15-24, 1965

(14) "Hysteretic moisture characteristics and hydraulic conductivities for glass-bead media", G.C. Topp, E.E. Miller, Soil Sci. Soc. Amer. Proc., 30, pp.156-162, 1966

(15) "Intermittent infiltration into soils with hysteresis", H.A. Ibrahim, W. Brutsaert, Jnl. of Hydraulics Divn., Proc. Am. Soc. Civ. Eng., No. HY1, pp.113-137, 1968

(16) "The mechanism of natural ground-water recharge and discharge", R.A. Freeze, Water Resou. Res., 5, No. 1, pp.153-171, 1969

(17) "Soil water hysteresis measured in a sandy loam and compared with the hysteretic domain model", G.C. Topp, Soil Sci. Soc. Amer. Proc., 33, pp.645-651, 1969

(18) "The effect of hysteresis of pore-water on the hydraulic conductivity", A. Poulovassilis, Jnl. of Soil Science, 20, No. 1, pp.52-56, 1969

(19) "Soil water hysteresis. The domain theory extended to pore interaction conditions", G.C. Topp, Soil Sci. Soc. Amer. Proc., 35, pp.219-225, 1971.

(20) "The hysteresis of pore water: the non-independence of domains", A. Poulovassilis, E.C. Childs, Soil Sci., 112, pp.301-312, 1971

(21) "The hydraulic conductivity-water content relationship during non steady flow through a sand column", J.S. Rogers, A. Klute, Soil Sci. Soc. Amer. Proc., 35, pp.695-700, 1971

(22) "Influence of hysteresis on moisture flow in an undisturbed soil monolith", F. Beese, R.R. van der Ploeg, Soil Sci. Soc. Am. Jnl., 40, pp.480-484, 1976

(23) "Hydraulic properties of a porous medium: measurement and empirical representation", R.W. Gillham, A. Klute, D.F. Heermann, Soil Sci. Soc. Am. Jnl., 40, No. 2, pp.203-207, 1976

(24) "A general approach to hysteresis. Part 2", D.H. Everett, F.W. Smith, Trans. of Farad. Soc., 50, pp.187-197, 1954

(25) "A general approach to hysteresis. Part 1", D.H. Everett, W.I. Whitton, Trans. of Farad. Soc., 48, pp.749-757, 1952

(26) "A general approach to hysteresis, Part 3", D.H. Everett, Trans. of Farad. Soc., 50, pp.1077-1096, 1954

(27) "A general approach to hysteresis, Part 4", D.H. Everett, Trans. of Farad. Soc., 51, pp.1551-1557, 1955

(28) "The domain model of hysteresis, Part 1", J.A. Enderby, Trans. of Faraday Soc., 51, pp.835-848, 1955

(29) "The domain model of hysteresis, Part 2", J.A. Enderby, Trans. of Farad. Soc., 52, pp.106-120, 1956

General References

Section 2

(30) "Physical Surfaces", J.J. Bikerman, Academic Press, 1970

(31) "Interfacial phenomena", J.T. Davies, E.K. Rideal, Academic Press, 2nd Ed. 1963

(32) "Physical chemistry of surfaces", A.W. Adamson, Interscience Publishers, 1960

(33) "Surface tension and adsorption", R. Defay, I. Prigogine, A. Bellemans, D.H. Everett, Longmans Green & Co. Ltd., 1966

(34) "Review of some elements of soil moisture theory", I. Rempson, J.R. Randolph, Geolog. Survey Profess. paper No. 411-D, 39 pages, 1962

(35) "Principles of penetration of liquids into solids", N.K. Adam, Discussions of Farad. Soc., No. 3, pp.5-11, 1948

(36) "Dynamics of fluids in porous media", J. Bear, Am. Elsevier Publ. Co. inc., 1972

(37) "Some fundamental aspects of liquid distribution in porous solids related to interfacial characteristics", F. De Bisschop, F. De Wulf, I.F.I.P. Working Conf., Computer Simulation of Water Resources Systems, Ghent, Belgium, July 30 - Aug 2, 1974, Publ. North Holland Publ. Co., Amsterdam

Section 3

(38) "The physics of flow through porous medium", A.E. Scheidegger, Univ. of Toronto press, revised 2nd Ed. 1963

(39) "Flow of fluids through porous materials", R.E. Collins, Rheinhold Publ. Corp. New York, 1961

(40) "Dynamics of flow in porous media", J. Bear, Am. Elsevier Publ. Co. inc., 1972

(41) "Oil reservoir engineering", S.J. Pirson, McGraw Hill Book Co. Inc.

(42) "The energy concept of soil moisture and mechanics of unsaturated flow", M.B. Russel, M.G. Spangler, Proc. 21st Am. Meeting Highway Research Board, pp.435-450, 1941

(43) "The movement of water in unsaturated soils", J.W. Holmes, Proc. of 1st Australia-New Zealand, Conf. on soil mech. and foundation eng., pp.1-9, 1952

Section 4

(44) "The solid-gas interface", Ed. E.A. Flood, Edward Arnold (Publishers) Ltd., London, Vol. 2, 1967

(45) "On the existence of two equilibrium series in soil capillary phenomena", W.B. Haines, Proc. and papers of the 2nd Int. Congress of Soil Science, Russia, 1930

(46) "Studies in physical propeties of soils, IV", W.B. Haines, Jnl. of Agric. Sci., 17, pp.264-290, 1927

(47) "Studies in physical properties of soils, V", W.B. Haines, Jnl. of Agric. Sci., 20, pp.97-116, 1930

(48) "Studies in physical properties of soils, VI", W.B. Haines, Jnl. of Agric. Sci., 20, p.283 1930

(49) "The drying of granular solids", N.H. Ceaglske, O.A. Hougen, Trans. Am. Inst. Chem. Eng., 33, pp.283-314, 1937

CHAPTER THREE

EQUATION OF MOTION OF MOISTURE IN AN UNSATURATED POROUS MATERIAL

1. Introduction

The equation of motion describes the movement of moisture within saturated and unsaturated porous materials. The equation was developed from the fundamental Navier-Stokes expression and expanded into a series of diffusivity type expressions, which were initially proposed by Philip[1]. Diffusivity type coefficients were derived for moisture flow in both the liquid and vapour phase, when influenced by gradients of pressure, temperature, electricity and solute concentration. The free energy gradients associated with each of these potential gradients are investigated. To conclude this chapter the influence of various factors upon the magnitude of the diffusivity type coefficients is also examined.

2. The Navier-Stokes equation

The flow of a fluid is described by the Navier-Stokes equation, which relates the viscous, inertial, body and pressure forces involved in the flow process and is usually written[2][3]

$$\frac{D\underline{u}}{Dt} = \frac{\partial \underline{u}}{\partial t} + (\underline{u}\cdot\nabla)\underline{u}$$

$$= -\nabla F' - \frac{\nabla P}{\rho} + \frac{\mu}{\rho}\left(\frac{1}{3}\nabla(\nabla\cdot\underline{u}) + \nabla^2 u\right) \qquad (1)$$

where ρ is the fluid density; μ, the fluid viscosity; $\underline{u}$, the linear fluid velocity vector; F', the body forces per unit mass of fluid (e.g. gravity); P, the pressure. The first term on the right includes all body forces, the second term represents forces associated with the pressure potential, the remainder of the terms on the right hand side represent viscous forces.

For an incompressible fluid, $(\nabla\cdot\underline{u}) = 0$, and the Navier-Stokes equation is reduced to

$$\frac{D\underline{u}}{Dt} = \frac{\partial \underline{u}}{\partial t} + (\underline{u}\cdot\nabla)\underline{u} = -\nabla F' - \frac{\nabla P}{\rho} + \left(\frac{\mu}{\rho}\right)(\nabla^2 u) \qquad (2)$$

Furthermore for slow steady flow; and combining the pressure and body forces which are now represented by a general potential Φ, equation (2) may be expressed as

$$\nabla\Phi = \frac{\mu}{\rho}(\nabla^2 u) \tag{3}$$

Differentiating eqn.(3) with respect to direction gives

$$\nabla^2\Phi = \frac{\mu}{\rho}\left(\frac{\partial^2}{\partial x^2} + \frac{\partial^2}{\partial y^2} + \frac{\partial^2}{\partial z^2}\right)\left(\frac{\partial u}{\partial x} + \frac{\partial v}{\partial y} + \frac{\partial w}{\partial z}\right) \tag{4}$$

where the operator $\nabla^2 = \left(\frac{\partial^2}{\partial x^2} + \frac{\partial^2}{\partial y^2} + \frac{\partial^2}{\partial z^2}\right)$ and u, v, w are the respective fluid velocities in the x, y, z directions of a set of orthogonal axes. In complete vector form eqn.(4) is written

$$\nabla^2\Phi = \frac{\mu}{\rho}\nabla^2(\nabla\cdot\underline{u}) \tag{5}$$

but for an incompressible fluid, the div of a velocity vector, $(\nabla\cdot\underline{u})$, is equal to zero, hence

$$\nabla^2\Phi = 0 \tag{6}$$

Generally the velocity of fluid flowing through a porous material is small, and the passages in which the fluid flows are also small. Assuming that the magnitude of the inertial terms, $(\underline{u}\cdot\nabla)\underline{u}$, are small in comparison to the viscous terms and that there is steady flow of an incompressible, (constant density), fluid then the mass flow is given by equation (6).

Most treatments of flow in porous media are based upon Poiseuille's Law and Darcy's Law. It is of some interest to consider these laws and interpret them in relation to the Navier-Stokes equation.

3. Poiseuille's Law

Poiseuille's Law for steady laminar flow of a fluid in a straight cylindrical pipe is

$$Jv = -\frac{r^2\rho}{8\mu}\frac{d\Phi}{dx} \tag{7}$$

where Jv, the mean flow velocity; r, the radius of the pipe; $d\Phi/dx$, the potential gradient in terms of energy per unit mass of fluid.

4. Darcy's Law

For steady linear flow of an incompressible fluid through a porous material, Darcy's Law is expressed as

$$Jv = -\frac{k\rho}{\mu} \nabla\Phi \qquad (8)$$

where Jv, the mean flow velocity; k, the permeability to the fluid; $\nabla\Phi$, the potential gradient expressed in terms of energy per unit mass of fluid. Jv, Φ are averages over regions whose dimensions are large compared with those of the individual pores.

Differentiating the velocity terms (Jv) of equations (7) and (8) with respect to distance, leads to the Laplacian equation described by equation (6).

Equation (7) refers to an exactly linear flow in a special and precise geometry, whereas equation (8) applies to conditionally linear flows (inertial terms very small) in a generally unknown geometry exhibiting certain statistical regularities, but both state that a macroscopic flow velocity is proportional to a macroscopic potential gradient. For laminar flow in a cylindrical tube, a parcel of fluid possesses a constant linear velocity throughout, whilst in the porous medium the magnitude and direction of the velocity change continuously. The failure of linearity of the two systems is expressed by a critical Reynolds number, which, relates the inertial forces to the viscous forces.

For flow in straight cylindrical pipes, Reynolds number N_{Re} is defined as[4]

$$N_{Re} = \frac{d\ u\ \rho}{\mu} \qquad (9)$$

where d, the pipe diameter; u, the macroscopic mean fluid velocity

of the pipe; μ, the fluid viscosity; ρ, the fluid density.

The critical Reynolds number for laminar flow in pipes has been found experimentally to be in the neighbourhood of 2200.

Similarly a Reynolds number for flow in porous materials can also be defined[5)-(11)]. The characteristic length is now taken as the square root of the permeability instead of the pipe diameter; hence

$$N_{Re_k} = \frac{\sqrt{k}\ u\ \rho}{\mu} \tag{10}$$

where k is the permeability to fluid and has the dimensions of length squared.

The critical Reynolds number for flow in porous media has been experimentally found to be in the neighbourhood of 0.1. By substituting the permeability Reynolds number, N_{Re_k}, into Darcy's Law, another dimensionless group, the permability friction factor is defined

$$N_{f_k} = \frac{1}{N_{Re_k}} = \frac{\sqrt{k}}{u^2} \nabla\Phi \tag{11}$$

where N_{f_k}, the permeability friction factor group; $\nabla\Phi$, the potential gradient per gram of fluid.

The laminar flow of fluid along a cylindrical pipe is restricted in the sense that fluid flow is parallel to the axes of the cylinder whereas flow through porous media can take place in all directions. If the permeability (or hydraulic conductivity) varies with direction, the porous material is said to be anistropic, and the permeability (hydraulic conductivity) variation is expressed by a symmetrical second order tensor[11)]. In the simpler case where the permeability is independent of direction, the material is said to be isotropic and the permeability (hydraulic conductivity) is a scalar quantity only. For the sake of

simplicity, it is assumed that the permeabilities (hydraulic conductivities) of porous building materials are isotropic.

5. The principles of moisture movement in unsaturated porous materials

The flow of fluid through a fully saturated porous material is described by Darcy's Law (eqn.(8)). The permeability to fluid, k, of the porous material is normally regarded as being a constant. However for flow through an unsaturated porous material the permeability is no longer constant. As the fluid saturation of a partially saturated medium is reduced, the area for fluid flow is correspondingly reduced, with a consequent reduction in the value of the permeability. Darcy's Law for an unsaturated porous material can be written as

$$Jv = - K'(\theta)\ \nabla\Phi \qquad (12)$$

where Jv, the macroscopic fluid velocity; $K'(\theta)$, the Darcy coefficient which is now a function of the volumetric moisture content, θ; Φ, the potential which for present purposes is composed of only the pressure and gravitational potentials.

In addition to the law of motion, i.e. Darcy's Law, the flow of fluid must obey the principle of conservation of matter. This, for free space, is usually expressed as "the net excess of mass flux per unit time, into or out of any infinitesimal volume element in the fluid, is equal to the rate of change of fluid density with respect to time in the volume element multiplied by the free volume of the element". Mathematically the above statement can be expressed as

$$\frac{\partial\rho}{\partial t} = - \nabla\cdot(\rho\underline{u}) \qquad (13)$$

where ρ is the fluid density and $\underline{u}$, the fluid velocity vector.

For flow within porous materials eqn.(13) must be modified to allow for the fact that not all the space in the elementary

volume is available for fluid flow. For isothermal fluid flow through an unsaturated porous material, eqn.(13) is modified to yield[12][13]

$$\frac{\partial \rho_B}{\partial t} = -\nabla \cdot (\rho \underline{u}) \tag{14}$$

where ρ_B is the bulk density of the volume element including both the mass of solid matrix and the mass of fluid.

If the liquid density is assumed to be constant, eqn.(14) can be reduced to

$$\frac{\partial \theta}{\partial t} = -\nabla \cdot \underline{u} \tag{15}$$

where θ, the volumetric moisture content (i.e. cm^3 of fluid per cm^3 of pore matrix inclusive of the void space).

Combining equation (15) with equation (12) noting that Jv is equivalent to $\underline{u}$

$$\frac{\partial \theta}{\partial t} = \nabla \cdot K' \nabla \Phi \tag{16}$$

If the potential, Φ, is expressed as energy per unit weight of fluid (i.e. dimensions of length) then K' becomes equal to the hydraulic conductivity, K, which has dimensions of velocity ($L\ T^{-1}$). Usually the potential Φ is expanded into the form $\Phi = \psi + h_w$ (where h_w is taken as positive in an upwards direction) to allow for the gravitational potential in the vertical, h_w, direction. ψ, which also has dimensions of length, is limited to the pressure potential only and has the same numerical value as Φ in the x, y directions. Hence equation (16) can be expanded to yield

$$\frac{\partial \theta}{\partial t} = \nabla \cdot K \nabla \psi + \frac{\partial K}{\partial z} \tag{17}$$

Alternatively eqn.(17) can be expressed in terms of the volumetric moisture potential[1][3][14]-[21]

$$\frac{\partial\theta}{\partial t} = \nabla\cdot D_{\theta L}\nabla\theta + \frac{\partial K}{\partial z} \tag{18}$$

where $D_{\theta L}$ (= $K\ \partial\psi/\partial\theta$), the liquid moisture diffusivity at constant temperature and θ, the volumetric moisture content.

Similarly for isothermal polyphase flow of moisture, it can be shown[1]

$$\frac{\partial\theta}{\partial t} = \nabla\cdot(D_{\theta L} + D_{\theta V} + D_{\theta A})\nabla\theta + \frac{\partial K}{\partial z} \tag{19}$$

where D_θ refers to moisture diffusivity and the other subscripts, L, V, A refer to liquid, vapour and adsorbed phase fluid flow.

Diffusivity type expressions have also been derived[22]-[24] for thermally driven flow, which when combined with eqn.(19) yield

$$\frac{\partial\theta}{\partial t} = \nabla\cdot(D_\theta\nabla\theta) + \nabla\cdot(D_T\nabla T) + \frac{\partial K}{\partial z} \tag{20}$$

where D_T is the net thermal diffusivity, and it represents the sum of the thermal flow coefficients in the liquid, vapour and adsorbed phases. Discussion of the applicability and limitations of eqns. (19) and (20) can be found elsewhere[1][3][17][18][20].

In addition to pressure and temperature potentials, solute and electrical potentials also induce moisture to move through a porous material; the next flux of water may be expressed as

$$Jv = -K_P(\nabla f)_P - K_T(\nabla f)_T - K_C(\nabla f)_C - K_E(\nabla f)_E \tag{21}$$

where Jv is the macroscopic mean fluid velocity; (∇f), the free energy potential gradient and the subscripts (P, T, C, E) refer to the free energy gradients produced by pressure, temperature, solute and electrical potential differences. Note that the gravity potential has been combined with the pressure potential and the free energy gradient can be expressed as energy per unit volume, unit mass and unit weight or even per mole of fluid. K_P, K_T, K_C and K_E are the coefficients that relate the flux of moisture to the corresponding potential gradient. It is assumed that the moisture flux is linearly related to the respective free energy

potential gradients. Combining eqn.(21) with eqn.(15) leads to

$$\frac{\partial\theta}{\partial t} = \nabla\cdot\left[K_P(\nabla f)_P + K_T(\nabla f)_T + K_C(\nabla f)_C + K_E(\nabla f)_E\right] \quad (22)$$

Eqn.(22) can be re-arranged into the more familiar diffusion type equation, where the individual diffusivities are defined by

$$K_\alpha(\nabla f)_\alpha \simeq K_\alpha\frac{\partial f}{\partial\alpha}\nabla_\alpha = D_\alpha\nabla_\alpha$$

$$= (D_{\alpha L} + D_{\alpha V} + D_{\alpha A})\ \nabla_\alpha \quad (23)$$

D_α is the net diffusivity corresponding to the potential α, and it is the sum of the diffusivities of the liquid, vapour and adsorbed phases.

Equation (22) expressed in diffusivity form

$$\frac{\partial\theta}{\partial t} = \left[\nabla\cdot D_\theta\nabla\theta + \frac{\partial K}{\partial z}\right] + \nabla\cdot\ (D_T\nabla T - D_C\nabla\pi + D_E\nabla E) \quad (24)$$

Note the terms in square brackets represent the separated potentials of pressure and gravity.

Equations (22) and (24) are expressions that describe movement of moisture due to free energy gradients of pressure, temperature, concentration and electricity. The net diffusivity associated with each potential is the sum of the diffusivities of the liquid, vapour, and adsorbed phases. However the adsorbed phase may be considered as an extension of the liquid phase, but with physical properties that are different to those observed in the bulk solution. Furthermore these same physical properties are no longer constant but vary in relation to their distance measured from the solid surface.

For the sake of simplicity, flow in the adsorbed phase will be assumed to be an extension of flow in the liquid phase, and as such will not be discussed as a separate flow. Combination of the adsorbed flux and the liquid phase flux is justified on the basis that adsorbed phase flow will only be significant for very dry porous materials of high internal surface area and noting that

in relation to Rising Damp, the main problem is that of excess moisture and hence the magnitude of the adsorbed flux is likely to be small in comparison to the liquid phase flux.

Theories relating to adsorbed phase flow have been developed by Philip[1] and Babbitt[25]. Flow in thin films near solid surfaces has been examined both theoretically and experimentally from a macroscopic standpoint in a series of papers by Kemper[26]-[29]. Kemper treated the adsorbed phase as an extension of the liquid phase but with physical properties different to the bulk solution.

Transport of moisture can either be classified as convective or diffusive in character, and that both types of transport can occur in any of the phases. Convective transport is opposed by viscous forces and driven by mechanical forces, i.e. gravity, pressure. Diffusive transport of moisture may be considered as due to a gradient of thermodynamic potential, i.e. osmotic free energy. Klute[20] stated that additional contributions to the moisture flux could occur because of deformation of the solid matrix. However for rigid materials, as are most building materials, these contributions will be non existent.

Determination of the magnitudes of individual diffusivities is difficult owing to the interference and interaction of the various potentials upon the proportionality coefficients, upon the solid-liquid interaction and upon each other. Before discussing the interacting effects of the potentials and coefficients, it is necessary to define the free energy of moisture in an unsaturated porous material.

6. Free energy per unit mass of moisture in an unsaturated porous material[30]

The absolute free energy of a system has been defined as[30]

$$f = U + P\upsilon - Ts \qquad (25)$$

where U, the internal energy of the fluid (sum of the internal

kinetic and potential energies); P, the pressure; υ, the specific volume per gram of fluid; T, the absolute temperature; s, the entropy per gram of fluid.

f is an arbitrary chosen function, useful because of its property that at equilibrium, df = 0, for all possible infinitesimal changes.

For a reversible process the change in free energy, df, may be expressed as

$$df = dU + Pd\upsilon + \upsilon dP - Tds - sdT \tag{26}$$

From the 1st Law of Thermodynamics

$$dU = dq - dW = Tds - dW \tag{27}$$

where dq (= Tds) is the heat energy change of the process; dW, the total amount of work. Note dW can be defined as $Pd\upsilon + dW_m$ where dW_m represents all mechanical work excluding that of expansion of a gas against a pressure P.

Combining eqns. (26) and (27) yields

$$df = \upsilon dP - sdT - dW_m \tag{28}$$

For isothermal changes

$$df = \upsilon dP - dW_m \tag{29}$$

and if the pressure also remains constant

$$-df = dW_m \tag{30}$$

Equation (30) states that the decrease of free energy equals the work performed (excluding that of expansion against constant pressure) by the system. However with irreversible processes some of the work will appear as heat, and hence

$$df = -d'W_m - dW_{heat}$$

i.e. $-df > d'W_m$.

For irreversible (finite) changes the decrease in free energy is a measure of the maximum work dW_m that can be performed by the

system at constant temperature and pressure on its surroundings. If water is removed from a porous material, the free energy decreases as a consequence of the work done. If $f_{free\ water}$ is chosen as a datum such that $f_{free\ water}$ was equal to zero then the free energy changes of water in a porous material is always less than zero (c.f. term capillary suction). A more useful expression therefore is the free energy relative to free pure water, f_o, where in finite difference form, the free energy difference is expressed by

$$\Delta f = \upsilon\Delta P - s\Delta T - \Delta W_m \tag{31}$$

6.1 Effect of pressure on free energy

From equation (31) and for isothermal changes where no mechanical work is performed, and in the absence of soluble salts

$$\Delta f = f_B - f_A = \int_A^B \upsilon dP \tag{32}$$

For incompressible fluids, i.e. liquid, where the specific volume, υ, is almost independent of pressure

$$\Delta f = \upsilon \int_A^B dP = \upsilon\Delta P \tag{33}$$

and noting, that for water, in the c.g.s. system of units, υ_L is approximately unity.

With gases (compressible fluids) and assuming the gases to be ideal, i.e. $P\upsilon_G = RT$, where R is the universal gas constant per gram of gas then

$$\Delta f = \int_A^B \upsilon_G\, dP = \int_A^B RT \frac{dP}{P} = RT \ln \frac{P_B}{P_A}$$

as R, T are constant. With vapours, and assuming them to be ideal, the expression may be written thus,

$$\Delta f = RT \ln \frac{p}{p_o} \tag{34}$$

where p is the vapour pressure of the liquid (water) in the porous material and p_o is the vapour pressure of free pure liquid (water)

at the same temperature. Note that (p/p_o) may be taken as the relative humidity of vapour above the porous material.

For a liquid and vapour in equilibrium with each other, combining eqns. (33) and (34)

$$\upsilon_L \Delta P = RT \ln \frac{p}{p_o}$$

which for water ($\upsilon_L \simeq 1$)

$$\Delta P = RT \ln \frac{p}{p_o} \tag{35}$$

Equation (34) can be used to derive the effect of surface tension and radius of curvature of the air-water interface upon the vapour pressure and free energy of porous material moisture[15], i.e.

$$-\ln \frac{p}{p_o} = \frac{1}{\rho_L RT} \left[\gamma_{LG} \left(\frac{1}{R_1} + \frac{1}{R_2} \right) - (p - p_o) \right] \tag{36}$$

Noting that υ_L is equal to $(1/\rho_L)$, and that if the principal radii of curvature are the same $R_1 = R_2 = r$ and that the variation of vapour pressure with height is small ($(p - p_o) \simeq 0$) then

$$\ln \frac{p}{p_o} = -\left(\frac{\upsilon_L}{RT}\right) \frac{2\gamma_{LG}}{r} \tag{37}$$

and $$p = p_o \exp - \left(\frac{2\gamma_{LG}}{r} \frac{\upsilon_L}{RT} \right)$$

The minus sign is included in eqn.(37) because the actual values of R_1, R_2, r are assumed as positive if the meniscus is concave towards the vapour. If positive values of r are substituted into eqn.(37), the pressure comes out less than that over a flat surface. Note that in a raindrop (spherical), the radii of curvature are convex towards the vapour, and hence the vapour pressure over a raindrop is greater than that of a flat surface.

Combination of eqn.(37) and (35) yields

$$\upsilon_L \Delta P = RT \ln \frac{p}{p_o} = \frac{-2\gamma_{LG}\,\upsilon_L}{r} \tag{38}$$

$$\Delta P = -\frac{2\gamma_{LG}}{r} \tag{39}$$

The pressure term, ΔP, of eqn. (38) can be expanded, and

$$RT \ln \frac{p}{p_o} = g(-h_w) \tag{40}$$

where g, the gravitation acceleration; h_w, the pressure head of liquid. Equation (38) expresses the relationship between the pore pressure, humidity, and surface tension - principal radius of curvature upon the vapour pressure and free energy of moisture within a porous material.

6.2 Effect of solutes on free energy

Assuming Raoult's Law is applicable to a solvent in a dilute solution, the vapour pressure, p, of the solution is proportional to its mole fraction x_L i.e.

$$p = c' x_L$$

where c', a constant of proportionality and x_L, the mole fraction of solvent. For two solutions of differing compositions x_L, x_{LO} then

$$\frac{p}{p_o} = \frac{x_L}{x_{LO}} \quad \text{and}$$

$$RT \ln \frac{p}{p_o} = RT \ln \frac{x_L}{x_{LO}} = \Delta f = f - f_o \tag{41}$$

If x_{LO} represents pure solvent (i.e. $x_{LO} = 1$, $f_o = 0$) then

$$f = RT \ln x_L$$

$$\left(\frac{\partial f}{\partial x_L}\right)_{P,T} = \frac{RT}{x_L} \tag{42}$$

where the subscripts P,T refer to constant temperature and pressure.

The mole fraction of solvent and solute can be expressed by

$$x_L = \frac{M_L}{M_L+M_S} \quad ; \quad x_S = \frac{M_S}{M_L+M_S}$$

where M_L, the moles of solvent; M_S, the number of moles of ionic species in solution[31]. Note, for present purposes, the degree of dissociation of the solute is assumed to be constant, and independent of the concentration of the solute.

Furthermore

$$x_L + x_S = 1 \quad ; \quad \text{and} \quad dx_L = - dx_S \tag{43}$$

Combining eqns. (42), (43)

$$\left(\frac{\partial f}{\partial x_L}\right)_{P,T} = - \left(\frac{\partial f}{\partial x_L}\right)_{P,T} = \frac{RT}{x_L}$$

which upon integration with respect to x_S, and noting that for pure solvent $x_{SO} = 0$.

$$\Delta f = - \frac{RT}{x_L} \Delta x_S \tag{44}$$

Equating eqn. (44) and (41)

$$\Delta f = \frac{-RT\Delta x_S}{x_L} = RT \ln \frac{p}{p_o}$$

where Δf is equal to $f - f_o$ and Δx_S is equal to $x_S - x_{SO}$.

For isothermal changes and where no external work is involved, the free energy change of the liquid is a function of the pressure and concentration of the solute only and

$$df_L = \left(\frac{\partial f_L}{\partial P}\right)_{x_S,T} dP + \left(\frac{\partial f_L}{\partial x_S}\right)_{P,T} dx_S$$

Changes in pressure and concentration may be adjusted such that the overall free energy change is zero.

$$\left(\frac{\partial f_L}{\partial P}\right)_{x_S,T} dP = - \left(\frac{\partial f_L}{\partial x_S}\right)_{P,T} dx_S$$

and substituting for the partial differentials

$$\upsilon_L \, dP = \frac{RT}{x_L} \, dx_S \quad \text{and upon re-arranging}$$

$$\frac{dP}{dx_S} = \frac{RT}{x_L} \frac{1}{\upsilon_L}$$

With dilute solutions, it is reasonable to assume that x_L is approximately equal to unity. On integration, the expression above yields

$$\Delta\pi = \frac{RT}{x_L} \frac{\Delta x_S}{\upsilon_L} \tag{45}$$

The pressure difference, $\Delta\pi$, is known as the osmotic pressure, and eqn. (45) is known as Van't Hoff's Law. Note that ΔP is equal to $P_2 - P_1$ and $\Delta\pi$ is equal to $\pi_2 - \pi_1$ and Δx_S is equal to $x_{S2} - x_{S1}$. Comparison of equations (33), (44), (45) shows that $\Delta\pi$ is equal to $-\Delta P$ and that free energy increases as mechanical pressure increases but free energy decreases as osmotic pressure increases, i.e. as concentration difference of solute increases. In other words addition of solute to a solution has a similar action to that of applying a suction to the solvent in the porous material.

6.3 Effect of a force field on free energy

Assuming that the temperature and external pressure remain constant the free energy difference is given by,

$$\Delta f = -\Delta W_m$$

The free energy change produced by a force field is the sume of two components. One component being due to the hydrostatic pressure, $(\Delta f)_P$ caused by the attraction of the force field on the overlying superincumbent layers of fluid, and the other component being due to position in the force field, $(\Delta f)_F$.

The pressure energy component is given by

$$(\Delta f)_P = \int_A^B \upsilon \, dP \tag{46}$$

and the force field component (Fig. 1a)

$$(\Delta F)_{F'} = \int_A^B \underline{K} \cdot d\underline{L} = \int_A^B K d\ell \cos \theta^o \qquad (47)$$

where K is the magnitude of the field $\underline{K}$; $d\ell \cos \theta^o$ represents the component of distance travelled in a cirection parallel to that of the force field. When the force field vector $\underline{K}$ and the path vector $\underline{L}$ are colinear, $\cos \theta^o = 1$ (when the particle moves in the direction of the force field) and $\cos \theta^o = -1$ (when the particle moves in the opposite direction of the force field).

Consider the following example of a column of water at equilibrium (Fig. 1b), in a force field $\underline{g}$ (gravitational) whose intensity is independent of the height y, measured from a datum s. The force field component is given by

$$(\Delta f)_{F'} = \int_B^A \underline{g}\, dy = g \int_B^A dy \qquad (48)$$

The total free energy is the sum of the hydrostatic and force field components

$$\Delta f = (\Delta f)_P + (\Delta f)_{F'} = \int_B^A \upsilon\, dP + \int_B^A g\, dy \qquad (49)$$

Since the column is in equilibrium the free energy difference between the points A and B (and all other points in the column) is zero, and

$$\frac{dP}{dy} = \frac{-g}{\upsilon} = -g\rho \qquad (50)$$

Equation (50) shows the rate of change of hydraulic pressure with height in a column of fluid of density ρ (and specific volume).

6.4 Effect of electrical potential upon free energy

Under isothermal isobaric conditions the free energy change is

$$\Delta f = -\Delta W_m$$

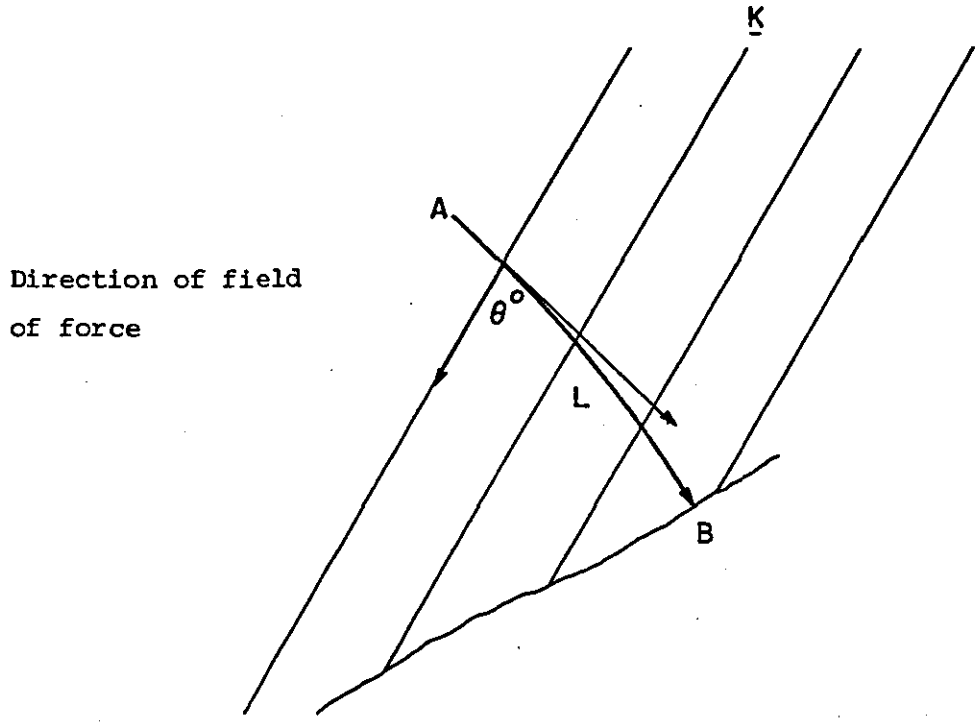

Fig. 1a. Relation between the direction of the force field acting on a body and its path of motion.

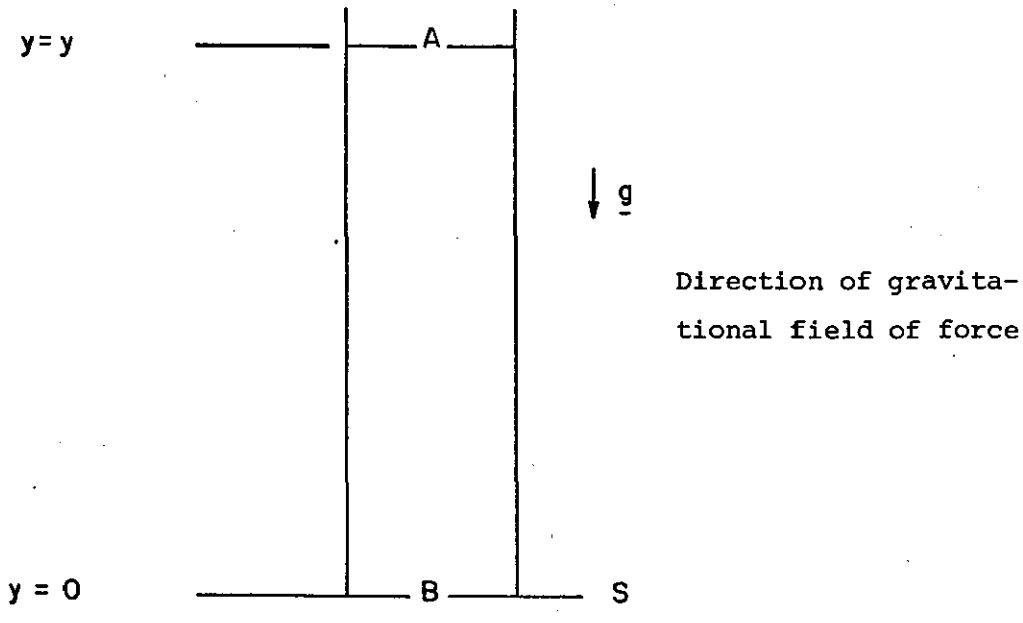

Fig. 1b. Column of fluid at equilibrium under a gravitational force field.

Assuming that there are charged particles (ions) present in the moisture within the porous material, and that the whole of the mechanical work involved is solely by the action of the electrical potential difference upon the charged particles, then

$$\Delta f = (\sigma)^{+}\Delta E \qquad (51)$$

where $(\sigma)^{+}$ is the amount of charge associated with unit mass of fluid, and ΔE is the electrical potential difference.

The electrical free energy difference eqn. (51) is similar to the pressure free energy difference

$$\Delta f = \upsilon\, \Delta P \qquad (52)$$

The mechanical pressure difference, ΔP (force over area) can be replaced by an electrical pressure difference which can be expressed thus

$$\Delta P_E = (\sigma)'\, \Delta E \qquad (53)$$

where ΔP_E is the electrical pressure; $(\sigma)'$, electric charge density per unit volume of fluid; ΔE, electrical potential difference.

Equations (52) and (53) can be combined to yield eqn. (51).

6.5 Effect of temperature on free energy

From eqn. (31) for conditions of constant pressure, zero mechanical work and in the absence of force fields and soluble salts,

$$\left(\frac{\partial f}{\partial T}\right)_P = -s \quad \text{and}$$

$$\Delta f = (f_B - f_A) = -(s_B - s_A)T = -\Delta s\, T \qquad (54)$$

where T is the absolute temperature at which the process is carried out.

Since the free energy of state B and reference state A, are both temperature dependent, the free energy change Δf is also temperature dependent and the change of free energy with respect to temperature is given by

$$\left(\frac{\partial(\Delta f)}{\partial T}\right)_P = -\Delta s_P \qquad (55)$$

The subscript P denotes that the free energy change is carried out at constant pressure, and that the free energy changes are also carried out at constant (fixed) temperature although different free energy differences are obtained at different fixed temperatures (ref.(3) p.98).

7. Factors affecting the diffusivity coefficients

The factors affecting the diffusivity coefficients can be grouped into three categories:-

(i) Intrinsic changes, i.e. changes which directly affect the solid matrix, altering the pore sizes and pore geometry. Examples of intrinsic changes are swelling of the matrix because of salt or moisture adsorption; dissolution or deposition of materials (salts, ice); thermal expansion and in extreme cases melting, deformation of the matrix by pressure and gravity forces, particularly with unconsolidated materials.

(ii) Direct changes in the fluid properties which are explicitly expressed in the diffusivity, i.e. viscosity of the fluid.

(iii) Changes of fluid properties, which indirectly affect the diffusivity, by their action upon the hydraulic functions and their derivatives.

For most building materials it can be assumed that thermal and pressure variations on the matrix geometry are negligible and, likewise, that thermal and pressure changes in the fluid, which indirectly affect the matrix goemtry are negligible. The remaining intrinsic factors are (a) alteration of the pore sizes and structure by leaching (which is discussed in Chapter Six) and deposition of salts. (b) swelling of the matrix through hydration or adsobtion of salts.

Changes of fluid properties mentioned in (ii) and (iii) above, are discussed under the appropriate diffusivity sections. In addition because of the simularity of the adsorbed phase to the liquid, i.e. a region where the fluid properties are no longer constant, and the joint diffusivity D_α, is given by

$$D'_{\alpha L} = D_{\alpha L} + D_{\alpha A}$$

and the net diffusivity, D_α

$$D_\alpha = D'_{\alpha L} + D_{\alpha V} \tag{56}$$

Because of the high moisture contents associated with Rising Damp, it is assumed that the contribution of the adsorbed phase can be neglected. Also, for future reference the joint diffusivity $D'_{\alpha L}$ will simply be denoted by $D_{\alpha L}$.

7.1 Moisture liquid diffusivity

The liquid phase diffusivity, $D_{\theta L}$ is defined as

$$D_{\theta L} = \frac{k_\theta}{\mu} \left(\frac{\partial h_w}{\partial \theta}\right)_\theta \rho_w \, g \tag{57}$$

where k_θ is the unsaturated permeability at a given moisture content, θ; μ, the fluid viscosity; $(\partial h_w/\partial\theta)_\theta$ is the rate of change of suction pressure head of water, of density ρ_w, with respect to the volumetric moisture content of the fluid; g, the gravitational acceleration.

The diffusivity is affected by changes of viscosity and/or moisture content. The relationship between the diffusivities at different viscosities and moisture contents is given by

$$\frac{D_{\theta 1}}{D_{\theta 2}} = \frac{k_{\theta 1}}{k_{\theta 2}} \frac{\mu_2}{\mu_1} \left(\frac{\partial h_w}{\partial \theta}\right)_{\theta 1} \left(\frac{\partial h_w}{\partial \theta}\right)^{-1}_{\theta 2} \tag{58}$$

as shown in Fig. 2a, b.

Assuming that the viscosity does not change and that the solid-liquid contact angle is unaffected by changes of temperature, pressure, salts, and electrical potential, then for a given

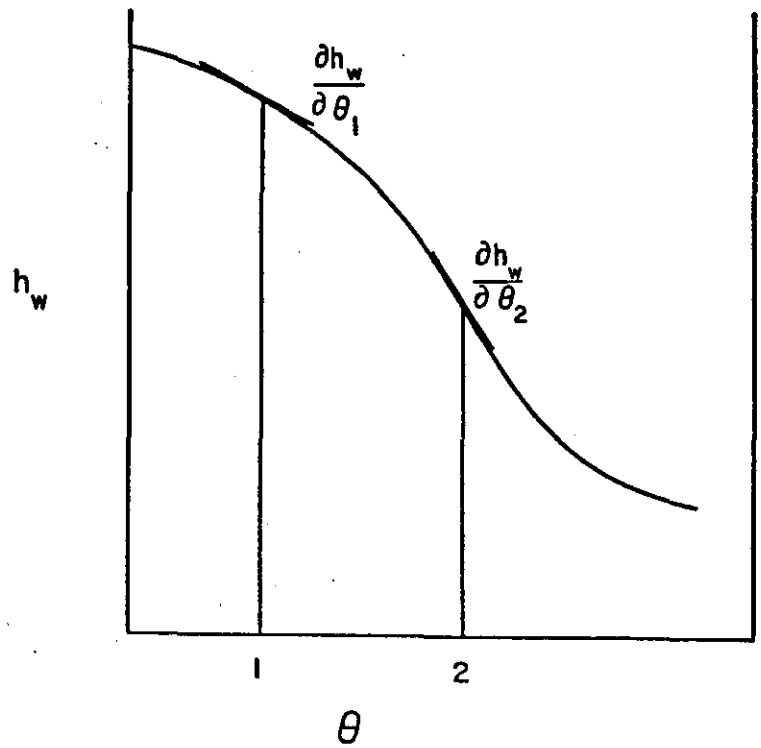

Fig. 2a. Change in suction pressure head (h_w) with respect to moisture content (θ) at point 1 and 2.

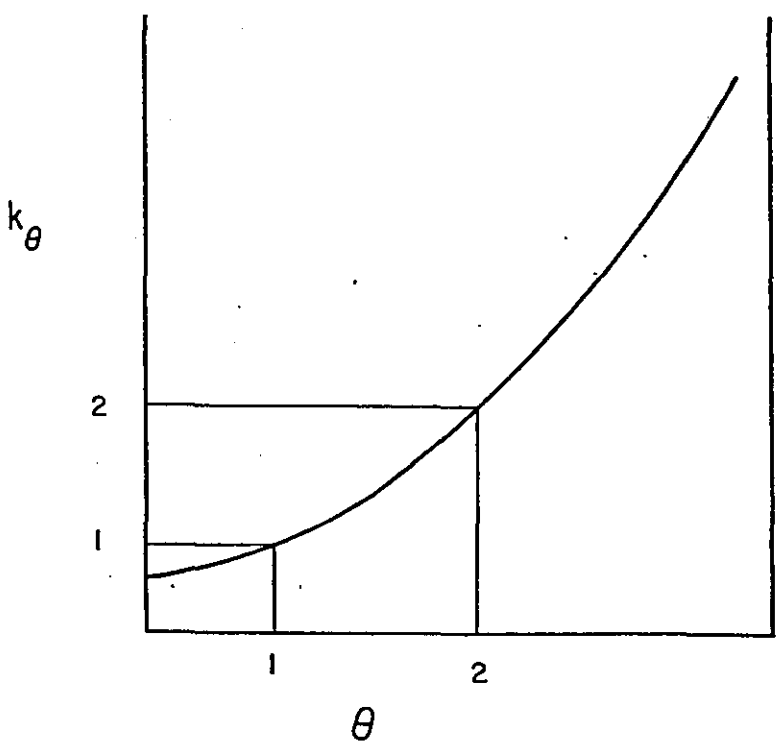

Fig. 2b. Change in unsaturated fluid permeability (k_θ) with respect to moisture content (θ) at points 1 and 2.

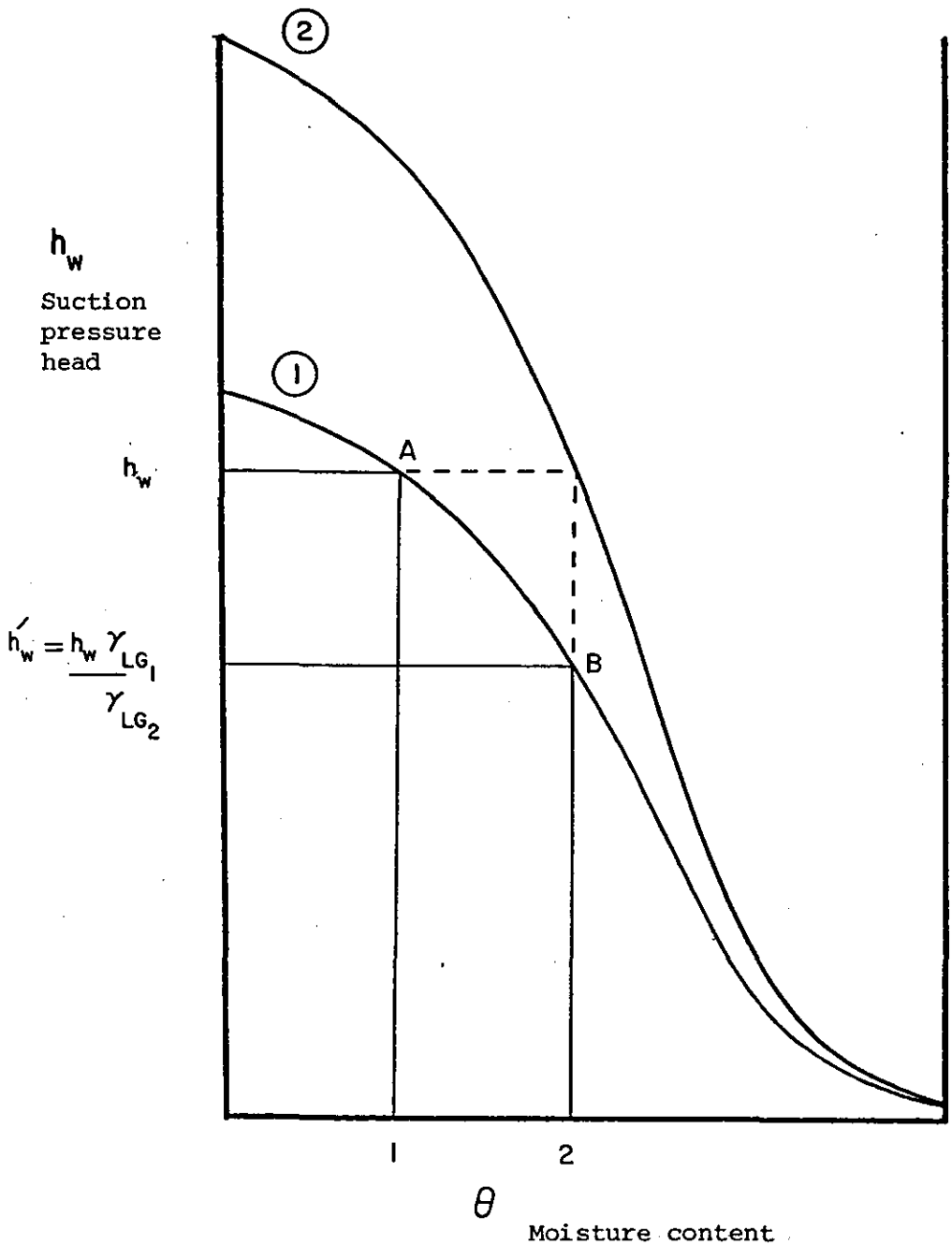

Fig. 3. Equivalent curves of suction pressure head (h_w) and moisture contact (θ) owing to changes of interfacial tension (liquid-gas) for the same porous material.

porous material, the moisture content is only affected by variations of surface tension.

Consider a liquid whose surface tension has increased from γ_{LG1} to γ_{LG2}. Because of the higher surface tension, the fluid meniscus will support an increased pressure difference before collapsing. The increased pressure difference (h_w) is represented in Fig. 3 by curve 2 . If the surface tension is doubled then, for any given moisture content, the new liquid height (h_w) will obviously be twice the equivalent height as that on curve 1 . Alternatively for any given suction, (i.e. h_w, Fig. 3), increasing the surface tension is equivalent to reducing the suction by the ratio $\gamma_{LG1}/\gamma_{LG2}$, with a consquent increase in moisture content from θ_1 to θ_2[32]. The ratio of the two diffusivities is given by (58), where the permeabilities are determined at their respective moisture contents. $\left(\frac{\partial h_w}{\partial \theta}\right)_{\theta 1}$ is determined at point A and $\left(\frac{\partial h_w}{\partial \theta}\right)_{\theta 2}$ is determined at point B.

Surface tension and viscosity are both affected by temperature and salt concentration. For the sake of simplicity it is assumed that the temperature coefficients of surface tension and viscosity for pure water are the same as those for salt solutions. Prediction of the solute coefficients is more difficult since the individual diffusivity coefficients for each salt will be different and furthermore with respect to Rising Damp, the moisture contains a mixture of salts of varying compositions.

The change of viscosity and surface tension of water with respect to some common salts can be found[33]. The effect of electrical potential fields on the surface tension of salt solutions has been found to ne negligible[34] since electric fields as high as 6700 volts per cm produced a change of surface tension of less than two percent of its normal salt free value.

Equation (58) is not applicable to porous materials whose pore structure is altered intrinsically by adsorption of ions or water. A typical example of intrinsic alteration is that of swelling of clays particularly those containing sodium montmorillonite. The alteration of pore structure can be produced by simple swelling or by failure of the material because of unequal swelling or by deflocculation. The liquid moisture diffusivity is affected by both the permeability function and the $(\partial h_w/\partial\theta)$ function. Pore conductivity is approximately proportional to the fourth power of the pore radius and hence the conductivity can be greatly influenced by small changes in radius although the magnitude of any overall change will also be influenced by the pore size distribution.

It is obvious that for the same degree of swelling, porous materials composed of fine pores will be affected to a greater extent than coarser pored porous materials, since the relative change in pore radius in the latter material is much smaller.

Because of the difficulty in predicting the degree of swelling in response to external conditions and predicting the effect of this swelling upon the hydraulic functions, calculation or theoretical prediction of intrinsically induced change in diffusivity value is very difficult if not impossible. For this reason, it is assumed that for rigid porous building materials intrinsic changes are negligible and hence can be ignored.

7.2 Moisture vapour diffusivity

Philip[1] proposed that the equation representing water vapour diffusion through a salt-free porous material in a non-turbulent free atmosphere was

$$Q_{\theta v} = -\alpha(\phi-\theta)D_{atm}\,\nabla\rho_v \qquad (59)$$

where $Q_{\theta v}$, is the vapour flux density (g cm^{-2} sec^{-1}); α, tortuosity factor approximately equal to 0.66; ϕ, the porosity; θ, the volumetric moisture content; D_{atm}, the molecular diffusivity of water vapour in air; ρ_v, the density of the vapour.

Eqn. (59) was modified[22] by the inclusion of a flow factor, ν, to allow for the mass flow of vapour arising from the difference in boundary conditions governing the air and vapour components of diffusion.

$$Q_{\theta v} = -\alpha\nu(\phi-\theta)D_{atm}\nabla\rho_v \tag{60}$$

and ν is equal to (P/P-p) where P is the total pressure and p is the partial pressure of the vapour.

Introducing the relationship,

$$\rho_v = \rho_{sv}h = \rho_{sv}\exp\left[\frac{-h_w g}{RT}\right] \tag{61}$$

where ρ_{sv} is the density of saturated vapour; h, the relative humidity; h_w, the suction water pressure head; g, the gravitation acceleration; T, the absolute temperature; R, the universal gas constant per gram of water; into equation (60)

$$Q_{\theta v} = \alpha\nu(\phi-\theta)D_{atm}\frac{\rho_{sv}g}{RT}\exp\left[\frac{-h_w g}{RT}\right]\nabla h_w \tag{62}$$

Expressed in diffusivity form eqn. (62) becomes

$$J_{\theta v} = \frac{Q_{\theta v}}{\rho_w} = \alpha\nu(\phi-\theta)D_{atm}\frac{\rho_{sv}}{\rho_w}\frac{g}{RT}\exp\left[\frac{-h_w g}{RT}\right]\frac{\partial h_w}{\partial\theta}\nabla\theta \tag{63}$$

$$= -D_{\theta v}\nabla\theta = -\left(k_{\theta v}\frac{\partial h_w}{\partial\theta}\right)\nabla\theta \tag{64}$$

where $D_{\theta v}$ is the moisture vapour diffusivity; $k_{\theta v}$, the vapour conductivity; $J_{\theta v}$, the vapour flux expressed as a velocity of liquid water; ρ_w, the density of water.

Currie[35] has shown that the simple relationship $\alpha(\phi-\theta)$ is only of limited applicability and that, in general, a more complex

expression must be used. This complex reltionship will be represented for brevity by an unspecified function $f_n(\phi-\theta)$, which is not simply a function of the gas-filled porosity alone.

Using Currie's modified tortuosity functions, Rose[36][37] expressed the vapour flux in the form

$$J_{\theta v} = \frac{\rho_{sv}}{\rho_w} D_{atm} \frac{g}{RT} \cdot \frac{D_T}{D_O} \cdot \frac{\nu h D}{D_T} \cdot \left[\frac{\partial h_w}{\partial \theta}\right] \nabla\theta \qquad (65)$$

where D is the gaseous diffusion coefficient through the porous material; D_T, the gaseous diffusion coefficient through the porous material when the pore space is full of gaseous mixture; D_O, is the gaseous diffusion coefficient in free air; (D/D_O) is the function $f_n(\phi-\theta)$ which is equal to the terms $\alpha(\phi-\theta)$ in the expression presented by Philip.

The first factor on the right hand side of eqn. (65) is a constant of water, the second factor, (D_T/D_O), is a constant of the porous material which accounts for the tortuosity or presence of the soil matrix. Finally the third factor, $(\nu hD/D_T)$, is a variable determined by the h_w-θ curve.

The density of saturated water vapour, ρ_{sv}, is a function of temperature only. Similarly the mass flow factor, ν, is also temperature dependent because of its relationship to ρ_{sv}. In addition the flow factor is obviously pressure dependent as is the molecular diffusion coefficient of water vapour in air (D_{atm}). Up to twenty atmospheres, the molecular diffusion coefficient is inversely proportional to the total pressure, P, and roughly varies with the absolute temperature at $T^{1.5}$ [38].

For pure water, Philip et al[22] has shown that h is virtually independent of temperature. However, when salts are dissolved in the water, determination of the relative humidity becomes more complicated. In the presence of salts, the relative humidity of the solution - pure water is given by[31][39]

$$h = (p/p_0) = \exp(-n/N) \tag{66}$$

where n is the number of molecules of solute and N, the number of molecules of solvent.

If the solute does not dissociate, the number of molecules of solute is proportional to the number of moles of solute, M_s dissolved in the solvent. Similarly, the number of molecules of solvent is proportional to the number of moles of solvent, M_w, in which the solute is dissolved. As an example, consider 1 gm-mole of sodium chloride dissolved in 180 gms of water (i.e. N = 10). If the sodium chloride does not dissociate then (n/N) is equal to (1/10). Alternatively if the sodium chloride is completely dissociated into sodium and chloride ions, the ratio (n/N) is now equal to (1/5). Generally the degree of dissociation is only fractional, $0 < x < 1$, and hence as an example for sodium chloride

$$\begin{array}{ccccc} NaCl & \rightarrow & Na^+ & + & Cl^- \\ 1-x & & x & & x \end{array}$$

Hence 1 mole of sodium chloride produces 1+x moles of particles in solution and hence the ratio of (n/N) is equal to (1+x)/10.

With dilute solutions of ionic salts, x may be regarded as equal to unity. Similarly for dilute solutions, the mole fraction of salt x_s $(=(M_s)/(M_s+M_w))$ can be simply expressed as the ratio (M_s/M_w), i.e. the number of molecules of solute divided by the number of molecules of solvent is proportional to the mole fraction of solute added (c.f. Raoult's Law - Section 8, eqns. (41)-(45)).

$$\frac{n}{N} = c' x_s \tag{67}$$

where c' is the number of moles of ionic species produced in solution per mole of solid salt. Note c' is a function of solute concentration.

Moisture in a wall contains several salts, and the number of each of the ionic species in the moisture will be governed by a

solubility matrix and also by a salt - reaction matrix both of which are temperature dependent. Because of the temperature dependence of the two matrices, the relative humidity of wall moisture will also be a function of temperature.

7.3 Thermal vapour diffusivity

A theory of vapour diffusion under thermal gradient has been proposed by Philip and De Vries[22]; where the thermal vapour flux, in terms of liquid water velocity, was defined as

$$J_{TV} = \frac{Q_{TV}}{\rho_w} = \frac{-\alpha \nu}{\rho_w} (\phi - \theta) \, D_{atm} \, h \frac{\partial \rho_{sv}}{\partial T} \nabla T \tag{68}$$

It is assumed that there are no salts in the water, i.e. h is not a function of temperature. Alternatively, using the notation of Rose (c.f. eqn. (63)-(65)) and the modified tortuosity factor, eqn. (68) may be expressed[40]

$$J_{TV} = \frac{-D}{\rho_w D_O} \nu \, D_{atm} \, h \frac{\partial \rho_{sv}}{\partial T} \nabla T$$

$$= -D_{TV} \nabla T \tag{69}$$

where D_{TV} is the thermal vapour diffusivity.

The rate of change of saturated vapour pressure with temperature, $(\partial \rho_{sv}/\partial T)$, is taken as that of pure free water. Discussion of the factors affecting the other variables can be found in the previous section.

7.4 Thermal liquid diffusivity

Darcy's law for flow within an unsaturated porous material is (c.f. eqn(18))

$$J_v = -K \nabla \Phi \tag{70}$$

where J_v is the macroscopic fluid velocity; K, the hydraulic conductivity; Φ, the pressure head potential (restricted to pressure and gravity).

When the potential difference is produced by a temperature gradient, flow in the liquid phase, corresponding to eqn.(70) is

$$J_{TL} = - K(\theta) \frac{\partial h_w}{\partial T} \nabla T \tag{71}$$

where J_{TL} is the macroscopic mean velocity of thermally induced moisture movement; $K(\theta)$, the hydraulic conductivity, shown as a function of volumetric moisture content, θ; $(\partial h_w/\partial T)$ is the rate of change of suction pressure head with respect to temperature, T.

Assuming that the difference in h_w is determined only by capillarity[22] [40]

$$J_{TL} = -K(\theta) \frac{\partial h_w}{\partial \gamma_{LG}} \frac{\partial \gamma_{LG}}{\partial T} \nabla T \tag{72}$$

where γ_{LG} is the surface tension of the liquid. However, since the potential h_w is directly proportional to the surface tension, then

$$J_{TL} = -K(\theta) \frac{h_w}{\gamma_{LG}} \frac{\partial \gamma_{LG}}{\partial T} \nabla T$$

$$= -K(\theta)\, h_w\, \gamma'' \nabla T = -D_{TL} \nabla T$$

where D_{TL} is thermal liquid diffusivity which is equal to $K(\theta)h_w\gamma''$ and γ'' is equal to $\frac{1}{\gamma_{LG}} \frac{d\gamma_{LG}}{dT}$.

γ'' is slightly dependent upon temperature, however, in the range 10^oC to 30^oC, a constant value of $-2.02 \times 10^{-3} (^oC^{-1})$ can be assumed. Assuming a constant value introduces an error of approximately $\pm 2\%$ over the range 10^oC to 30^oC.

7.5 Solute vapour diffusivity

Addition of a solute to a solvent lowers the free energy and vapour pressure of the solvent. This effect may be thought of as being equivalent to directly increasing the suction of the liquid phase. Because of the close relationship between the two processes upon the vapour pressure and relative humidity of the solvent, moisture movement in the vapour phase due to differences in solute concentration (c.f. eqn.(66)) has been included in the

section discussing moisture vapour diffusivity (i.e. Section 14) and as such will not be treated as a separate diffusivity in this work.

7.6 Solute liquid diffusivity

Because of the similarity between the free energy changes produced by addition of a solute to a solvent and the application of a negative mechanical pressure (suction) to the solvent, it is convenient to express solute-induced moisture flow in terms of osmotic pressure rather than concentration difference,

$$J_{CL} = -K_C(\Delta f)'_C = K_C(\nabla\pi) \tag{73}$$

where $(\Delta f)'_C$ is the free energy difference, per unit volume of moisture; K_C the proportionality coefficient; $\nabla\pi$, the osmotic pressure; J_{CL}, the macroscopic mean velocity of moisture in the liquid phase.

Combining osmotically induced moisture flow and mechanically induced moisture flow yields[20][41][42][46]

$$J_v = J_{\theta L}+J_{CL} = -K_P\nabla P + K_C\nabla\pi \tag{74}$$

or $$J_v = K_P(-\nabla P + \sigma\nabla\pi) \tag{75}$$

where σ, is known as the reflection coefficient or osmotic efficiency coefficient.

The difference in sign, in equations (73),(74),(75), between the mechanical pressure gradient and osmotic gradient is introduced because the osmotic moisture flux is in the direction of increasing solute concentration (greater suction) whereas the pressure flux is in the direction of decreasing pressure.

σ is the osmotic efficiency coefficient and it is equal to the ratio (K_C/K_P)[41][46]. The range of σ is from 0 to 1. σ will equal 0 where K_C is equal to 0, i.e. salt concentration gradients cause no moisture flow. σ will equal 1 when K_C is equal to K_P, in which case the osmotic pressure gradient is as efficient

in causing moisture to flow as is the mechanical pressure gradient, (i.e. a semi-permeable membrane).

Although values of σ can be used to determine the value of K_C, caution is required in a direct conversion of σ to get values of K_P, because the osmotic efficiency coefficient is also influenced by K_P. Thus a factor may alter the value of σ but not necessarily alter the value of K_C and hence the value of σ is altered because of variations in K_P.

The osmotic efficiency coefficient and flow of moisture and ions in thin films adjacent to charged mineral surfaces has been investigated by Kemper and co-workers[(26)-(29) (41)-(47)]. The major theme of Kemper's study is an investigation of the relative movement of moisture and salts in the films, assuming that only pressure and solute gradients are active in producing moisture movement.

The close proximity of the solid surface has considerable influence on the relative motion of solute and solvent particularly with flow in the thinner films. Differences in the relative mobility of solutes and solvent in thin films give rise to the process of salt-sieving, whereby the concentration of solute in the bulk solution is reduced on passing through a fine-pored membrane or a membrane containing thin films of solution. Conversely, the greater the restriction of solute, the greater will be the efficiency of the osmotic potential in causing moisture movement. When the solute is totally restricted, the osmotic efficiency coefficient is equal to unity and the osmotic potential is equally effective as the pressure potential in producing moisture flow.

Charged solid surfaces play an important role in the restriction of solute. The charged surface attracts ions of

opposite polarity and repels those of similar polarity, and providing the film is thin enough, these ions will be partially or totally restricted from the film. Obviously this electrostatic effect is increased as the film thickness is decreased. In addition, the diffusion coefficients of the various ions are lower, measured near to the solid surface, than in the bulk liquid, which also contributes to the restriction of solute. The decrease in ionic diffusivity is attributed to the increased viscosity of water near the solid surface[42] and furthermore Wang et al[48] has shown that the diffusion of ions through water is approximately inversely proportional to the viscosity of water.

In addition to the above mechanisms of solute restriction Kemper[42] investigated the effects of geometric factors upon the restriction of solute to solvent. He developed an equation to predict the value of σ in relation to the radius of the solute molecules and found that there was good agreement between the theoretical values of σ and experimentally determined values.

The experimental values of σ were measured for relatively large organic molecules, however further experiments[45] using ionic materials showed that geometrical restriction is practically negligible as a factor causing restriction of ions. Furthermore for ionic materials the electrostatic effects (negative adsorption of ions possessing a similar polarity of charge to that of the solid surface) are the most important factors determining the degree of salt restriction.

Kemper stated that the ability of salt concentration gradients to cause solution movement is increased by:- (i) saturating the material with monovalent rather than divalent cations. (ii) using divalent rather than monovalent anions. (iii) decreasing the water

content (i.e. reducing the film thickness). (iv) decreasing the average concentration of the bulk electrolyte. It is important to note that the porous membranes (clays) used by Kemper were negatively charged and that for positively charged surfaces the role of the cations (+ve ions) and anions (-ve ions) in (i) and (ii) above is reversed.

Kemper's conclusion that in the case of ions, the electrostatic effects are the major factor in determining solute restriction is in agreement with predictions based upon the "diffuse double layer" concept. Consider an infinite plane surface of fixed charge density, $(\sigma_0)^-$ (i.e. surface is assumed to be negatively charged). In the absence of other charged particles the field intensity of the charge would decrease linearly with distance, x, normal to the charged surface (curve 1 Fig. 4). However, when ionic solutions are present, cations will be attracted towards the surface and anions will be repelled from the surface. The increased cation concentration near the surface reduces the field intensity in excess of the rate when no ions are present (curve 2 Fig. 4).

The charge density variation with respect to distance from the surface can be expressed as the gradient of an electrical potential, as given by[(49)-(55)]

$$\nabla^2 E = \frac{-4\pi(\sigma)'}{\varepsilon} \qquad (76)$$

where E is the electrical potential; ∇^2, the Laplacian operator $\left(\frac{\partial^2}{\partial x^2} + \frac{\partial^2}{\partial y^2} + \frac{\partial^2}{\partial z^2}\right)$; $(\sigma)'$, the volumetric charge density and ε, the dielectric constant of the medium.

In the case of monovalent ions at room temperatures (i.e. $E/k'T << 1$), the change in electrical potential with respect to distance, x, from the solid surface is [(53)]

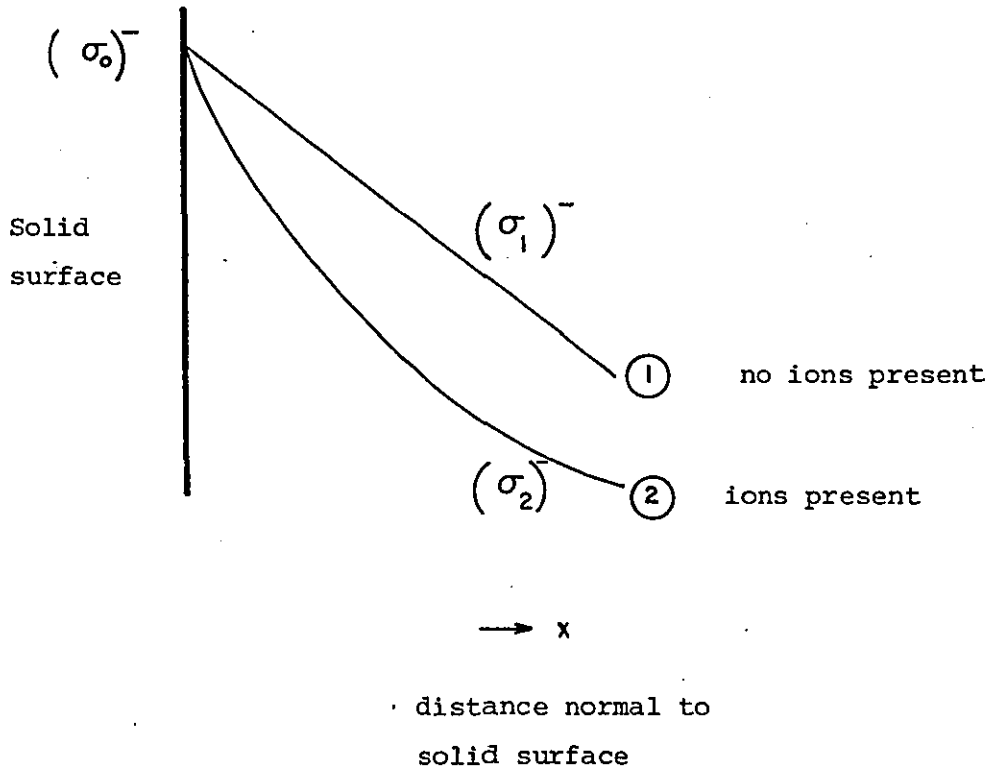

Fig. 4. Variation of charge $(\sigma)^-$ near a solid surface in the absence of ions (curve 1) and in the presence of ions (curve 2).

$$E = E_0 \exp\left[-\left(\frac{8\pi n_o z^2 e^2}{k' T}\right)^{0.5} x\right] \tag{77}$$

where E is the electrical potential at a distance x measured normal to the surface; E_0 is the surface potential; n_o, the concentration of ions at a large distance from the surface, i.e. the bulk liquid concentration; z, the valency of the ion; e, the charge on an electron; ε, the dielectric constant; k', Boltzmann constant; T, the absolute temperature.

The concentration of ions associated with this potential is given by (ref. (53) page 180)

$$n^+ = n_o \exp(z^+ e E/k'T) \quad \text{and}$$

$$n^- = n_o \exp(-z^- e E/k'T) \tag{78}$$

Both the fluid velocity and solute concentration are determined by their distance from the surface and it is the relative difference between the two functions that gives rise to the process of salt-sieving when an ionic solution is induced to move by a pressure gradient acting parallel to the solid surface.

From eqn. (77) we can see that as the solute concentration (proportional to n_o) is increased, the potential normal to the surface is correspondingly reduced at all distances. This means that the relative concentration of anions near the surface has increased and more salts are transported across the membrane, (i.e. σ is reduced). Similarly if monovalent cations are replaced by divalent cations, then once again the potential normal to the surface is reduced and σ, the osmotic efficiency coefficient is correspondingly reduced. When divalent anions are replaced by monovalent anions, the relative concentration of anions, given by eqn. (78) is increased and consequently the osmotic efficiency is lowered. Finally, if the film thickness is increased, then the relative flow area affected by the diffuse layer is decreased and because of this more anions will be transported across the film

consequently reducing the osmotic efficiency coefficient once again.

The changes in the value of σ as determined and predicted by Kemper, are in complete agreement with the predictions based upon a qualitative analysis of the "diffuse double layer" theory.

7.7 Electro osmotic coefficient

The theory of electro osmosis and the derivation of the electro osmotic coefficient is discussed more fully in Chapter Four. The electro osmotic coefficient derived in Chapter Four is the same (diffusivity) coefficient as defined in equation (23) where α is the electrical potential. For the sake of consistency the coefficient should nominally be called the electrical liquid diffusivity but because of the greater popularity, and not wishing to create further confusion, usage of the term "electro osmotic coefficient" will be continued.

Liquid flow is induced by the action of an (externally applied) electrical potential gradient upon the mobile part of the diffuse double layer. The magnitude of the electro osmotic coefficient is increased by raising the temperature owing to the relative lowering of the fluid viscosity[56][57].

The effect of solute concentration upon the electro osmotic coefficient is more complex. Initially the coefficient increases with increasing concentration[58]. However, further increases in the salt concentration result in a lowering of the value of the coefficient[59].

The magnitude of the electro osmotic coefficient is approximately related to the excess viscous drag force between the cations and the anions. At high concentrations, an increase in solute concentration has little effect upon the drag force. It does however, lower the electrical efficiency of the process since

the additional ions reduce the electrical resistance of the solution and in order to maintain the same moisture flux a higher electrical current is required.

At lower concentrations, increasing the amount of solute increases the differential drag force, because the degree of adsorption or repulsion of anions (or cations) has correspondingly been increased.

Consider an initially uncharged membrane that preferentially adsorbs anions (or desorbs cations) at the solid surface such that they may be regarded as immobile. On the addition of a small amount of ionic solute, the surface acquires a negative charge and the cations form the diffuse double layer. Further addition of solute results in a larger number of anions becoming attached to the surface and correspondingly a greater number of cations becoming associated with the diffuse layer; which consequently increases the electro osmotic effect.

This process will continue until the surface has become saturated with anions. Further increases in solute concentration merely result in an increased anion (and cation) concentration in the bulk liquid, which as stated above ultimately reduces the electro osmotic effect. It is obvious that for the example above, any factors which reduce the mobility of anions will consequently increase the electro osmotic effect. Restriction of anions has been discussed in the previous section with respect to salt-sieving and the osmotic efficiency coefficient, σ.

It has been stated that film thickness (i.e. moisture content or for fully saturated porous materials, porosity) is a factor which affects the degree of restriction of anions, when the solid surface has acquired a negative charge. Alterations of the film thickness gives rise to two opposing processes which affect the efficiency of the electro osmotic effect.

Increasing the film thickness results in a greater volume of fluid being transported across the membrane, together with an increased number of anions. The greater anion flow is directly due to greater anion concentration in the outer region of the film away from the solid.surface.

The anions are also affected by the externally applied electrical potential and their movement tends to oppose the bulk liquid flow. It is obvious that for a certain concentration and at a given distance from the surface, the relative drag in this layer of fluid will be zero (i.e. no movement) and that at greater distances from the surface, the fluid velocity will be in the opposite direction to bulk electro osmotic flow. This reversal of flow lowers the efficiency of the electro osmotic effect in two ways (i) the negative convection of fluid lowers the net (positive) moisture flux. (ii) a fraction of the electrical current is carried by the anions (partial short-circuiting) which lowers the electrical efficiency of the process.

The ion reversal of flow is an example of circulation (i.e. the electrical energy is merely used to circulate fluid rather than transport it in a particular direction). The process is not restricted to single film thickness but may occur when pores of dissimilar size are in contact with each other. In fact the process described above has been presented as an explanation for the temporary blocking of membranes[60].

At low moisture contents the increase in positive convective flow, when solute is added, is greater than the opposing anion effect and hence the elctro osmotic coefficient initially increases with concentration. However, when the system has become "saturated" with salt the coefficient decreases with increasing salt concentration.

A similar mechanism will also occur when the concentration is kept constant and the film thickness varied. At low moisture contents the increase in positive convective flux is greater than the opposing ion effect and hence the electro osmotic coefficient will initially increase. However, a situation is reached when the effects of the opposing ion process are greater than the relative increase in positive flux and hence the electro osmotic coefficient is consequently lowered[56] [57] [61] [62].

List of symbols and units of Chapter Three

D_θ	net moisture diffusitivity of a porous material ($cm^2 sec^{-1}$)
$D_{\theta L}$	moisture liquid diffusivity of a porous material ($cm^2 sec^{-1}$)
$D_{\theta V}$	moisture vapour diffusivity of a porous material ($cm^2 sec^{-1}$)
$D_{\theta A}$	moisture adsorbed diffusivity of a porous material ($cm^2 sec^{-1}$)
D_{TL}	thermal liquid diffusivity of a porous material ($cm^2 sec^{-1}$)
D_{TV}	thermal vapour diffusivity of a porous material ($cm^2 sec^{-1}$)
D_{TA}	thermal adsorbed diffusivity of a porous material ($cm^2 sec^{-1}$)
D_{atm}	molecular diffusion coefficient of water vapour in air ($cm^2 sec^{-1}$)
D	gaseous diffusion coefficient through the porous material ($cm^2 sec^{-1}$)
D_O	gaseous diffusion coefficient in free air ($cm^2 sec^{-1}$)
D_T	gaseous diffusion coefficient through the porous material when the pore space is full of gaseous mixture ($cm^2 sec^{-1}$)
d	diameter of a pipe (cm)
E	an applied voltage (stat volts)
e	charge on an electron (stat coulombs)
F'	body forces per unit mass of fluid ($cm\ sec^{-2}$)
$(\nabla f)_\alpha$	free energy gradient
g	gravitational acceleration ($cm\ sec^{-2}$)
h	relative humidity
h_w	pressure head of fluid (cm)
J_v	macroscopic mean fluid velocity ($cm\ sec^{-1}$)

K'	Darcy coefficient; coefficient relating the flux J_v, and the applied potential Φ. The dimensions of K' are dependent upon the dimensions adopted for Φ.
K	Hydraulic conductivity of a porous material to fluid (cm sec^{-1})
K_α	a coefficient relating the flux of moisture to the corresponding free energy gradient $(\nabla f)_\alpha$; where the subscript α is denoted by E or C or T or P referring to free energy gradients produced by voltage, solute concentration, temperature or pressure differences respectively.
k	permeability of the porous material to fluid (cm^2)
k'	Boltzmann's constant (g cm^2 sec^{-2} $^oK^{-1}$)
N_{Re}	Reynolds number
N_{Re_k}	permeability Reynolds number
N_{f_k}	permeability friction factor
N	number of moles of solvent (mole)
n	number of moles of solute (mole)
n_o	concentration of ion in bulk solution (ions cm^{-3})
n^-	concentration of anions in solution (ions cm^{-3})
n^+	concentration of cations in solutions (ions cm^{-3})
P	pressure (g $cm^{-1}sec^{-2}$)
ΔP_E	pressure difference arising from an applied voltage gradient (g $cm^{-1}sec^{-2}$)
p_o	vapour pressure of free pure liquid (g $cm^{-1}sec^{-2}$)
p	vapour pressure in equilibrium with liquid within a porous material (g $cm^{-1}sec^{-2}$)
$Q_{\theta v}$	mass flow of vapour (g $sec^{-1}cm^{-2}$)
q	heat energy per gram of fluid (cm^2sec^{-2})
R	Universal gas constant per gram of fluid (cm^2sec^{-2} $^oK^{-1}$)

r	radius of a capillary (cm)
s	entropy per gram of fluid ($cm^2 sec^{-2}\ {}^oK^{-1}$)
T	temperature (${}^oC$, ${}^oK$)
t	time (sec)
U	internal energy per gram of fluid ($cm^2 sec^{-2}$)
u	fluid velocity ($cm\ sec^{-1}$)
$\underline{u}$	fluid velocity flow vector ($cm\ sec^{-1}$)
W	work per gram of fluid associated with a process ($cm^2 sec^{-2}$)
W_m	all mechanical work per gram of fluid, associated with a process, excluding that of expansion of a gas against a pressure P ($cm^2 sec^{-2}$)
x_L	mole fraction of solvent
x_S	mole fraction of solute
z	valency of an ion
α	tortuosity coefficient
γ_{LG}	surface tension between liquid and gaseous phases ($g\ sec^{-2}$)
ε	dielectric constant (stat $coulombs^2 sec^2\ g^{-1}\ cm^{-3}$)
ε_o	dielectric (or permittivity) of free space (stat $coulombs^2\ sec^2\ g^{-1}\ cm^{-3}$)
θ	volumetric moisture content of a porous material
μ	fluid viscosity ($g\ cm^{-1} sec^{-1}$)
ν	a factor to allow for the mass flow of vapour arising from the difference in boundary conditions governing the air and vapour components of diffusion (= P/P-p)
π	osmotic pressure ($g\ cm^{-1} sec^{-2}$)
ρ	density of the fluid ($g\ cm^{-3}$)
ρ_L	density of moisture in the liquid phase ($g\ cm^{-3}$)
ρ_V	density of moisture in the vapour phase ($g\ cm^{-3}$)
ρ_{SV}	density of moisture in the vapour phase when saturated in air ($g\ cm^{-3}$)

σ	osmotic efficiency coefficient
$(\sigma)^{+}$	charge density per unit mass of fluid (stat coulombs g^{-1})
$(\sigma)'$	volumetric charge density of the fluid (stat coulombs cm^{-3})
υ	specific volume of the fluid ($cm^3\ g^{-1}$)
υ_L	specific volume of moisture in the liquid phase ($cm^3\ g^{-1}$)
υ_G	specific volume of moisture in the gaseous phase ($cm^3\ g^{-1}$)
Φ	a generalised potential combining both pressure and body forces ($cm^2\ sec^{-2}$)
ϕ	porosity of a porous material

References Chapter Three

(1) "The concept of diffusion applied to soil water", J.R. Philip, Proc.Nat.Acad.Sci., India, No. 24A, pp.93-104, 1955

(2) "Fluid dynamics", V.L. Streeter, McGraw Hill Book Co. Inc., 1st Ed., 1948

(3) "Flow in porous media", J.R. Philip, Anuual review of fluid mech., 2, pp.177-204, 1970

(4) "Chemical engineering. Vol. one", J.M. Coulson, J.F. Richardson, Pergamon Press, revised 2nd Ed., 1970

(5) "Turbulent flow in porous media", J.C. Ward, Jnl. of Hydraulics Divn., Proc. Am. Soc. of Civ. Eng., No. HY5, pp.1-12, 1964

(6) "Non-Darcy flow through fibrous porous media", G.S. Beavers, E.M. Sparrow, Jnl. of App. Mech., 36, No. 4, pp.771-714, Trans A S M E 91, Series E, 1969

(7) "Experimental study of slurry separators for use in desalination", J. Shwartz, R.F. Probstein, Desalination, 6, pp.239-266, 1969

(8) "Influence of bed size on the flow characteristics and porosity of randomly packed beds of spheres", G.S. Beavers, E.M. Sparrow, D.E, Rodenz, Jnl. of App. Mech., Trans. A S M E pp.655-660, 1973

(9) "Laminar, turbulent, and transitional flow in porous sintered media", A. Lorenzi, Meccanica, 10, No. 2, pp.75-77, 1975

(10) "Visualisation of the transition to turbulent flow in porous media", J.D. McFarland, P.M. Dranchuk, Jnl. Canad. Petr. Tech. 15, No. 2, pp.71-78, 1976

(11) "Dynamics of flow in porous media", J. Bear, Elsevier Publ. Co. Inc., 1972

(12) "Some theoretical aspects of the flow of water in unsaturated soils", A. Klute, Soil Sci. Soc. Amer. Proc., 16, pp.144-148 1952

(13) "A numerical method for solving the flow equation for water in unsaturated materials", A. Klute, Soil Science, 73, pp.105-116, 1952

(14) "Some steady state solutions of the unsaturated moisture flow with application to evaporation from a water table", W.R. Gardner, 85, No. 4, pp.228-232, 1958

(15) "Review of some elements of soil moisture theory", I. Remson, J.R. Randolph, Geolog. Survey Professional Paper 411-D, 39 pages, 1962

(16) "Soil-water behaviour as described by transport coefficients and functions", D. Swartzendruber, Advances in Agron. 18, pp.327-370, 1966

(17) "Engineering concepts of moisture equilibria and moisture changes in soils. Statement of the review panel", Symp. moisture equilibria and moisture changes in soils beneath covered areas, (Butterworths) Australia, pp.7-21, 1965

(18) "Theory of infiltration", J.R. Philip, Advances Hydro Sci. 5, pp.215-296, 1969

(19) "Soil-water physics and hydrologic systems", J.R. Philip, I F I P Working Conf. Computer Simulation of Water Resources Systems, Ghent, Belgium, 30 July - 2 Aug. 1974, Publ. North Holland Publ. Co., Amsterdam, pp.85-97, 1975

(20) "Soil water theory and its application in field situations", A. Klute, Soil Sic. Soc. Am. Spec. Publ. No. 5, pp.9-35, 1973

(21) "Water movement in porous building materials", C. Hall, Building and Envir. 12, pp.117-125, 1977

(22) "Moisture movement in porous materials under temperature gradients", J.R. Philip, D.A. De Vries, Trans. Am. Geophy. Union 38, No. 2, pp.222-232, 1957

(23) "Evaporation, and moisture, and heat fields in the soil", J.R. Philip, Jnl. of Met., 14, pp.354-366, 1957

(24) "Physics of water movement in porous materials", J.R. Philip, High. Res. Board Spec. Rep. No. 40, pp.147-163, 1958

(25) "On the differential equation of diffusion", J.D. Babbitt, Canad. Jnl. of Research A28 , pp.449-474, 1950

(26) "Water and ion movement in thin films as influenced by the electrostatic charge and diffuse layer of cations associated with clay mineral surfaces", W.D. Kemper, Soil Sci. Soc. Amer. Proc., 24, pp.10-16, 1960

(27) "Chloride diffusion in soils as influenced by moisture content", L.K. Porter, W.D. Kemper, R.D. Jackson, B.A. Stewart, Soil Sci. Soc. Amer. Proc., 24, pp.460-463, 1960

(28) "Movement of water as affected by free energy and pressure gradients,I", W.D. Kemper, Soil Sci. Soc. Amer. Proc., 25, No. 4, pp.255-260, 1961

(29) "Movement of water as affected by free energy and pressure gradients, II", W.D. Kemper, Soil Sci. Soc. Amer. Proc., 25, No. 4, pp.260-265, 1961

(30) "Thermodynamics of soil moisture", N.E. Edlefsen, A.B.C. Anderson, Hilgardia, 15, No. 2, 298 pages, 1943

(31) "Chemical problems and calculations", R.H. Gibbs, Edward Arnold (Publ.) Ltd., London, (page 70), 1957

(32) "Hysteresis in moisture content-suction relationships in soils", N. Collis George, Proc. Natl. Acad. Sci., India, 24, pp.80-85, 1955

(33) "Langes handbook of chemistry", Ed. J.A. Dean, 11th Ed., McGraw Hill Book Co., 1973

(34) "Effects of electrostatic fields on the surface tension of salt solutions", G.M. Schmid, R.M. Hurd, E.S. Snavely, Jnl. of the Electrochem Soc. 109, No. 9, pp.852-858, 1962

(35) "Gaseous diffusion in porous media, Part I, II", J.A. Currie, British Jnl. of App. Phys., 11, pp.314-317, pp.318-323, 1960

(36) "Water movement in porous materials, I", D.A. Rose, Brit. Jnl. of Appl. Phys., 14, pp.256-262, 1963

(37) "Water movement in porous materials, II", D.A. Rose, Brit. Jnl. of Appl. Phys., 14, pp.491-496, 1963

(38) "The properties of gases and liquids", R.C. Reid, J.M. Prausnitz, T.K. Sherwood, 3rd Ed., McGraw Hill Book Co., 1977

(39) "Elements of physical chemistry", S. Glasstone, D. Lewis, 2nd Ed., Macmillan & Co. Ltd., 1960

(40) "Diurnal soil-water evaporation: comparison of measured and calculated soil-water fluxes", R.D. Jackson, R.J. Reginato, B.A. Kimball, F.S. Nakayama, Soil Sci. Soc. Amer. Proc., 38, No. 6, pp.861-866, 1974

(41) "Movement of water through soils as influenced by osmotic pressure and temperature gradients", J. Letey, Hilgardia, 39, No. 14, pp.405-418, 1968

(42) "Movement of water as affected by free energy and pressure gradients, III", W.D. Kemper, N.A. Evans, Soil Sci. Soc. Amer. Proc., 27, No. 5, pp.485-490, 1963

(43) "Mobility of water adjacent to mineral surfaces", W.D. Kemper, D.E.L. Maasland, L.K. Porter, Soil Sci. Soc. Amer. Proc., 28, No. 2, pp.164-167, 1964

(44) "Reduction in salt content of solution on passing through thin films adjacent to charged surfaces", W.D. Kemper, D.E.L. Maasland, Soil Sci. Soc. Amer. Proc., 28, pp.318-323, 1964

(45) "Osmotic efficiency coefficients across compacted clays", W.D. Kemper, J.B. Rollins, Soil Sci. Soc. Amer. Proc., 30, No. 5, pp.529-534, 1966

(46) "The effect of osmotic pressure gradients on water movement in unsaturated soil", J. Letey, W.D. Kemper, L. Noonan, Soil Sci. Soc. Amer. Proc., 33, pp.15-18, 1969

(47) "Ion adsorption on charged surfaces", W.R. Heald, M.H. Frere, C.T. De Wit, Soil Sci. Soc. Amer. Proc., 28, No. 5, pp.622-627

(48) "Self-diffusion and structure of liquid water, III", J.H. Wang, C.V. Robinson, I.S. Edelman, Jnl. of Am. Chem. Soc., 75, pp.466-470, 1953

(49) "Electrocapillarity", J.A.V. Butler, Methuen & Co. Ltd., London, 1940

(50) "The principles of electrochemistry", D.A. MacInnes, 2nd Ed., Reinhold Publ. Corp., 1961

(51) "Review of some studies of electro kinetic phenomena", D. Zaslavsky, I. Ravina, Symp. Moisture equilibria and moisture changes in soils, (Butterworths), Australia, pp.55-69

(52) "Treatise on electrochemistry", G. Kortum, 2nd Ed., Elsevier Publ. Co., 1965

(53) "Physical chemistry of surfaces", A.W. Adamson, Interscience Publ., 1960

(54) "Interfacial phenomena", J.T. Davies, E.K. Rideal, 2nd Ed., Academic Press, 1963

(55) "Physical surfaces", J.J. Bikerman, Academic Press, 1970

(56) "Surface chemical properties of clay minerals and soils from theoretical and experimental developments in electro osmosis", H.F. Winterkorn, Symp. on exchange phenomena in soils, Am. Soc. Testing Matls., spec. publ. No. 142, pp.44-52, 1952

(57) "Mass transport phenomena in moist porous systems as viewed from the thermodynamics of irreversible processes", H.F. Winterkorn, Highway Research Board, Spec. Publ., No. 40, pp.324-338, 1958

(58) "Electro osmosis of aqueous electrolyte solutions across pyrex and zeokarb-226 membranes", R.P. Rastogi, K. Singh, J. Singh, R. Kumar, 5th Int. Symp. on fresh water from the sea, 3, pp.51-56, 1976

(59) "Electro osmotic water transport across ion-exchange membranes", A.S. Tombalakian, H.J. Barton, W.F. Graydon, Jnl. of Physical Chem., 66, pp.1006-1009, 1962

(60) "A study of the blocking effect of membranes", G.H. Bishop, F. Urban, H.L. White, Jnl. of Phys. Chem., 35, pp.137-143, 1931

(61) "Fundamental simularities between electro osmotic and thermo-osmotic phenomena", H.F. Winterkorn, Proc. Highway Research Board, 27, No. 1, pp.443- 55, 1947

(62) "Electro osmotic processes in clayey soils and dewatering during excavations", G.M. Lomize, A.V. Netushil, B.A. Rzhanitzin, Proc. of 4th Int. Conf. on Soil Mech. and Foundn. Eng., London, 1, pp.62-67, 1957

CHAPTER FOUR

ELECTROKINETIC PHENOMENA

1. Introduction

Electrical phenomena arise in porous materials because of the uneven attraction of the charged particles (ions, etc.) at the interface of solid-fluid surface, either in the solid, liquid or gaseous states. The differential charge distribution at the interface is most commonly observed in solid-liquid systems. The transfer of charge across the interface can basically occur in two ways, the solid may preferentially adsorb ions of the same polarity from the liquid phase, or alternatively ions may preferentially migrate from the solid into the liquid phase. In either case, an equal but opposite charge appears in the solid and liquid phases, (i.e. the Electrical Double Layer).

Relative motion between the solid and liquid phases gives rise to a series of electrokinetic phenomena, which briefly are (ref.(1) pp.190-195; ref.(2) pp.115-145; ref.(3) p.404):-

(1) Electrophoresis. This is the movement of charged particles through a solution when an electrical potential difference is applied. If the particles are small, i.e. ions, then the phenomena is called ionic conductance, and if the particles are of colloidal size, it is called cataphoresis. For larger molecules, the phenomenon is termed electrophoresis.

(2) Sedimentation potential. This phenomenon is the converse of electrophoresis. When particles move downwards, or bubbles upwards, through a solution, a potential difference is generated between the top and bottom layers of solution.

The two previous phenomena are related to the movement of the solid phase through the liquid phase, if we now consider the movement of the liquid phase through a fixed solid phase, two more electrical phenomena are produced:-

(3) Streaming potential (streaming current). Streaming potential is the potential developed when a liquid is forced

through a porous matrix when no external current is flowing. Streaming current is the current developed when a liquid is forced through a porous material when the potential across the matrix is zero.

(4) Active electro osmosis. As in the case of the two previous phenomena, the second phenomenon is the converse of the previous one, i.e. electro osmosis (active) is the movement of solution with respect to the fixed porous material in response to an externally applied electrical potential difference.

Of the four groups of electrokinetic phenomena, two are of particular interest (electro osmosis and streaming potential) and one is of slight interest (electrophoresis), in relation to Rising Damp. Obviously electro osmosis is of interest since it can be used as a cure for Rising Damp.

Streaming potential is of interest because it is likely to appear as a secondary effect of Rising Damp, being produced by the continual upward movement of ground water to replace that lost by evaporation.

Electrophoresis is of interest since it may also be a contributory factor in curing dampness when an external electrical potential difference is applied. Charged particles, free to move under the influence of the electric field, can become lodged in the narrow necks of the pores in the wall, thus reducing the capacity of the pores to transport water.

Although a permanent reduction in flow capacity, will only occur if the particle becomes permanently fixed in the porous matrix (cementation, consolidation) otherwise when the external field is removed, the particle(s) will become dislodged and the flow capacity will return to its previous value.

2. Electro osmosis

Reuss was first to demonstrate the movement of water through a porous material under the influence of an electric field. Further experiments by Wiedemann and Quinke enabled them to derive a set of empirical rules of electro osmosis (ref.(3) p.411). These basic rules were theoretically accounted for by Helmholtz, who also introduced the concept of the "double layer". The double layer concept was developed by Gouy and several other workers (ref.(1) p.181). The historical development of electro-osmosis has also been discussed by Fairbrother and Mastin[4].

The Gouy concept of a diffuse double layer and the corresponding theory is still the most acceptable explanation of electrokinetic phenomena. Although additional modifications of Gouy's theory have been introduced by Stern and other workers (ref.(1) page 184; ref.(2) p.79; ref.(3) p.371; ref.(5) p.75; ref.(6) p.389), the original Gouy theory is sufficient to provide an explanation of the electrokinetic phenomena.

3. Calculation of the electro osmotic effect

The distribution of charged particles in the diffuse double layer and the associated electric potential field is represented schematically in Fig. 1. Note that in the figure it is assumed that the solid surface is positively charged.

When an external electric field is applied in a direction parallel to the solid surface part of the diffuse double layer is induced to move. It is assumed that the motion is laminar and that after a short period of time, a thickness dx will move with a steady velocity, u. The net force acting upon this layer is therefore zero, i.e. the electrical force is balanced by the viscous drag force.

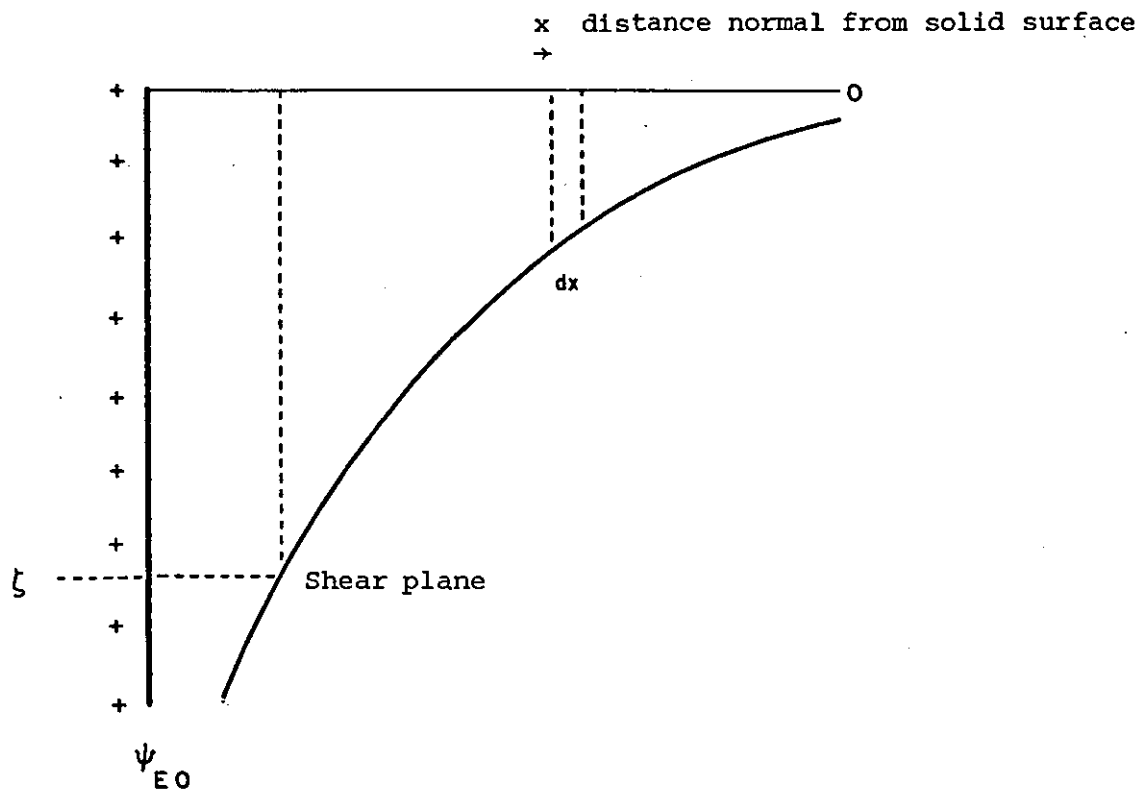

Fig. 1. Simplified representation of the change in electrical potential in a fluid, adjacent to a positively charged surface.

The electrical force, F_E, per unit area is expressed by

$$F_E = \nabla E\ (\sigma)'\ dx \tag{1}$$

where ∇E is the electrical potential field and $(\sigma)'$ is the volumetric charge density.

The viscous force for the layer, dx is expressed as

$$-F_\mu = \mu\left(\frac{\partial u}{\partial x}\right)_{x+dx} - \mu\left(\frac{\partial u}{\partial x}\right)_x = \mu\ \frac{\partial^2 u}{\partial x^2}\ dx \tag{2}$$

For steady state conditions equation (1) and (2) yield

$$\nabla E(\sigma)' = \mu\ \frac{\partial^2 u}{\partial x^2} \tag{3}$$

where u is the field velocity and μ is the fluid viscosity.

Assuming the existence of a Poisson equation, i.e.

$$\nabla^2\psi_E = -\frac{4\pi(\sigma)'}{\varepsilon} \tag{4}$$

where ψ_E is the electrical potential associated with the charged surface; ε, the dielectric constant of the fluid: then equation (4) can be used to eliminate the volume charge density from equation (3), so

$$-\frac{\nabla E\varepsilon}{4\pi}\ \frac{\partial^2\psi_E}{\partial x^2} = \mu\ \frac{\partial^2 u}{\partial x^2} \tag{5}$$

Note the Laplacian opperator, $\nabla^2 (= \frac{\partial^2}{\partial x^2} + \frac{\partial^2}{\partial y^2} + \frac{\partial^2}{\partial z^2})$ has been replaced by the derivative, $\frac{\partial^2}{\partial x^2}$, since there is no potential in the y, z directions. In fact, in these directions, it is assumed that the solid surface extends indefinitely.

On integration of equation (5) between the limits of $x = \infty$ and the slip surface, together with the boundary conditions,

$$x = \infty \qquad u_\infty = u \quad \left(\frac{\partial u}{\partial x}\right)_\infty = 0 \quad \psi_{E\infty} = 0 \quad \left(\frac{\partial \psi_E}{\partial x}\right)_\infty = 0 \tag{6}$$

$$x_{\text{slip surface}}\ u_{\text{slip surface}} = 0 \quad \psi_{E\ \text{slip surface}} = \zeta$$

we may obtain

$$u = \frac{\varepsilon \zeta \nabla E}{4\pi\mu} \tag{7}$$

where u is the steady laminar fluid velocity; ε, the dielectric constant; ∇E, the applied electric field strength; μ, the fluid viscosity; ζ, the "zeta" potential which is normally assumed to represent the electric potential of the shear surface and is regarded as a constant for any solid-fluid system assuming the concentration of solution remains constant (ref.(2) p.120; ref.(5) p.122; ref.(6) p.434).

Similar derivations to the one presented above can be found in the literature (ref.(1) p.192; ref.(2) p.114; ref.(3) p.411; ref.(6) p.424; ref.(7)).

In electro osmotic measurements, it is not the velocity in the middle of the pore that is determined but the volume transported in unit time. The expression for the volumetric flow rate of electrically induced flow Q_E is

$$Q_E = u A_1 = \frac{\varepsilon \zeta \nabla E}{4\pi\mu} A_1 \tag{8}$$

where A_1 is the cross-sectional area for flow which for a cylindrical capillary of radius, r, is simply πr^2. In this expression, it is assumed that the velocity is uniform throughout the cross-section of the pore. However, the velocity near the walls is lower than the mean velocity, in the pore, u. Equation (8) is therefore correct only if A_1 is large with respect to the area in the double layer which remains immobile. Noting that, generally, the thickness of the double layer is of the order of 10^{-5} cm. Winterkorn[8] stated that the Helmholtz theory was no longer applicable to pores of less than 0.05μm (5×10^{-6}cm), and Despic et al[9] also stated that the Helmholtz theory was not applicable to pores of approximately molecular dimensions.

For fine pored porous materials Schmid (found in ref.(8)) proposed an alternative theory. He assumed that the counterions to the wall charged were not concentrated in a diffuse double layer or even a simpler layer but are uniformly distributed throughout the entire liquid volume. The applied potential was assumed to act upon all the counterions rather than a fraction of them as determined by the slip-plane in the Helmholtz theory.

The electrical force, F_E, acting upon the fluid in a capillary of radius, r, and unit length, ℓ, was expressed as

$$F_E = \pi r^2 \ell (\sigma)' \nabla E \tag{9}$$

where $(\sigma)'$ is the volume charge density and ∇E, the applied electric potential field. If this electrical force is substituted into Poiseuille's equation (Chapter three eqn. (7)) then

$$Q_E = \frac{\pi r^4}{8\mu} (\sigma)' \nabla E \tag{10}$$

where Q_E is the volumetric flow of electrical induced moisture; μ, the viscosity of the fluid; $(\sigma)'$, the volumetric charge density of the fluid; ∇E, the applied electric field strength.

The effect of electro osmosis can also be studied via a mechanistic approach to the phenomenon. The fluid in the porous material contains ions of both polarities, and also of different valencies. Assuming, as before, that the solid surface is positively charged, then an excess of negatively charged ions will exist in the solution.

When an electrical potential difference ΔE is applied across the electrodes which are assumed to be a distance ℓ apart, an electric field, ∇E may be defined thus

$$\nabla E = -\frac{\Delta E}{\ell} \tag{11}$$

The force acting upon the water per unit volume, because of the ions present within the water is

$$F_E = \nabla E\ (\sigma)' \tag{12}$$

When steady state is attained, the same force is acting upon the solid skeleton of the porous matrix but in opposite direction to the acting upon the liquid solution, i.e. there is no net force on the porous matrix. To establish a linear relation between the field, ∇E, and the water discharge, Q_E, it must be assumed that the steady flow be proportional to the force, F_E,

$$Q_E \sim F_E = \nabla E\ (\sigma)' \tag{13}$$

The water discharge, Q_E is simply defined as (V/A), i.e. the volume of water per unit time passing through the porous matrix divided by the total cross-sectional area available for flow.

To satisfy the condition of linear proportionality as expressed in equation (13), several requirements are needed which briefly are:- (i) independence between $(\sigma)'$ and ∇E; (ii) that the water discharge be linearly proportional to the frictional stress of the liquid and solid; (iii) that both ∇E and $(\sigma)'$ be independent of the velocity distribution; (iv) independence between the viscosities and rates of shear[7].

It is important to note that the derivation of the electro osmotic effect, as presented in equations (1) through (8) is related to the c.g.s. system of units. Unfortunately the values of the electrical units of this system, (i.e. electric potential, electric charge, etc.) are different to those of the S.I. system, which are in "everyday' use. To distinguish between the S.I. units and the c.g.s. units, the c.g.s. electrical units will be preceded by the word "stat", as in electrostatic. Hence the volt (S.I.) is expressed as a statvolt (c.g.s.) and likewise the unit of charge, the coulomb becomes a statcoulomb. Other electrical properties are similarly named. The conversions factors of several common electrical units can be found in Appendix I.

Furthermore, to convert from the c.g.s. system to the S.I. system, slight adjustment of equations (4) through (8) is required. The adjustment is needed because of a fundamental difference in the definition of Coulomb's Law between the two systems of units. Coulomb's Law relates the force of attraction or repulsion between charged particles and the distance separating them. This basic difference is reflected in the formulation of the Poisson equation (eqn.(4)), which in the S.I. system is expressed as[10]

$$\nabla^2\psi_E = -\frac{(\sigma)'}{\varepsilon'\varepsilon_0}$$

where ε_0 is the permittivity of free space and has the value of 8.854×10^{-12} (Faraday metre^{-1} or coulombs^2 Newton^{-1} metre^{-2}). ε is the dielectric constant of the medium, which is the ratio of the value of the dielectric constant of the medium to that of free space. The other symbols have their usual meaning except that their units are now expressed with reference to the S.I. system.

The equation corresponding to equation (7), in the S.I. system of nomenclature becomes

$$u = \frac{\varepsilon'\varepsilon_0\zeta\nabla E}{\mu}$$

An example demonstrating the calculation of the electrically induced fluid velocity for both types of systems can be found in Appendix II.

4. Electro osmosis in porous materials and electro osmotic coefficient

Utilising the assumption of the previous section, an electro osmotic coefficient, k_E, may be defined thus

$$\frac{Q_E}{A} = k_E \nabla E \qquad (14)$$

where Q_E is the electro osmotic volumetric flow; ∇E, the applied electric field; k_E, the electro osmotic coefficient; A, the area

for flow including both the pores and solid material.

Using the above expressed, together with the Helmholtz flow velocity (eqn.(8)), the electro osmotic coefficient of a porous material, possessing a uniform porosity, ϕ, can be defined thus

$$k_E = \frac{\varepsilon \zeta \phi}{4\pi\mu} \tag{15}$$

Note, the actual area for liquid flow, A_1, is given by ϕA, where ϕ represents the porosity; and the proportionality coefficient relating Q_E to ∇E in equation (13) is defined as the electro osmotic coefficient. Care must be exercised, when using values for k_E, to determine whether k_E has been determined with respect to the pore flow area or whether k_E has been determined with respect to the total flow area.

5. Coupled flow of water and electricity through porous materials

Neglecting flow interactions produced by salt and temperature gradients together with their respective fluxes, the expressions describing the coupled flow of moisture and electricity within porous materials is[11][12][13]

$$J_V = -K_{11}\nabla\psi_P - K_{12}\nabla E \tag{16}$$

$$I = -K_{21}\nabla\psi_P - K_{22}\nabla E \tag{17}$$

where J_V is the macroscopic mean water velocity; I, the electrical current density; $\nabla\psi_P$, the hydraulic pressure head gradient; ∇E, the applied electric field gradient; K_{11}, the hydraulic conductivity; K_{12}, the electro osmotic coefficient (which is equivalent to k_E); K_{21}, the hydraulic coefficient; K_{22}, the electrical conductivity coefficient. Note that all the coefficients and fluxes are defined with respect to the whole of the porous material flow area. It is assumed that in eqns. (16),(17) the fluxes are linearly related to the corresponding potential fields.

It has been shown[7] that it is possible to define several so called electro-hydraulic coefficients, however, assuming Onsager's reciprocal law is applicable, only three of the flow coefficients are independent of each other namely K_{11}, K_{22} and either K_{12} or K_{21}, since they are interdependent upon each other.

6. Discussion of some electro kinetic phenomena

(1) Electro osmosis. The phenomenon of electro osmosis has been discussed in Section 3. of this chapter. It is evident from consideration of equation (16) that there should be no difference in hydraulic head across the porous material, ($\nabla\psi_P = 0$) when the electro-osmotic coefficient, K_{12}, is determined, i.e.

$$J_V = -K_{21} \nabla E \tag{18}$$

Similarly, from equation (17), the electrical current density required to drive the above liquid flow is

$$I = -K_{22} \nabla E \tag{19}$$

(2) Electro osmotic counter pressure. This phenomenon is very similar to that of electro osmosis. The only difference between the two phenomena is that instead of observing liquid flow with zero pressure gradient, the pressure gradient now is adjusted until there is no liquid flow. The pressure difference observed across the porous material when there is zero flow is called the electro osmotic counter pressure. Using equation (16), the electro osmotic pressure expressed in terms of field strength is

$$\nabla\psi_P = \frac{-K_{12}}{K_{11}} \nabla E \tag{20}$$

The electrical current density associated with the electro osmotic counter pressure can once again be obtained from eqn. (17) and if it is assumed that the electrical current density associated with this pressure potential is small ($I = -K_{21} \nabla\psi_P$ tends to zero)

when compared to the 'applied' electrical current density, then the applied current density is again represented by equation (19).

(3) Streaming current and streaming potential. When a liquid is forced through a porous material by a pressure gradient, ∇P, a part of the charged diffuse double layer is swept along with the liquid. By definition, this movement gives rise to an electrical current, namely the streaming current. In relation to the Gouy diffuse layer theory presented in Section 3. the expression for the current (ref.(2) p.119; ref.(3) p.416)

$$I'_{STR} = \frac{\varepsilon \zeta}{4\pi\mu} A_1 \nabla P \qquad (21)$$

where I'_{STR} is the streaming current; A_1, the area available for liquid flow; ε, the dielectric constant; μ, the viscosity of the fluid; ∇P, the pressure gradient.

If the liquid contained an excess of cations (positively charged particles), then a reservoir downstream of the porous material will become positively charged with respect to the upstream reservoir. This imbalance will produce a second electric current which, contrary to the first, utilises the whole of the cross-sectional area of each pore. If ΔE is the potential between the two reservoirs, then the expression for this current is

$$I'_2 = \kappa \frac{A_2}{\ell} \Delta E \qquad (22)$$

where κ is the electrical conductivity of liquid in the pores. Note the solid is assumed to be a perfect insulator. A_2 is the area available for back ionic flow; ℓ, the length of the porous material.

When steady state conditions have been attained, and no external current is flowing in the system, then I_2 must be equal and opposite to I_{STR}, consequently

$$\nabla E_{STR} = \frac{\Delta E}{\ell} = \frac{\varepsilon\ \zeta\ \nabla P}{4\pi\ \mu\ \kappa}\ \frac{A_1}{A_2} \tag{23}$$

where ∇E_{STR} is the streaming potential, expressed as a field strength.

Comparison of eqns. (17) and (21) when no external field is applied (i.e. $\nabla E = 0$), shows that the streaming current density to be given by

$$I_{STR} = -K_{21}\ \nabla\psi_P$$

with (24)

$$K_{21} = \frac{\varepsilon\ \zeta\ A_1}{4\pi\ \mu\ A}\ \rho_\omega\ g$$

where A is the area available for flow of the whole of the porous material; ρ_ω, is the density of the liquid; g, the gravitational acceleration. Note that the pressure gradient, ∇P, has been expanded into $\rho_\omega g \nabla\psi_P$.

The flow of water required to produce the streaming current density (c.f. eqn.(16) and note $\nabla E = 0$)

$$J_V = -K_{11}\ \nabla\psi_P \tag{25}$$

Furthermore, the expression for the streaming potential, from eqn.(17) noting that $I = 0$ is given by

$$\nabla E_{STR} = \frac{K_{21}}{K_{22}}\ \nabla\psi_P \tag{26}$$

The expression for the coefficient K_{21} has been expressed above. The value of K_{22} is obtained from eqn.(22)

$$I = \frac{I_2}{A} = \kappa\ \frac{A_2}{A}\ \nabla E = K_{22}\ \nabla E \tag{27}$$

where A is the cross-sectional area of the whole of the porous material; ∇E, the electrical potential gradient (i.e. ΔE divided by ℓ).

7. Electrical conductivity of the porous matrix system

The electrical conductivity of a porous material system is important since it directly affects the values of both the electro-osmotic flow and streaming potential. By combining eqns.(18),(19) to eliminate ∇E, the electro osmotic flux is given by

$$J_V = \frac{K_{12}}{K_{22}} I \tag{28}$$

Similarly the expression describing the value of the streaming potential (eqn.(26)) also contains the electrical conductivity coefficient, K_{22}. It is obvious that as K_{22} increases, then both the electro osmotic flux and streaming potential will decrease, provided the values of the other variables remain constant.

Under normal circumstances, electricity can be conducted by the solid phase and the liquid phase of the porous system, but it has been assumed that the solid phase is a perfect insulator, and hence the magnitude of the electrical conductivity coefficient will be governed solely by conductivity in the liquid phase.

The liquid phase conductivity is comprised of two parts. One component is the normal (bulk) conductivity of the solution as determined in a concentration cell. The other is an additional increment associated with the charged layer at the solid-liquid interface. This increment is known as surface conductivity. A brief description of surface conductivity can be found (ref.(2) p.208; ref.(3) p.418). For present purposes, however a detailed description of surface conductivity will not be required since it is assumed that the variation of surface conductivity with solute concentration is small and that the variation of the electrical conductivity coefficient, K_{22}, is governed by the concentration of ionic salts in the bulk liquid.

Noting that as the bulk salt concentration is increased, the value of K_{22} is also increased, which correspondingly reduces the

efficiency of the electro osmotic effect (i.e. cm^3 of moisture moved per stat amp of current). Likewise as the value of K_{22} is increased, the value of the streaming potential is correspondingly decreased.

List of symbols and units of Chapter Four

A	area of a porous material (cm^2)
A_1	area of a porous material available for liquid flow (cm^2)
A_2	area of a porous material available for bulk-ionic flow (cm^2)
E	applied voltage (stat volt)
∇E_{STR}	stream potential gradient (stat volt cm^{-1})
g	gravitational acceleration (cm sec^{-2})
I_{STR}	streaming current density (stat amp cm^{-2})
I'_{STR}	streaming current (stat amp)
I'_2	back-ionic current flow (stat amp)
J_V	macroscopic mean fluid velocity (cm sec^{-1})
K_{11}	Hydraulic conductivity (cm sec^{-1})
K_{12}	electro osmotic coefficient (cm^{-2} sec^{-1} stat $volt^{-1}$)
K_{21}	hydraulic coefficient (stat amp cm^{-2})
K_{22}	electrical conductivity coefficient (stat $ohm^{-1}cm^{-1}$)
k_E	electro osmotic coefficient (cm^2 stat $volt^{-1}$ sec^{-1})
ℓ	length of a porous material (cm)
∇P	applied pressure gradient (g cm^{-2} sec^{-2})
Q_E	electricity induced volume flow rate of moisture (cm^3sec^{-1})
u	fluid velocity (cm sec^{-1})
ε	dielectric constant (stat $coulomb^2sec^2g^{-1}cm^{-3}$)
ε_o	permittivity of free space (stat $coulomb^2sec^2g^{-1}cm^{-3}$)
ε'	ratio of the dielectric constant of the medium to that of free space
ζ	zeta potential (stat volt)
κ	electrical conductivity of liquid within the pores of a porous material (stat ohm^{-1} cm^{-1})
μ	viscosity of the fluid (g cm^{-1} sec^{-1})
ρ_ω	density of the fluid in the liquid phase (g cm^{-3})
$(\sigma)'$	volumetric charge density of the fluid (stat coulomb cm^{-3})

ψ_E electrical potential owing to the proximity of a charged surface (stat volt)

ψ_P pressure head of fluid (cm)

References Chapter Four

(1) "Physical chemistry of surfaces", A.W. Adamson, Interscience Publ., 1960

(2) "Interfacial phenomena", J.T. Davies, E.K. Rideal, 2nd Ed. Academic Press, 1963

(3) "Physical surfaces, J.J. Bikerman, Academic Press, 1970

(4) "Studies in electro-endosmosis, Part I", F. Fairbrother, H. Mastin, Jnl. of Chem. Soc., 24, pp.2319-2330, 1924

(5) "Electrocapillarity", J.A.V. Butler, Methuen & Co. Ltd., London, 1940

(6) "Treatise on electrochemistry", G. Kortum, Elsevier Publ. Co. Ltd., 2nd Ed., 1965

(7) "Review of some studies of electrokinetic phenomena", D. Zaslavsky, I. Ravina, Symp. Moisture equilibria and moisture changes in soils, (Butterworths), Australia, pp.55-69

(8) "Surface chemical properties of clay minerals and soils from theoretical and experimental developments in electro osmosis", H.F. Winterkorn, Symp. on exchange phenomena in soils, Am. Soc. Testing Matls., spec. publ. no. 142, pp.44-52, 1952

(9) "Electro osmosis in charged membranes", A. Despic, G.J. Hills, Disc. of the Farad. Soc., No. 21, pp.150-162, 1956

(10) "Electrolyte theory and S.I. units", R.I. Holliday, Jnl. of Chem. Education, 53, pp.21-22, 1976

(11) "On electro osmosis and streaming potentials in diaphragms", J. Th. G. Overbeek, P.W.O. Wijga, Rec. Trav. Chim., 65, pp.556-563, 1946

(12) "On electro-osmosis and streaming potentials in diaphragms", P. Mazur, J.Th.G. Overbeek, Rec. Trav. Chim., 70, pp.83-91, 1951

(13) "Cross-phenomenological coefficients, III Studies on electro-osmosis", R.P. Rastogi, K.M. Jha, Jnl. of Phys. Chem., 70, No. 4, pp.1017-1024, 1966

Appendix I

Conversion factors of several common electrical units

quantity	S.I. unit	electrostatic - cgs unit
electric charge	1 coulomb	2.9979×10^{9}
current	1 ampere	2.0079×10^{9}
voltage	1 volt	3.3356×10^{-3}
resistance	1 ohm	1.11263×10^{-12}

Appendix II

Calculation of the electro osmotic velocity.

Assumptions

applied voltage gradient, $\nabla E = 100$ ($v\ m^{-1}$)

zeta potential, $\zeta = 0.1$ (v)

dielectric constant, $\varepsilon = 80$

fluid viscosity, $\mu = 10^{-3}$ ($N\ s\ m^{-2}$)

permittivity of free space, $\varepsilon_o = 8.854 \times 10^{-12}$ ($C^2\ N^{-1}\ m^{-2}$)

(i) S.I. system

The expression representing the electro osmotic fluid velocity, u, is

$$u = \frac{\varepsilon' \varepsilon_o \zeta\ \nabla E}{\mu}$$

$$= \frac{80 \times 8.854 \times 10^{-12} \times 0.1 \times 100}{10^{-3}}$$

$$= 7.0832 \times 10^{-6}\ (m\ s^{-1})$$

(ii) cgs system

The expression representing the electro osmotic fluid velocity, u, is

$$u = \frac{\varepsilon\ \zeta\ \nabla E}{4\pi}$$

Note, the figures in parentheses represent conversion factors.

$$u = \frac{80 \times 0.1 \times (3.3356 \times 10^{-3}) \times 100 \times (10^{-2} \times 3.3356 \times 10^{-3})}{4\pi \times 10^{-3} \times (10)}$$

$$= 7.08317 \times 10^{-4}\ (cm\ s^{-1})$$

$$= 7.08317 \times 10^{-6}\ (m\ s\text{-}1)$$

The calculations show that the electro osmotic velocity to be same irrespective of the unitary system.

CHAPTER FIVE

EVAPORATION

1. Introduction

Evaporation of moisture from walls is an important part of the phenomenon of Rising Damp because evaporation plays a major part in determining the flow of moisture up a wall; the severity of moisture in the wall; and the additional problem of salts, either at the wall surface or in the interior of the wall.

Evaporation can be regarded as a naturally occurring example of 'drying of porous materials' albeit under much less harsh drying conditions.

There is a wide variety of methods of indirectly estimating evaporation. The methods range from the purely empirical to the highly theoretical. In addition several of the methods have been developed to estimate evaporation from large horizontal surfaces (fields, lakes) and for particular types of ground cover (crops). Obviously these methods cannot be modified to estimate evaporation from damp walls; even so there still remain several methods which can be modified to estimate evaporation from damp walls, although they almost all present the additional difficulty of estimating evaporation from a vertical surface rather than a horizontal one. In fact the close proximity of the ground surface doubly complicates this new problem.

Another complication is that evaporation can occur both from internal and external walls of buildings. Evaporation from external walls is characterised by atmospheric conditions similar to those occurring at other external surfaces (e.g. fields, lakes, etc.) whilst evaporation from internal surface is more closely related to evaporation into 'still' air. These differing conditions necessitate the development of different approaches to the problem of estimating evaporation, although some methods may be used to estimate evaporation under both types of conditions.

The description of the drying process and method of estimating evaporation is preceded by a section devoted to the terminology associated with evaporation and drying processes. This is followed by a section describing the moisture redistribution and moisture movement towards the evaporating surface. The chapter is concluded by a discussion of several methods of estimating evaporation, both at internal and external locations. However, there has been no attempt to specifically develop the evaporation methods with respect to Rising Damp.

2. Terminology

2.1 Water vapour pressure

Dalton's Law of partial pressures states that the presure exerted by a vapour (gas) is independent of the pressure exerted by the other gases present. Assuming that a fixed mass of water vapour behaves as an ideal gas, the water vapour pressure, p, can be represented by

$$p = \frac{\rho_v}{M_W} R_m T \qquad (1)$$

where ρ_v, the density of water vapour; M_W, the molecular weight of water; R_m, the universal gas constant per mole; T, the absolute temperature; p, the vapour pressure of water.

2.2 Saturated vapour pressure

When a liquid and its vapour are enclosed, a dynamic equilibrium is established whereby the number of molecules leaving the liquid is balanced by the number of molecules returning to the liquid. When the equilibrium is attained the vapour is said to be saturated. The vapour pressure is the maximum possible for the particular temperature of the enclosed system and the vapour is known as the saturated vapour pressure (s.v.p.) denoted here by the symbol, p_{as}.

It should be remembered that presence of solute within the water and curvature of the water-gas interface both affect the vapour pressure, and thus s.v.p. is normally associated with pure solvent and a flat liquid-gas interface. The variation of s.v.p. and temperature under these conditions is show in Fig. 1.

2.3 Saturation deficit

For a space in which the vapour pressure p is less than the s.v.p. p_{as} at the temperature, T, (Fig. 1) the saturation deficit is given by the difference $(p_{as}-p)$.

2.4 Relative humidity

It is defined as the ratio

$$h = \frac{p}{p_{as}} \quad \text{where } p < p_{as}$$

The ratio may sometimes be expressed as a percentage, i.e.

$$h = 100 \times (p/p_{as}) \text{ percent}$$

2.5 Absolute humidity or vapour density

The vapour density, ρ_v, in eqn. (1) is sometimes referred to as the absolute humidity.

2.6 Specific humidity

The specific humidity, q, is defined as the ratio of the mass of water vapour per unit mass of dry air and associated water vapour.

2.7 Humidity

The humidity, H', of moist air is the ratio of the mass of water vapour to the mass of dry air. The humidity may also be called the mixing ratio.

In unit volume of gaseous mixture (air-water vapour), the mass of vapour (water) is given by $(p.M_W)/(R_m.T)$. The mass of non-condensibles (air) is $(M_A.(P-p))/(R_m.T)$. Therefore the humidity, H', is defined as

$$H' = \left(\frac{p}{P-p}\right) \frac{M_W}{M_A} \tag{2}$$

Similarly the humdity of saturated gaseous mixture H'_s is

$$H'_s = \left(\frac{p_{as}}{P-p_{as}}\right) \frac{M_W}{M_A} \tag{3}$$

where M_W is the molecular weight of the vapour; M_A, the molecular weight of non-condensible gas; p, p_{as} is the vapour pressure and saturated vapour pressure; P, the total pressure.

For an air-water system, p, p_{as} are often small when compared to the total pressure, P, and hence eqn.(2) may be written as

$$H' = \left(\frac{p}{P}\right) \frac{M_W}{M_A}$$

The humidity may also be expressed as a ratio, normally as a percentage, i.e.

percentage humidity = $(H'.100)/(H'_s)$

which from eqn.(1),(2),(3) may be expressed as

$$= \left(\frac{P-p_{as}}{P-p}\right) \times (h \times 100) \tag{4}$$

2.8 Dew point temperature

The dew point temperature can be illustrated with reference to Fig. 1. Consider a fixed mass of partially saturated air-water vapour mixture, initially at temperature T, to be cooled at constant pressure and without any gain or loss of water vapour (constant H'). On re-arrangement of eqn.(2) it can be shown that

$$p = \frac{H'.\ P.\ M_A}{(M_W + M_A\ H')} \tag{5}$$

For constant total pressure, P and humidity, H', the right hand side of equation (5) is constant. Thus on cooling the air-water vapour mixture (initially at temperature T, denoted by A in Fig. 1), point A is moved horizontally to the left. Eventually the locus of point A will intersect the s.v.p. curve. The temperature corresponding

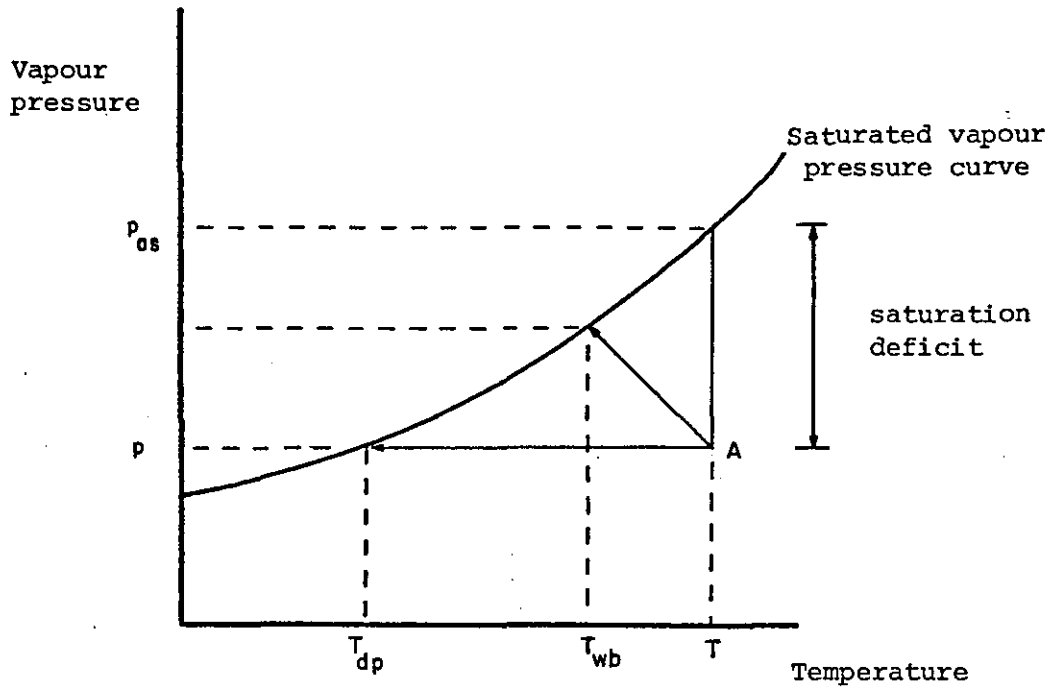

Fig. 1. The saturation vapour pressure of water shown as a function of temperature.

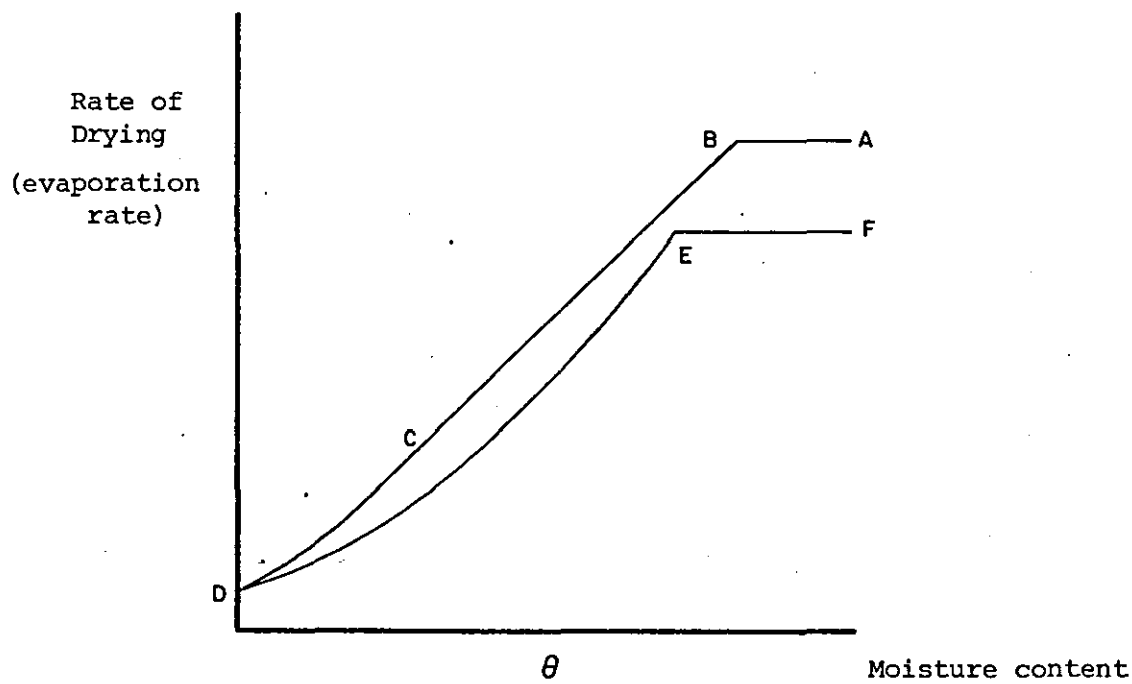

Fig. 2. Rate of drying curves of porous materials.

to the point of intersection is called the dew point temperature, T_{dp}.

2.9 Wet bulb temperature

The wet bulb temperature can also be illustrated with reference to Fig. 1. Consider the cooling of air as it flows over a wet surface. If point A (Fig. 1) represents the intial state of such an air flow, then evaporation of moisture into the air stream will increase the vapour pressure and simultaneously reduce the air stream temperature. Such a change can be represented by a path inclined upwards and to the left of A. The temperature at which this path intersects the s.v.p. curve will depend somewhat on the conditions of the air flow. The temperature of intersection is decreased as the air flow rate is increased. However, for air velocities greater than 2 metres per sec., a small wet surface achieves a steady lower temperature, which is rather insensitive to further increases in flow rate provided the small wet surface is to some extent thermally isolated from its surroundings. This steady lower temperature is defined as the wet bulb temperature, T_{wb}, corresponding to state A.

3. The drying process

3.1 Description of the drying process. External observations.

Originally the drying process within porous materials was thought to be purely diffusive in character [1] [5] [6] with moisture movement obeying Fick's laws of diffusion [7] :-

$$u = D \frac{\partial \theta}{\partial x} \tag{6}$$

$$\frac{\partial \theta}{\partial t} = D \frac{\partial^2 \theta}{\partial x^2} \tag{7}$$

where u is the velocity of moisture; θ, the volumetric moisture content; D, the diffusion coefficient; x, distance.

The diffusion coefficient was assumed to be constant and independent of moisture content. The results obtained for fine-pored porous materials (clays, soap, wood) tended to confirm the assumption. However, for coarser-pored materials Fick's laws were found to be inadequate to simultaneously predict the flux of moisture and corresponding moisture gradient. The moisture flow occurring in coarser-pored materials was shown to be determined initially by interfacial (capillary) forces and in the latter stages of drying by diffusional forces. The shape of the drying curve varies with the structure and type of material. Two typical shapes of drying curves are illustrated in Fig. 2.

In curve (1) there are three well defined stages; A-B constant rate of drying, B-C first falling rate period where the drying rate decreases linearly with moisture content, and C-D second falling rate period where the decrease in drying rate with respect to moisture content is no longer constant.

For curve (2), F-E represents the constant rate period which is similar to the region A-B of curve (1). The section E-D (curve (2)) is similar to the portion C-D of curve (1), there being no zone of linearly decreasing drying rate. Curve 2 is characteristic of the drying of fine pored porous materials (e.g. soap, clay, wood). Curve (1) is characteristic of coarser pored materials (e.g. sand, loam). The moisture content corresponding to points B, E is the respective critical moisture content of the material, the significance of which is discussed later.

3.2- Constant rate period

During the constant rate period evaporation is assumed to take place at the surface of the wet solid. The rate of drying is limited by the rate of diffusion of water vapour through a stationary air film near the solid curface. Drying in this period is similar to the evaporation from a free liquid surface[8]. The

solid assumes a constant equilibrium temperature, just as a free liquid surface is maintained at the wet bulb temperature of the air. When the heat required for vaporisation is supplied only by conduction through the same surface gas film through which water vapour diffuses, the solid surface temperature is the same as the wet bulb temperature of the air. When additional heat is supplied by radiation, or conduction through the solid, the solid surface temperature is higher than the wet bulb temperature, also the rate of drying is consequently increased[2] [9].

Experiments by Powell and Griffiths[10] have shown that the rate of evaporation is affected by the dimensions of the drying surface and the tangential air velocity across the surface. For air velocities between 100 and 300 cm per sec, the overall evaporation rate, $E_{v\ell b}$ is given by

$$E_{v\ell b} = 2.12 \times 10^{-7} \ell^{0.77} B(p_{es}-p_a)(1 + 0.121 u^{0.85}) \quad (8)$$

and for air velocities less than 100 cm per sec

$$E_{v\ell b} = 4.3 \times 10^{-7} \ell^{0.77} B^{0.8} (p_{es}-p_a)(1 + 0.121 u^{0.85}) \quad (9)$$

where $E_{v\ell b}$ is the overall rate of evaporation (g sec^{-1}) for a surface of ℓ (cm) and width B (cm). p_{es} is the saturation vapour pressure at the temperature of the surface and p_a is the vapour pressure of water in the bulk air stream, both are expressed in m.m. of mercury. u is the tangential air velocity (cm.sec^{-1}).

The variation of evaporation rate with respect to the dimensions of the wet surface has also been discussed by Powell[11] and Chakravorty[12].

Evaporation from a wet surface will remain constant, until a situation is reached, when moisture from the interior of the porous material is unable to migrate to the surface at a sufficient rate to replace that lost by evaporation. The moisture content that determines the end of the constant rate period and the onset of the falling rate period is called the critical moisture content.

It is affected by the structure and type of porous material, and also by bed conditions which affect the moisture content and the moisture conductivity of the material (temperature, salt content). Assuming that the bed conditions remain the same, then the rate of evaporation will also affect the critical moisture content since to sustain a higher evaporation rate, a higher fluid conductivity (and hence a higher moisture content) is required.

3.3 First falling rate period

The points B-C in Fig. 2 curve (2) represent the condition where the porous material is unable to supply sufficient moisture to saturate the air in close contact with it. It is believed that the linear decrease in drying rate after the critical point is due to a decrease in the surface actually wetted[(2) (3) (5) (13)]. The rate of drying per unit of free liquid surface does not decrease, but as the network of raised portions of the solid dry, the rate of drying per unit total surface area decreases. The belief that the zone of evaporation is still at the solid surface has been confirmed by the work of Sherwood[(2) (5)], who by monitoring the temperature gradients within the porous material and subsequently calculating the overall heat transfer coefficient, showed it to remain essentially constant. From this result Sherwood inferred that there was no change in the thermal resistance of the process (evaporation still at the surface).

Since evaporation is still occurring at or very near to the surface, in this drying period, the rate of evaporation will be greatly influenced by the external climatic conditions (surface temperature, air humidity and air velocity)[(2) (5) (13) (14)].

3.4 Second falling rate period

When the zone of evaporation has receded into the interior of the porous material, migration of moisture to the solid surface, can

only occur by diffusion of vapour, and obviously the overall process of evaporation will predominantly become diffusion controlled. The evaporation rate now being inversely proportional to the distance between the solid surface and the constantly receding zone of internal evaporation. Eventually the process of vapour diffusion will also cease. The remaining moisture content, when no further loss of moisture occurs, is called the equilibrium moisture content. The value of this moisture content is determined by the solid structure, by the humidity of the external air stream, and by the salt content of the remaining moisture, which is in equilibrium with the moisture in the bulk air stream.

3.5 Description of the drying process. Internal considerations[4] (5) (13)-(16)

Consider a totally saturated porous material (i.e. suction in the liquid is zero), which is allowed to dry in a stream of air. Initially the suction increases rapidly with only a corresponding slight decrease in moisture content owing to the formation of liquid menisci at the surface.

Eventually the curved liquid surface in the largest pore collapses and air replaces the liquid which is redistributed throughout the porous material. This redistribution of liquid causes a slight reduction in liquid suction. However, the suction recovers rapidly and as drying continues more and more of the finer pores at the surface area emptied. Secondary emptying of larger sized pores below the surface may occur when the suction at that level is sufficient to rupture any air-water meniscus present.

Assuming the frictional forces associated with moisture flow to be negligible then the suction at a distance, z, below the surface is given by

$$h_{wz} = h_{ws} + \rho_{\omega} g z \qquad (10)$$

where h_{wz} is the suction at a vertical distance, z, below the surface; h_{ws}, the suction at the surface; ρ_{ω}, the density of the liquid; g, the gravitational acceleration.

As drying proceeds, fluid conductivity in the liquid phase is restricted to the finer pores and to the films of water adjacent to the solid surfaces of the larger pores. When secondary emptying below the surface becomes widespread, rapid desaturation of the porous material occurs at approximately constant suction; and provided that there is still sufficient liquid conductivity to the surface, the evaporation rate and surface temperature will remain constant[13].

Eventually, liquid continuity will become less than that required to maintain the constant rate of evaporation and consequently partial drying of the wetted surface will occur. This condition marks the onset of the first (linear) falling rate period, which is characterised by an increase in surface suction and a more rapid increase in the rate of liquid suction.

As drying proceeds moisture at the surface will become isolated from the rest of the liquid; i.e. liquid conductivity has failed and the saturation regime has changed from funicular to pendular. The isolated liquid adjacent to the sharp recesses between the solid surfaces tends to adopt menisci such that the liquid is in equilibrium with the surrounding vapour, consequently there is little further loss of moisture in this dry zone.

The suction in the continuous liquid phase is at a maximum at the onset of the formation of a dry zone. Loss of moisture can now only occur by vapour diffusion through this dry (pendular) layer which marks the beginning of the second falling rate period.

The rate of evaporation now decreases inversely as the thickness of the pendular layer increases. Finally the pendular zone exists throughout the porous material and the remaining liquid eventually

attains equilibrium with the vapour in the bulk air stream (equilibrium moisture content).

It can be recalled that potentials of pressure, temperature, solute concentration and voltage are responsible for the movement of moisture in a porous material. Neglecting the potentials of temperature, solute concentration and voltage; and including the gravitational potential, then the only forces inducing moisture movement are pressure forces (induced by capillarity) and gravity. These forces are opposed by frictional forces generated by the movement of moisture.

In a bed composed of large particles and pore spaces gravitational forces will be greater than capillary forces and frictional effects will be negligible. The amount of liquid movement to the surface during drying will be small and most of the drying will occur in the first and second falling rate periods.

For intermediate sized particles, gravitational and capillary forces will be comparable in magnitude and frictional effects will be small. For beds of very fine particles frictional forces will predominate and capillary and frictional forces will far outweigh those due to gravity.

Newitt[13] predicted from theoretical considerations that for beds of uniform spheres and for laminar fluid flow:- (i) gravity and capillary force were the controlling forces for spheres greater than 10^{-2} cm. (ii) For spheres of radius 10^{-3} to 10^{-4} cm the controlling forces were mainly capillary. (iii) For spheres less than 10^{-5} cm capillary and frictional forces were the controlling forces.

However, experiments showed that the theoretical predictions were only partially correct. For glass beads of radius 6×10^{-3} cm, the controlling forces were gravitational and capillary. For

spheres of 2.35×10^{-3} cm the controlling forces were almost all capillary and that for spheres of 7.5×10^{-4} cm capillary and frictional forces were controlling. Finally for spheres of 2.5×10^{-4} cm the controlling forces were almost totally frictional.

The theoretical predictions were obtained from calculations and upon the assumption that the spheres were packed as closely as possible. The results for the larger spheres (6×10^{-3} cm) indicate that the sphere packing is more open than assumed, which in turn leads to greater pore sizes than expected. Newitt[17] proposed that a possible explanation of the significant increase of frictional forces, above that predicted, for the smaller spheres (2.5×10^{-4} and 7.5×10^{-4} cm) was due to disruption of the capillary pathways by air-vapour bubbles. The disruption is caused by expansion of entrapped air, or by separation and consequent expansion of air from solution at high suctions. This problem is aggravated at higher temperatures when the vaporisation of the liquid also contributes to the size of the air-water vapour bubbles.

4. Methods of estimating evaporation

The evaporation process involves the transfer of heat, momentum and mass, which are intimately related. Methods of estimating evaporation include an energy balance approach; estimation by mass transport treatments, either empirically or theoretically. Another approach involves the measurement of all the components of a water balance equation, except that of the rate of evaporation, which is then estimated to be the residual flux after the sum of the component fluxes have been subtracted from the net moisture flux.

The methods of estimating evaporation discussed in the following sections are:- (i) empirical or semiempirical Dalton type formulae. (ii) Turbulent aerodynamic methods. (iii) Energy balance approach. (iv) A dimensionless correlation of evaporation

into still air. The first two methods are more applicable to external building surfaces, whilst number (iv) is more applicable for internal building surfaces whilst method number (iii) can be used to estimate evaporation from both types of surfaces.

4.1 Requirements for evaporation

For evaporation, from a wet surface, to continue three physical requirements must be continually fulfilled. Firstly there must be a continual supply of heat energy to vaporise the liquid. Secondly the vapour pressure in the overlying air must be less than that at the evaporating surface. Finally, a sufficient quantity of moisture must be transported to the surface.

4.2 Dalton method

The beginnings of a scientific study of evaporation are due to Dalton, who was first to state clear views on the nature and properties of vapours in general. He designed experiments to elucidate the factors controlling natural evaporation and showed his results to be consistent with the equation which workers now refer to as the "Dalton" form

$$E_v = a\,(p_{es}-p_d)\,(1 + bu) \qquad (11)$$

where E_v is the evaporation per unit area; a, b are empirical constants; p_{es} is the saturation vapour pressure at the surface temperature T_{es}. p_d is the saturation vapour pressure at the dew point temperature T_{dp}; u, the velocity in the x direction.

There is however, lack of agreement concerning the value of the constants. The value of a has been found to lie between 0.3 and 0.5 when E_v is measured in mm of water per day; u in miles per hour and p_{es}, p_d in mm of mercury. The value of b shows a much greater variation. Several possible reasons have been presented to account for the variation of b; some of the more common reasons being the sizes, depths and exposures of the evaporating pans, the height at which the wind velocity is measured.

Another possible explanation is the determination of p_d, since for evaporation to continue, p_d must decrease with height; however, the greatest fall in vapour pressure occurs in the laminar sub-layer near the surface, and that further changes in vapour pressure with height are small. Provided p_d is determined at the height of a few metres above the surface, it is expected that no serious error in the value of p_d will be incurred. Rohwer[18] made a comprehensive investigation of evaporation from free water surfaces, which has been discussed further by Penman.[19] [20]

Rohwer's measurements were obtained for a tank 3-ft square (approx, 1m x 1m) and his results can be summarised by the formula

$$E_v = 0.40\ (1. + 0.27\ u_o)\ (p_{es} - p_d) \qquad (12)$$

where E_v is the evaporation rate in mm of water per day; u_o is the velocity at the surface, obtained by extrapolation and has units of miles per hour; p_{es}, p_d are the vapour pressures in mm of mercury.

Penman[19] modified this formula by substituting a new wind speed which was measured at a height of two metres above the surface

$$E_v = 0.40\ (1 + 0.17\ u_2)\ (p_{es} - p_d) \qquad (13)$$

where u_2 is the velocity measured two metres above the damp surface.

Dalton type formulae have also been presented by several workers[10] [11] [12] [21]-[24].

4.3 Turbulent aerodynamic methods

These methods have their origins in classical turbulent transfer theory. The main assumption associated with this approach is that the magnitude of the eddy momentum diffusivity is numerically equal to the eddy mass diffusivity. The momentum

eddy diffusivity is evaluated from wind speed measurements. This value is then used together with air moisture measurements to calculate the evaporative flux.

Eddy momentum transfer coefficients were developed from fundamental principles together with the concepts of 'eddy velocity' and 'mixing length' together with an expression describing the velocity profile near to the surface.

The theory of momentum transfer developed from fundamental principles has been discussed by O.G. Sutton[(25)-(27)] and W.G.L. Sutton[(28)]. The theory was subsequently found to be in reasonable accord with experimental fact[(29)].

Sutton's method of evaluating the eddy momentum coefficient for aerodynamically smooth surfaces was slightly modified by Frost[(30)] to extend the method to aerodynamically rough surfaces. The results predicted by both theories was confirmed by Calder[(31)]. The problem of turbulence and evaporation has also been discussed by Davies[(32)].

A slightly different approach to the problem of measuring turbulent natural evaporation from any type of surface has been developed by Thornthwaite and Holzman[(33)(34)]. The difference between this method and that pioneered by Sutton arises from an assumption associated with the definition of "mixing length", which in turn is reflected by the expression for the velocity profile of fluid associated with the solid surface. A roughness factor is also included in the velocity profile expression. The approach resulted in a different expression for the eddy momentum diffusivity.

The concluding part of the method however is similar to the method of Sutton, in that the eddy mass diffusivity is assumed to the eddy momentum diffusivity, and from which an expression for

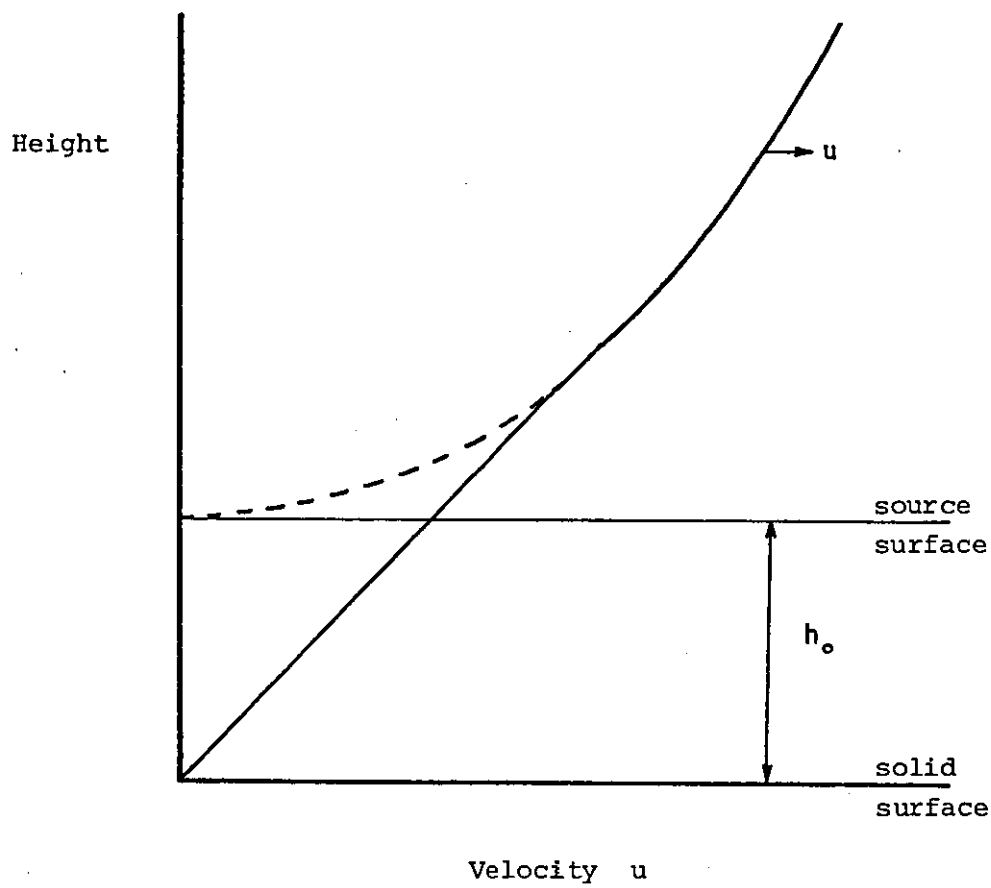

Fig. 3. Schematic representation of the wind velocity profile near to the ground. Solid line actual wind velocity profile. Dotted line is an extrapolation of an assumed velocity profile. h_o is the height of surface roughness.

the evaporative flux was derived.

Equality of the eddy diffusivities has been verified by Pasquill[35], who has also shown that under certain circumstances the evaporation expression could be simplified to yield a "Dalton" type of expression[36].

Further aspects associated with turbulent transfer methods are atmospheric stability and its effect upon the velocity profile and evaporation expressions, and the definition of aerodynamically smooth and rough surfaces. These aspects are influenced by the type of flow regimes associated with a particular surface. The type of flow regime is itself a function of Reynolds number. The flow regime is described as either laminar, transitional or fully turbulent. The criteria for determining the type of flow regime and treatment of boundary layer motion can be found in most fluid mechanics textbooks, e.g.[37].

A schematic representation of the velocity profile over a surface elucidating the meaning of 'surface roughness' can be found in Fig. 3 (ref.(33), page 25). The surface roughness variable is denoted by the height h_o in the figure. The continuous line represents the actual velocity profile whilst the dotted line is an extrapolation of an assumed velocity profile to the axis of zero velocity. The source surface is assumed to represent the height at which moisture is liberated or the height from which moisture is assumed to be evaporated.

The importance of atmospheric stability is that it influences the profiles of velocity, humidity and temperature in the air. This is reflected by variability of the mixing length[29][38] and the velocity profile which are used to determine the eddy momentum coefficients. The criterion of stability was expressed in terms of the ratio of the buoyancy force to the frictional force, the ratio is known as the Richardson number[39][40][41].

The question of stability in Sutton's method, can easily be accounted for by adjustment of a variable, designated by 'n' in the original papers[25][26][27]. The variable n is a measure of the degree of mixing and lies between 0 and 1.

Adjustment of the theory when using the approach of Thornthwaite and Holzman[33][34] is more difficult since an additional "correlating" factor was introduced into the equations[35][42][43]. An alternative treatment involved redefinition of the velocity profile with a variable exponent, a modification which is very similar to the original approach presented by Sutton[44].

Pasquill[35], using the modified velocity profile, developed expressions for the rate of evaporation. The agreement between the above theoretical modification and experimental observations has been discussed by Rider[45][46].

Description and limitations of the turbulent transfer methods, and further discussion are given by Halstead and Covey[47]; Rider and Robinson[48]; Deacon, Priestley and Swinbank[49]; Blackwell[50]; and Rose[51].

The discussion above is merely an outline of the development of the turbulent transfer methods. These methods have been included since they represent an established approach of estimating evaporation. The discussion has been abbreviated because complete derivation of the evaporation expressions from fundamental principles is tedious and often difficult to follow.

With turbulent transfer methods the apparatus, accuracy of measurement and adherence to boundary conditions are generally more critical than in other methods of estimating evaporation. These stringent requirements make it doubtful as to whether these methods could be successfully applied to prediction of evaporation from damp walls. There are however, less demanding but equally valid methods of estimating evaporation (e.g. energy balance

method) which preclude the frequent use of turbulent transfer methods for estimating evaporation.

4.4 Energy balance approach

This method of estimating evaporation is based upon an energy balance at ground level. The equation representing the various heat fluxes can be expressed as

$$R_n = G + H + L\,E'_v \qquad (14)$$

where R_n is the net radiation flux density, adsorbed at the ground surface; G, the heat flux density conducted into the ground; H, the sensible (or non-latent) heat flux density into the atmosphere; L, the latent heat of evaporation; E'_v, the evaporation rate per unit area of surface. The product $L\,E'_v$ comprises the latent heat flux density.

4.5 Discussion and evaluation of R_n

Most of the radiant energy from the sun has a wavelength between 0.3 μm and 3 μm whereas terrestrial radiation is effectively of wavelength greater than 3 μm[52][53]. There is little overlap between the radiation spectra[51]. Because of this terrestrial radiation is referred to as 'Long Wave' radiation to distinguish it from the 'Short Wave' radiation from the much hotter sun.

Short wave radiation from the sun is affected by passage through the atmosphere. On clear days much of the solar radiation is directly transmitted to the ground. However, on cloudy days, the sun's radiation is reflected in all directions (diffuse reflection), and solar radiation reaching the ground, via the clouds is called reflected radiation. Part of the solar (short wave) radiation is absorbed by clouds and re-emitted as long wave radiation either back into space or towards the ground. Similarly, dust or smoke particles, in the atmosphere, also reflect and

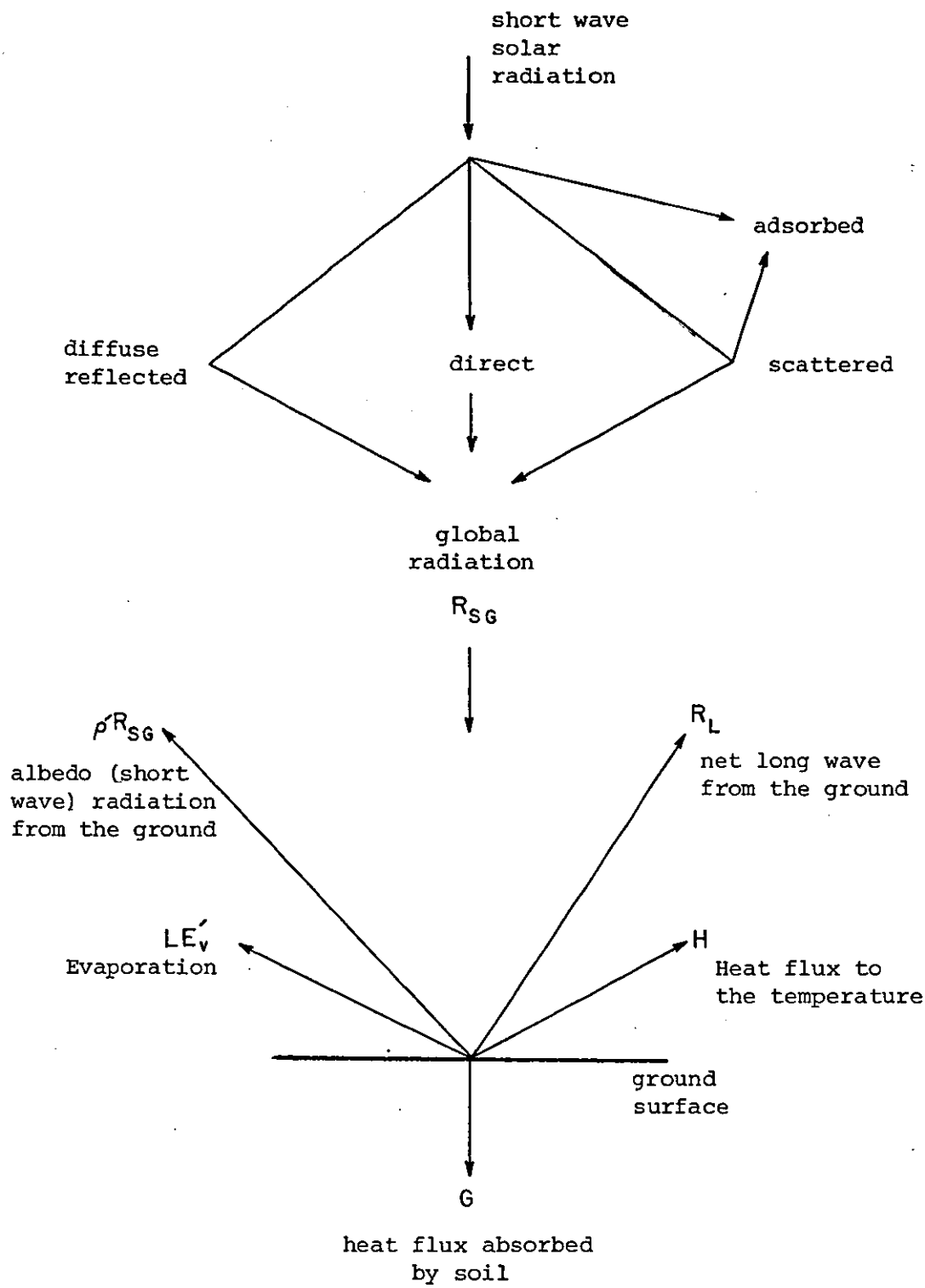

Fig. 4. Component of the heat exchange at the earth's surface.

adsorb solar radiation. However, because the concentration of these particles is much lower: the solar radiation reflected by these particles is referred to as scattered radiation[52].

The net shortwave radiation reaching the ground is referred to as global radiation (R_{SG}). Some of the short wave radiation is reflected by the ground back into space, and albedo is the term used to denote the reflection coefficient of short wave radiation only.

It is important to distinguish between short wave radiation reflected from a surface, i.e. still as short wave radiation and short wave radiation that is adsorbed by the surface and, because of the lower surface temperature, re-emitted as long-wave radiation.

If the difference in long wave radiation received and emitted by the ground surface is denoted by R_L and the reflection coefficient of the surface (albedo) is denoted by ρ', and finally if R_{SG} denotes short wave received at the ground surface then the net radiation flux density (R_n), available at the ground surface, is

$$R_n = R_{SG}(1 - \rho') - R_L \qquad (15)$$

The various components of the energy balance are shown schematically in Fig. 4.

The gases which appreciably affect the long wave portion of the radiation spectrum are carbon dioxide and water vapour. The overall effect of carbon dioxide is less important because of its lower concentration and fewer adsorption bands than water vapour. Also since the proportion of carbon dioxide in the atmosphere is practically constant, its effects may be considered as fixed for most purposes. The evaluation of long wave radiation in the atmosphere has been discussed by several workers[52] [54]-[59].

Brunt[54] derived a semi empirical expression for the incoming long wave radiation in a cloudless sky,

$$R'_L = \sigma_r T^4 (a + b\sqrt{p}) \tag{16}$$

where a, b are constants for a given location; p, the vapour pressure of water in the atmosphere; T, the absolute temperature of air at the screen height; R'_L, the downward (incoming) radiation from the atmosphere for a clear sky; σ_r, the Stefan-Boltzman constant.

Penman[19] modified Brunt's expression to allow for cloud coverage

$$R'_{Lm} = R'_L (1 - \alpha m) \tag{17}$$

where R'_{Lm}, the net incoming long wave radiation on a cloudy day; m, the fractional cloudiness; α, a variable which depends on the cloud type. For high clouds (cirrus, $\alpha = 0.025$); for medium height (alto, $\alpha = 0.06$); and finally for low clouds (cumulus, $\alpha = 0.09$).

Monteith[56] developed a similar expression for cloudy skies

$$R'_{Lm} = R'_L (1-m) + m \sigma_r T_c^4 \tag{18}$$

where m, the fractional cloudiness; σ_r, the Stefan-Boltzman constant; T_c the absolute temperature of the cloud surface.

Monteith expanded eqn.(18) to allow for differences in temperature between the ground surface and the air temperature, and by inclusion of a suitable correction factor, expressed the cloud temperature in terms of air temperature, the final expression was

$$R'_{Lm} = - \{ (1-m)(\varepsilon-1) \} \sigma_r T_A^4 + m \Delta L_1 + \Delta L_2 \tag{19}$$

where ε is equal to $R'_L/(\sigma_r T_A^4)$; T_A. the absolute temperature of the air; R'_L, the incoming radiation from a cloudless sky; ΔL_1, the correction for the difference between T_A and the cloud base temperature, T; ΔL_2, the correction for the difference between

T_A and the surface radiative temperature.

For clear skies and an air temperature, T_A, Swinbank[57] proposed two equivalent equations, which are solely dependent upon the air temperature,

$$R'_L = -17.09 + 1.195\ \sigma_r\ T_A^{\ 4} \tag{20}$$

or

$$R'_L = 5.31 \times 10^{-14}\ T_A^{\ -6} \tag{21}$$

where R'_L is the incoming long wave radiation (milli watts cm^{-2}); σ_r, the Stefan-Boltsman constant, which has a value of 5.77×10^{-9} (milli watts $cm^{-2}\ {}^{o}K^{-4}$); T_A, the absolute air temperature.

Short wave radiation received at ground level is often expressed in the form[20]

$$R_{SG} = R_S\ (a + b\ \frac{n}{N}) \tag{22}$$

where R_{SG} is the short wave radiation received at ground level on a cloudy day; R_S, the short wave radiation received at ground level on a clear day; a, b are constants for a given location; n, is the total period of bright sunshine; N, is the maximum period of bright sunshine. Note, a fraction of R_{SG} is reflected, as short wave, back into space; and if the reflection coefficient (albedo) is denoted by ρ', the net short wave radiation available at the surface is $(1-\rho')R_{SG}$. In addition the value of ρ' may be affected by the amount of moisture at the surface.

4.6 Discussion of the soil heat flux

Heat may be transferred through a porous material by conduction, convection and radiation. However, the heat flux of the two latter processes is much smaller than that of conduction, and hence they may be ignored. Part of the heat energy absorbed by a porous material is used to increase the temperature of the material itself (i.e. storage), the remainder of the heat energy is transferred through the material.

When the supply of heat is removed, and provided the temperature of the porous material is greater than ambient temperature, the stored heat is transferred back to the surroundings. Likewise, this reverse flow of heat, may be transferred back to the surroundings by conduction.

The heating and cooling process produced what is known as a temperature wave in the porous material[51][60]-[63]. Consider as an example the surface of the soil. During the day solar radiation impinges on the ground. If the rate of incoming energy is greater than the rate at which energy can be dissipated to the atmosphere, the soil surface temperature will rise. Heat conduction into the soil will occur because of the difference in surface and lower soil temperatures. Also the upper layers of soil will become warmer. At night the reverse process will occur since the soil temperature at the surface is less than that immediately below it.

The greatest observed daily difference in temperature (i.e. amplitude of the temperature wave) is at the soil surface. West[60] has shown, that with soils and especially at greater depths, the diurnal and annual temperature waves can be represented by a simple sine wave expression. Furthermore, by assuming the thermal diffusivity of the soil to be constant, the amplitude of the temperature wave was shown to be a linear function of soil depth. In addition, West, by measuring the difference in time between the peak temperature at each depth (measurement of phase lag), showed that the phase lag of the temperature wave at different soil depths varied linearly with depth.

Variation of temperature affects the thermal conductivity and thermal capacity of damp porous materials, because of the inter-

action of these properties and the (temperature dependent) moisture content of the material[64]-[66]. In addition, there is a thermal component arising from the bulk movement of moisture to the evaporating surface, which will modify the temperature wave and hence indirectly affect the thermal capacity and conductivity of the porous material[67-(70)].

If the upward rate of moisture flow is less than the rate of evaporation at the surface (flow-limiting), then the variation of surface conditions is much more extreme than is the case where the rate of evaporation is limited by the supply of energy (energy limiting)[71]. The interaction between the rate of evaporation, surface and sub-surface conditions is discussed in greater detail by Philip[67] and De Vries[69].

4.7 Bowen ratio

In employing the energy balance approach, the net energy available at the surface is denoted by R_n-G, where R_n is the net radiation energy at the surface and G, the heat energy conducted into the soil. The available energy at the surface has usually been partitioned between that required to heat the air, H and that required for evaporation, E'_v. Working on evaporation from open water surfaces, Bowen[72] expressed the ratio, $\beta = H/(L\ E'_v)$ in terms of properties at two heights, one usually was taken as the evaporating surface.

The flux of heat was expressed by

$$H = -K_h\ \rho_a\ cp_a\ \frac{\partial T}{\partial z} \qquad (23)$$

where H is the flux of heat into the air; ρ_a, the density of the air; cp_a, the specific heat of the air; $(\partial T/\partial z)$, the thermal gradient in the air and finally K_h, the thermal diffusivity of the air. Note that for turbulent air conditions the thermal diffusivity is synonymous with the thermal eddy diffusivity (section 4.3) and

furthermore is numerically equal to the eddy diffusivities of momentum and mass transfer under all conditions of atmospheric stability. Hence by employing the corresponding expressions for heat and mass (water vapour) transfer, the Bowen ratio may be expressed as

$$\beta = \frac{H}{L\ E'_v} = \frac{cp_a}{L}\ \frac{K_h}{K_v}\ \frac{(\partial T/\partial z)}{(\partial q/\partial z)} = \frac{cp_a}{L}\ \frac{\partial T}{\partial q}$$

$$= \gamma_E\ (\partial T/\partial q) \qquad (24)$$

where K_v is the eddy mass diffusivity; q, the specific humidity (c.f. section 2.6) and γ_E is the ratio cp_a/L.

Both the temperature gradient and the specific humidity gradient are normally measured over the same height interval. Frequently, the amount of moisture in an air-water system is small and hence the specific humidity, q (section 2.6) can be equated to the humidity, H' (section 2.7); also as a consequence of the low air moisture content, the vapour pressure of the moisture in the air will also be small in comparison to the total pressure, P. Utilising these approximations the Bowen ratio can be expressed as

$$\beta = \gamma'_E\ (\partial T/\partial p) \qquad (25)$$

where p is the vapour pressure of water; γ'_E, the ratio $(cp_a\ P\ M_a)/(L\ M_W)$: M_a, M_W are the molecular weights of air and water respectively.

Recalling eqn.(14) and dividing by $L\ E'_v$ then

$$\frac{R_n - G}{L\ E'_v} = 1 + \beta \qquad (26)$$

which on re-arrangement yields

$$L\ E'_v = (R_n - G)/(1+\beta) \qquad (27)$$

By evaluating β from eqns. (24) or (25) and inserting it into eqn. (27), the evaporation rate E'_v can be determined. To overcome the problem of determining the surface temperature and vapour pressure

(the same problem that is encountered in Dalton type expressions) Penman[20] combined the energy balance approach and the Dalton method to eliminate measurements at the surface, i.e.

$$L\,E'_v = \frac{(R_n - G)\Delta' + L\,E'_{va}\,\gamma'_E}{(\Delta' + \gamma'_E)} \tag{28}$$

where Δ' is the slope of the vapour pressure/temperature curve at the air temperature T_a; E'_{va}, the evaporation rate obtained by substituting p_{as} for p_{es} in the Dalton expression (c.f. eqn.(11)) to yield

$$L\,E'_{va} = f(u)\,(p_{as} - p_d) \tag{29}$$

where f(u) is expression for the variation of wind velocity, u; p_{es}, p_{as}, p_d are the saturation vapour pressures of water at the surface temperature T_e, air temperature T_a, and dew point temperature of the air respectively (see Fig. 1).

Note that the latent heat of vaporisation of moisture, L, is included in equations (28), (29) because the evaporation rate is expressed as a mass flux whilst the radiation and soil conduction terms are expressed as energy fluxes.

The "combination" method above (eqns.(28),(29)), proposed initially by Penman[20] has been subject to further study by several workers[73]-[84].

An important development was introduced by Tanner and Fuchs[83] who showed that the combination method could be used to estimate evaporation from partially saturated porous materials, whereas originally the Penman method estimated the "potential evapotranspiration" rate, i.e. the evaporation from a free water surface.

The modification proposed by Tanner and Fuchs means that the combination method could be successfully applied to the problem of estimating evaporation from damp walls.

4.8 Evaporation into still air

The preceding theories and methods of measuring evaporation are concerned with the evaluation of evaporation into currents of air, (i.e. losses from the exterior of damp buildings). For damp interior walls, the evaporation process can be regarded as occurring into 'still' air; the evaporation rate is now controlled by buoyancy forces rather than convective forces.

An early empirical formula, expressing the rate evaporation of (free) water from a horizontal surface into still air, was proposed by Hinchley and Himus[21], the expression being

$$W = \frac{(p_e - p)^{1.2}}{50} \qquad (30)$$

where W is the evaporation rate per square metre per hour; p_e, p are the vapour pressures at the evaporating surface and the bulk air, respectively.

Further study of evaporation of water from free horizontal water surfaces has been conducted by Powell[11]; Wade[22], who discussed the correctness of an expression to represent evaporation into both still and moving air; Priestley[85][86], who discussed evaporation from large open horizontal surfaces into calm air; and by Boelter et al.[23][24], who expressed the evaporation rate in terms of the following dimensionless parameters:- Grashof No., modified Nusselt No. (also known as Sherwood No.), and modified Prandtl No. (more commonly known as the Schmidt No.).

Use of a dimensionless correlation for natural convection from horizontal surfaces is obviously not applicable to evaporation from a wall (vertical surface). However, a dimensionless comparison between free convective heat transfer and mass transfer from a vertical surface can be obtained provided the Prandtl group (heat transfer) is replaced by the Schmidt group (mass transfer),

and the Nusselt group (heat transfer) is replaced by the Sherwood group (mass transfer)[37][87]-[92].

The dimensionless groups are defined as follows

Nusselt No. $= \frac{h_e \ell}{k_c}$; Prandtl No. $= \frac{c_p \mu}{k_c}$; Grashof No. $= \frac{\beta_E g \Delta T \ell^3 \rho^2}{\mu^2}$;

Sherwood No. $= \frac{h_D \ell}{D_{atm}}$; Schmidt No. $= \frac{\mu}{\rho D_{atm}}$. The Schmidt (or Prandtl) No. is often combined with the Grashof No., the combination being called the Rayleigh No. and where h_e is the heat transfer coefficient; h_D, the mass transfer coefficient; ℓ, the characteristic length; k_c, the thermal conductivity of the fluid; c_p, the specific heat of the fluid, at constant pressure; μ, the fluid viscosity; β_E is the cubical expansion, which for an ideal gas β_E is equal to reciprocal of the absolute temperature. Furthermore if the temperature difference is small, the expansion coefficient can be written as $1/T_o$ where T_o is the absolute temperature in the gas outside the boundary layer. ΔT the temperature difference; ρ, the fluid density; D_{atm}, the diffusivity of the vapour.

The problem of free convective mass transfer at vertical surfaces has been correlated by several researchers[93]-[97]. The correlation for the average mass transfer rate at a vertical surface is usually expressed in the form

$$N_{Sh} = c' \, (N_{Sc} \times N_{Gr})^{0.25} \qquad (31)$$

where N_{Sh}, N_{Sc}, N_{Gr} are the Sherwood, Schmidt and Grashof numbers respectively and c' is a constant.

For small Schmidt numbers, a more accurate expression is[93]

$$N_{Sh} = 0.667 \, N_{Sc}^{0.5} \, (0.952 + N_{Sc})^{-0.25} \, H_{Gr}^{0.25} \qquad (32)$$

which for large N_{Sc} (i.e. $0.952 \ll N_{Sc}$), eqn.(32) reduces to eqn. (31). Similarly by direct analogy with heat transfer studies,

the theoretical correlation for the local mass transfer rate during laminar free convection at a vertical plate can be formulated as[95]

$$1.99 \frac{N_{Sh_x}}{N_{Ra_x}^{0.25}} = f_1(Sc) \qquad (33)$$

where the subscript x denotes local values, i.e. values at a height x from the base of the surface; $f_1(Sc)$ is a function of the Schmidt number as shown in Fig. 5.

Natural evaporation from internal walls may be regarded as an example of evaporation into still air and hence the rate could be predicted by eqn.(32) and (33) provided measurements of the physical properties used in the correlation were recorded or estimated.

4.9 Summary

Natural evaporation from damp walls occurs under two widely differing conditions, i.e. evaporation into turbulent air (external surfaces) and evaporation into still air (internal surfaces).

Early attempts of estimating evaporation employed simple empirical formulae (Dalton-formulae). Later more sophisticated and complicated methods were developed, utilising fundamental principles of turbulence theory (aerodynamic methods); however, difficulties of application and measurement of atmospheric conditions limited the use of such methods.

A more modern and less stringent method of estimating evaporation is the energy balance approach. This method is essentially a heat balance, with the 'evaporation' surface used as a datum level. The various energy components of the heat balance are measured or estimated such that the evaporation rate from the surface can be predicted. The method has been extended to estimate evaporation from unsaturated surfaces. A further advantage of this method is that it can also be used to estimate

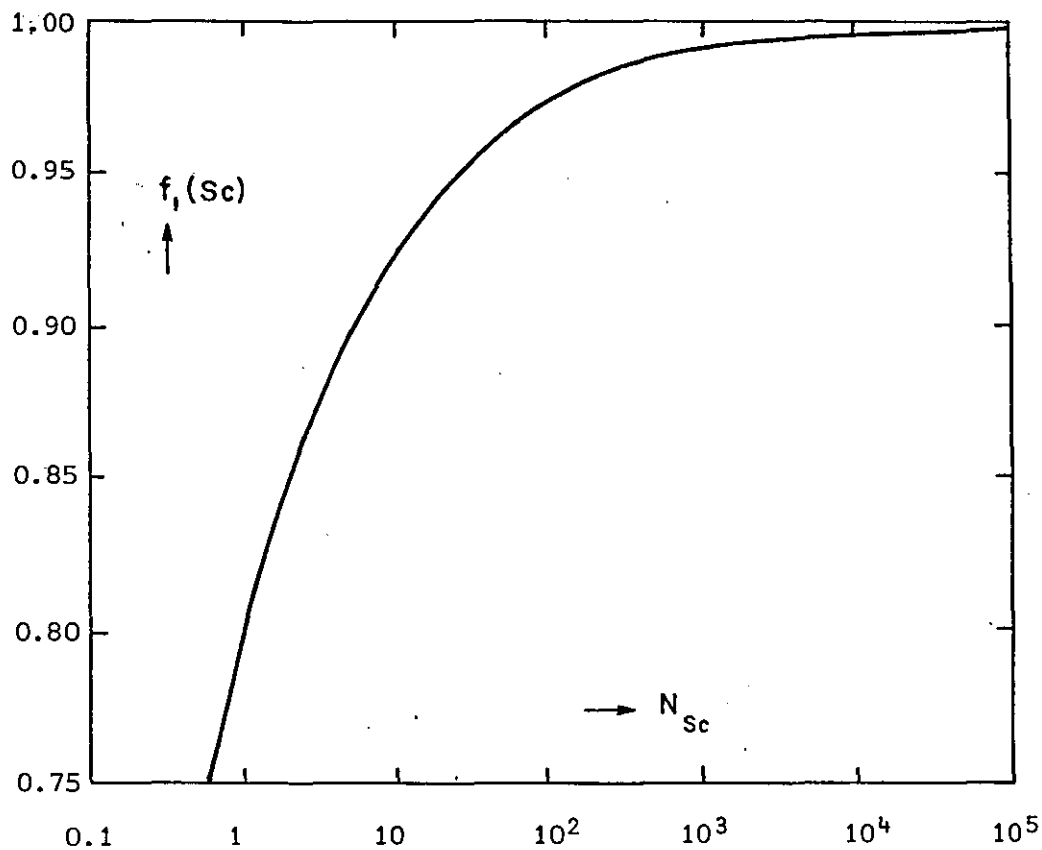

Fig. 5. The function f_1 (Sc or Pr) constructed from heat transfer data.[95]

evaporation from internal surfaces.

Internal evaporation may also be regarded as an example of evaporation into "still" air and hence could be predicted by the dimensionless correlation that has been developed to estimate evaporation occurring under still air conditions.

List of Symbols and units of Chapter Five

cp	specific heat of unit mass of material at constant pressure ($cm^2\ sec^{-2}\ {}^oK^{-1}$)
cp_a	specific heat of unit mass of air at constant pressure ($cm^2 sec^{-2}\ {}^oK^{-1}$)
D	diffusion coefficient of a vapour ($cm^2 sec^{-1}$)
D_{atm}	diffusion coefficient of water vapour ($cm^2 sec^{-1}$)
E_v	evaporation rate of moisture per unit area of porous material, usually expressed as a velocity of moisture in the liquid phase ($cm\ sec^{-1}$)
E_v'	mass flow rate of moisture per unit area ($g\ cm^2\ sec^{-1}$)
G	heat flux density conducted into the ground ($g\ sec^{-3}$)
g	gravitational acceleration ($cm\ sec^{-2}$)
H	sensible (or non-latent) heat flux density into the atmosphere ($g\ sec^{-3}$)
H'	humidity (or mixing ratio) of a vapour
H'_s	saturated humidity of a vapour
h	relative humidity of a vapour
h_e	heat transfer coefficient ($g\ sec^{-3}\ {}^oK^{-1}$)
h_D	mass transfer coefficient ($cm\ sec^{-1}$)
K_v	eddy mass diffusivity ($cm^2\ sec^{-1}$)
K_h	eddy thermal diffusivity ($cm^2\ sec^{-1}$)
k_c	thermal conductivity of a material ($g\ cm\ sec^{-3}\ {}^oK^{-1}$)
ℓ	characteristic length (cm)
L	latent heat of evaporation per unit mass of moisture ($cm^2\ sec^{-2}$)
M_A	molecular weight of air ($g\ mole^{-1}$)
M_W	molecular weight of water ($g\ mole^{-1}$)
m	fractional cloudiness
N_{Gr}	Grashof number $\left((\beta_E\ g\ \Delta T\ \ell^3 \rho^2)/\mu^2\right)$
N_{Sh}	Sherwood number ($h_D\ \ell/D_{atm}$)

N_{Sc}	Schmidt number $(\mu/\rho\ D_{atm})$
N_{Ra}	Rayleigh number $\left((\beta_E\ g\ \Delta T\ \ell^3\rho)/(D_{atm}\ \mu)\right)$
P	total pressure $(g\ cm^{-1}\ sec^{-2})$
p	vapour pressure of water at an air temperature T_a $(g\ cm^{-1}\ sec^{-2})$
p_a	vapour pressure of moisture in air at temperature T_a $(g\ cm^{-1}\ sec^{-2})$
p_{as}	saturated vapour pressure of moisture in air at temperature T_a $(g\ cm^{-1}\ sec^{-2})$
p_{es}	saturated vapour pressure of moisture in air at the surface temperature T_{es} $(g\ cm^{-1}\ sec^{-2})$
p_d	saturated vapour pressure of moisture in air at the dewpoint temperature T_{dp} $(g\ cm^{-1}\ sec^{-2})$
q	specific humidity
R_m	Universal gas constant per mole of fluid $(g\ cm^2 sec^{-2}\ mole^{-1}\ {}^oK^{-1})$
R_n	net radiation flux density absorbed at the ground surface $(g\ sec^{-3})$
R_S	net short wave radiation reaching the ground on a clear day $(g\ sec^{-3})$
R_{SG}	net short wave radiation reaching the ground surface $(g\ sec^{-3})$
R_L	net long wave radiation leaving the ground surface $(g\ sec^{-3})$
R'_L	incoming long wave radiation from the atmosphere $(gsec^{-3})$
R'_{Lm}	incoming long wave radiation from the atmosphere on a cloudy day $(g\ sec^{-3})$
T	temperature $({}^oC,\ {}^oK)$
T_{wb}	wet bulb temperature $({}^oC)$
T_{dp}	dew point temperature $({}^oC)$

T_{es}	surface temperature of a moist porous material (^{o}C)
ΔT	temperature difference (^{o}C)
t	time (sec)
u	fluid velocity (cm sec^{-1})
x	distance (cm)
β	Bowen ratio defined as the ratio of sensible (or non-latent) heat flux density to the atmosphere to the latent heat flux density of evaporation
β_E	coefficient of cubical expansion ($^{o}K^{-1}$)
γ_E	the ratio of the specific heat of air at constant pressure to the latent heat of evaporation of moisture ($^{o}K^{-1}$)
γ'_E	a factor (= $(cp_a\ P\ M_A)/(L\ M_W)$
θ	volumetric moisture content of a porous material
μ	fluid viscosity (g cm^{-1} sec^{-1})
ρ	fluid density (g cm^{-3})
ρ_a	density of air (g cm^{-3})
ρ_v	density of water vapour in air
ρ'	albedo coefficient
σ_r	Stefan-Boltzmann constant (= 5.6697×10^{-5} g sec^{-3} $^{o}K^{-4}$)

References Chapter Five

(1) The drying of solids I, T.K. Sherwood, Ind. and Eng. Chem. 21, No. 1, pp.12-16, 1929

(2) The drying of solids II, T.K. Sherwood, Ind. and Eng. Chem. 21, No. 10, pp.976-980, 1929

(3) The drying of solids III. Mechanism of the drying of pulp and paper. T.K. Sherwood, Ind. and Eng. Chem., 22, No. 2, pp.132-136, 1930

(4) The drying of solids VII. Moisture movement by capillarity in drying granular materials, E.W. Comins, T.K. Sherwood. Ind. and Eng. Chem., 26, No. 10, pp.1096-1098, 1934

(5) The air drying of solids, T.K. Sherwood. Trans. Am. Inst. Chem. Eng., 32, pp.150-168, 1936

(6) The drying of porous solids: diffusion and surface emission equations. A.B. Newman, Trans. Am. Inst. Chem. Eng., 27, pp.203-220, 1931

(7) Diffusion in solids, liquids and gases. W. Jost. Academic Press Inc., Publ. 1960

(8) Fundamentals of drying and air conditioning, E.R. Gilliland. Ind. and Eng. Chem., 30, No. 5, pp.506-514, 1938

(9) The mechanism of the drying of solids, Part VII: Drying with heat transfer by conduction, A.R. King, D.M. Newitt. Trans. Inst. Chem. Eng., 33, pp.64-71, 1955

(10) The evaporation of water from plane and cylindrical surfaces, R.W. Powell, E. Griffiths. Trans. Inst. Chem. Eng., 13, pp.175-198, 1935

(11) Further experiments on the evaporation of water from saturated surfaces, R.W. Powell. Trans. Inst. Chem. Eng., 18, pp.36-55, 1940

(12) Evaporation from free surfaces, K.R. Chakravorty. Jnl. Imp. Coll. Chem. Eng. Soc., 3, pp.46-53, 1947

(13) The mechanism of the drying of solids. Part I: The forces giving rise to the movement of water in granular beds, during drying. J.F. Pearse, T.R. Oliver, D.M. Newitt. Trans. Jnl. Inst. Chem. Eng., 27, pp.1-8, 1949

(14) The drying of granular solids, N.H. Ceaglske, O.A. Hougen. Trans. Am. Inst. Chem. Eng., 33, pp.283-314, 1937

(15) Studies in the physical properties of soils, IV. A further contribution to the theory of capillary phenomena in soils. W.B. Haines. Jnl. Agric. Sci., 17, pp.264-290, 1927

(16) Studies in the physical properties of soils, V. The hysteresis effect in capillary properties, and the modes of moisture distribution associated therewith. W.B. Haines. Jnl. of Agric. Sci., 20, pp.97-116, 1930

(17) The mechanism of the drying of solids. Part II. The measurement of suction potentials and moisture distribution in drying granular solids. T.R. Oliver, D.M. Newitt. Trans. Inst. Chem. Eng., 27, pp.9-18, 1949

(18) Evaporation from free water surfaces, C. Rohwer. U.S. Dept. of Agric. Tech. Bull., No. 217, 96 pages, 1931

(19) Evaporation in nature, H.L. Penman. Rep. Prog. in Phys., 11, pp.366-388, 1946/47

(20) Natural evaporation from open water, bare soil and grass, H.L. Penman. Proc. Roy. Soc. (London), Ser. A., 193, pp.120-145, 1948

(21) Evaporation in currents of air. J.W. Hinchley, G.W. Himus. Trans. Inst. Chem. Eng., 2, pp.57-64, 1924

(22) Evaporation of liquids in currents of air. S.H. Wade. Trans. Inst. Chem. Eng., 20, pp.1-13, 1942

(23) Evaporation of water into quiet air. B.F. Sharpley, L.M.K. Boelter. Ind. and Eng. Chem., 30, No. 10, pp.1125-1131, 1938

(24) Free evaporation into air of water from a free horizontal quiet surface. L.M.K. Boelter, H.S. Gordon, J.R. Griffin. Ind. and Eng. Chem., 38, No. 5, pp.596-600, 1946

(25) A theory of eddy diffusion in the atmosphere. O.G. Sutton. Proc. Roy. Soc., (London), Ser. A, 135, No. 826, pp.143-165, 1932

(26) Wind structure and evaporation in a turbulent atmosphere. O.G. Sutton. Proc. Roy. Soc. (London), Ser. A, 146, pp.701-722, 1934

(27) The problem of diffusion in the lower atmosphere. O.G. Sutton. QUART. Jnl. Roy. Met. Soc., 73, pp.257-281, 1947

(28) On the equation of diffusion in a turbulent medium. W.G.L. Sutton. Proc. Soy. Soc. (London), Ser. A, 182, pp.48-75, 1943

(29) Evaporation from a plane, free-liquid surface into a turbulent air stream. F. Pasquill. Proc. Roy. Soc. (London), Ser. A, 182, pp.75-95, 1943.

(30) Turbulence and diffusion in the lower atmosphere. R. Frost. Proc. Roy. Soc. Ser. A, 186. pp.20-35, 1946

(31) Eddy diffusion and evaporation in flow over aerodynamically smooth and rough surfaces. K.L. Calder. Quart. Jnl. Mech. and Appl. Math. 2, No. 2, pp.153-175, 1949

(32) A note on three-dimensional turbulence and evaporation in the lower atmosphere. D.R. Davies. Proc. Roy. Soc. Ser. A, 202, pp.96-103, 1950

(33) Measurement of evaporation from land and water surfaces. C.W. Thornthwaite, B. Holzman. U.S. Dept. of Agric. Tech. Bull. No. 817, 75 pages, 1942

(34) The determination of evaporation from land and water surfaces. C.W. Thornthwaite, B. Holzman. Monthly Weather Review, 67, pp.4-11, 1939

(35) Eddy diffusion of water vapour and heat near the ground. F. Pasquill. Proc. Roy. Soc., 198, pp.116-140, 1949

(36) Some estimates of the amount and diurnal variation of evaporation from a clayland pasture in fair spring weather. F. Pasquill. QUART. Jnl. of Roy. Met. Soc., 75, pp.249-256 1949

(37) Chemical Engineering, Vo. I. J.M. Coulson, J.F. Richardson. Revised 2nd Ed., Pergamon Press, 1964

(38) The aerodynamic drag of the earth's surface and the value of von Karman's constant in the lower atmosphere. P.A. Shephard. Proc. Roy. Soc. Ser. A, 188, pp.208-222, 1947

(39) The supply of energy from and to atmospheric eddies. L.F. Richardson. Proc. Roy. Soc. Ser. A, 97, pp.354-373, 1920

(40) The criterion of turbulence in a fluid of variable density, with particular reference to conditions in the atmosphere. K.L. Calder. Quart. Jnl. Roy. Met. Soc., 75, pp.71-88, 1949

(41) The conditions for dynamical simularity of motions of a frictionless perfect-gas atmosphere. G.K. Batchelor. Quart. Jnl. of Roy. Met. Soc., 79, pp.224-235, 1953

(42) The influence of stability on evaporation. B. Holzman. Ann. New York Acad. Sci., 44, pp.13-18, 1943

(43) The turbulent transfer of momentum in the lowest layers of the atmosphere. E.L. Deacon. C.S.I.R.O., Australia, Divn. of Met. Phys. Tech. paper No. 4, 36 pages, 1955

(44) Vertical diffusion in the lowest layers of the atmosphere. E.L. Deacon. Quart. Jnl. Roy. Met. Soc., 75, pp.89-103, 1949

(45) Eddy diffusion of momentum, water vapour and heat near the ground N.E. Rider. Phil. Trans. Roy. Soc. Ser. A, 246, pp.481-501, 1954

(46) An account of the development of the aerodynamic method for the evaluation of natural evaporation conducted in Great Britain from 1947 to 1953. N.E. Rider. L'Assoc^{n}. Int. d'Hydrologie, No. 38, pp.135-141, 1954

(47) Some meteorological aspects of evapotranspiration. M.H. Halstead, W. Covey. Soil Sci. Soc. Amer. Proc. 21, No. 5, pp.461-464, 1957

(48) A study of the transfer of heat and water vapour above a short grass surface. N.E. Rider, G.D. Robinson. Quart. Jnl. Roy. Met. Soc., 77, pp.375-401, 1951

(49) Evaporation and the water balance. E.L. Deacon, C.H.B. Priestley, W.C. Swinbank. Climatology, Reviews and Research. UNESCO, pp.9-34, 1958

(50) The role of evaporation in the surface energy balance. M.J. Blackwell. "The water relations of plants", A symposium, Brit. Ecol. Soc., London,1961, Blackwell Scientific Publ. (1963)

(51) Agricultural Physics. C.W. Rose. Pergamon Press, 1966

(52) Radiation and the thermal balance. A.J. Drummond. Climatology, Reviews and Research, UNESCO, pp.56-74, 1958

(53) Practical Microclimatology. R.O. Slayter, I.C. McIlroy. C.S.I.R.O., Australia, UNESCO 1961

(54) Notes on radiation in the atmosphere. D. Brunt. Quart. Jnl. of Roy. Met. Soc., 58, pp.389-418, 1932

(55) Notes on the measurement and estimation of atmospheric radiation. G.D. Robinson. Quart. Jnl. of Roy. Met. Soc. 73, pp.127-150, 1947

(56) An empirical method for estimating long-wave radiation exchanges in the British Isles. J.L. Monteith. Quart. Jnl. of Roy. Met. Soc., 87, pp.171-179, 1961

(57) Long wave radiation from clear skies. W.C. Swinbank. Quart. Jnl. of Roy. Met. Soc., 89, pp.339-348, 1963

(58) Estimating incident terrestrial radiation under all atmospheric conditions. E.A. Anderson, D.R. Baker. Water Resou. Res., 3, No. 4, pp.975-988, 1967.

(59) Generalised estimates of free-water evaporation. M.A. Kohler, L.H. Parmele. Water Resou. Res. 3, No. 4, pp.997-1005

(60) A study of the annual soil temperature wave. E.S. West. Aust. Jnl. Scientific Research, Ser. A, 5, pp.303-314, 1952

(61) The annual and diurnal heat-exchange cycles in upper layers of soil. J.E. Carson, H. Moses. Jnl. Appl. Meterorology, 2, pp.397-406

(62) Water transport in soil with a daily temperature wave I. Theory and experiment. C.W. Rose. Aust. Jnl. of Sci. Res., 6, pp.31-44, 1968

(63) Water transport in soil with a daily temperature wave II. Analysis. C.W. Rose. Aust. Jnl. of Sci. Res., 6, pp.45-57 1968

(64) A non-stationary method for determining thermal conductivity of soil in situ. D.A. De Vries. Soil Science, 73, No. 2, pp.83-89, 1952

(65) The thermal conductivity of granular materials. D.A. De Vries. Bull. Inst. Int. du Froid (Annexe), pp.115-131, 1952

(66) A note on the physics of soil temperature. N.E. Rider. Weather, 12, pp.241-246, 1957

(67) Evaporation, and moisture and heat fields in the soil. J.R. Philip. Jnl. Meteorology, 14, pp.354-366, 1957

(68) Simultaneous transfer of heat and moisture in porous media. D.A. De Vries, Trans. Am. Geophys. Union, 39, No. 5, pp.909-916, 1958

(69) The influence of irrigation on the energy balance and the climate near the ground. D.A. De Vries. Jnl. Meteorology, 16, pp.256-270, 1959

(70) Rates of vertical ground water movement estimated from the earth's thermal profile. J.D. Bredehoeft, J.S. Papadopulos, Water Resou. Res. 1, No. 3, pp.325-328, 1965

(71) Calculation of evaporation rates during the transition from energy-limiting to soil-limiting phases using albedo data. R.D. Jackson, S.B. Idso, R.J. Reginato. Water Resou. Res., 12, No. 1, pp.23-26, 1976

(72) The ratio of heat losses by conduction and by evaporation from any water surface. I.S. Bowen. Phys. Review, 27, pp.779-787, 1926

(73) Estimating Evaporation. H.L. Penman. Trans. Am. Geophys. Union, 37, No. 1, pp.43-50, 1956

(74) Evaporation: an introductory survey. H.L. Penman. Netherlands Jnl. Agric. Sci., 4, pp.9-29, 1956

(75) The rate of natural evaporation from shallow ponds. J. Ferguson. Australian Jnl. Sci. Res., No. 5A, pp.315-330, 1952

(76) Some recent advances in hydrologic physics. J.R. Philip. Jnl. Inst. Eng. Austr., 26, pp.255-259, 1954

(77) The measurement of natural evaporation. I.C. McIlroy. Jnl. Austr. Inst. Agric. Sci., 23, pp.4-17, 1957

(78) A surface energy-balance computer. G.J. House, N.E. Rider, C.P. Tugwell. Quart. Jnl. Roy. Met. Soc., 86, pp.215-231, 1960

(79) Evaluation of some practical methods of estimating evapotranspiration in arid climates at low latitudes. W. Brutsaert. Water Resou. Res., 1, No. 2, pp.187-191, 1965

(80) Potential evaporation: the combination concept and its experimental verification. C.H.M. Van Bavel. Water Resou. Res., 2, No. 3, pp.455-467, 1966

(81) Potential evapotranspiration estimates by the approximate energy balance method of Penman. C.B. Tanner, W.L. Pelton. Jnl. of Geophys. Res., 65, No. 10, pp.3391-3413, 1960

(82) Energy balance approach to evapotranspiration from crops. C.B. Tanner. Soil Sci. Soc. Amer. Proc., 24, No. 1, pp.1-9, 1960

(83) Evaporation from unsaturated surfaces: a generalised combination method. C.B. Tanner, M. Fuchs. Jnl. of Geophys. Res., 73, No. 4, pp.1299-1304, 1968

(84) On the assessment of surface heat flux and evaporation using large-scale parameters. C.H.B. Priestley, R.J. Taylor. Monthly Weather Review, 100, pp.81-92, 1972

(85) Convection from a large horizontal surface. C.H.B. Priestley. Austr. Jnl. of Physics, 7, pp.176-201, 1954

(86) Free and forced convection in the atmosphere near the ground. C.H.B. Priestley. Quart. Jnl. of Roy. Met. Soc., 81, No. 348, pp.139-143, 1955

(87) The effect of pressure upon natural convection in air. O.A. Saunders. Proc. Roy. Soc. Ser. A, 157, pp.278-291, 1936

(88) Natural convection in liquids. O.A. Saunders. Proc. Roy. Soc. Ser. A, 172, pp.55-71

(89) Diffusion and convection at electrodes. J.N. Agar. Discussions of the Farad. Soc., No. 1, pp.26-37

(90) The use of dimensionless groups in electrochemistry. N. Ibl. Electrochimica Acta, 1, pp.117-129, 1959

(91) Analysis of heat and mass transfer. E.R.G. Eckert, R.M. Drake. McGraw Hill Book Co., 1972

(92) Transport phenomena. R.B. Bird, W.E. Stewart, E.N. Lightfoot. J. Wiley and Sons Inc., 1960

(93) Free-convection mass transfer at vertical plates. C.R. Wilke, C.W. Tobias, M. Eisenberg. Chem. Eng. Progress, 49, No. 12, pp.663-674

(94) Correlation of limiting currents under free convection conditions. C.R. Wilke, M. Eisenberg, C.W. Tobias. Jnl. of the Electrochem. Soc., 100, No. 11, pp.513-523

(95) Theoretical and electrochemical investigation of free convection mass transfer at vertical cylinders. E. Ravoo, J.W. Rotte, F.W. Sevenstern. Chem. Eng. Sci., 25, pp.1637-1652, 1970

(96) Laminar, transition and turbulent natural convection adjacent to inclined and vertical surfaces. J.R. Lloyd, E.M. Sparrow, E.R.G. Eckert. Int. Jnl. Heat Mass Transfer, 15, pp.457-473, 1972

(97) Natural convection mass transfer adjacent to vertical and downward-facing inclined surface. W.R. Moran, J.R. Lloyd. Trans. of the A.S.M.E., Aug., pp.472-474, 1975

CHAPTER SIX

LEACHING OF POROUS MATERIALS

1. Introduction

It has been proposed by Mason[1] that leaching of lime mortar was the most likely cause of the continual increase of height of dampness in a wall.

Leaching of mortar is an example of a group of phenomena characterised by a change of pore structure resulting from the interaction of a penetrating fluid with a porous solid material. Leaching of mortar is an undesirable example of this type of phenomenon. Other unwanted examples include deactivation of catalysts and plugging of microfilters. Sometimes the change of hydraulic properties accompanying the modification of the pore structure are highly desired. An important example is the acidisation (stimulation) of oil wells.

Because of the simularities between leaching of mortar and acidisation of oil wells, the theories and mathematical models developed to explain the increase of fluid permeability of rock formations should be applicable, at least partially so, to the problem of estimating the increase in permeability of mortar in a wall which is affected by Rising Damp.

Coincidentally a further development of leaching theory arises from another branch of the oil production industry, specifically that of immiscible displacement of oil by water injection. The theory of immiscible displacement will be modified to explain the effects accompanying a change of pore structure by leaching.

The acidisation models are discussed first, followed by a discussion of a moving boundary model. The defects and advantages of each type of model are discussed at the rear of each particular section. The chapter is terminated by a general discussion of all models.

2. Acidisation models

2.1 Capillaric approach

The earliest important model of acidisation was formulated by the French researchers Nougaro and Labbé[2]. They assumed the pore space to be composed of straight cylindrical capillaries of uniform radius, and that the pore surface dissolved uniformly along the whole length of the capillaries. This model resulted in a comparatively simple expression, which furnished a linear relationship between the square root of the rock permeability to fluid and the volumes of acid consumed.

$$(k_v)^{0.5} = (k_i)^{0.5} + \lambda V \qquad (1)$$

where k_i is the initial permeability of the material; k_v, the permeability after a volume of acid, V, had passed through the sample; λ, is a constant.

Equation (1) is developed in the paper presented by Mason[1] and more fully by Rowan[3]. Nougaro and Labbé provided evidence from laboratory studies upon a number of vesicular limestones in support of this model.

An extension of this basic model was introduced by Rowan[3], who like Nougaro and Labbé, assumed the pore space to be composed of straight cylindrical capillaries, and that the acid attacked the pore surface uniformly along its length. However, Rowan assumed that the pore space could be expressed in terms of a pore size distribution.

Using this modification Rowan calculated that the rate of change of permeability was always greater than that predicted by the Nougaro and Labbé expression. Experimental studies upon limestone samples, which were characterised by a wide pore size distribution, were in agreement with his computations. Rowan also showed that the larger pores became increasingly more dominant in

determining the rate of change of permeability as acidisation proceeded.

There are two serious defects in Rowan's analysis. First of all, the rate of acid attack does not enter his calculations so that neither the diffusivity nor surface reactivity play any part at all. The second defect is that spatial and temporal changes in pore size distribution are not considered. Both of these important considerations were included in a sophisticated model proposed by Schecter and Gidley[4].

The pore space in the Schecter model was assumed to be composed of randomly distributed pores of varying length and area, although the pore shape was assumed to be geometrically similar. The sample was reduced to a series of thin slices, the thickness of each slice was assumed to be constant and equal to the mean pore length, $\bar{\ell}$.

The distribution of pore sizes is expressed as a reduced pore size density function, $\bar{\eta}$. The change in area of a pore is expressed by a growth rate function, $\bar{\psi}$. Growth of pores was thought to be produced by two mechanisms. First of all the pore area may be changed by the action of the reacting fluid. The second mechanism is that a pore may grow as a result of a collision with a neighbouring pore, and that for a given pore range, pores can either be introduced or removed from the range by collisions.

The growth rate attributed to the first mechanism was discussed with respect to the interaction of the fluid and the solid, the final expression being

$$\bar{\psi} = \frac{C(x,t)\ \bar{\gamma}\ A\ \bar{u}}{\rho_s\ \bar{\ell}} \left[1 - \exp\left\{\frac{-\bar{\alpha}\ \bar{k}\ \Gamma\ \bar{\ell}}{A\ \bar{u}}\right\}\right] \qquad (2)$$

Equation (2) shows that the rate of increase of area, denoted by $\bar{\psi}$, is linear in the concentration of reactant, C(x,t) and depends upon the pore geometry (area of the pore, A; the perimeter of the pore,

Γ; and the mean pore length, $\bar{\ell}$); the surface dissolution rate (the reaction rate constant, $\bar{k}$); the ratio of the mass of solid dissolved per mass of acid expended, $\bar{\gamma}$; the mean velocity of fluid in the pore, $\bar{u}$; and finally the ratio of the mean surface concentration to the mean bulk concentration, $\bar{\alpha}$. All the above variables were well defined except $\bar{\alpha}$, which is dependent upon the pore shape. Schecter and Gidley showed however, that the value of $\bar{\alpha}$ was not particularly sensitive to the configuration of the pore.

Schecter and Gidley discussed the evolution of the pore distribution under conditions of highly reactive and retarded acids. For highly reactive acids (dissolution process diffusion controlled), and ignoring collisions between pores, eqn.(2) may be expressed as

$$\bar{\psi} = FXA^2 \{1 - \exp\left(\frac{-18.1\ D}{F\ A^2}\right)\} \qquad (3)$$

where F is equal to $(Q/(K\bar{\ell}w^2))$ and X is equal to $C(x,t)\bar{\gamma}/\rho_s$; A, the area of the pore; Q, the volumetric acid flow rate; K, a factor proportional to the permeability; $\bar{\ell}$, the mean pore length; w^2, the area available for fluid flow; C, the acid concentration (function of position, x and time, t); $\bar{\gamma}$, the mass of solid dissolved per mass of acid expended; ρ_s, the density of the solid; D, the molecular diffusion coefficient of the acid; X is the dissolving power of the acid expressed as volume of rock dissolved per volume of acid expended.

As the pore becomes very large ($(A^2F)/(18.1D) > 1$) $\bar{\psi}$ tends to 18.1 DX, and for a given dissolving power, X, the pore growth rate function will tend to a constant. Thus regardless of the size a pore achieves, it will continue to grow but not at the rate predicted by Rowan (growth rate proportional to the square of the pore area). From this result, Schecter and Gidley concluded that the growth of large pores (wormholing) was a result of preferential flow through large pores and a growth rate that was diffusion

controlled.

The two defects of this method relating to the calculation of the result above are:- (1) The acid feed to the next segment was assumed to be a mixture of all the acid emerging from the different pores of the previous segment. Thus no allowance can be made for the localised high acid concentrations preferentially flowing along a wormhole. (2) No allowance was made for the sequential arrangement of pores, which is important in determining the overall relative flow along each sequence of pores.

However, these two defects are minimal when the case of dissolution by a retarded acid is considered, as little reaction occurs whilst the acid is injected into the porous material. For the case of "stationary" dissolution by a very retarded acid the change in permeability and the corresponding change in porosity was found to follow a unique relationship[(5)-(9)] as theoretically predicted by Schecter and Gidley[(4)].

When the retarded acid was pumped at constant velocity through the sample, the growth function $\bar{\psi}$ was theoretically predicted to be proportional to $A^{0.5}$ which was found to be in agreement with experimental observations[(6)].

It is assumed that leaching of lime mortar is an example of simple dissolution (i.e. diffusion controlled) and that there are no chemical reactions at the peripheral surfaces of the pores as is the case with acid injection. Thus the most relevant example of acidisation with respect to Rising Damp is acidisation using a highly reactive acid, since this type of dissolution tends to be diffusion controlled.

Matrix acidisation with highly reactive acids has been investigated by Guin and Schecter[(10)] who used a simulation technique. Four types of pore size distribution were compared, with the pores

being selected by Monte Carlo methods, and placed randomly in the matrix. The growth of the pores was controlled by the pore growth function, $\bar{\psi}$. Studies of pore evolution with and without collisions were examined and compared with the corresponding exact analytical solutions of the change in the reduced pore size density function, $\bar{\eta}$. There was good agreement between the simulation method and the analytical solutions. Further studies using the simulation technique showed that the change in permeability to be dependent on the initial pore size distribution, when the case of no pore collisions was investigated. However, when collisions are allowed for, the permeability change of each pore size distribution is much less diverse. The change in permeability with respect to porosity of each distribution was shown to lie within a certain band of values, the width of the band becoming progressively narrower as the porosity increases.

Guin and Schecter[10] stated that in principle, there was no reason for all the initial pore size distributions to fall within the band, and they showed that the initial change in permeability was very dependent on the variety of pore sizes present in the system. Their explanation for the convergence of the permeability-porosity curves was the phenomenon known as "wormholing".

Wormholes are a result of pore collisions, which results in a few large pores dominating the response of the pore matrix to the acid injected. The large pores are generated, irrespective of the initial pore size distribution. The practical significance of wormhole creation is that it is not necessary to know the initial rock pore configuration to a high degree of accuracy to be able to estimate the results of some acidisations.

2.2 Dimensionless model

A different approach to the problem of estimating the change of hydraulic properties caused by acidisation has been presented by

Fogler and co-workers[11)-(18)] who studied the effect of constant flowrate of hydrochloric acid and mixtures of hydrochloric and hydroflouric acid mixtures upon sandstones.

A theory was developed which contained two dimensionless parameters, the Damkohler number and the acid capacity number, which together characterised the acidisation process. The Damkohler number is a measure of the rate of acid reaction as compared to the rate of convection of the acid.

$$D_a' = \frac{\bar{k}\ (W_O - W_I)\ \ell}{u} \tag{4}$$

where $\bar{k}$ is the reaction rate, which for the Fogler method has units of cm^3 of acid per gm. mole per sec (cm^3 g $mole^{-1}$ sec^{-1}); W_O, the initial concentration of minerals in the solid phase; W_I, the irreducible concentration of minerals in the solid phase; ℓ, the core length; u, the superficial velocity of the acid solution.

The acid capacity number is the molar ratio of the acid present in the pore space to the acid needed to dissolve all the dissoluble minerals in the corresponding solid space.

$$A_c = \frac{\phi_o\ C_o}{\bar{\gamma}_m (1-\phi_o)\ (W_O - W_I)} \tag{5}$$

where ϕ_o is the initial porosity of the sample; C_o, the inlet concentration of the acid; $\bar{\gamma}_m$, the moles of acid required to dissolve one mole of dissoluble minerals.

The Fogler method is essentially a combination of the rate of reaction law of hydroflouric acid with the dissoluble minerals and the differential mole balances of the dissoluble rock minerals and hydroflouric acid. This combination leads to a set of coupled non-linear differential equations, their solutions being[(14) (16)-(18)]

$$1/\psi' = 1 + \exp\ \{D_a'\ A_c\ \left[(1+1/A_c)\ \varepsilon' - \theta_p\right] \tag{6}$$

$$1/\eta' = 1 + \exp\ \{-D_a' A_c \left[(1+1/A_c)\varepsilon' - \theta_p\right]\} - \exp\ (-D_a'\varepsilon') \tag{7}$$

where ψ' is equal to C/C_o which is the concentration of acid at position x (along the core) divided by the original inlet acid concentration; ε' is equal x/ℓ, i.e. the fractional length along the sample core; $\theta_p = (u\ t)/(\phi_o\ \ell) = t/\tau$ which is the number of pore volumes of acid injected. u is the superficial velocity of acid solution; t, the time; ϕ_o, the original porosity of the matrix; ℓ, the length of the sample; τ, the space time of the core $(= (\phi_o \ell)/u)$; η', the dimensionless concentration of minerals $(= (W-W_I)/(W_O-W_I)$.

In considering eqn.(6), (7) two different fronts can be recognised, each of which moves with its own characteristic velocity through the sample. A front may be considered as a zone in the sample where the value of the derivative of the property, (i.e. permeability, porosity) changes rapidly with respect to the distance along the fluid flow path compared to other positions along the flow path.

The first is given by $\varepsilon' = 0$ (or $x = u\ t/\phi_o$). This front is the interface between the distilled water (which was used to initially saturate the sample) and the injected acid mixture. The velocity of this front is given by the ratio

$$x/t = u/\phi_o \quad . \tag{8}$$

The second front is the reaction front, its position is found from

$$\theta_p = (1 + 1/A_c)\varepsilon' \tag{9A}$$

or

$$ut/\phi_o\ell = (1 + 1/A_c)(x/\ell) \tag{9B}$$

The velocity of the reaction front is once again given by the ratio x/t

$$\frac{x}{t} = \frac{u}{\phi_o}\left(\frac{A_c}{1+A_c}\right) \tag{10}$$

Equation (7) may be used to estimate the change in porosity, $\Delta\phi$, at

any point, according to

$$\Delta\phi = (1 - \eta')(\Delta\phi)_{max} \tag{11}$$

where $(\Delta\phi)_{max}$ is the maximum porosity increase when all the dissoluble minerals accessible to the acid have been dissolved, which can be determined experimentally.

Similarly a relationship between the permeability change and porosity change was also determined experimentally[11], the expression being

$$\frac{k}{k_i} = \exp\left(\beta' \frac{(\Delta\phi)}{(\Delta\phi)_{max}}\right) \tag{12}$$

where k_i is the initial permeability and k, the local permeability. β' is an experimentally determined parameter.

It is important to determine β' as accurately as possible, because if the permeability is a strong function of porosity, it will lead the acid front, whereas if the permeability is only a weak function of porosity it will lag behind the acid front.

The overall permeability of the core is determined by integrating the local permeability over the length of the core

$$k_T = \frac{1}{\int_o^{\ell} \frac{dx}{k}} \tag{13}$$

where k_T is the overall permeability of the core.

Since the integration is performed on the reciprocal of the local permeability, the sections with low permeability will be dominating and k_{max} will have little effect upon the overall permeability. Hence the determination of the value of k_{max} corresponding to ϕ_{max} is not of critical importance.

The dimensionless groups can be modified slightly to form the ratios (D_a'/τ) and $A_c\bar{\gamma}_m/C_o$ whose values depend only on the initial properties of the porous material (sandstone). Noting that τ, the space time, is given by the expression $\phi_o\ell/u$ then

$$\frac{D'_a}{\tau} = \frac{\bar{k}\ (W_O - W_I)}{\phi_o} \tag{14}$$

$$\frac{A_c \bar{\gamma}_m}{C_o} = \frac{\phi_o}{(1-\phi_o)(W_O - W_I)} \tag{15}$$

The actual fitting of the experimental model to the permeability data from each experiment was performed by choosing the highest value of the permeability ratio, k/k_i, as possible without the latter showing signs of approaching a maximum.

A value of D'_a/τ was chosen and then the group $A_c\bar{\gamma}_m/C_o$ was selected such that the experimental and computed curves met at a given permeability ratio. A best estimate of D'_a/τ was found by choosing a value of D'_a/τ which makes the variance of the calculated $A_c\bar{\gamma}_m/C_o$ value from all the experiments small, and which simultaneously produces a good agreement between the calculated and measured concentration of acid. The effluent acid concentration can be calculated by substituting the value of $\varepsilon' = 1$ into eqn.(6). Also the groups D'_a/τ and $A_c\bar{\gamma}_m/C_o$ can be estimated from first principles[14].

The Damkohler number is a measure of the rate at which acid reacts compared to the rate at which it is transported by convection. As the value of the Damkohler number is increased, the degree of reaction between the acid and sandstone is likewise increased and therefore we could expect the internal reaction front to become much sharper.

Similarly if the acid capacity number is increased, then the reaction and permeability fronts are expected to transverse the core at a greater velocity, as indicated by equation (10). Thus both the Damkohler number and the acid capacity number will affect the shape of the permeability versus time curve.

An advantage of the Fogler method is that it is a non-geometric model, i.e. the expression depicting the permeability change has

been developed independently of the geometry of the pores in the porous material. Similarly the overall permeability, local permeability and reaction front are likewise expressed in terms of non-geometric parameters.

A disadvantage is that no knowledge can be gained of the physical mechanism producing the changes. Consider the example of a permeability front in a cylindrical core, the front may be a wormhole growing longitudinally through the core with little change to the surrounding material or alternatively may be a uniform broad band extending across the whole of the flow area. Obviously these two flow regimes can be characterised by the appropriate D_a' and A_c numbers, but it is obvious that the interstitial fluid flow will be very different.

In addition, it was assumed that there was no radial flow. It is very difficult to comment upon how this might affect the development or shape of the permeability front since the shape of the front has not been defined "physically".

For example one would expect there to be considerable radial flow from a wormhole due to its very existence and that the localised flows from the sides and the end of the wormhole will affect its growth rate. However, this point may not be of great importance since Fogler et al[14] has stated that once a front has become fully developed, it moves with constant velocity through the sample.

A major weakness of the Fogler method is the experimental correlation of the ϕ-k relationship. It has been shown by Schecter and Gidley[4] that there is no unique ϕ-k relationship which was also noted by Fogler[11]. Fogler assumed however, that for a given porous material one should expect the permeability, k, to increase in a prescribed manner as the porosity increases. Fogler does not state whether the acid reactivity (which affects the Damkohler

number) was altered, which, recalling the investigations of Schecter et al., plays an important part in determining the pore growth function and consequently the resulting ϕ-k relationship. Thus each Damkohler number would be related to a particular ϕ-k curve and that, generally, it would be wrong to apply the ϕ-k relationship obtained for a given Damkohler number, to the observed porosity changes for a system having a different Damkohler number.

3. Moving boundary models

Let us now consider a more "physical" approach to the problem of describing the evolution of a frontal system. A typical example is that of immiscible displacement of oil by water, where the oil-water interface is regarded as the front or moving boundary. It will soon become apparent that the oil-water displacement example can be simply and directly translated into a frontal system across which there is a discontinuity of fluid permeability. The water phase may be regarded as a zone of increased but constant permeability, k_f, and the oil phase may be regarded as the zone of unleached (original) permeability, k_o. The movement of the front, u_f, can be simply related to the flow of water, u_w.

3.1 Muskat Model

Treatment of the oil displacement process is based upon what has been called the Muskat model. This model is based upon the assumptions that there is a sharp front between the displacing and displaced fluid, and that on each side of the interface flow proceeds according to Darcy's law. Consider the following example of linear displacement (Fig. 1) where the velocity of fluid in the pores is u_p.

If the displacement process is total and stable, the displacement front also moves with a velocity u_p. The front moves a distance dx in time dt such that

$$dx = u_p \, dt \tag{16}$$

The volume of fluid is ϕ a dx, where a is the cross-sectional area available for flow and ϕ is the porosity of the porous material.

Application of Darcy's law to both the oil and water phases yields

$$\text{grad } P_w = \frac{\mu_w \, \phi \, u_p}{k_w} \tag{17a}$$

$$\text{grad } P_o = \frac{\mu_o \, \phi \, u_p}{k_o} \tag{17b}$$

where grad P is the pressure gradient; μ, the fluid viscosity; k, the fluid permeability and o, w refers to the oil and water phase respectively. The stable type of displacement described above will be referred to as case A.

Consider now displacement where a "finger" or "wormhole" might develop, (case B). Case B is shown schematically in Fig. 2. Once again a volume of water, a dx, is injected in time dt. The possibility of the existence of a finger, compared to the stable displacement process is dependent upon the following conditions:-

(i) Volume condition. The volume of fluid injected must be equal to the volume swept out by movement of the front and its associated fingers

$$\phi \, a \, dx = \phi \, (a' \, dx' + a'' \, dx'') \tag{18}$$

where $a = a' + a''$.

(ii) Equilibrium condition. A finger can only be maintained if there is no tendency for it either to spread out or become squeezed to nothing. This entails that the pressure gradient in the finger must be the same as that in the surrounding fluid. This condition can mathematically be expressed by equating expressions (17a) and (17b)

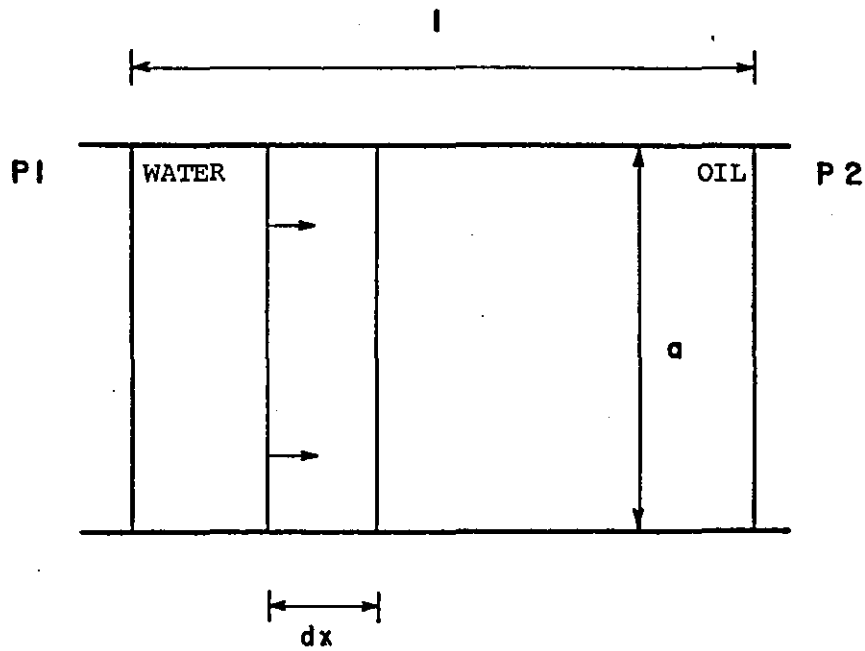

Fig. 1. Stable displacement front.

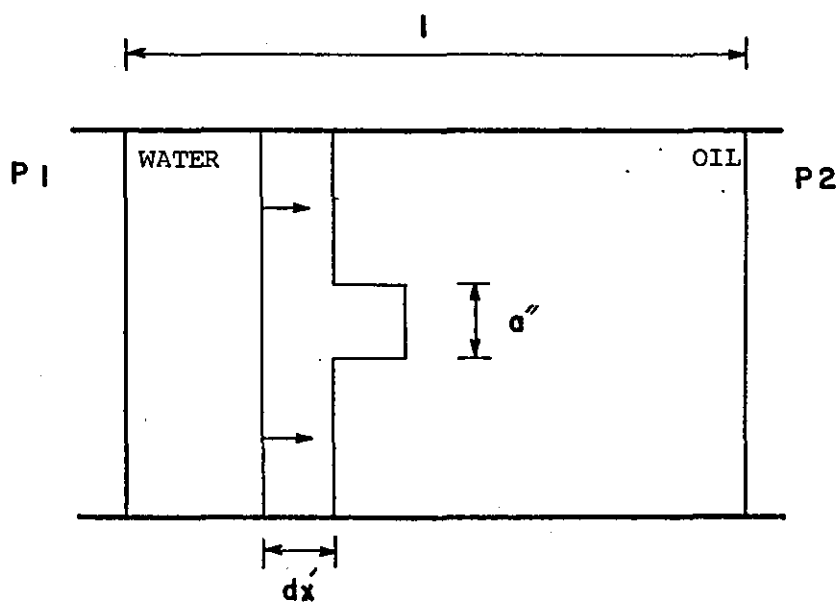

Fig. 2. Model of a finger.

$$\frac{\phi\ \mu_w\ u_w}{k_w} = \frac{\phi\ \mu_o\ u_o}{k_o} \tag{19}$$

which on substitution of $m_i = k_i/\mu_i$ and $u_i = dx_i/dt$, yields

$$m_w\ dx' = m_o\ dx''$$

or

$$dx''/dx' = m_w/m_o = \eta \tag{20}$$

(iii) Energy condition. A finger will develop if, by its formation, it consumes less energy than the corresponding stable displacement of the whole front, i.e. the energy consumed in case B must be less than that of case A. Scheidegger[19][20][21] has shown that the energy condition can be expressed as follows

$$dx'\left[\frac{\mu_w}{k_w}\ a'(dx')^2 + \frac{2\mu_o}{k_o}\ a''(dx'')^2 + \frac{\mu_o}{k_o}\ a'(dx')^2\right] \leqslant a\ dx^3\left[\frac{\mu_w}{k_w} + \frac{\mu_o}{k_o}\right] \tag{21}$$

On combination of the three conditions, represented by eqns. (18), (19), (20) and using the following notation

$$\frac{a'}{a} = \alpha'\ ;\ \frac{a''}{a} = \alpha''\ ;\ \frac{dx'}{dx} = \xi'\ ;\ \frac{dx''}{dx} = \xi''\ ;\ \frac{k_w}{\mu_w}\cdot\frac{\mu_o}{k_o} = \frac{m_w}{m_o} = \eta \tag{21a}$$

equation (21) can be reduced to

$$\xi''^2\left[\frac{\xi}{\eta^2} - \frac{1}{\eta^2} + 2\eta - 2\xi'' + \frac{1}{\eta}\ \xi'' - \frac{1}{\eta}\right] \leqslant \eta^2 - 1 \tag{22}$$

From the definition of a finger ξ'' must be greater than one. Taking the limiting case $\xi'' = 1$, eqn. (22) reduces to

$$\eta^2\ (\eta^2 - 2\eta + 1) \geqslant 0 \tag{23}$$

which is always satisfied.

Equation (20) implies that geometrically a finger can only exist if $\eta > 1$, since the very definition of a finger implies that $\xi'' > \xi'$. The last result shows that the Muskat model automatically indicates that fingering will occur as soon as the mobility ratio of the displacing fluid versus the displaced fluid is greater than unity, (i.e. $\eta > 1$: c.f. eqn. (20)).

Furthermore, using y to denote the energy condition (c.f. eqn.(22))

$$y = \xi''^3(1-2\eta^2+\eta) + \xi''^2(-1+2\eta^3-\eta) - \eta^2(\eta^2-1) \leqslant 0 \qquad (24)$$

which is the limiting case of $\xi'' = 1$ reduces to

$$y_{\xi''=1} = -\eta^2(\eta^2-2\eta+1) \qquad (25)$$

Inspection of equation (25) shows that there are double roots at $\eta=0$ and at $\eta=1$ and that for all other values of η, the value of y, is less than zero. This confirms that for $\eta>1$, there is always a range of values of ξ'' for which the energy condition (eqn.(24)) is satisfied.

This range of values of ξ'' may not necessarily be the whole domain $\xi''>1$. For large values of ξ'', y is negative. However, y may attain a range of positive values between $\xi''=1$ and $\xi''\to\infty$ (infinity). Since y is negative for large ξ'' then the range of positive values, if any, must have an extreme value (i.e. a peak) where the value of the derivative $\partial y/\partial\xi''$ is zero. Differentiating equation (24) with respect to ξ'' yields

$$\frac{\partial y}{\partial \xi''} = 3\xi''^2(1-2\eta^2+\eta) + 2\xi''(-1+2\eta^3-\eta) \qquad (26)$$

and thus, extreme values are at

$$\text{(i)} \qquad \xi'' = 0 \qquad (27a)$$

$$\text{(ii)} \qquad \xi'' = \frac{-2}{3}\left(\frac{-1+2\eta^3-\eta}{1-2\eta^2+\eta}\right) \qquad (27b)$$

For large η, eqn.(27b) reduces to

$$\xi''_{max} \simeq 2/3\ \eta \qquad (28)$$

and consequently $y(\xi''_{max})$ becomes (for large η and retaining only the highest powers of η)

$$y(\xi''_{max}) \simeq (8/27)\ \eta^5 \qquad (29)$$

The shape of the curve $y(\xi'')$ is shown in Fig. 3. An inspection of the curve, shows that the energy function y is positive (for large η) for a certain range of ξ''. This implies that there

is a forbidden range for the speed of a finger.

A further geometrical condition for the evolution of a finger is[19]

$$\alpha'' = \frac{1}{\xi''} \frac{\eta - \xi''}{\eta - 1} \tag{30}$$

Equation (30) shows that the fingers cannot be of arbitrary size. Or, in other words, if a certain fraction of the cross-section of a porous material, during linear displacement, is fingered out, then the velocity (ξ'') of these fingers is determined by eqn.(30).

The oil-water displacement problem has also been discussed by Collins[22]. Collins assumed that the initially oil-saturated porous material contained some irremovable water, whose saturation is denoted by S_c (connate water saturation). The displacement of oil was also assumed to be incomplete, the residual oil saturation is denoted by S_{ro}. If the superficial flow rate of water per unit area normal to the oil-water interface is u_w, then the velocity of the front u_f is given by

$$u_f = \frac{u_w}{\phi(1-S_{ro}-S_c)} \tag{31}$$

where ϕ is the porosity and it is assumed that the fluids are immiscible and incompressible. The velocity of water, u_w, can be substituted for by employing Darcy's law

$$u_f = \frac{d\,x_f}{dt} = \frac{-k_{wr}}{\mu_w} \frac{\partial\, p_w}{\partial\, x} \frac{1}{\phi(1-S_{ro}-S_c)} \tag{32}$$

where k_{wr} is the permeability to water at the residual oil saturation and $\partial\, p_w/\partial\, x$ is the pressure gradient in the water phase.

Furthermore, the aqueous pressure gradient may also be substituted for, to yield (ref(22) page 173)

$$u_f = \frac{d\,x_f}{dt} = \frac{k_{wr}}{\mu_w\,\phi} \frac{\Delta P}{(1-S_c-S_{ro})} \frac{1}{\eta\ell+(1-\eta)x_f} \tag{33}$$

where η is the mobility ratio, $(k_{wr}\,\mu_o)/(k_{oc}/\mu_w)$, and k_{oc}, is the

permeability to oil at the connate water saturation.

If the injection rate of water, u_w, is kept constant, then the pressure difference across the sample will vary linearly with the position of the front, x_f. Alternatively if the pressure difference across the sample is kept constant, then the front either accelerates or decelerates accordingly as $\eta>1$ or $\eta<1$. In the special case of $\eta=1$ the front moves with constant velocity and also the pressure distribution is independent of x_f. Note that the derivation above is essentially the same as case A (c.f. eqns. (16), (17a) (17b)).

Consider, the example as shown in Fig. 4, where there is a small bump on an otherwise plane oil-water interface (ref.(22) page 196). To discover the subsequent history of this bump, let us divide the flow domain into two isolated flow systems, one being a tube parallel to the direction of flow contained by the bump, the other being the remainder of the flow area, as shown in Fig. 4. The position of the front in each domain is measured from the inflow end; the distance for the domain containing the bump is $(x_f+\delta)$, whilst the distance for the other domain is x_f. δ is the length of the bump which is considered to be infinitesimal.

According to eqn.(33) the velocity of the front in each system is

$$\frac{d\,x_f}{dt} = \frac{k_{wr}\,\Delta P}{\mu_w\,\phi(1-S_c-S_{ro})}\left(\frac{1}{\eta\,\ell + (1-\eta)x_f}\right) \tag{34a}$$

$$\frac{d(x_f+\delta)}{dt} = \frac{k_{wr}\,\Delta P}{\mu_w\,\phi(1-S_c-S_{ro})}\left(\frac{1}{\eta\,\ell + (1-\eta)(x_f+\delta)}\right) \tag{34b}$$

If δ is very small in comparison to x_f, then eqns. (34a), (34b) yield

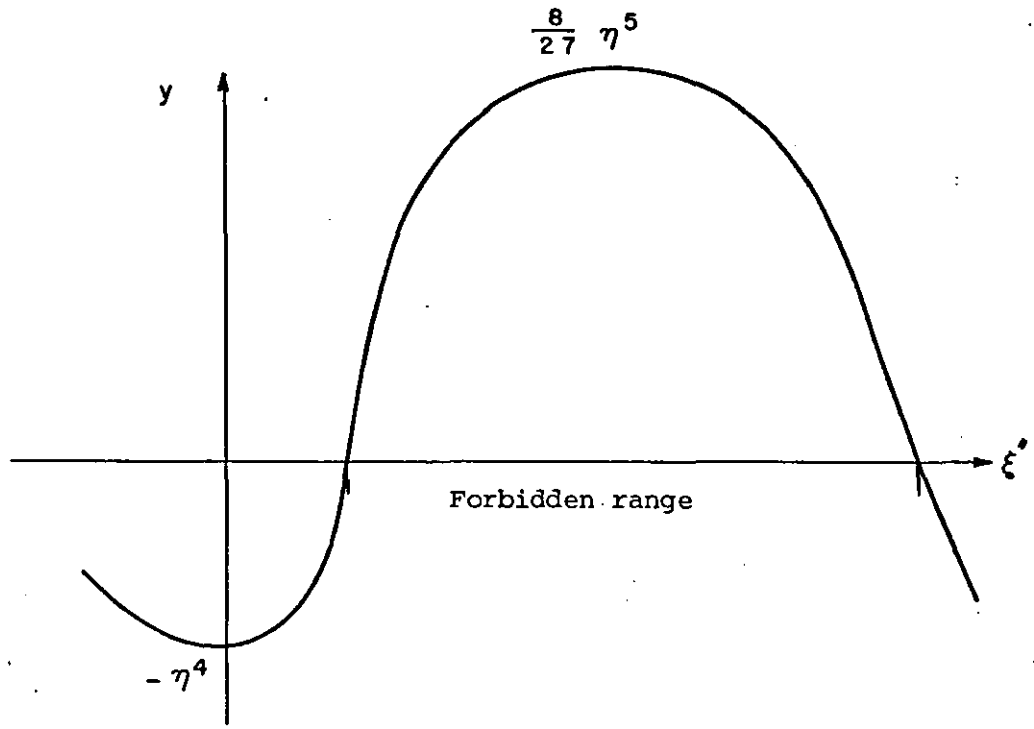

Fig. 3. Plot of the energy function y versus the dimensionless distance, $\xi''(dx''/dx)$.

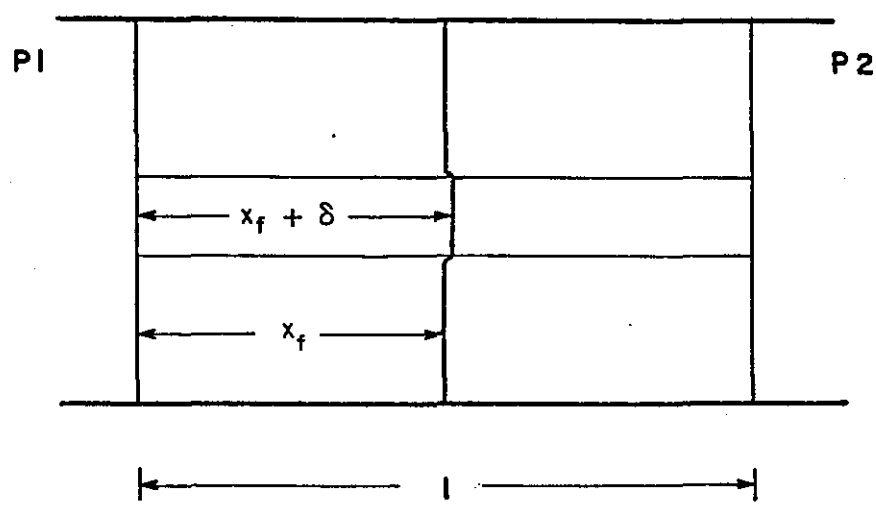

Fig. 4. Simplified model of a "small" frontal instability.

$$\frac{d\delta}{dt} = \frac{-k_{wr}\Delta P}{\mu_w \phi (1-S_c-S_{ro})} \left(\frac{(1-\eta)\delta}{[\eta\ell + (1-\eta)x_f]^2} \right) \tag{35}$$

Equation (35) shows that δ grows exponentially with time after inception of the bump, provided $\eta>1$; or decays exponentially with time if $\eta<1$. For $\eta= 1$, δ does not alter with time. This simple analysis shows that if the displacing fluid is more mobile than the displaced fluid, any small irregularities of the front, grow rapidly to take the form of "wormholes" or "fingers".

Equation (35) cannot predict the behaviour of large fingers. To determine the behaviour of large fingers, it is necessary to examine the displacement process from a macroscopic viewpoint, that is, we shall only be interested in the average behaviour of the two fluids[23]. The individual shape and size of fingers will be disregarded except for the fact that the sum of their individual areas will be used to determine an average cross-sectional area of one large finger (Fig. 5).

This example is also based upon the Muskat model. Even though the front is now irregular, it is assumed that there is a sharp interface between the two fluids, and that displacement is complete (i.e. $S_c = 0$ and $S_{ro} = 0$). Darcy's law is assumed to apply to both fluids which are taken to be immiscible and incompressible. Finally, it is assumed that the pressure P does not vary along any line normal to the overall direction of fluid flow, as indicated at level x (Fig. 5). The average fractional area occupied by either of the two fluids is denoted by S_w for water, and S_o for oil and that at all x

$$S_w + S_o = 1 \tag{36}$$

Furthermore S_w and S_o are taken as functions of position (x) and time (t) only.

Application of Darcy's law to either fluid at any level, x, yields

$$U_i = -k \frac{k_i'}{\mu_i} \text{grad } P \tag{37}$$

where U_i is the superficial velocity of the ith fluid; k, the permeability of the material when completely saturated with fluid; k_i', the relative permeability which is a function of saturation (or area) occupied by the ith fluid at that level; grad P, the pressure gradient.

The problem is determined, if in addition to the two equations of motion (eqn.(37)) two continuity conditions are considered

$$\phi \frac{\partial S_i}{\partial t} = - \text{div } U_i \tag{38}$$

Equations (36),(37),(38) may be combined to yield the following differential equation

$$\left[\frac{U_T}{\phi} \frac{df_w}{dS_w}\right] \frac{dS_w}{d\ x} = - \frac{\partial S_w}{\partial t} \tag{39}$$

where U_T is the total fluid velocity $(=U_w+U_o)$; U_w the water velocity may be defined as Q_w/A, where Q_w is the volumetric water flow rate and A the area for flow. Similarly the oil velocity, U_o, is given by Q_o/A. The ratio of the water flow rate to the total flow rate, f_w is expressed by

$$f_w = \frac{U_w}{U_T} = \frac{U_w}{U_w+U_o} = \frac{Q_w}{Q_w+Q_o} = \frac{k_w'/\mu_w}{(k_w'/\mu_w)+(k_o'/\mu_o)} \tag{40}$$

The problem now is to find a relationship between k_i' and S_i. This can be easily done by considering oil-water flow through unit area of porous material as can be found in Fig. 6. The equation of motion is expressed in terms of relative permeability (eqn.(37)), which for the water phase is

$$U_w = -k \frac{k_w'}{\mu_w} \frac{\Delta P}{\ell} \tag{42}$$

Alternatively Darcy's law can be applied only to that portion of the porous material containing the aqueous phase

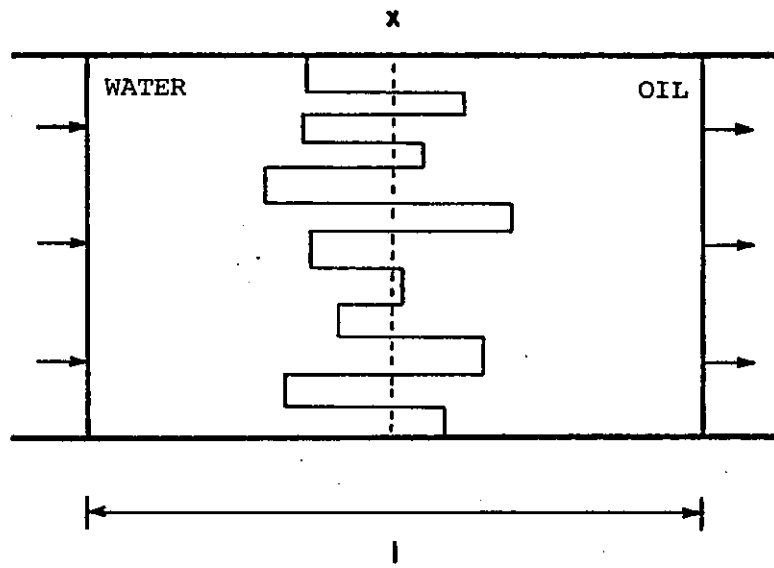

Fig. 5. Schematic representation of fingers.

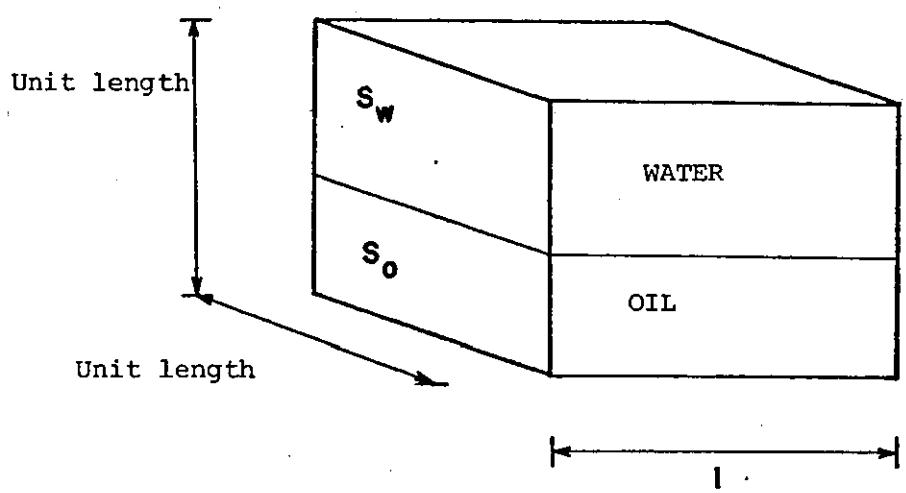

Fig. 6. Schematic representation of the simultaneous flow of oil and water through a porous material.

$$U_w = -k \frac{S_w}{\mu_w} \frac{\Delta P}{\ell} \tag{42}$$

From (41) and (42) we have the equality

$$k'_w = S_w \tag{43}$$

and hence

$$f_w = \frac{(S_w/\mu_w)}{(S_w/\mu_w)+((1-S_w)/\mu_o)} = \frac{m'}{m'-1 + (1/S_w)} \tag{44}$$

where m' is defined as

$$m' = \mu_o/\mu_w \tag{45}$$

Equation (43) shows that the relative permeability curve (k'_i as fn. of S_i) are straight lines as shown in Fig. 7. It is obvious that $f(S_w)$ has no inflection point, so that no "shock front" can develop[(20)-(22)(24)].

The total derivative of $S_w(x,t)$ with respect to time is

$$\frac{dS_w}{d\,t} = \frac{\partial S_w}{\partial\, x}\frac{dx}{dt} + \frac{\partial S_w}{\partial\, t} \tag{46}$$

and if $x = x(t)$ is chosen to coincide with a surface of constant S_w

$$dS_w = 0 \tag{47}$$

$$\left[\frac{dx}{dt}\right]_{S_w} \frac{\partial S_w}{\partial\, x} = -\frac{\partial S_w}{\partial\, t} \tag{48}$$

Using equations (39) and (48) to eliminate $\partial S_w/\partial t$

$$\left[\frac{dx}{dt}\right]_{S_w} = \left[\frac{U_T}{\phi}\frac{d\,f_w}{d\,S_w}\right] \tag{49}$$

Equation (49) is known as the Buckley-Leverett equation. Substitution of the derivative of $f_w(S_w)$ yields

$$\left[\frac{dx}{dt}\right]_{S_w} = \frac{U_T}{\phi}\frac{m'}{[S_w(m'-1)+1]^2} \tag{50}$$

If U_T is kept constant, then eqn. (50) can be integrated to yield

$$[x]_{S_w} = \frac{U_T}{\phi} \frac{m'}{[S_w(m'-1) + 1]^2} t \qquad (51)$$

Eqn.(50) shows that the speed of a particular area (S_w) is constant as it traverses the sample, and that there is no stabilisation of any array of fingers which have developed. Further treatment of this model has been discussed by Scheidegger et al[25][26], who confirmed that for a homogeneous porous material, no stabilisation of fingers was possible.

In order to compare the analogous oil-water process to that of a moving permeability front, it is necessary to make the following assumptions:- (1) Dissolution of the porous matrix at the front only occurs over a small distance, i.e. there is a sharp permeability front. (2) Fluid moving toward the front is unsaturated with respect to the material being dissolved from the matrix, and that fluid moving away from the interface is completely saturated with dissolved material. (3) The actual movement of the front is proportional to the flux of unsaturated fluid at that point, i.e.

$$U_f = c' U_u \qquad (52)$$

where U_f is the velocity of the front; U_u, the velocity of the unsaturated fluid (c.f. U_w in the oil displacement example); c', a constant relating the amount of material dissolved to the volume of unsaturated fluid passing across the interface. Equation (52) corresponds to equation (31). (4) The change in pore volume ($\Delta\phi$) accompanying dissolution of the matrix is small in comparison to the volume of fluid required to produce this porosity difference. That is the constant c' in equation (52) is small. (5) Darcy's law is applicable to fluid in front of and behind the interface.

These assumptions do not alter the findings of the stability criteria (Eqn.(16) through (30)) or the behaviour of small fingers (Eqn.(31) through (35)) but merely affect the

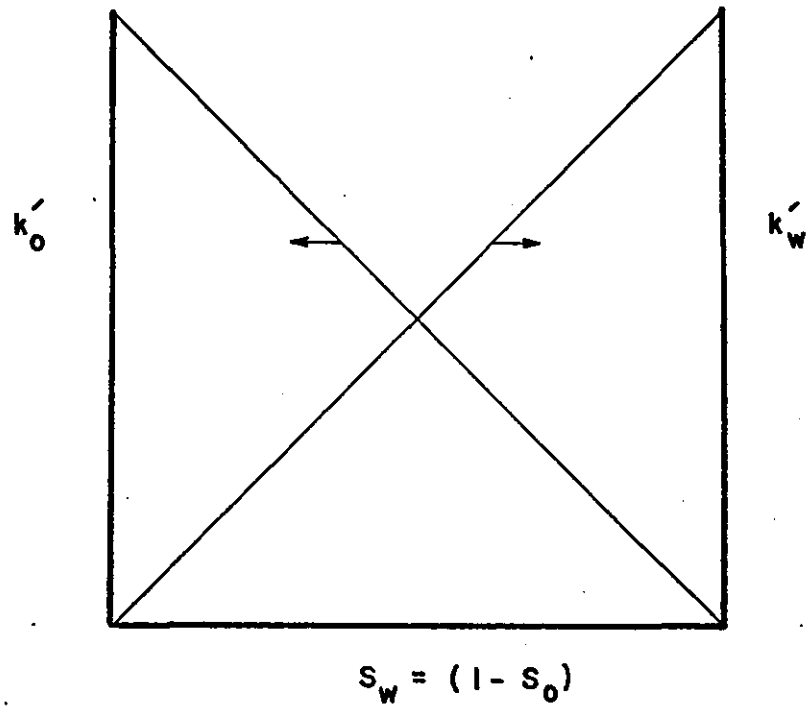

Fig. 7. Fictitious relative permeability curves.

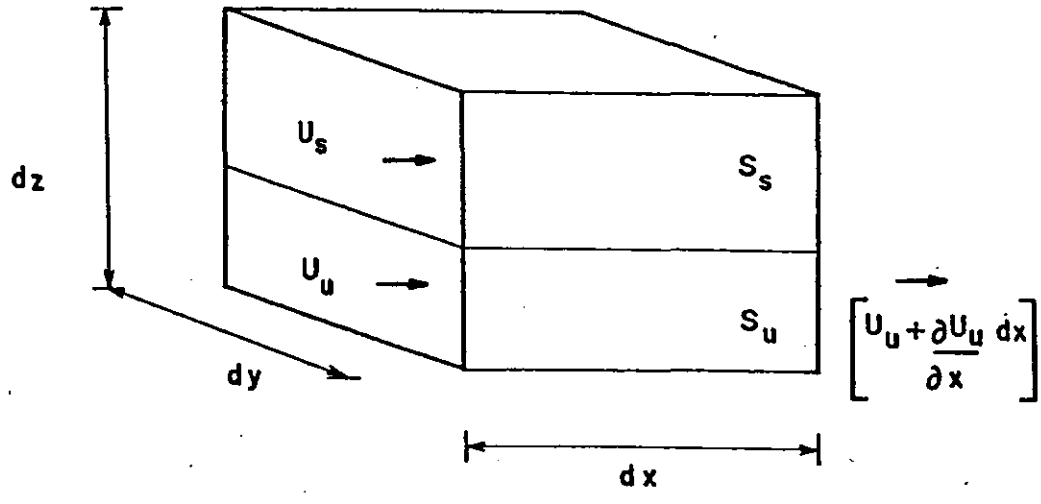

Fig. 8. Schematic representation of the simultaneous flow of unleached and leached fluid within a porous material.

notation of symbols in the corresponding expressions. However, the analogy relating the behaviour of large fingers is not so straight forward, as is shown below.

Consider the partial dissolution of a small elemental volume dx, dy, dz, as shown in Fig. 8, where the direction of fluid is parallel to the x axis. "Unsaturated" fluid flows into the cube, with velocity U_u. Similarly fluid saturated with dissolved material has a velocity, U_s. It is assumed that the change in pore volume, by dissolution is small in comparison to the volume of unsaturated fluid needed to produce the change in pore volume.

If the fluid is incompressible then applying the equation of continuity to the saturated and unsaturated flows

$$\frac{-\partial U_u}{\partial x} = c' \frac{\partial S_u}{\partial t} \tag{53}$$

$$\frac{-\partial U_s}{\partial x} = c' \frac{\partial S_s}{\partial t} \tag{54}$$

S_u and S_s represent the fractional areas occupied by the unsaturated and saturated fluid respectively. c' is a constant relating the volume of material dissolved to the volume of unsaturated fluid needed to dissolve the solid. Equation (53) simply relates the loss of unsaturated fluid to the overall increase in volume of the porous material that has been leached away by passage of unsaturated fluid.

The fractional areas are related by

$$S_u + S_s = 1 \tag{55}$$

which together with equations (53), (54) yields

$$\frac{-(U_u+U_s)}{\partial x} = \frac{(S_u+S_s)}{\partial t} = 0 \tag{56}$$

Equation (56) implies that the overall fluid velocity, U_T, is constant and

$$U_T = (Q_T/A) = U_u + U_s = (Q_u + Q_s)/A \tag{57}$$

The fractional flow rate, f_u, of unsaturated fluid with respect to the overall flow rate

$$f_u = \frac{Q_u}{Q_u+Q_s} = \frac{Q_u}{Q_T} \tag{58}$$

Combination of (53) and (58) yields

$$\frac{-Q_T}{A}\frac{\partial f_u}{\partial x} = c' \frac{\partial S_u}{\partial t} \tag{59}$$

Since the fractional flow of unsaturated fluid is simply a function of the fractional area occupied by the unsaturated fluid, then

$$\frac{\partial f_u}{\partial x} = \frac{d f_u}{d S_u}\frac{\partial S_u}{\partial x} \tag{60}$$

and

$$\frac{-Q_T}{A}\frac{d f_u}{d S_u}\frac{\partial S_u}{\partial x} = c' \frac{\partial S_u}{\partial t} \tag{61}$$

The total derivative of $S_u(x,t)$ with respect to time is

$$\frac{d S_u}{dt} = \frac{\partial S_u}{\partial x}\frac{dx}{dt} + \frac{\partial S_u}{\partial t} \tag{62}$$

and, if $x(t)$ is chosen to coincide with a surface of fixed S_u

$$\frac{d S_u}{dt} = 0 \tag{63}$$

and

$$\left(\frac{dx}{dt}\right)_{S_u} = \frac{-\partial S_u}{\partial t}\left(\frac{\partial S_u}{\partial x}\right)^{-1} \tag{64}$$

Using eqn. (61) to eliminate $\partial S_u/\partial t$ from eqn. (64)

$$\left(\frac{dx}{dt}\right)_{S_u} = \frac{1}{c'}\frac{Q_T}{A}\frac{d f_u}{d S_u} \tag{65}$$

This expression is similar to the Buckley-Leverett equation (c.f. eqn. (49)).

Applying Darcy's law to equation (58)

$$f_u = \frac{(k_u\ S_u/\mu_u)}{(k_u\ S_u/\mu_u)+(k_s\ S_s/\mu_s)} = \frac{(k_u\ S_u/\mu_u)}{(k_u\ S_u/\mu_u)+(k_s\ (1-S_u)/\mu_s)} \quad (66)$$

where k_u is the permeability of the leached porous material; k_s, the original (unleached) permeability of the porous material.

If we make the arbitrary simplifying assumption that $\mu_u = \mu_s$ and that $m'' = k_u/k_s$, then equation (66) reduces to

$$f_u = m'' \ / \ (m''-1 + 1/S_u) \quad (67)$$

It is obvious that eqn. (67) corresponds to eqn.(44) and eqn. (65) corresponds to equation (49). Hence the speed at which a given fractional area of leached porous material will traverse the sample is given by

$$\left[\frac{dx}{dt}\right]_{S_u} = \frac{1}{c'} \ \frac{Q_T \quad m''}{A\ \left[S_u\,(m''-1) + 1\right]^2} \quad (68)$$

Equation (68) shows that, if the total flow rate, Q_T, remains constant, then the velocity of a given area will also be constant for any given m". Furthermore, the assumption that the pressure across planes normal to the direction of flow is constant, implies that there is no radial flow of fluids; and recalling that the velocity of any interface remains constant, then the flow rate through any given area of interface must be constant irrespective of its longitudinal position. This condition is equivalent to case A, (Fig. 1). Also as every high pressure (unleached) element of the porous matrix is steadily replaced by a correspondingly low pressure element (leached), the total pressure drop across the sample will fall linearly as the interface moves through the core.

4. Discussion of the models predicting the change of permeability

The three most useful models with respect to leaching are the acidisation models of Schecter and Gidley (capillaric model) and Fogler (non-geometric) and the oil displacement model.

(1) The problem of fully describing the flow pattern (longitudinal and radial) in a cylindrical core has been avoided in all

three models. In the two acidisation models, the core is subdivided into a series of thin discs and the subsequent effect of acid upon each disc is then ascertained. The inlet acid concentration to the next disc is an average value of the effluent acid from the previous disc.

The effluent acid mixing process is one of the major defects of the models, since the effect of localised acid concentrations, both radially and longitudinally, cannot be accounted for. Note that both the radial and axial fluid flow components affect the shape and growth of wormholes; and hence the permeability response of the material to penetrating fluid.

The major defect of the oil-displacement model, when applied to predicting the behaviour of large fingers, is the assumption that the pressure is constant across all planes perpendicular to the direction of flow. This assumption prohibits the possibility of there being any radial flow.

(2) The experimental results of Fogler et al[13] show that there is, initially, a period of constant permeability, whilst the frontal system becomes fully developed. The initial period of constant permeability is followed by a period of rapidly increasing permeability. The experimental behaviour can be predicted theoretically by the appropriate choice of acid capacity number and Damkohler number[14]. Further analysis predicted that once a frontal system has become fully developed, the front then moves through the sample with constant velocity.

(3) Foglers' findings are similar to the theoretical predictions derived via the oil-displacement model. For the oil-displacement model, it has been shown that for small fingers, their growth follows an exponential law (eqn.(35)) whereas for large fingers, each element of the frontal interface moves with its own constant velocity (eqn.(68)).

The implications to be concluded from the oil-displacement model are that once a front has become fully established, the flow rate of fluid through each area remains constant; and that areas of the interface then move through the sample with constant velocity. This steady motion simultaneously produces a linear decrease of the total pressure drop across the sample, provided that the overall injection rate of fluid remains constant.

For a fully developed frontal system, the Fogler model predicts that the whole interface moves with constant velocity whilst the displacement model predicts that each element of the interface moves with its own constant characteristic velocity.

(4) Interpretation of capillaric model results of Schecter and Gidley are more difficult. Predictions of permeability versus porosity, using a simulation technique employing four types of pore size distribution, were made for cases where highly reactive and retarded acids were used. With highly reactive acids, and neglecting pore collisions, the response of each pore size distribution was found to vary; however, inclusion of the pore collision mechanism produced a similar response for all the pore distributions irrespective of the initial values[10]. From this result, Schecter et al, concluded that the convergent behaviour of the pore distribution was governed by the production of wormholes which tended to dominate the overall flow pattern; (i.e. a fully developed frontal system has become developed, which is the same frontal system irrespective of the initial pore size distribution).

Similarly, with the study of flowing retarded acid systems, the permeability response of each type of pore size distribution was found to lie within a certain band, albeit a different one to that obtained for flowing highly reactive acids[6]. Unfortunately the pressure (or permeability) response versus injected volume of fluid

(or pressure versus time, if the injection rate of fluid is constant) has not been included in their data and hence no comparison of their findings and those of Fogler or the displacement method has been attempted.

(5) The evolution of a frontal system within a porous material is not satisfactorily described by any of the models. The Fogler method suffers a major defect in the method of determining a localised experimental permeability versus porosity relationship and the subsequent fitting of the Damkohler and acid capacity numbers to the experimental curves.

The Schecter model is of limited usefulness since a knowledge of the pore size distribution and pore structure is required. A common fault of all the models, with respect to evolution of a frontal system, is theirneglection of the fluid radial flow component which plays an important part in determining the width and moderating the longitudinal growth rate of the wormhole.

(6) A difficulty with the displacement model is deciding when the frontal system has become fully established, and hence when calculation of the steady interfacial velocities may be performed. However, the displacement method does provide the simple result that the overall pressure across the sample should fall linearly once the front has become established.

(7) The determination of the increase in permeability of a porous material because of leaching is of considerable importance to the phenomenon of Rising Damp. since rate of change of permeability affects the breakthrough time of the moisture barrier, (i.e. failure time of the damp-proof course or moisture barrier, and the amount of moisture entering into the wall).

A fundamental difference between the acidisation and oil-displacement methods, discussed above, and leaching associated with Rising Damp is that the former methods are characterised by constant

fluid flow velocity and reducing pressure gradient across the sample. Leaching is a process which can most likely be considered as being characterised by a constant pressure difference and increasing flow rate.

The sample may be regarded as a leaky damp proof course. On one side of the sample, the wall can be considered as very wet, (i.e. low suctions) and on the other side of the sample, the wall is very dry, (i.e. high suctions). If the amount of moisture required to leach the sample is small in comparison to the capacity of the dry wall to absorb moisture, without altering its (high) suction, then the leaching process will occur at constant pressure difference. The pressure difference will remain constant until the latter stages of the leaching process, when by this time the flow rate of moisture will be so high that the 'dry' section of wall can be regarded as a new section of damp wall.

At this stage the leaching process then proceeds to attack the next moisture barrier in exactly the same fashion, except the barrier will now be higher up the wall, or at a greater distance from the source of moisture.

In order to elucidate the difference between constant flow leaching and constant pressure leaching processes, let us examine the response of the two systems; one where the flow rate of injected fluid is kept constant whilst the pressure difference across the sample is allowed to vary; and the alternative system where the overall pressure difference is kept constant whilst the fluid flow rate is allowed to increase. In all other respects the two systems are exactly the same. A schematic representation of the porous system can be found in Fig. 9.

The flow rate of fluid, of constant viscosity, μ, within the system is denoted by Q; the area for flow denoted by A. The velocity of the fluid, u is thus denoted by Q/A. The total

pressure difference, ΔP_T, across the sample is the sum of the pressure differences of the leached and unleached regions. The permeability of the leached region is denoted by k_f and the initial permeability (unleached material) by k_i. The ratio of the two permeabilities, k_f/k_i is denoted by m". The position of the interface is shown at a distance x_f from the inlet face of the material, which is of total length ℓ.

It is assumed that the change of porosity, because of leaching, with respect to the volume of fluid passing through the sample is small.

Application of Darcy's law to both regions of the material yields the expression

$$\frac{\Delta P_T}{u} = \frac{\mu\ (x_f + m''(\ell - x_f)\ )}{k_f} \tag{69}$$

In eqn. (52) it was assumed that the velocity of the front, u_f, was directly proportional to the flow of moisture, u, passing across the interface, i.e.

$$u_f = c'\ u_u \tag{70a}$$

and

$$\frac{d\ x_f}{dt} = c'\ u_u = \frac{c'}{A}\ \frac{dV}{dt} \tag{70b}$$

where c' is a constant relating the velocity of the front to the velocity of unsaturated fluid passing across the front. V is the volume of fluid and t the time.

The time for breakthrough for the constant flow (case (1)) and constant pressure (case (2)) systems will be developed subject to the following boundary conditions:- (1) the net initial pressure difference is denoted by ΔP_{TO}, and the initial superficial fluid velocity by u_o. At time t=0, the volume of fluid, V = 0, and there is no frontal interface, i.e. $x_f = 0$.

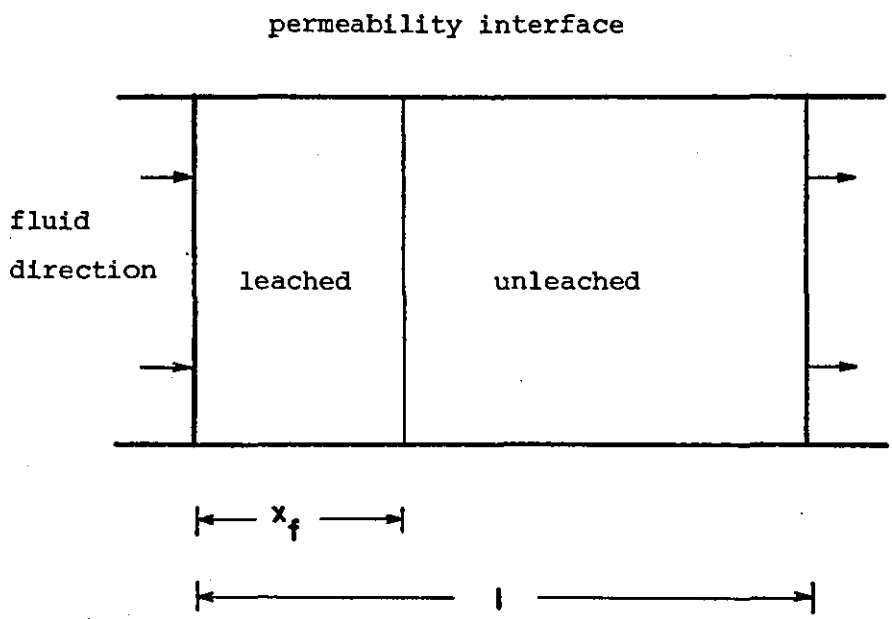

Fig. 9. Schematic representation of a permeability interface moving through a porous material.

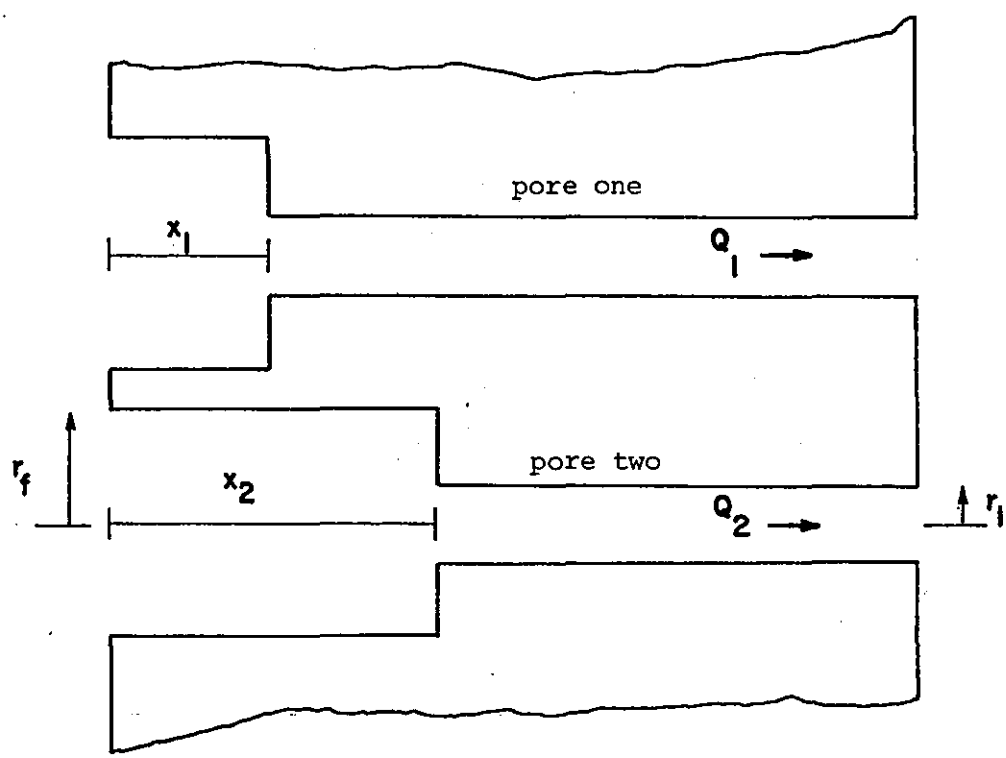

Fig. 10. Section of a porous material containing two pores of differing step lengths.

Case (1) Constant flow velocity, u.

Integration of eqn.(70b), which with the boundary conditions $V = 0$, $x_f = 0$ yields

$$x_f = (C'V)/A \tag{71}$$

Similarly eqn.(70a) can be re-arranged to yield

$$d\,V = A\,u\,dt \tag{72}$$

which on integration, using the boundary conditions $V = 0$, $t = 0$, yields

$$V = A\,u\,t \tag{73}$$

Combining eqns. (73) and (69), and noting that for the initial conditions $u = u_o$, $\Delta P_T = \Delta P_{TO}$ and $x_f = 0$ then

$$t^1 = \frac{V\,\mu\,m''\,\ell}{A\,\Delta P_{TO}\,k_f} \tag{74}$$

Case (2) Constant pressure difference, ΔP_T.

From eqn. (69)

$$u = \frac{\Delta P_T\;k_f}{\mu\,\left[x_f + m''(\ell - x_f)\right]} \tag{75}$$

which together with eqn. (72) yields

$$\left[x_f + m''(\ell - x_f)\right]\,d\,V = \frac{A\,\Delta P_T\,k_f\,dt}{\mu} \tag{76}$$

Substituting for x_f (eqn.(71)) in eqn. (76) and integrating, with the boundary conditions $t = 0$, $V = 0$, and noting that $\Delta P_T = \Delta P_{TO}$;

$$t^2 = \frac{\mu}{A\,\Delta P_{TO}\,k_f}\left[\frac{c'V^2}{2A} + m''\ell V - \frac{m''\,c'\,V^2}{2A}\right] \tag{77}$$

Note that for very small volumes, i.e. $V^2 \to 0$), eqn. (77) reduces to eqn. (74).

If V in eqn. (74) and (77) represents the volume required for 'breakthrough' of the fluid, or in other words, if V is the volume of fluid which causes the moisture barrier to fail then t represents the breakthrough time. Note that for the assumed conditions of dissolution, the volume of fluid required to dissolve

the matrix is the same for cases (1) and (2).

Since the fluid is allowed to accelerate through the porous material in case (2), one would expect the breakthrough time of case (2), t^2, to always be less than the breakthrough time of case (1), t^1; hence

$$\frac{t^2}{t^1} = \frac{\frac{c' V^2}{2A} + m'' \ell V - \frac{m'' c' V^2}{2A}}{m'' \ell V} < 1 \qquad (78)$$

m" is the permeability ration k_f/k_i, which is always greater than unity; thus the equality of eqn. (78) is always satisfied.

If t = 0 corresponds to the beginning of the linear failure rate, and t = t corresponds to breakthrough, then eqn. (78) can be used to predict the accelerated failure rate due to the continually increasing flow rate. Furthermore inspection of eqn. (78) shows the importance of the permeability ration, k_f/k_i, and the breakthrough time.

(8) Let us now examine the implications of the linear failure rate, predicted by the oil displacement method, with respect to the permeability response of individual porous samples. The effect of linear failure can be more easily visualised via a capillaric model.

The porous material can be regarded as a series of capillary tubes of initial radius, r_i, and after leaching the radius has increased to a maximum value, r_f. The interface between the leached and unleached region in a pore is assumed to be sharp, i.e. a step increase in radius as shown in Fig. 10. This assumption that the mass transfer rate of solid into solution is very high and remains constant irrespective of the position of the step within the pore.

For the sake of simplicity, only two capillaries have been reproduced in Fig. 10, each with a different step length (x_1, x_2). According to the oil displacement model, for large fingers, the

flow down each pore is constant. This means that each step moves along each pore, with its own characteristic velocity, which for the model described in Fig. 10, will depend on the intial configuration of the pores. In addition, the permeability or pressure response of the pore network will also be determined by the initial pore configuration, (i.e. the individual position of the steps within the pores at the start of the leaching process).

For a fixed number of pores per unit area, and for a given initial step pore length (sum of the individual step lengths, which for Fig. 10 is given by x_1+x_2), then the individual step lengths can be arranged in an infinite variety of different step arrangements, each of which characterised by its own permeability response. Hence the response (permeability and breakthrough time) of each porous material will be unique.

It is to be expected though, that similar porous materials will exhibit common statistical pore size properties, and hence will exhibit similar permeability - porosity responses, when the number of samples examined is large. However, problems will be encountered in correlating the response of similar porous materials due to the variability of time required to establish a frontal system measured from the beginning of fluid injection; and due to the difficulty of determining the pore size distribution existing at the onset of the linear failure rate, especially so if these variables are also unique functions of each individual porous material.

List of symbols and units of Chapter Six

A pore area (cm^2)

A_c acid capacity number ($= (\phi_o C_o)/(\bar{\gamma}_m(1-\phi_o)(W_O-W_I))$)

C concentration of acid

C_o initial concentration of acid

D molecular diffusion coefficient of acid ($cm^2 sec^{-1}$)

D_a' Damkohler number ($= \bar{k}(W_O-W_I)\ell/u$)

F a factor ($= Q/(K\,\bar{\ell}\,w^2)$)

f_w fractional water flowrate with respect to the total flow rate within the porous material

f_u fractional flowrate of unsaturated fluid with respect to the overall flowrate within a porous material

K a factor proportional to the permeability to fluid of rock

k local permeability to fluid of the porous material (cm^2)

k' relative permeability

k_i initial permeability to fluid of the porous material (cm^2)

k_v permeability to fluid of the porous material after a volume, V, of fluid has passed through the porous material (cm^2)

k_f final permeability of the porous material (cm^2)

k_T overall permeability to fluid of the porous material (cm^2)

k_{wr} permeability of the porous material to water at the residual oil saturation (cm^2)

k_{oc} permeability of the porous material to oil at the connate wate water saturation (cm^2)

$\bar{k}$ reaction rate constant

ℓ length (cm)

$\bar{\ell}$ mean pore length (cm)

m' viscosity ratio (μ_o/μ_w)

m'' permeability ratio of leached to unleached porous matrix

grad P pressure gradient ($g\ cm^{-2} sec^{-2}$)

Q volumetric flowrate ($cm^3 sec^{-1}$)

Q_w volumetric flowrate of water ($cm^3 sec^{-1}$)

Q_o volumetric flow rate of oil ($cm^3 sec^{-1}$)

S_o fractional area occupied by oil phase

S_s fractional area occupied by saturated fluid

S_u fractional area occupied by unsaturated fluid

S_w fractional area occupied by water phase

t time (sec)

U_s superficial velocity of unsaturated fluid ($cm\ sec^{-1}$)

U_u superficial velocity of unsaturated fluid ($cm\ sec^{-1}$)

u superficial velocity of acid solution ($cm\ sec^{-1}$)

$\bar{u}$ mean fluid velocity in a pore ($cm\ sec^{-1}$)

u_f velocity of a front ($cm\ sec^{-1}$)

u_o superficial velocity of oil ($cm\ sec^{-1}$)

u_p velocity within a pore ($cm\ sec^{-1}$)

u_T overall superficial velocity of fluids ($cm\ sec^{-1}$)

u_w superficial velocity of water ($cm\ sec^{-1}$)

V volume of fluid pumped through the porous material (cm^3)

W concentration of minerals in the solid phase ($g\ mole\ cm^{-3}$)

W_I irreducible concentration of minerals in the solid phase ($g\ mole\ cm^{-3}$)

W_O initial concentration of minerals in the solid phase ($g\ mole\ cm^{-3}$)

w^2 area of porous material available for fluid flow inclusive of both solid and pore space (cm^2)

X dissolving power of acid solution

x distance measured along the porous material

x_f position of a frontal interface measured fron the inlet surface of the porous material

$\bar{\alpha}$ a dimensionless ratio of mean reactant concentration within a pore to the mean surface concentration

Γ perimeter of a pore (cm)

$\bar{\gamma}$ mass of solid dissolved per unit mass of acid expended

$\bar{\gamma}_m$ moles of acid required to dissolve one mole of dissoluble minerals

ε' fractional length along a porous material (= x/ℓ)

η mobility ration (= $(k_1\mu_2)/(k_2\mu_1)$)

$\bar{\eta}$ pore size density function

η' a factor (= $(W-W_I)/(W_O-W_I)$)

θ_p number of pore volumes of acid

λ a constant

μ_o viscosity of oil (g $cm^{-1}sec^{-1}$)

μ_w viscosity of water (g $cm^{-1}sec^{-1}$)

ρ_s density of solids within a porous material

ϕ porosity of a porous material

ϕ_o original porosity of a porous material

$\bar{\psi}$ pore growth rate function ($cm^2 sec^{-1}$)

ψ ratio of acid concentration within a porous material to inlet acid concentration

τ space time constant of fluid within a porous material (= $\phi\ell/u$) (sec)

References Chapter Six

1. "Rising Damp", G. Mason, Building Sci., 9, pp.227-231, 1974

2. "Etude des lois de l'acidification", J. Nougaro, C. Labbe, Rev. de l'institut Francais du petrole, 10, No. 5, pp.354-364

3. "Theory of acid treatment of limestone formations", G. Rowan, Jnl. of Inst. of Petroleum, 45, No. 431, pp.321-334, 1959

4. "The change in pore size distributions from surface reactions in porous media", R.S. Schecter, J.L. Gidley, Am. Inst. Chem. Eng. Jnl., 15, No. 3, pp.339-350, 1969

5. "Chemically induced changes in porous media", J.A. Guin, R.S. Schecter, I.H. Silberberg. Ind. Eng. Chem. Fundam., 10, No. 1, pp.50-54, 1971

6. "Dissolution of a porous matrix by a slowly reacting acid", W.E. Sinex, R.S. Schecter, I.H. Silberberg. Ind. Eng. Chem. Fundam., 11, No. 2, pp.205-209, 1972

7. "Hydrofluoric acid reaction with sandstone", B.B. Williams, M.E. Whiteley. Soc. Pet. Eng. Jnl., 11, pp.306-314, 1971

8. "Dissolution of a homogeneous porous medium by surface reaction" M.C. Glover, J.A. Guin. Am. Inst. Chem. Eng. Jnl., 19, No. 6, pp.1190-1195, 1973

9. "Errata (for reference No. 8)" J.A. Guin. Am. Inst. Chem. Eng. Jnl., 20, No. 2, p.415

10. "Matrix acidisation with highly reactive acids", J.A. Guin, R.S. Schecter. Soc. Pet. Eng. Jnl, 11, pp.390-398, 1971

11. "An experimental technique for obtaining permeability-porosity relationships in acidisation", C.C. McCune, H.S. Fogler. Paper No. 52e, 74th Natl. Meeting Am. Inst. Chem. Eng., New Orleans, Louisiana 1973

12. "Acidisation III. The kinetics of the dissolution of sodium and potassium feldspar in HF/HCl acid mixture", H.S. Fogler, K. Lund, C.C. McCune. Chem. Eng. Sci., 30, pp.1325-1332, 1975

13. "Acidisation IV. Experimental correlations and techniques for the acidisation of sandstone cores", K. Lund, H.S. Fogler, C.C. McCune, J.W. Ault. Chem. Eng. Sci., 31, pp.373-380, 1976

14. "Acidisation V. The prediction of the movement of acid and permeability fronts in sandstone", K. Lund, H.S. Fogler. Chem. Eng. Sci., 31, pp.381-392, 1976

15. "Acidisation VI. On the equilibrium relationships and stoichiometry of reactions in mud acid", Y. Hekim, H.S. Fogler. Chem. Eng. Sci., 32, pp.1-9. 1977

16. "On the extension of the model of matrix acid stimulation to different sand stones", H.S. Fogler, C.C. McCune. Am. Inst. of Chem. Eng. Jnl., 22, No. 4, pp.799-805, 1976

17. "A new model of the physical and chemical changes in sandstone during acidisation", C.C. McCune, H.S. Fogler, K. Lund, J.R. Cunningham, J.W. Ault. Soc. Pet. Eng. Jnl., 15, pp.361-370, 1975

18. "Predicting the flow and reaction of HCl/HF acid mixtures in porous sandstone cores", H.S. Fogler, K. Lund, C.C. McCune. Soc. Pet. Eng. Jnl., 16, No. 5, pp.248-260, 1976

19. "On the stability of displacement fronts in porous media: A discussion of the Muskat-Aronofsky model", A.E. Scheidegger. Canad.Jnl. Physics, 38, No. 2, pp.153-162, 1960

20. "The physics of flow through porous media", A.E. Scheidegger. Univ. of Toronto Press, Toronto, 2nd Ed. 1960

21. "Dynamics of fluids in porous media", J. Bear. Am. Elsevier Publ. Co. Inc., New York, 1972

22. "Flow of fluids through porous materials", R. Collins. Rheinhold Chemical Engineering Series, Rheinhold Publ. Corp., New York, 1961

23. "The statistical behaviour of instabilities in displacement processes in porous media", A.E. Scheidegger, E.F. Johnson. Canad. Jnl. of Phys., 39, pp.326-334, 1961

24. "One-dimensional, incompressible, non-capillary, two-phase fluid flow in a porous medium", J.W. Sheldon, B. Zondek, W. T. Cardwell. Petroleum Trans. A.I.M.E., 216, T.P.8089, pp.290-296, 1959

25. "Stability conditions for displacement processes in porous media", A.E. Scheidegger. Canad. Jnl. Phys., 47, pp.209-214, 1969

26. "Statistical behaviour of fingering in a displacement process in heterogeneous porous medium with capillary pressure", A.P. Verma . Canad. Jnl. of Phys., 47, pp.319-324, 1969

CHAPTER SEVEN

EXPERIMENTAL WORK

1. Introduction

This chapter has been devoted to describing the experimental work performed in relation to Rising Damp. The phenomenon has been discussed theoretically in the previous chapters and it has been shown that the phenomenon extends across many disciplines and subjects. Unfortunately this wide variety of subjects is accompanied by a general lack of experimental data, particularly in relation to the hydraulic functions of building materials (bricks, cement, plaster, etc.) and in relation to the seasonal moisture conditions in damp walls. Thus a wide choice of experiments was originally available.

Three experiments were finally chosen. One designed to investigate the effects of leaching upon plaster of Paris cores. A second experiment was undertaken as a long term investigation of the suction (or tension) developed by walls affected by Rising Damp. The final experiment was to develop an experimental procedure to investigate the hydraulic properties of building materials.

The individual aims of the experiments are discussed as each experimental study is introduced.

2. Experimental study number one. Leaching.

2.1 Introduction

The theories and models relating to the leaching of porous materials have been discussed in Chapter Six. It has been shown that the passage of a reacting fluid through a porous material should increase the permeability of the porous material to the fluid. The theories do not physically describe the mechanism producing the increased permeability nor do they predict the final permeability ratio (k_f/k_i).

Mason[1] has indicated that the permeability ratio would have to increase by a value of fifty fold, or greater, to account for the increase in dampness of a wall. It is the aim of this experi-

mental study to determine whether increases of permeability of at least fifty fold can be achieved and to identify, if possible, the mechanism producing the permeability increase, together with the rate of failure of porous materials.

The composition of mortars used for bricklaying and building construction has been varied considerably[(2)-(5)]. Initially mixtures of 3 parts sand to 1 part lime were used until Portland cement became common, when some of the lime was replaced by Portland cement. The combinations of lime and Portland cement most commonly used was a mixture lime/cement/sand in the ratios of 1/1/6 respectively. Further discussion of building mortars can be found[(2)-(6)].

Both Portland cement and lime shrink upon drying. This fact causes problems when casting cylindrical cores for subsequent use in leaching - permeability studies, because a tight fit between the porous core and sample holder is essential. This problem may be overcome by using tapered cores and matching sample holders, the seal being obtained by forcing the core into the sample holder[(6)].

The shrinkage problem can be avoided by using plaster of Paris as the cementing material. Additional advantages are that plaster of Paris sets more rapidly than cement or lime; it is more permeable than Portland cement (no lime permeability data was available); plaster of Paris is a simple chemical material (calcium sulphate) whereas Portland cement contains several chemicals[(3)] of differing solubilities. The solubility of lime (calcium hydroxide), especially in damp walls, is expected to be of the same magnitude as the solubility of plaster of Paris, because of solubility restrictions upon their common ion (Ca^{2+}). Hence plaster of Paris was chosen as the cementing material to be used in the permeability - leaching investigation.

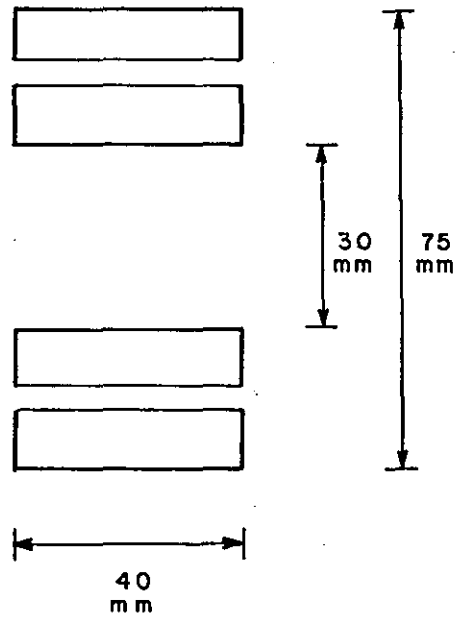

Fig. 1. Sectional view of sample holder.

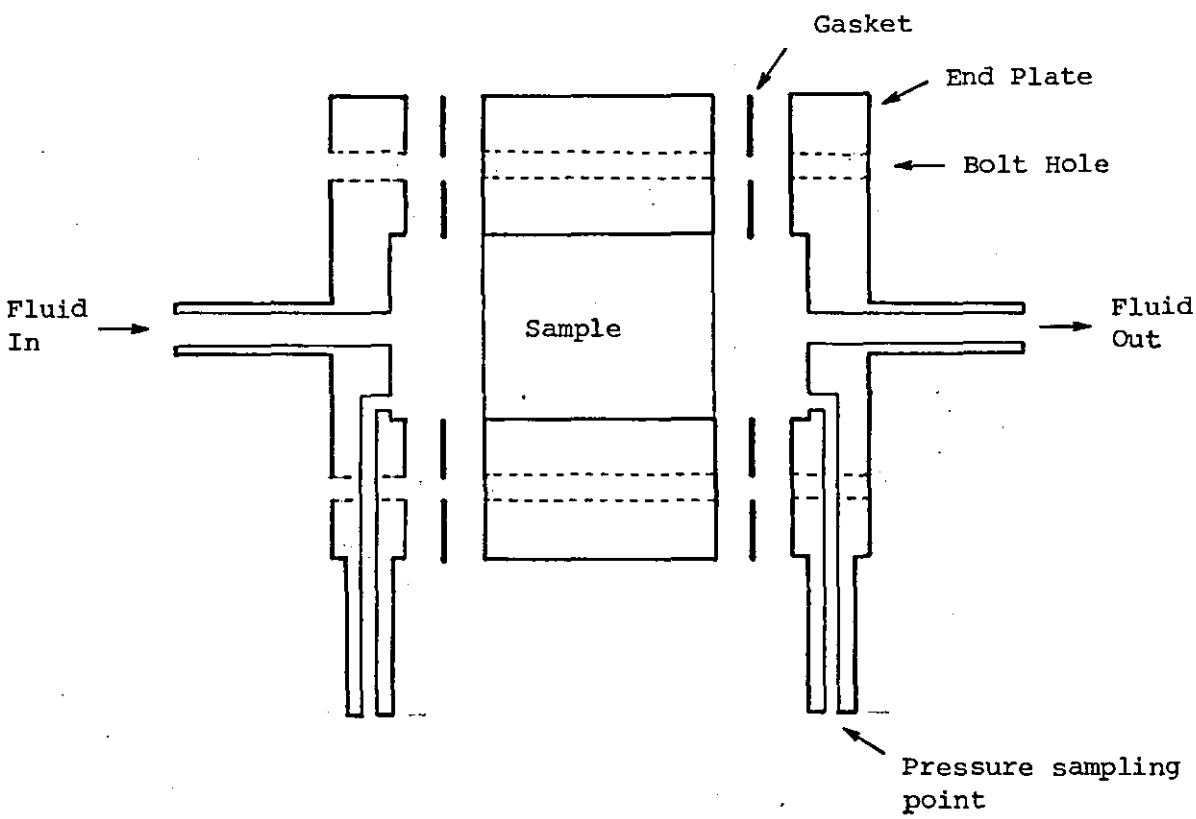

Fig. 2. Sectional view of sample holder and end plates.

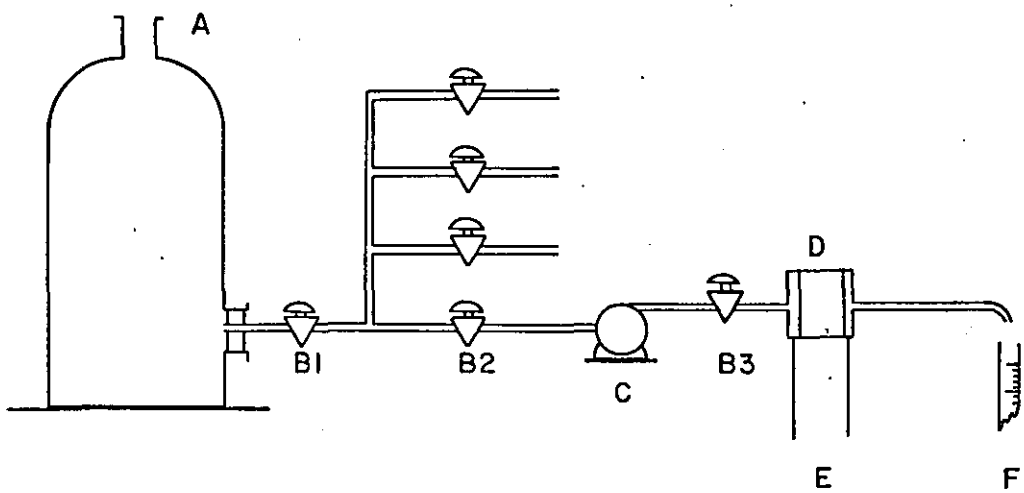

Key

A aspirator containing distilled ater

B glass tap

C constant flow rate pump

D sample holder and end plates

E mercury manometer

F graduated container

Fig. 3. Schematic representation of leaching apparatus.

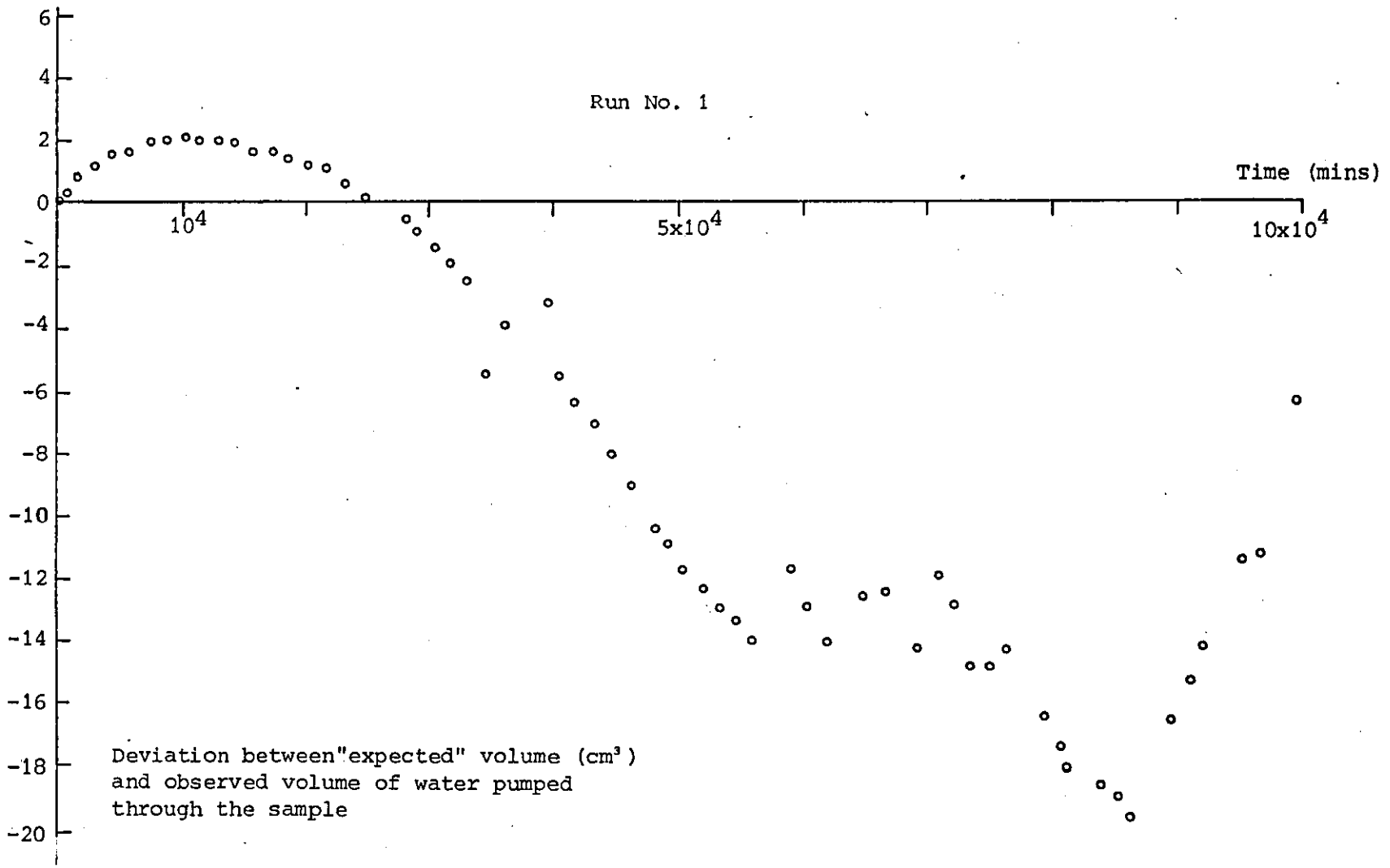

Fig. 4. Difference between the observed volume of water pumped through sample No. 1 and the volume of water calculated using an "expected" flowrate of 8.334×10^{-3} (cm^3 min^{-1})

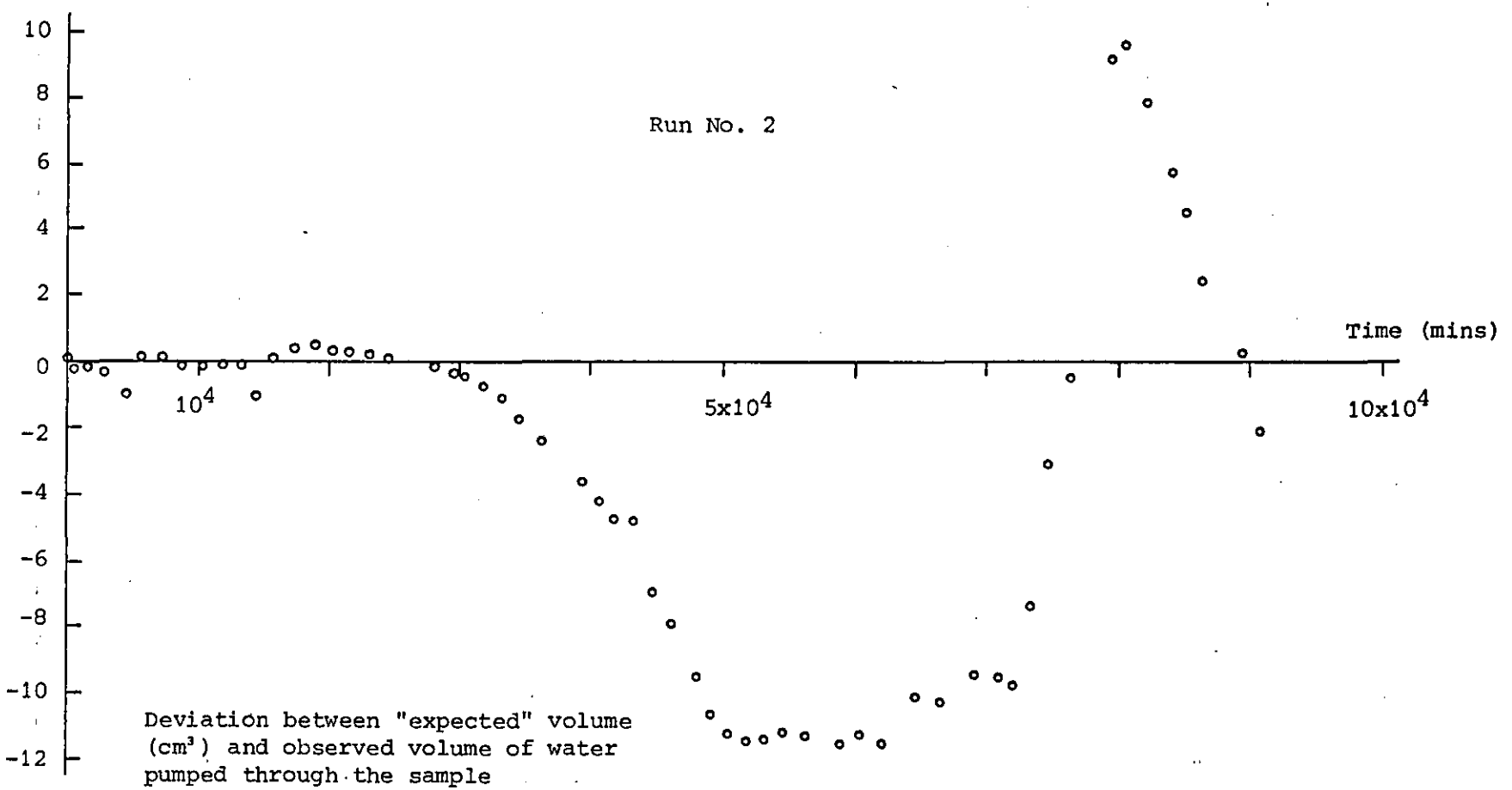

Fig. 5. Difference between the observed volume of water pumped through sample No. 2 and the volume of water calculated using an "expected" flowrate of 7.14×10^{-3} (cm^3 min^{-1})

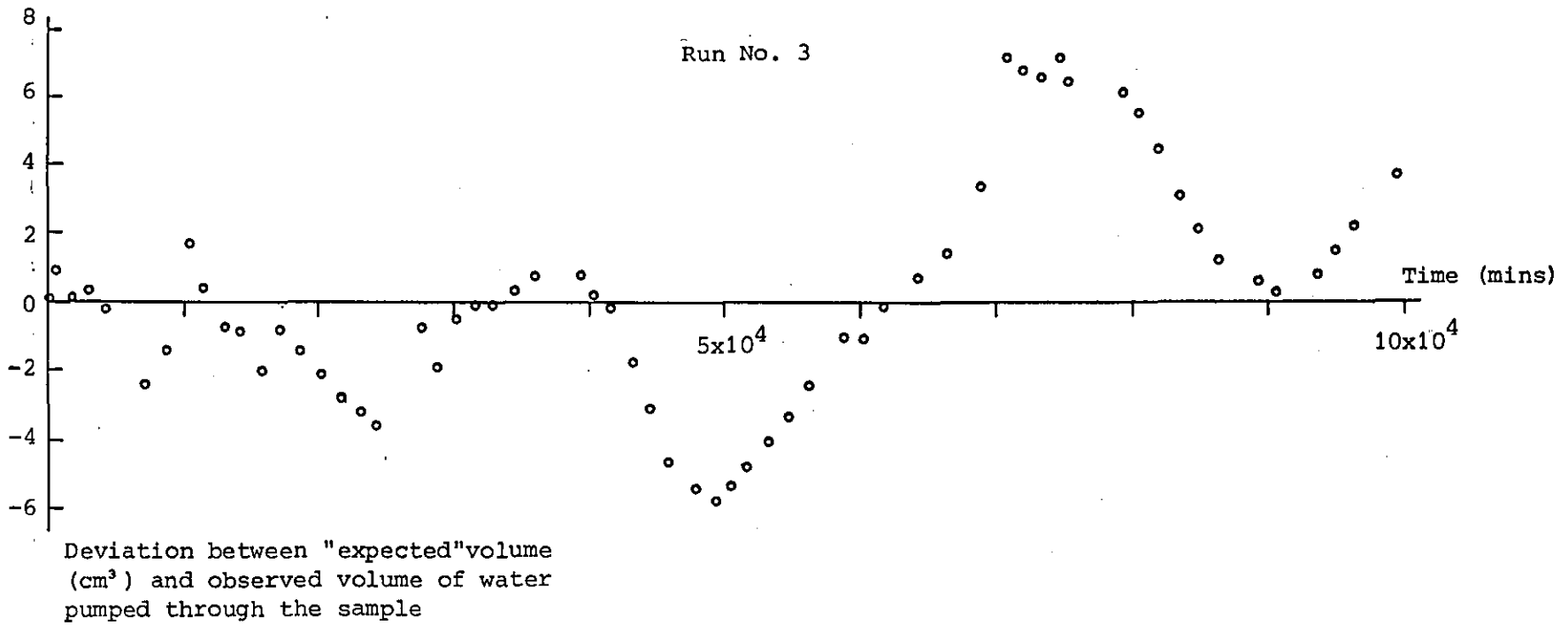

Fig. 6. Difference between the observed volume of water pumped through sample No. 3 and the volume of water calculated using an "expected" flowrate of 6.225×10^{-3} ($cm^3\ min^{-1}$)

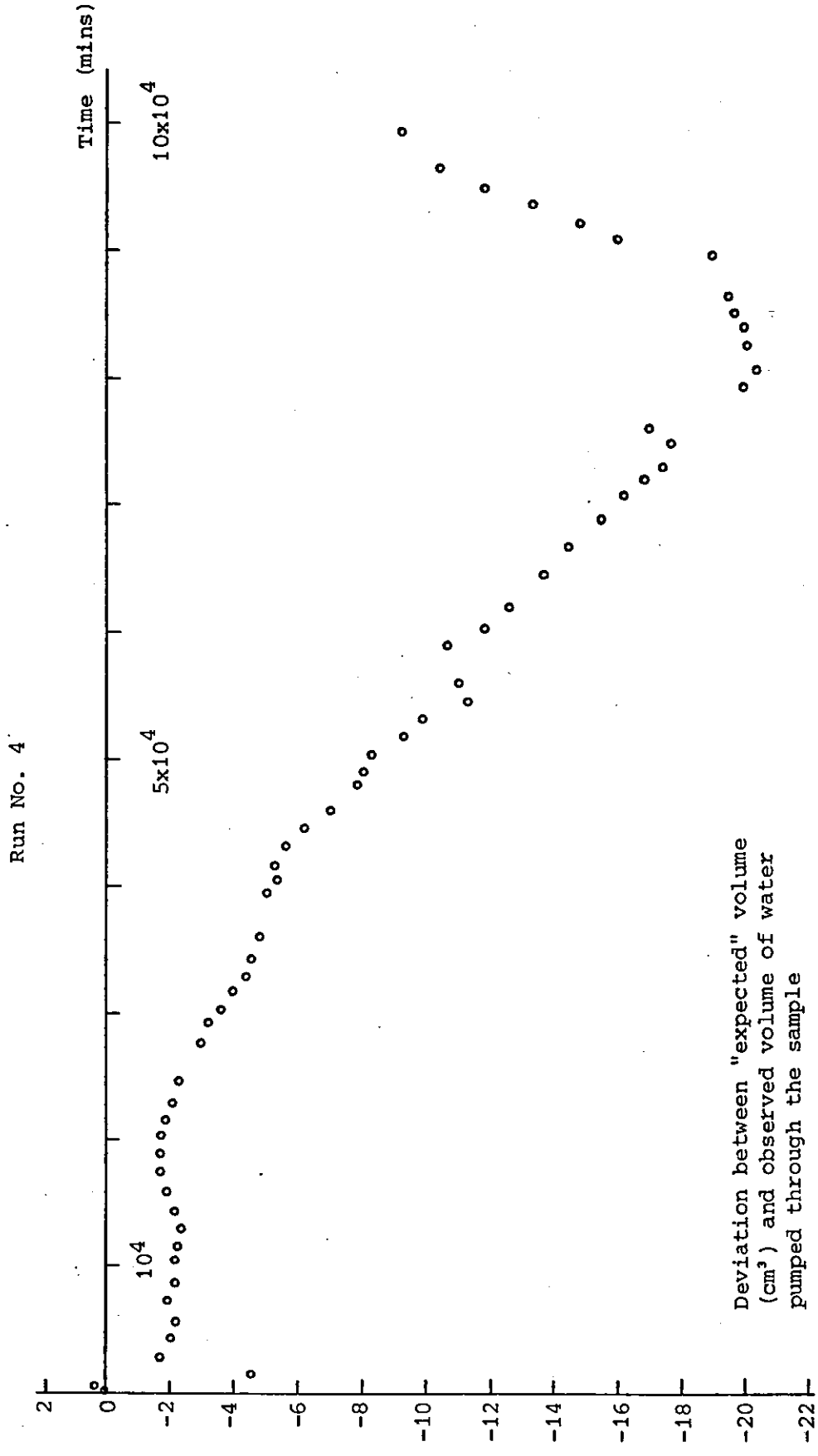

Fig. 7. Difference between the observed volume of water pumped through sample No. 4 and the volume of water calculated using an "expected" flowrate of 8.2×10^{-3} (cm^3 min^{-1})

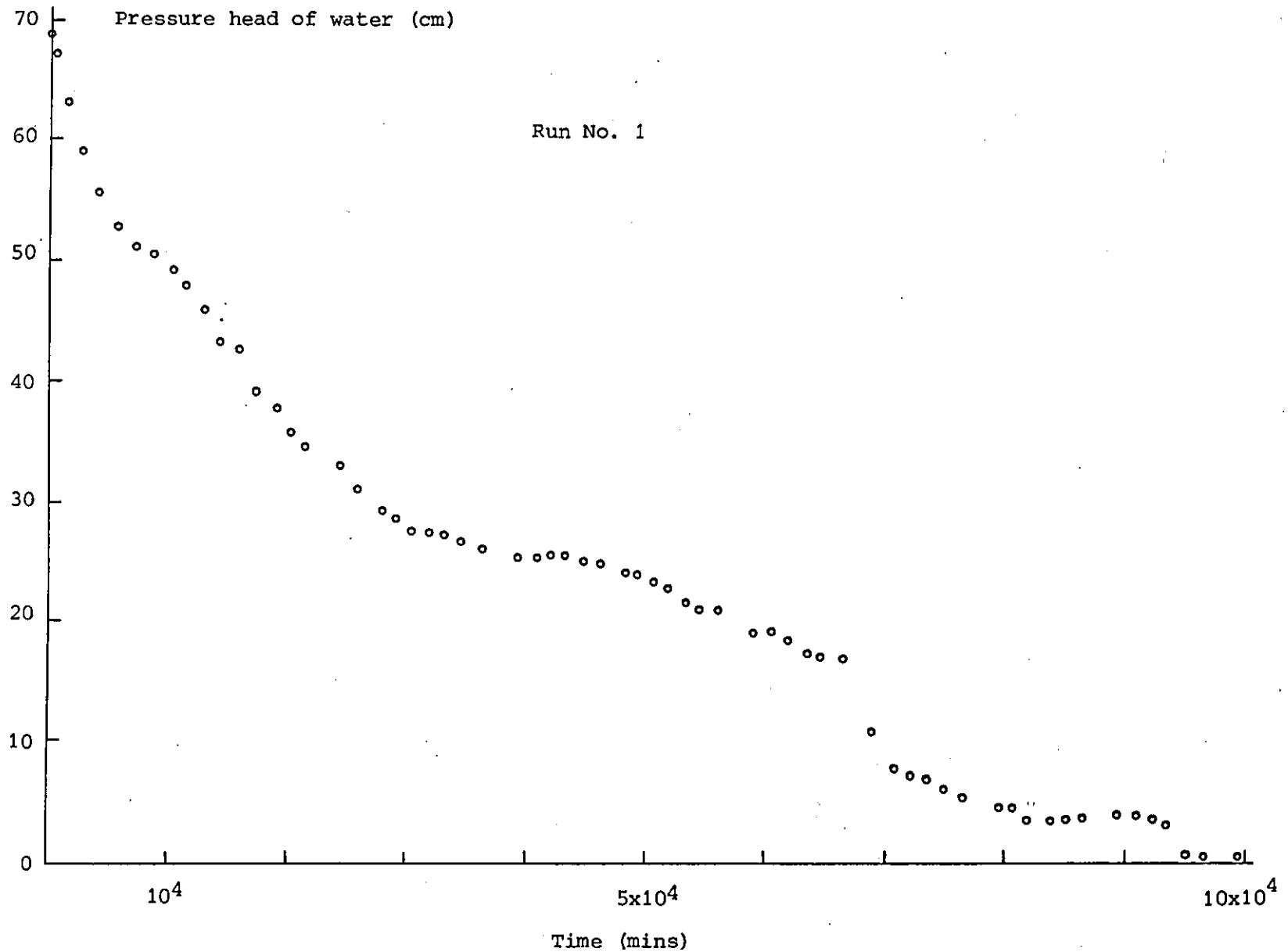

Fig. 8. Pressure head of water (cm) measured across sample No. 1 with respect to time (min).

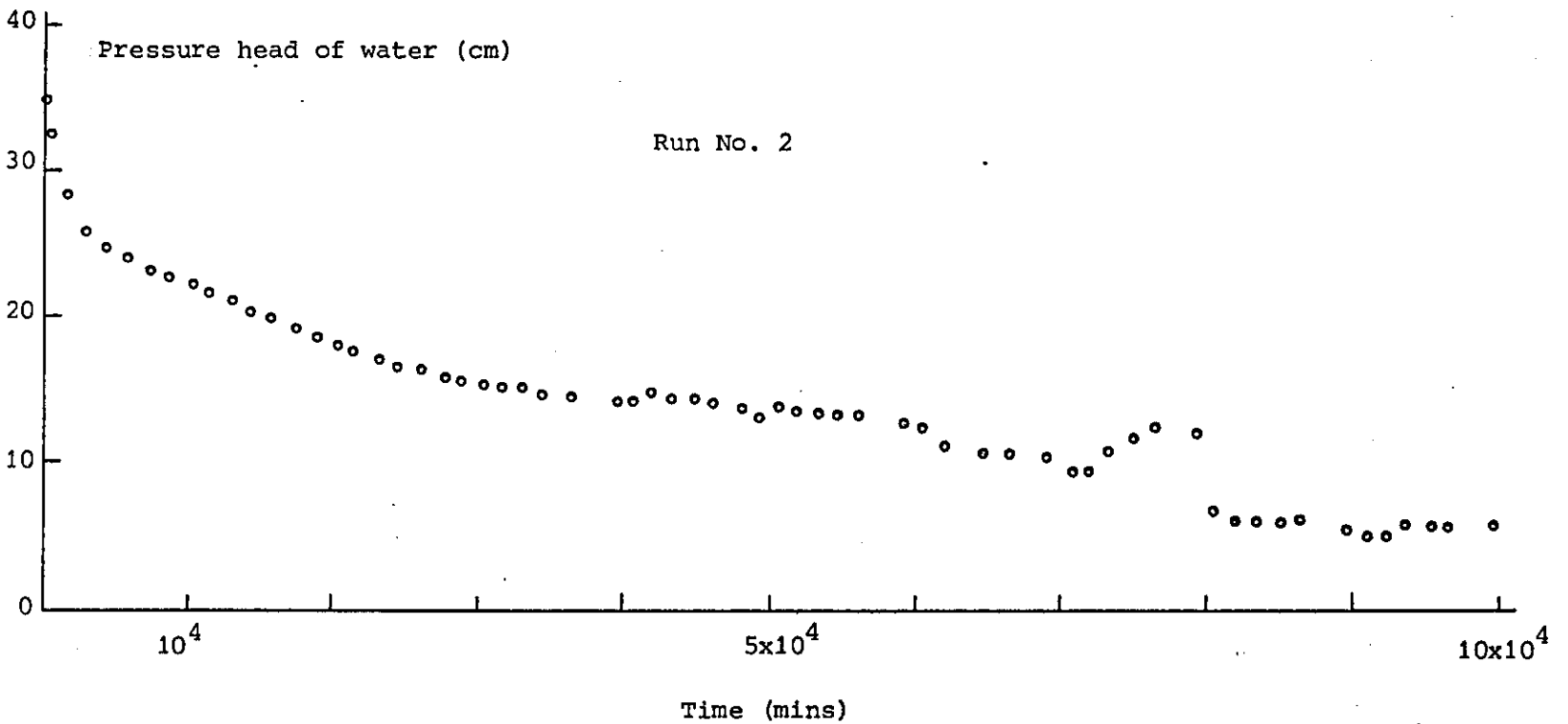

Fig. 9. Pressure head of water (cm) measured across sample No. 2 with respect to time (min).

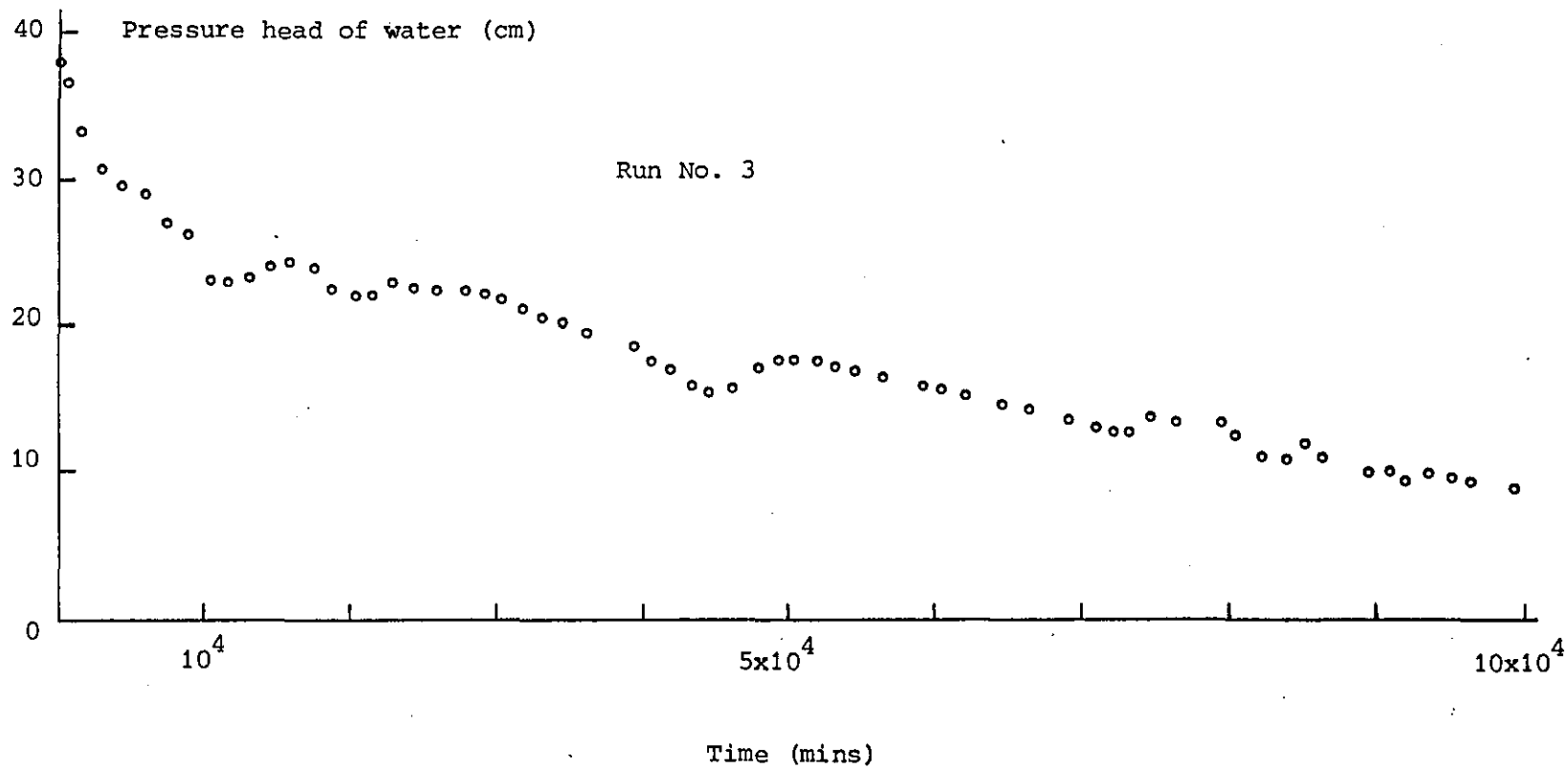

Fig. 10. Pressure head of water (cm) measured across sample No. 3 with respect to time (min).

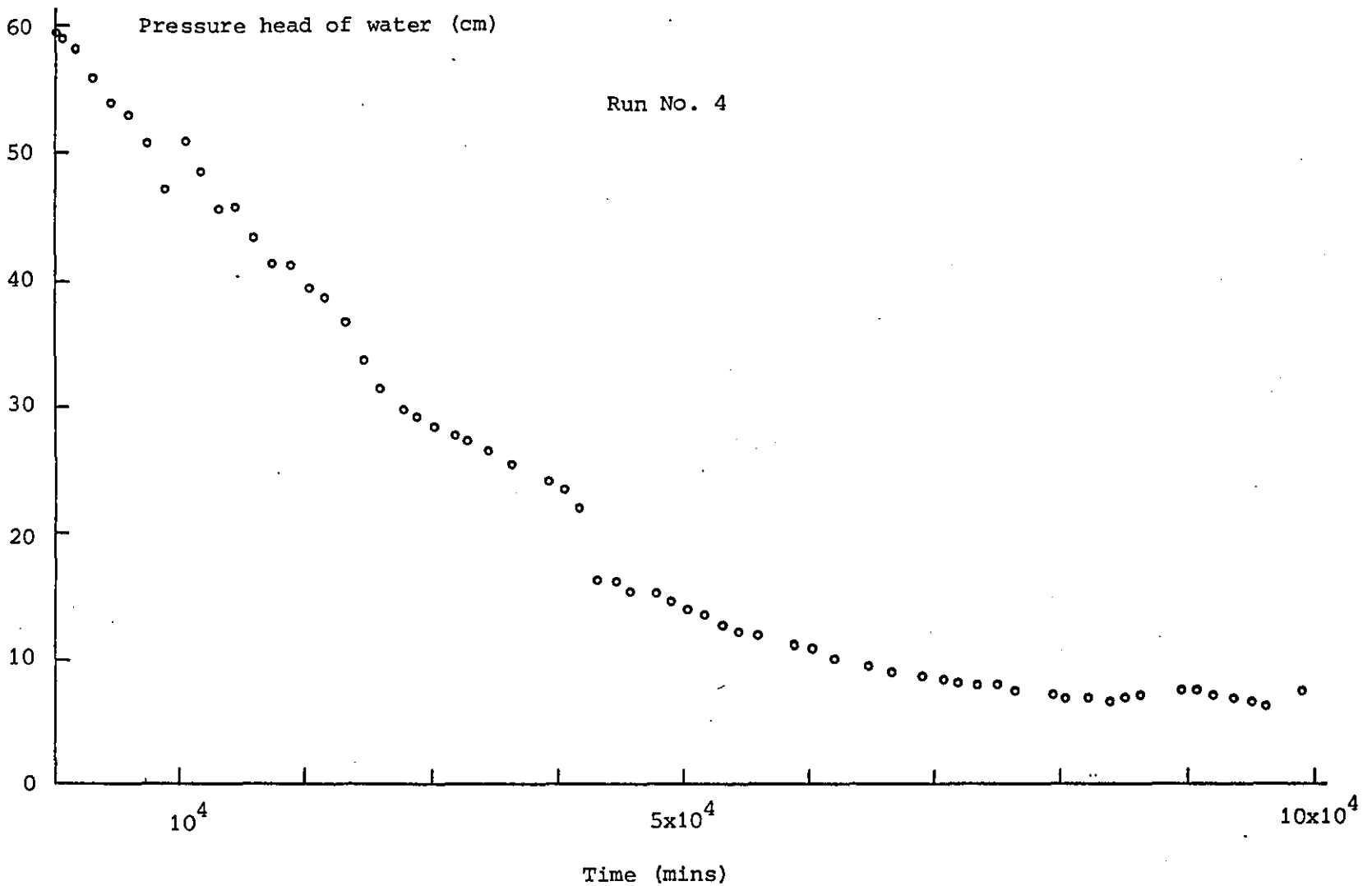

Fig. 11. Pressure head of water (cm) measured across sample No. 4 with respect to time (min).

2.2 Experimental procedure. Run numbers 1-4.

The experimental procedure was modified on several occasions during the course of the investigation. The following represents an account of the experimental procedure.

A mixture of three parts building sand to one part plaster of Paris (by weight) was prepared. Distilled water was added to the sand-plaster mix to produce a slurry. The slurry was poured into the centre of a hollow cylindrical perspex sample holder and left to set. The length and diameter of the central core were both the same (2.54 cm). The end faces of the hardened mixture were ground away such that the surfaces of the mortar were flush with the faces of the perspex sample holder (Fig. 1). End plates were bolted onto the sample holder as shown in Fig. 2.

The sample holder and end plates were fitted into the remainder of the apparatus, which is shown schematically in Fig. 3. Glass taps B1, B2, B3 were opened and the apparatus was completely filled with distilled water, such that all air bubbles both upstream and downstream of the sand-plaster core were removed. The peristaltic pump was started and its speed of rotation adjusted until a suitable pressure difference was developed across the sand plaster core. Daily readings of pressure difference and liquid volume exuded through the core were recorded.

The latter measurements have been reproduced in Figs. 4, 5, 6, 7. It was assumed that fluid flow through the samples remained constant. The assumed flow rate, calculated from approximate flow measurements, was used as an "expected" flow rate. Experimentally observed differences from the "expected" flowrate, were expressed along the ordinate axis, whilst measurements of time were shown on the abscissa. The corresponding measurements of pressure difference versus time can be found in Figs. 8-11.

Four samples were arranged in parallel. The flowrate through each sample could be adjusted, albeit in a limited fashion, by loosening or tightening its individual P.V.C. tubing that circumscribed the rotor of the peristaltic pump.

Distilled water was injected through the sand-plaster cores for about ten weeks. The experiment was terminated when the rate of change of pressure difference became small. The sample holders were removed fron the experimental apparatus and washed to remove particles of loose sand, particularly from the front face of the samples. The plaster cores were removed from the sample holders and left to dry. Photographs of the dry cores were taken (Figs. 12-15). In view of the lengthy failure time of the sand-plaster cores it was decided to omit the sand from the cores and to continue with cores containing plaster of Paris only.

A modification to the apparatus at this time was the replacement of the manometer by a pressure transducer. The electrical output of the transducer was recorded continuously using a chart recorder. The technical data relating to the pressure transducer (type AE 830 A) has been reproduced in Appendix I. The transducer was calibrated using a mercury-water manometer together with a travelling microscope. The calibration curves (three) are shown in Fig. 16. The mercury pressure readings have been converted into cm of water head (y axis) against millivolt readings (from pressure transducer). A straight line was fitted to each set of measurements using a least squares regression technique.

Further modifications that were subsequently introduced into the apparatus were:-

(1) Introduction of a temperature controlled water bath ($\pm 0.1^{\circ}C$). The main function of the bath was to limit the temperature dependent fluctuations of water viscosity. Secondary benefits of the bath were that it limited the variation of solubility with temperature

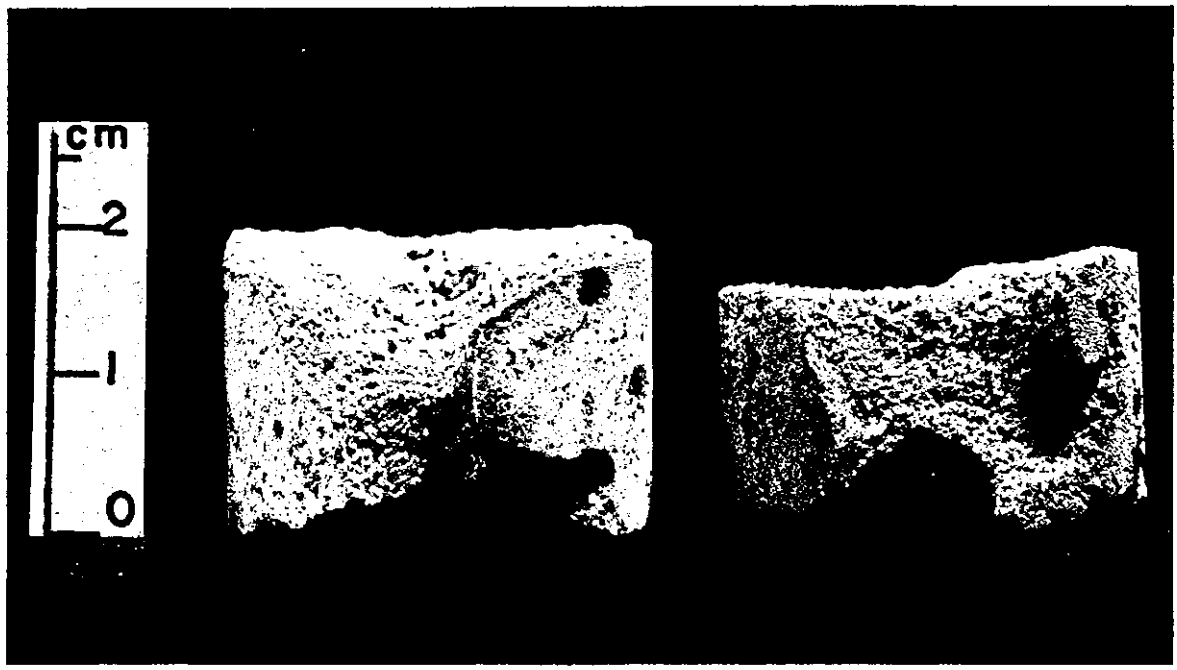

Fig. 12 (left) Fingers developed in sample cores of Run No. 1
Fig. 13 (right) and Run No. 2 respectively.

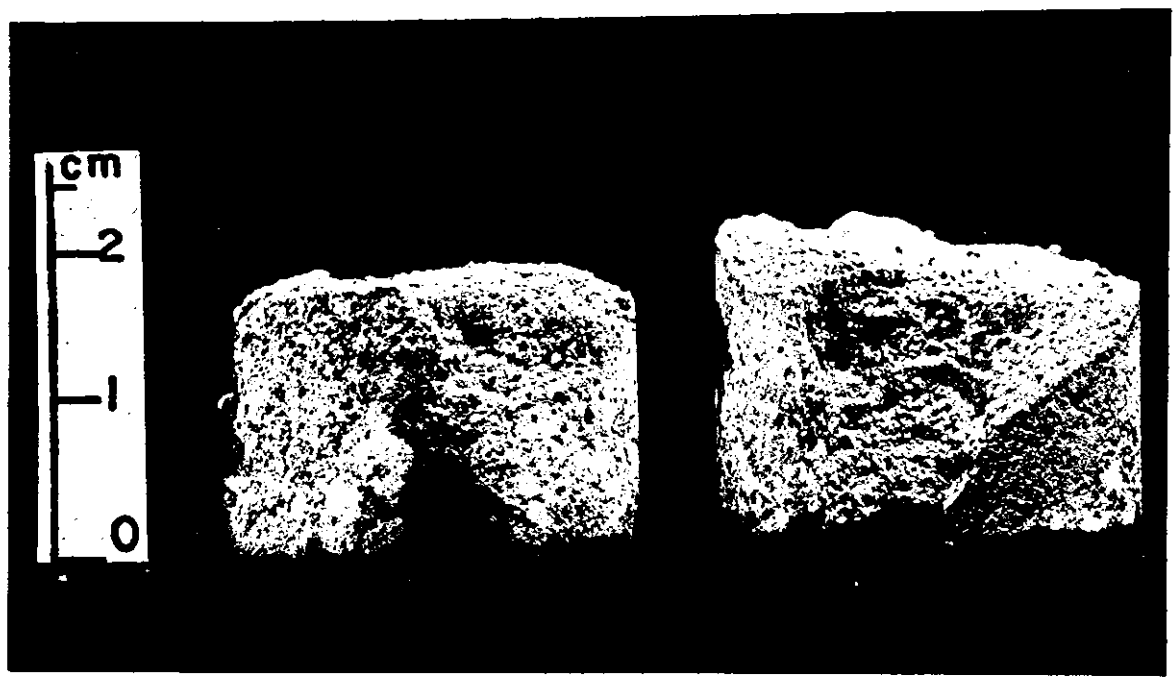

Fig. 14 (left) Fingers developed in sample cores of Run No. 3
Fig. 15 (right) and No. 4 respectively

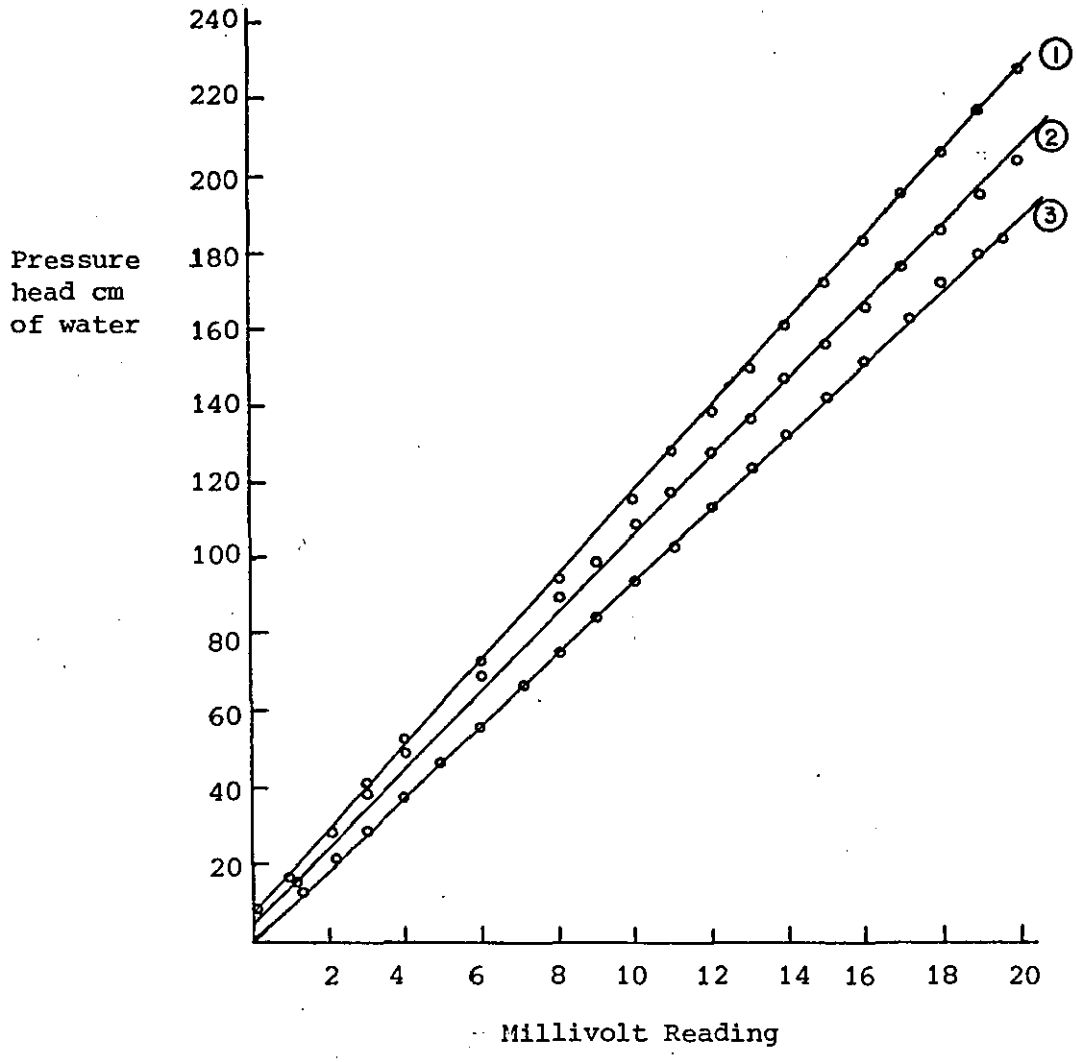

Fig. 16. Calibration curves of the three pressure transducers, relating the output of the transducers (millivolts) to the pressure head (cm) of water. Curve 1 was used for runs 5-8, curve 2 for runs 9-22, and curve 3 was used for runs 23-44.

of the plaster of Paris; and that it reduced the effect of thermal expansion of P.V.C. tubing used to connect the pieces of apparatus together; the water bath was also used to regulate the temperature variations upon the output of the pressure transducer.

(2) Inclusion of a stratified sand-glass bead filter bed between the peristaltic pump and the porous sample. Initially the inclusion of the filter was to prevent build up of a thin scum at the front face of the sample. The scum may have originated because of internal friction of the tubing circumscribing the pump rotor. An alternative source may be a result of fungus growing in the connecting tubes of the apparatus. A further benefit of the filter is discussed in (3).

(3) Inclusion of a glass T-piece which was sealed at one of its ends. The position of the T-piece was between the peristaltic pump and the filter. Approximately 0.5 cm^3 of air was injected into the sealed arm of the T-piece. The purpose of this modification was to reduce the magnitude of the cyclical pressure variation produced by the interaction of the rotor tubing and the rotor itself. The filter also assisted in reducing the magnitude of the pressure variation, observed at the inlet face of the sample. The filter increased the flow resistance along the path to the sample, compared to the resistance in the sealed arm of the T-piece.

(4) The inner radius of the sample holder was increased to 3 cm. The standard length of the sample holder was reduced to 2.5 cm. An additional length of 4 cm was also used.

(5) The casting procedure and subsequent shaping of the porous cores was modified. Three perspex sample holders were assembled as a tower. Each sample holder was separated from its neighbours by a layer of perspex approximately 6 mm thick. An additional spacer was placed at the base of the tower. The spacers were cut in half to facilitate their removal from the tower after the plaster had

become firm.

When the tower had been assembled, plaster slurry was poured into the hollow centre of the tower and agitated slightly to remove any entrapped air. A mixture of 2 parts plaster to 1 part water, by weight, was experimentally found to produce a suitable slurry for casting.

After the plaster in the tower had become firm, some 10 minutes after pouring, the spacers in the tower were removed. The sample holders were separated, the uppermost in the tower being discarded. The remaining cores were allowed to dry in the open air of the laboratory for one week. After this time had elapsed, excess plaster was removed from the end faces until a continuous flat surface of plaster and perspex was attained.

The core and holder were weighed and then the core vacuum saturated with distilled water. The pressure in the vacuum chamber was reduced to 6.5 ($KN\ M^{-2}$); the core remained in the chamber for fifteen minutes. The core was removed from the chamber and wiped to remove excess water, particularly from the bolt holes. The sample holder and "saturated" core were reweighed. The difference in the dry and wet weighings was used to calculate the porosity of the core.

End plates were bolted onto the sample holder and the assembly was connected into the rest of the apparatus, which is shown schematically in Fig. 17. The experiment was conducted as has been described earlier.

Measurements of pressure difference versus time were recorded automatically via the chart recorder. The volume of liquid pumped through the sample was recorded as described previously.

Experimental measurements of millivolts versus time, recorded by the chart recorder, have been reproduced in Figs. 18-56. A summary of experimental results and data can be found in Appendix II.

2.3 Discussion

The aims of this study were to determine whether increases of permeability of at least fifty fold could be produced by leaching; and to identify, if possible the mechanism producing the permeability increase.

Examination of the experimental results presented in Appendix II shows that the permeability increase can be as little as four fold or as high as one thousand five hundred fold. The accuracy of measurement of the increase of permeability is governed by the value of the pressure difference, Δh_w, at the end of an experimental run. Unfortunately, the final value of Δh_w is often comparable to the accuracy to which the pressure difference can be measured, consequently large errors are incurred. However, the large decrease of Δh_w is indicative of a correspondingly large increase of permeability. Since the final pressure difference cannot be determined accurately, the value of the permeability ratio presented in Appendix II should be used as an indicator of change rather than an accurate assessment.

Examination of the permeability ratio for runs 2-4 (sand-plaster cores) in Appendix II shows that the permeability had not increased by more than a factor of ten whereas the permeability increase of run 1 was approximately one hundred and seventy. The large divergence of values is largely attributed to the fact that the core of run 1 partially collapsed, causing a reduction of the pressure head of water from 3.0 cm to 0.45 cm; a rise in permeability of approximately six fold at this point.

The experiment was terminated shortly after the collapse of the core in run 1, which occurred after 9.35×10^4 minutes. It is expected that had the experiment continued further increases in permeability for runs 2-4 would have been attained, although no attempt can be made to predict the ultimate values of permeability

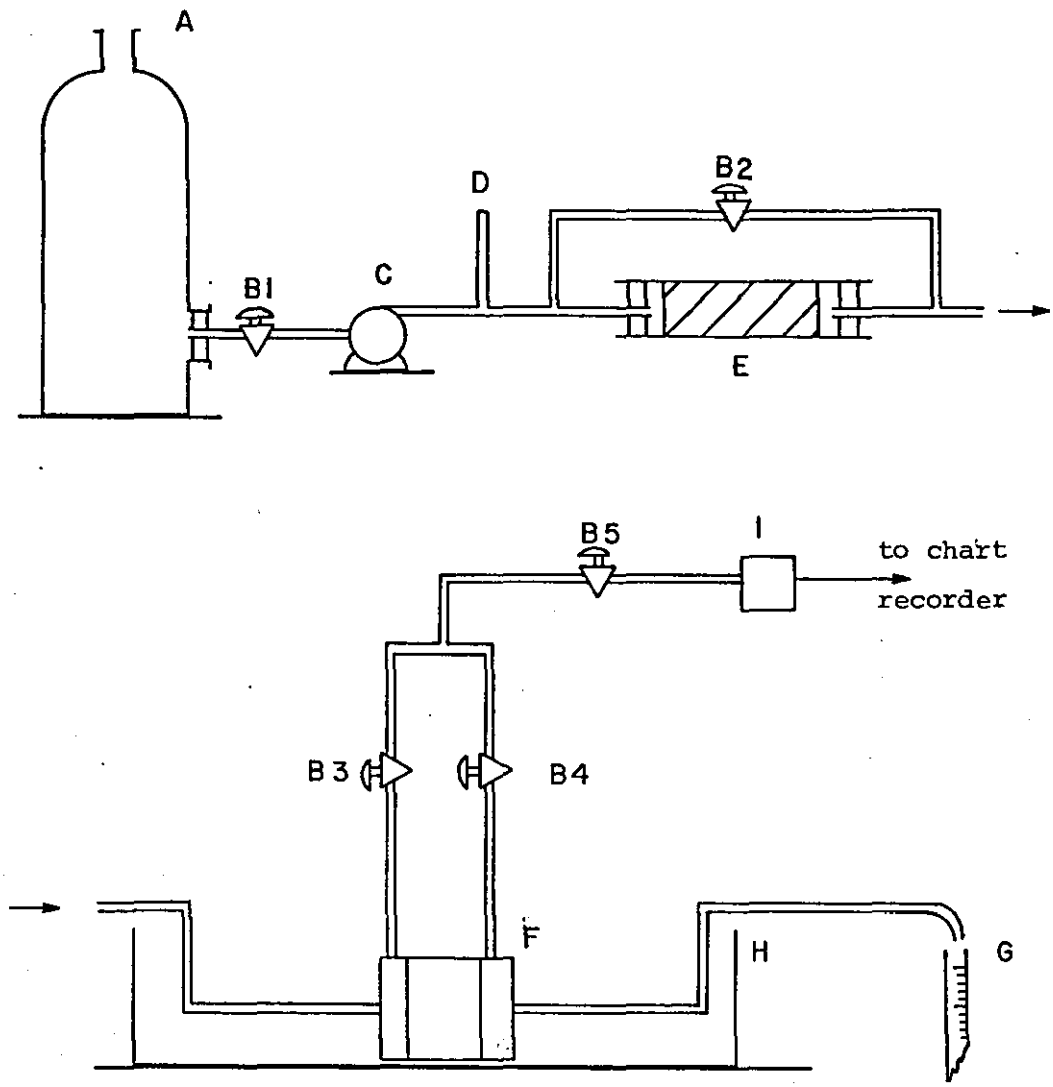

Key

A	aspirator containing distilled water
B	glass tap
C	constant flow rate pump
D	glass T piece, with sealed end
E	glass bead filter bed
F	sample holder and end plates
G	graduated container
H	temperature controlled water bath
I	pressure transducer

Fig. 17. Schematic representation of the modified leaching apparatus.

Fig. 18 to Fig. 56.

Pressure trace versus time of Run No. 5 - Run No. 44 (excluding Run No. 13). The pressure difference across the porous sample is expressed in millivolts, the time in hours.

Millivolt conversion factors can be obtained from Fig. 16 and the physical properties of each core from Appendix II.

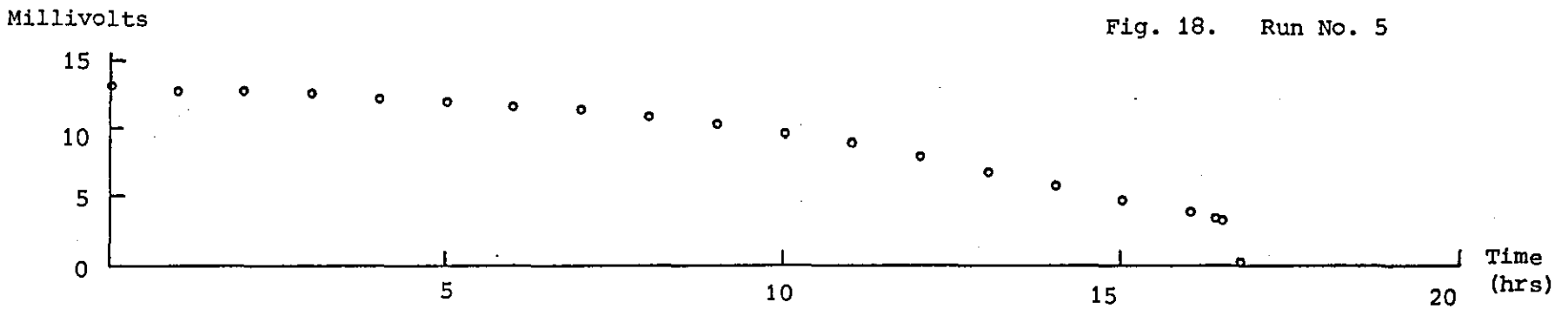

Fig. 18. Run No. 5

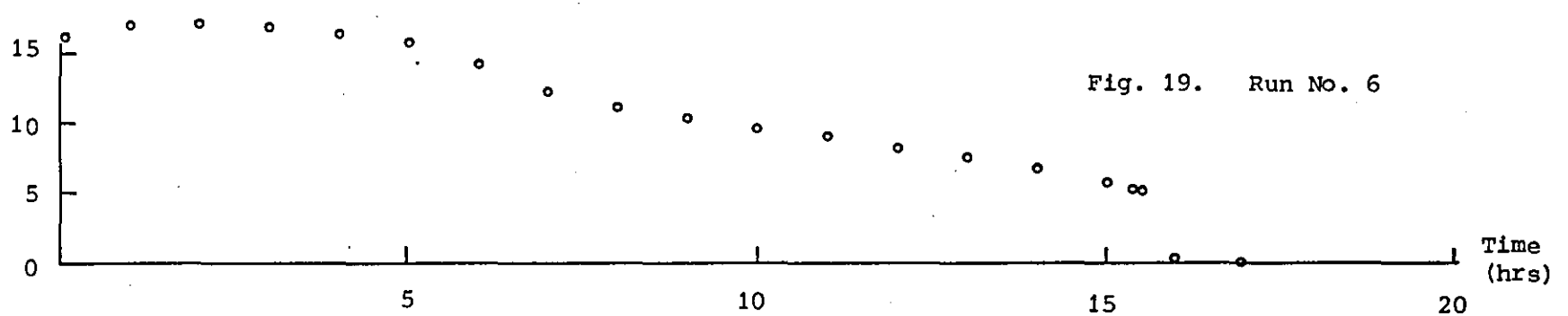

Fig. 19. Run No. 6

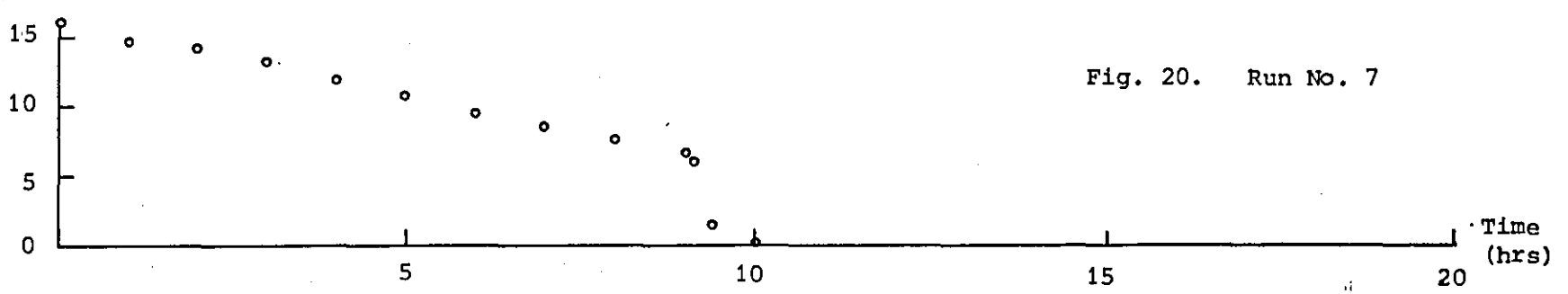

Fig. 20. Run No. 7

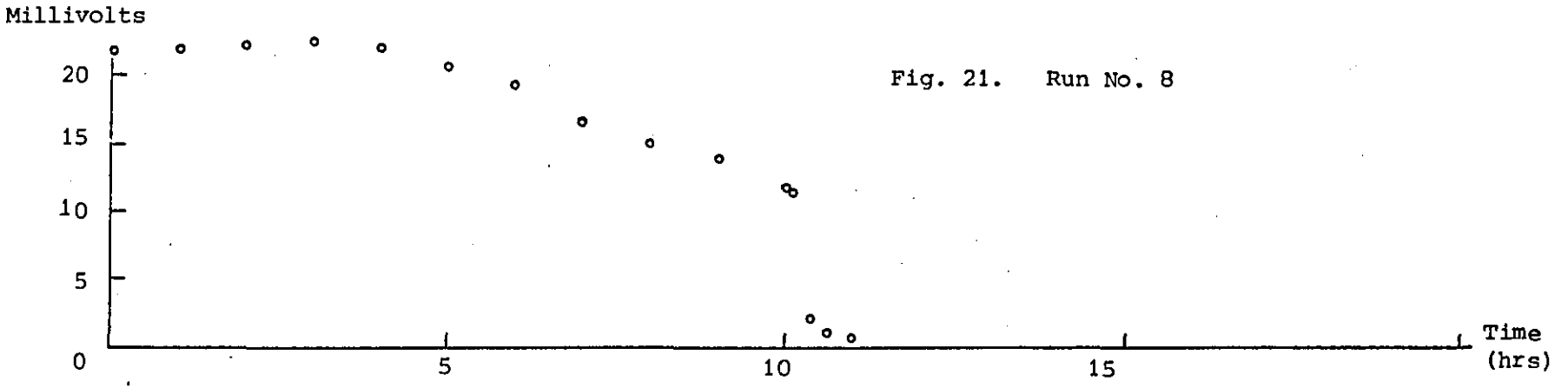

Fig. 21. Run No. 8

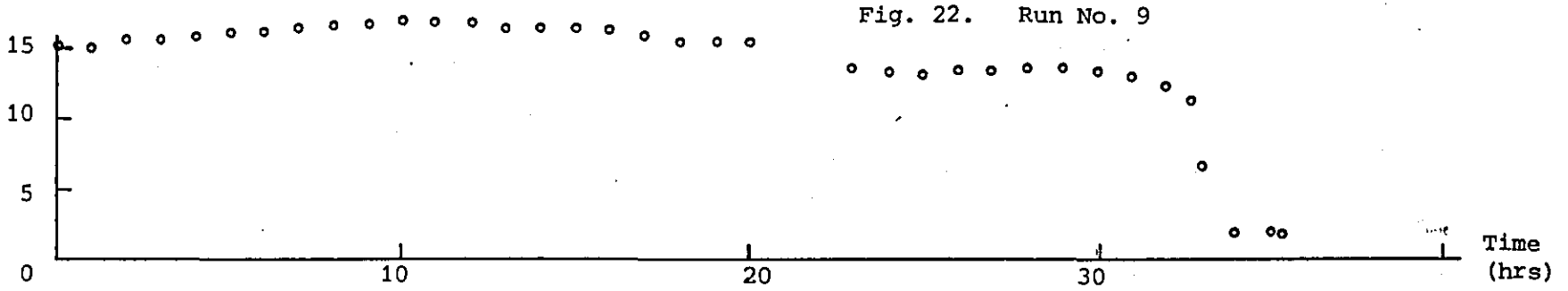

Fig. 22. Run No. 9

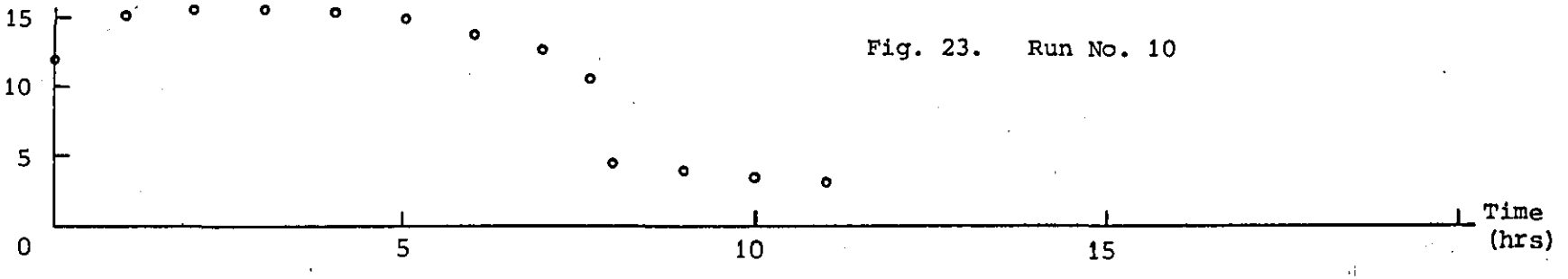

Fig. 23. Run No. 10

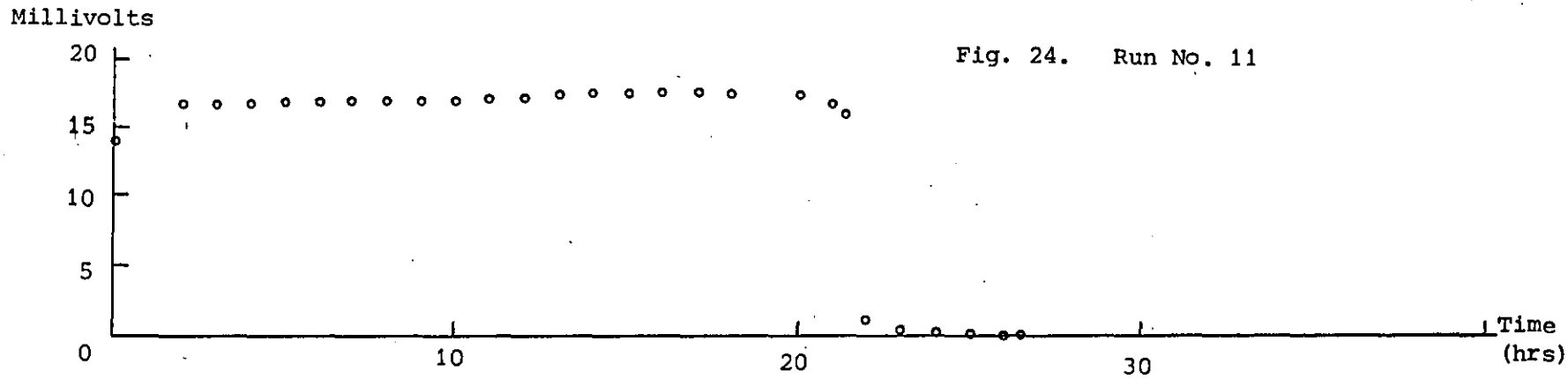

Fig. 24. Run No. 11

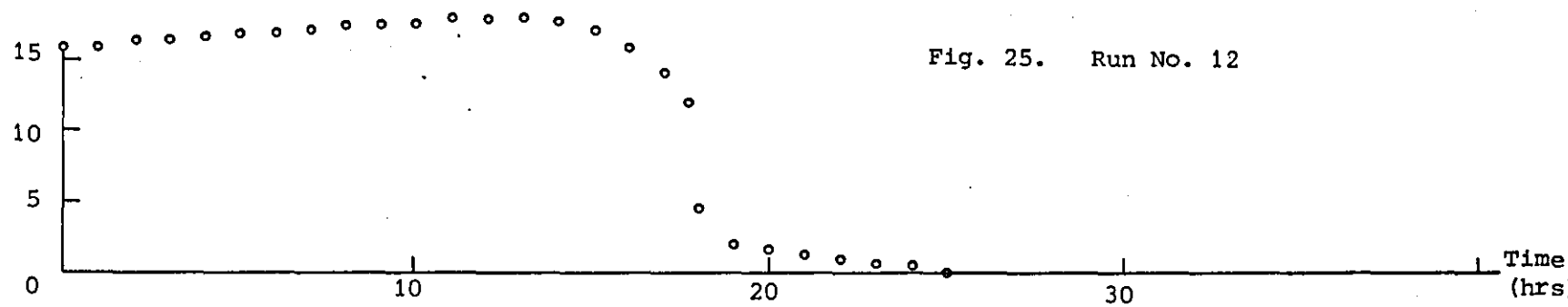

Fig. 25. Run No. 12

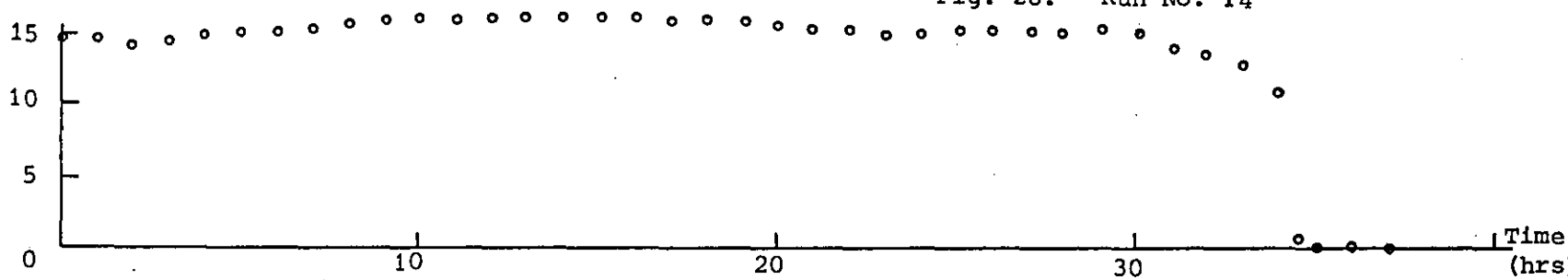

Fig. 26. Run No. 14

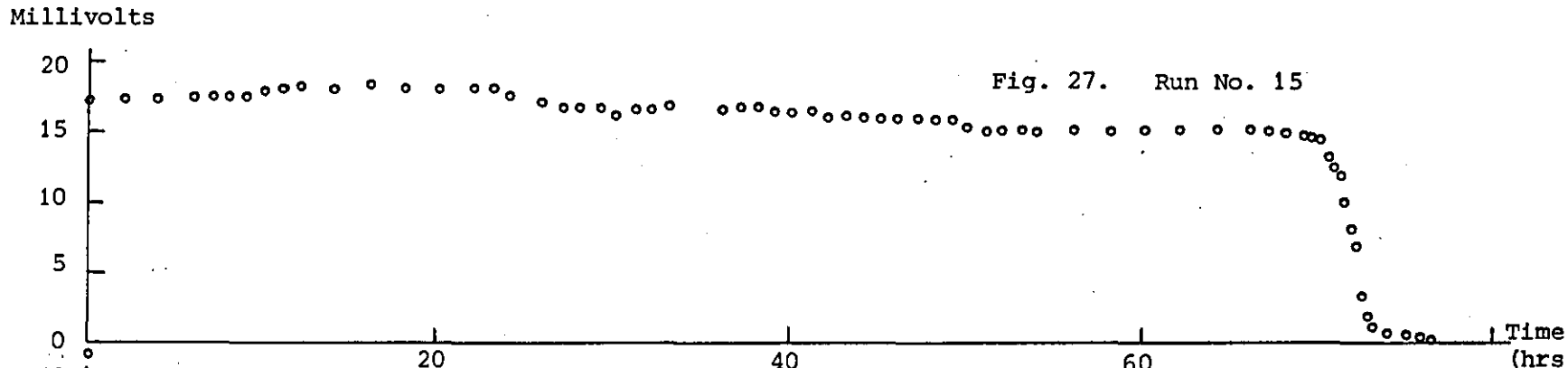

Fig. 27. Run No. 15

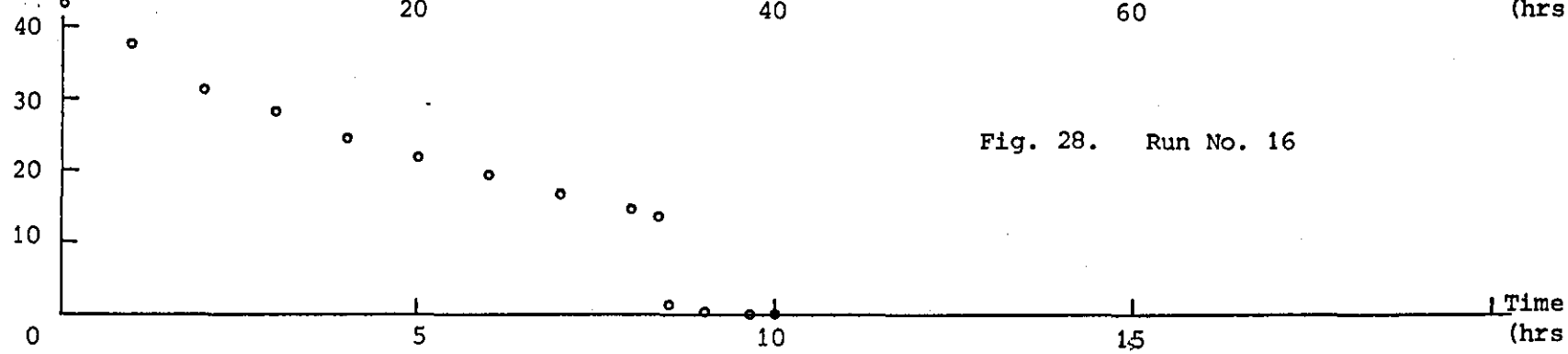

Fig. 28. Run No. 16

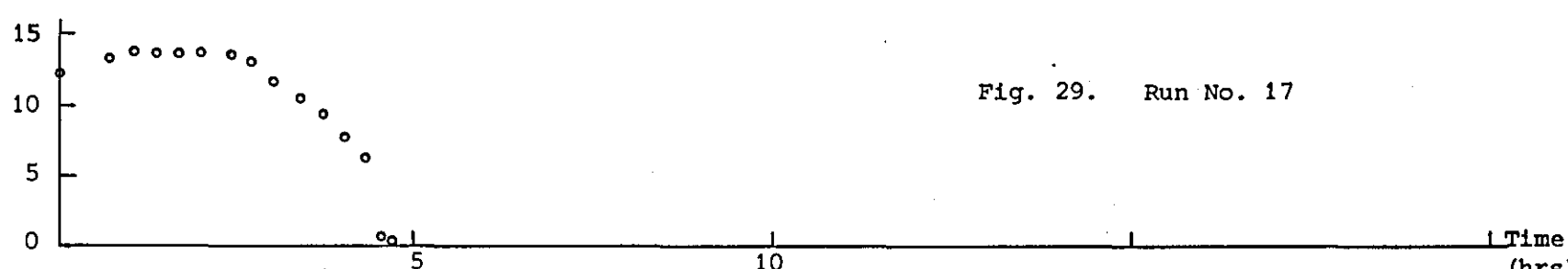

Fig. 29. Run No. 17

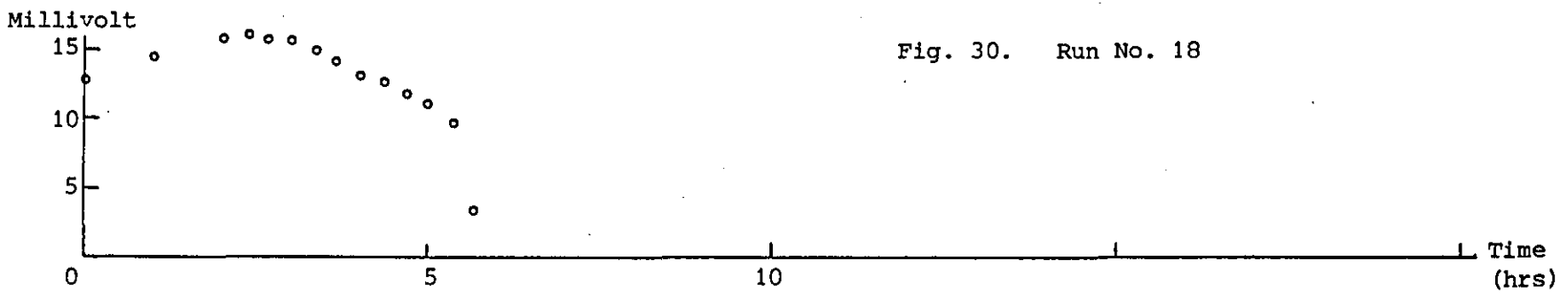

Fig. 30. Run No. 18

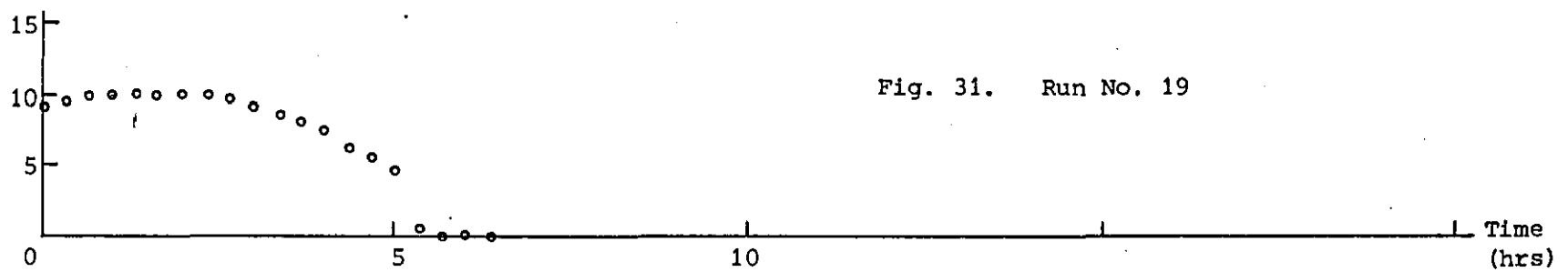

Fig. 31. Run No. 19

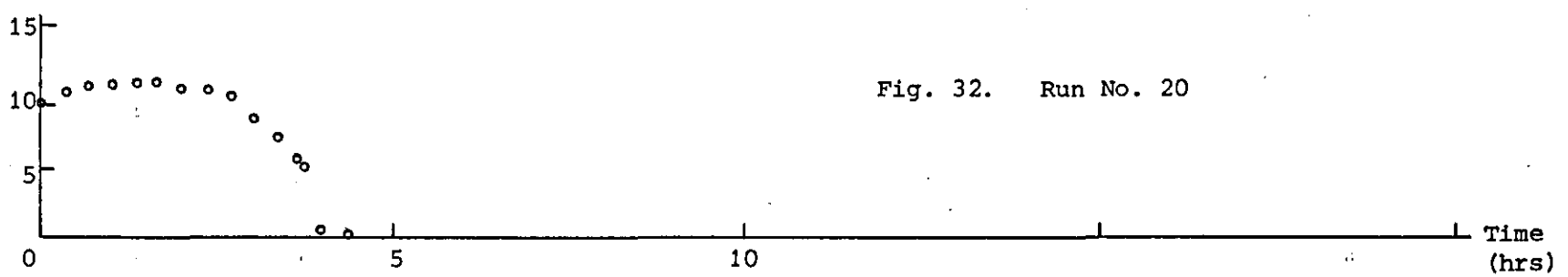

Fig. 32. Run No. 20

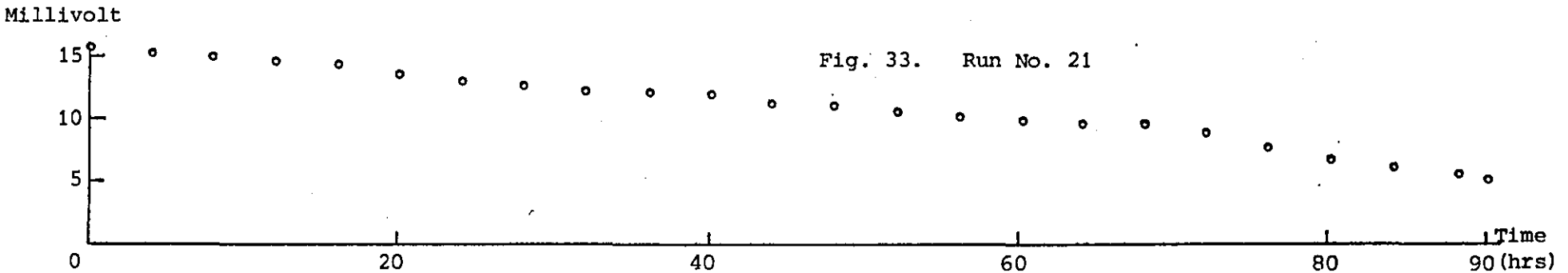

Fig. 33. Run No. 21

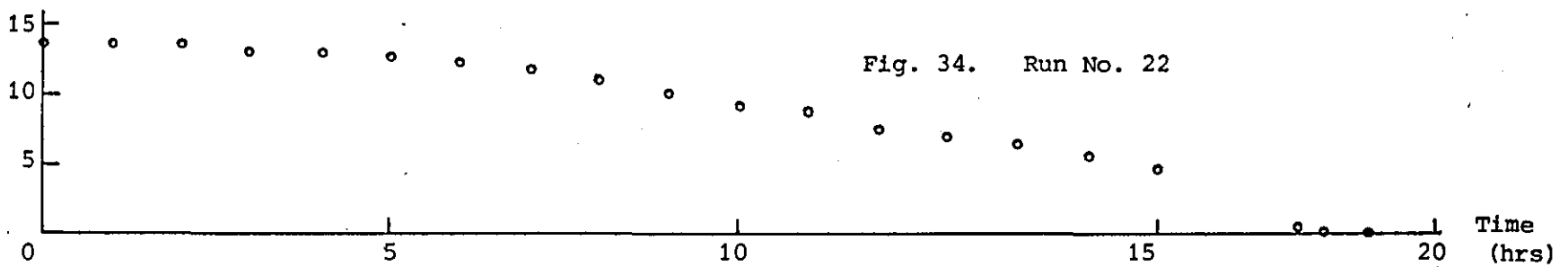

Fig. 34. Run No. 22

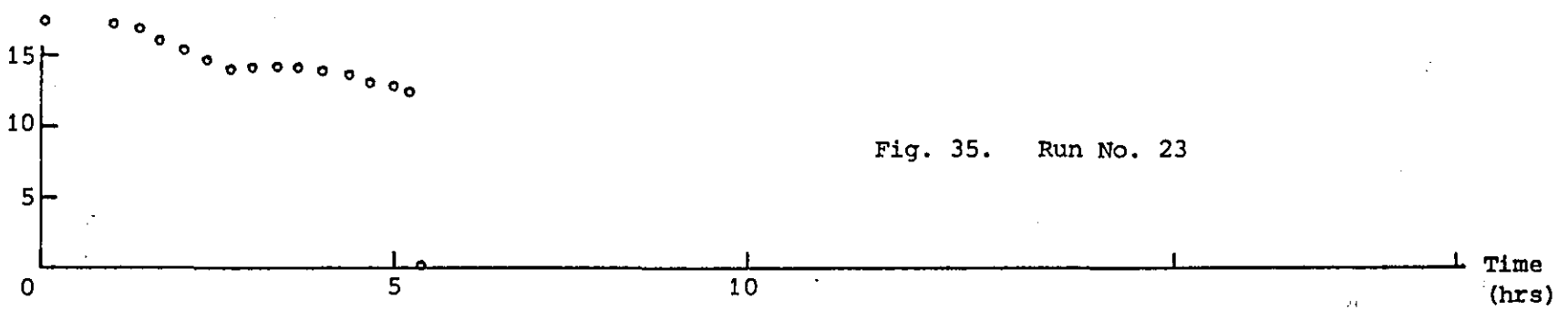

Fig. 35. Run No. 23

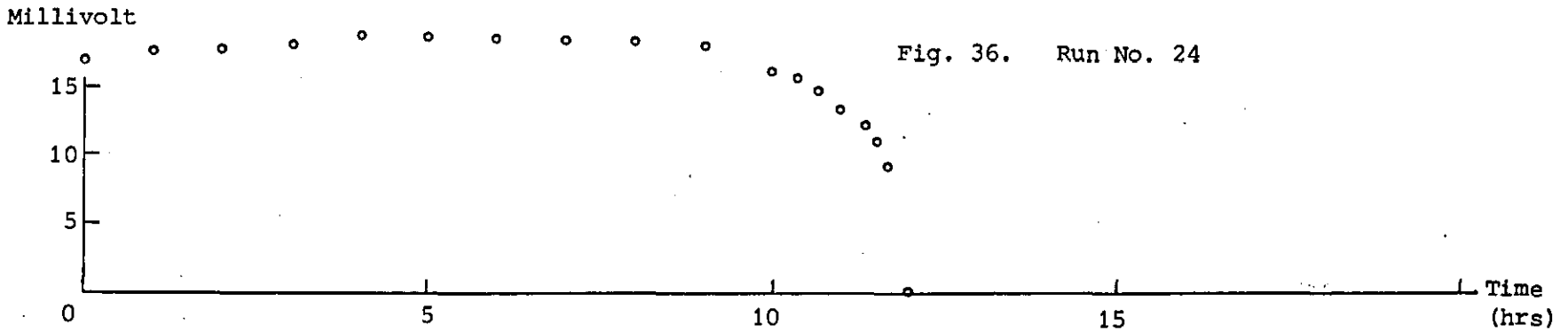

Fig. 36. Run No. 24

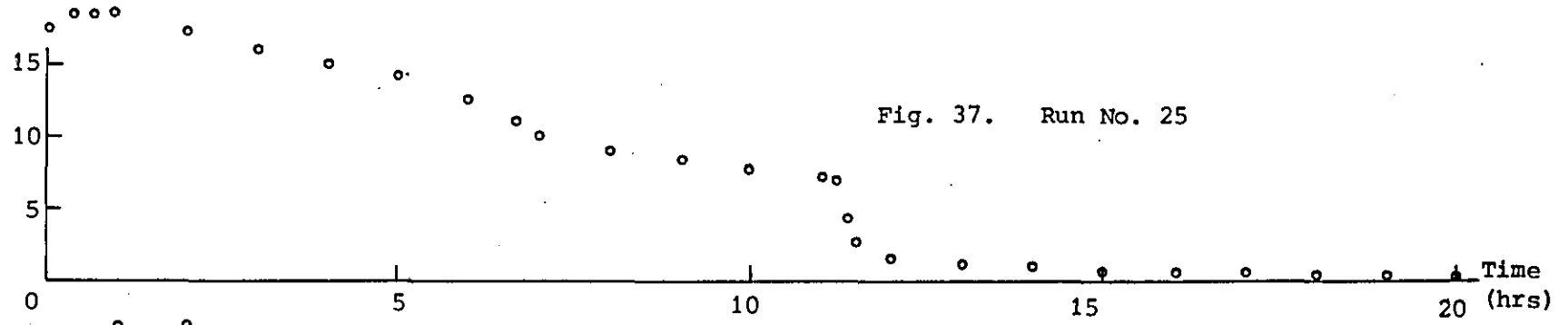

Fig. 37. Run No. 25

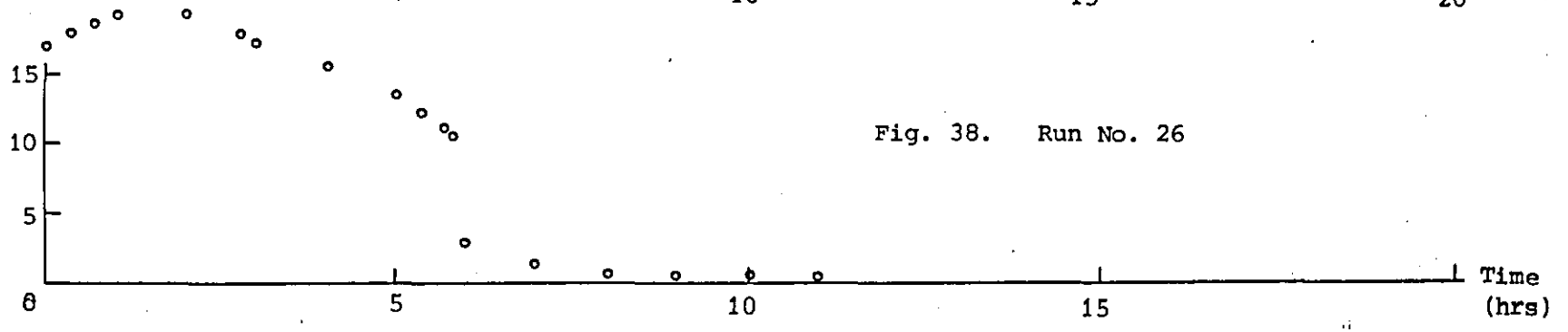

Fig. 38. Run No. 26

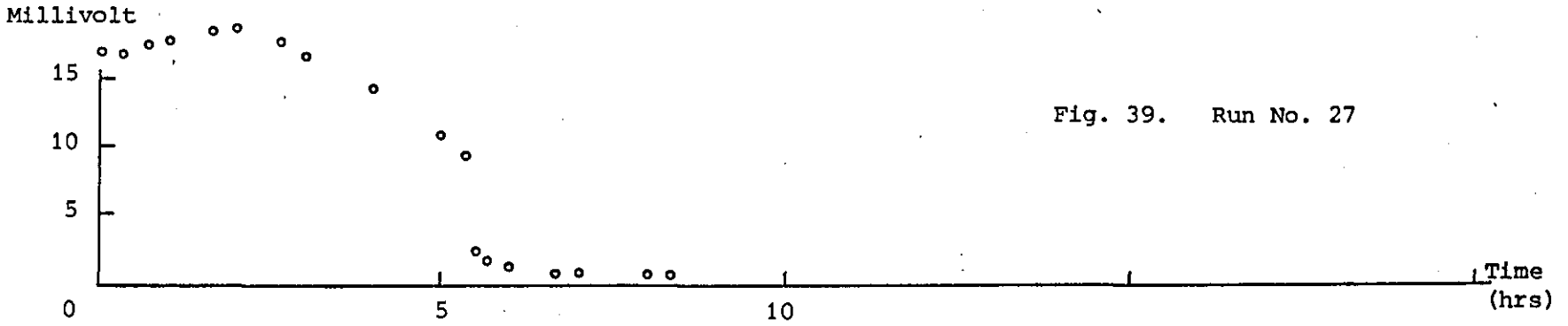

Fig. 39. Run No. 27

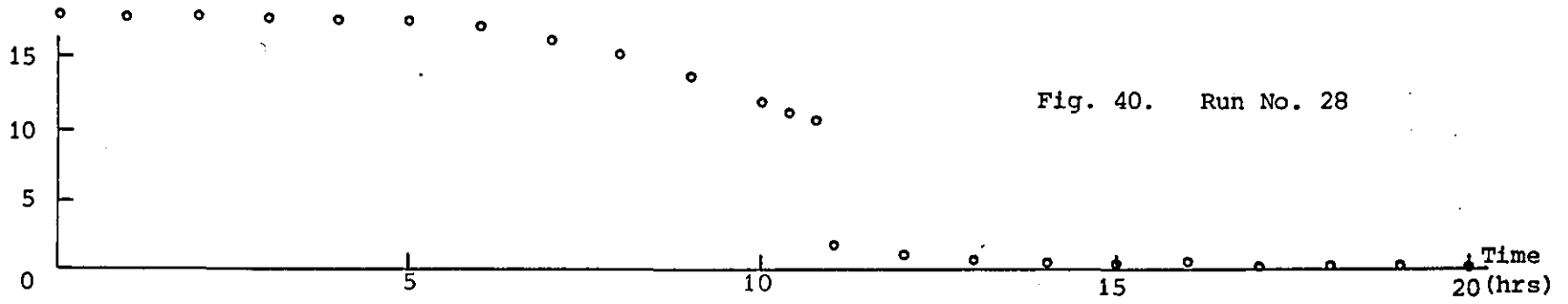

Fig. 40. Run No. 28

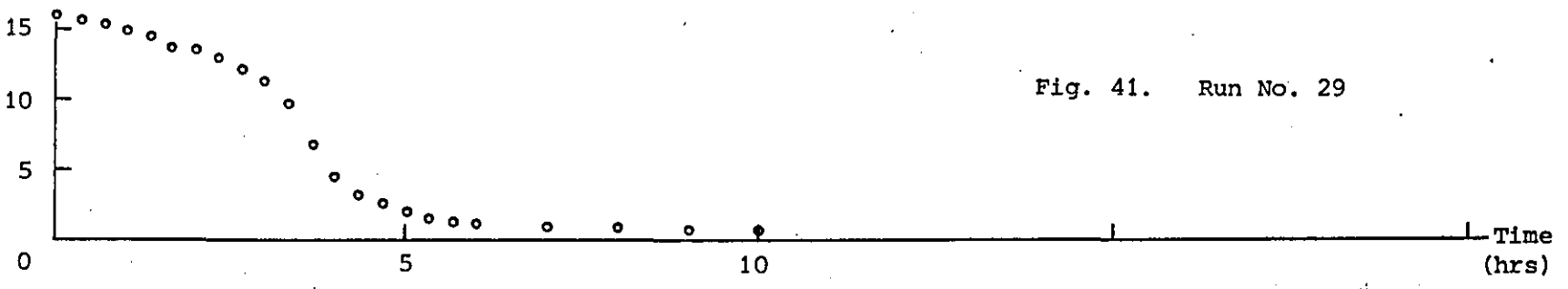

Fig. 41. Run No. 29

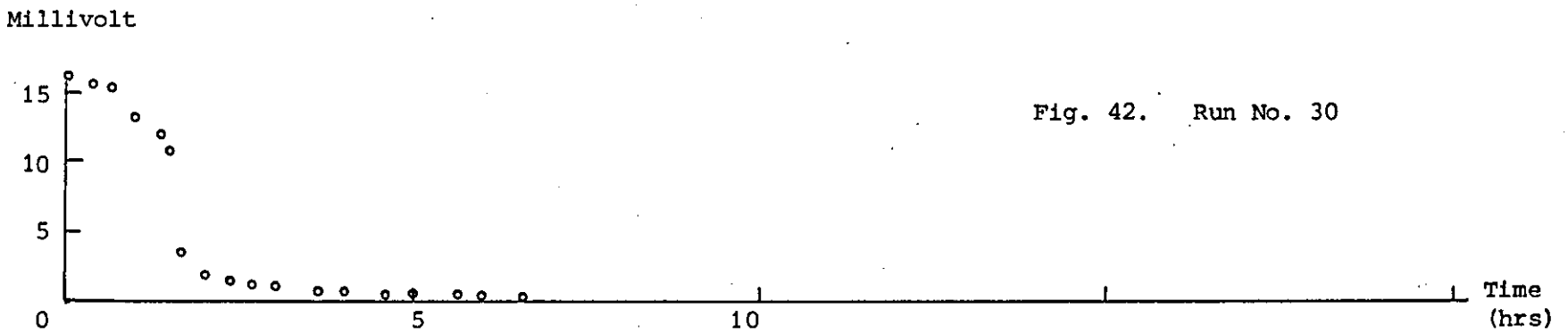

Fig. 42. Run No. 30

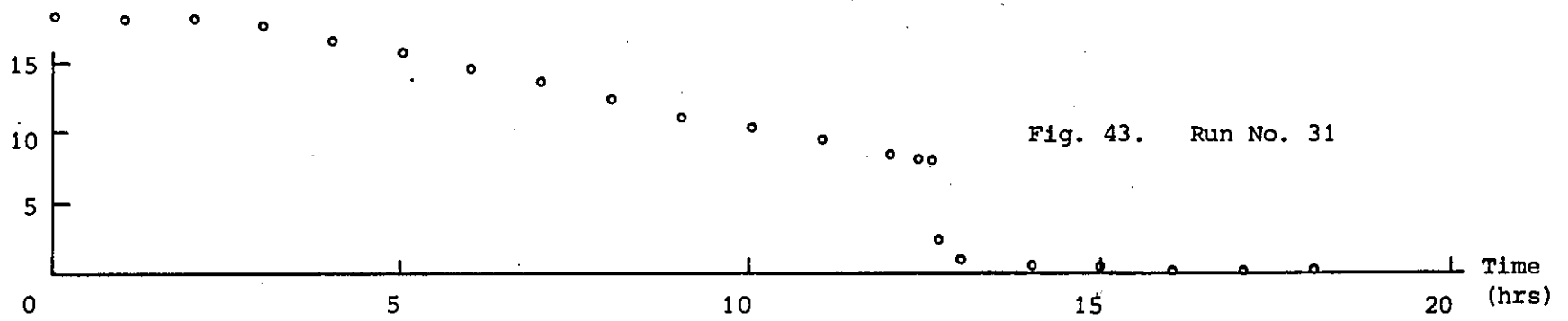

Fig. 43. Run No. 31

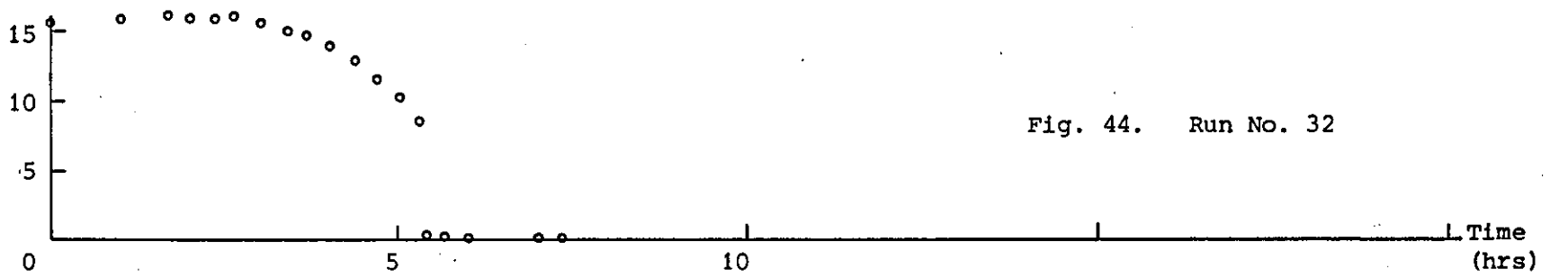

Fig. 44. Run No. 32

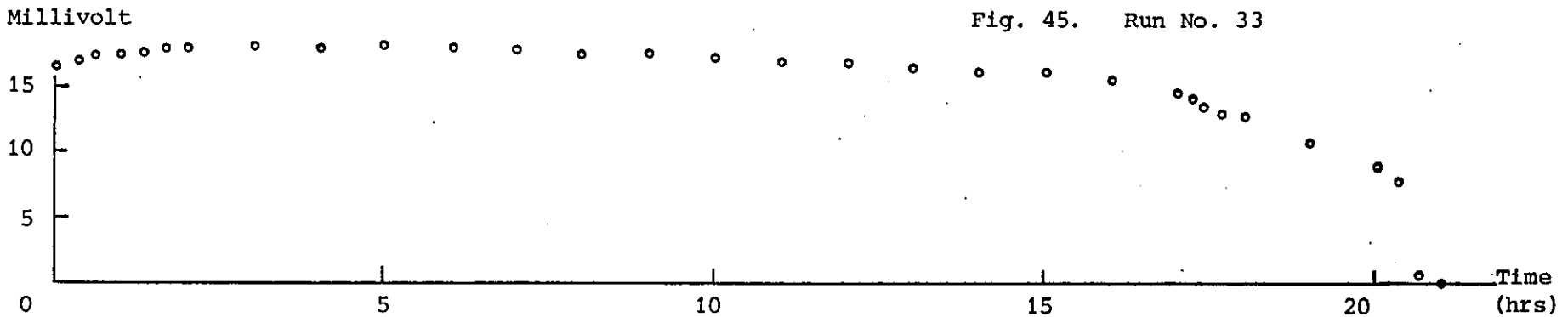

Fig. 45. Run No. 33

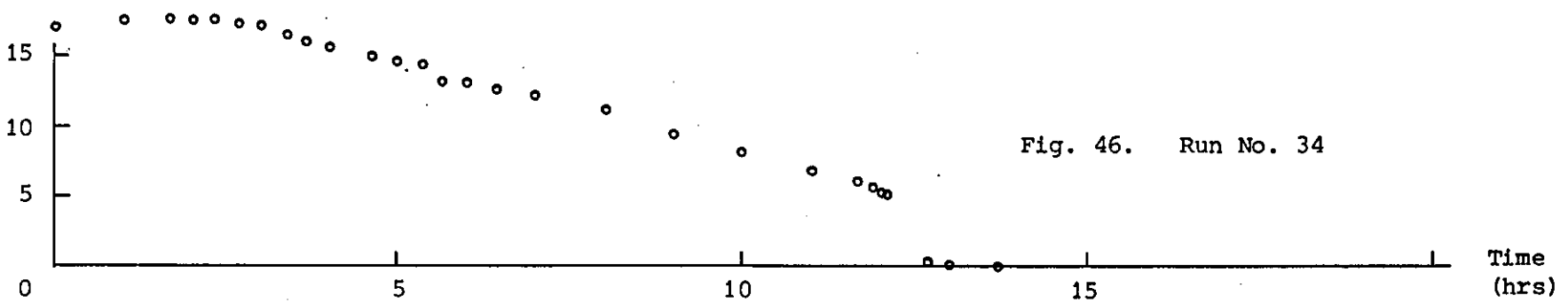

Fig. 46. Run No. 34

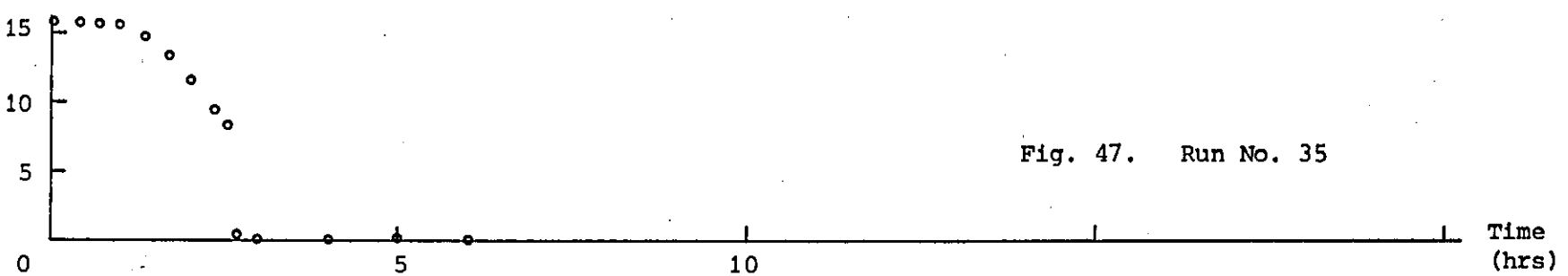

Fig. 47. Run No. 35

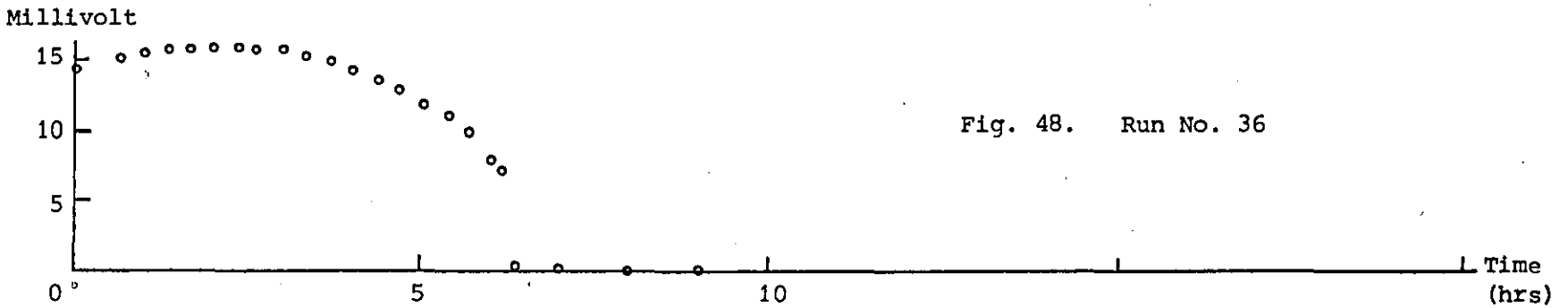

Fig. 48. Run No. 36

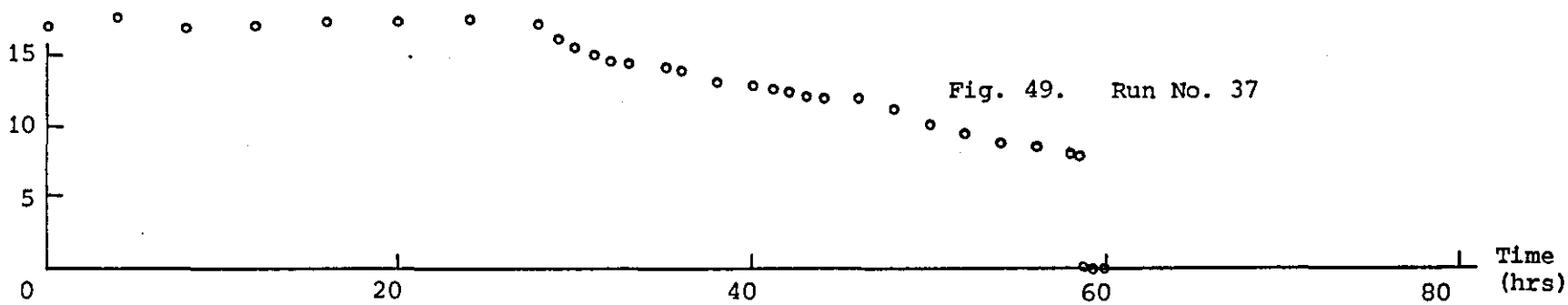

Fig. 49. Run No. 37

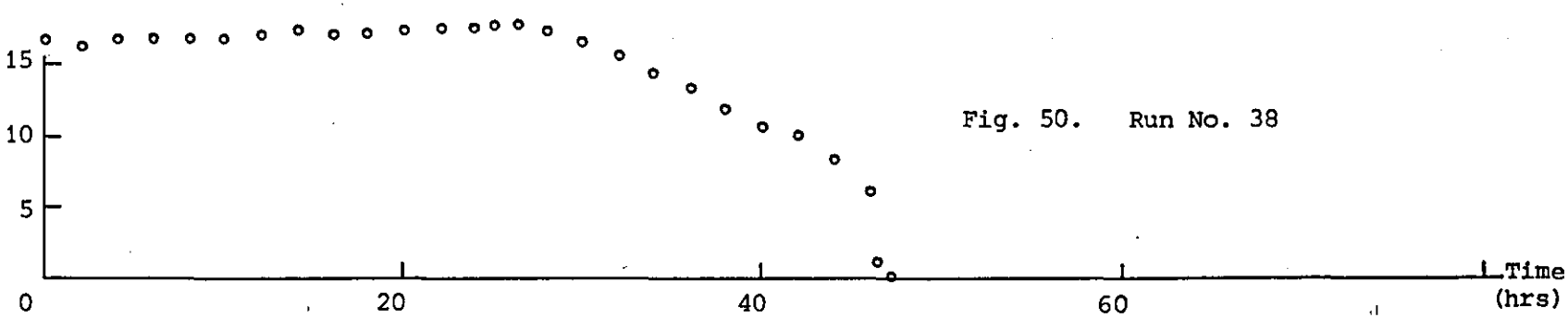

Fig. 50. Run No. 38

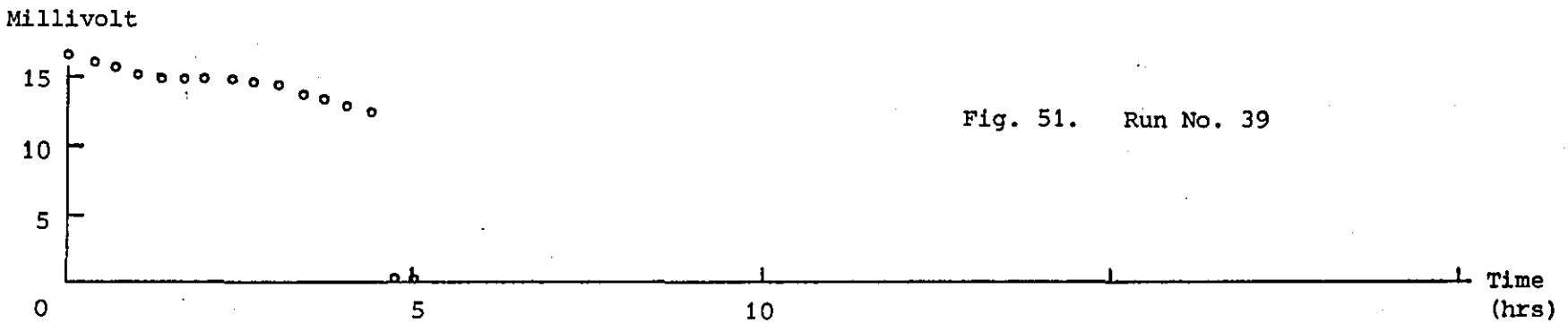

Fig. 51. Run No. 39

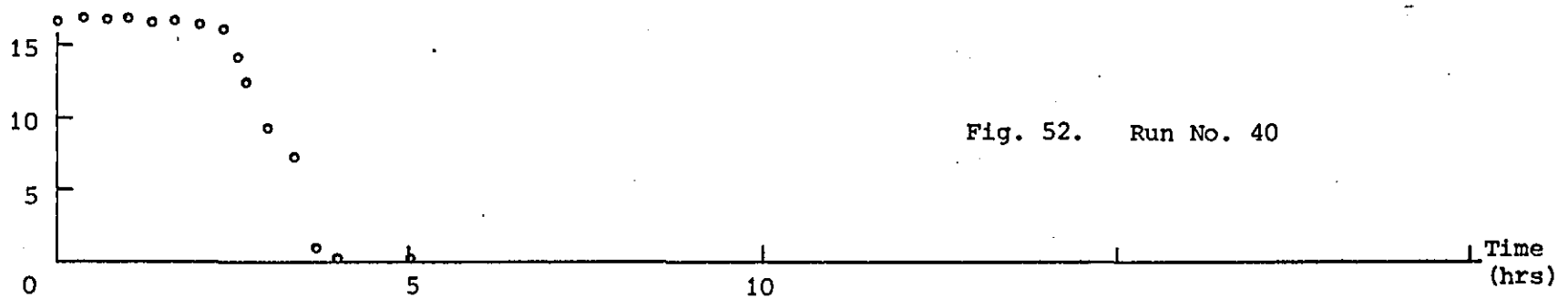

Fig. 52. Run No. 40

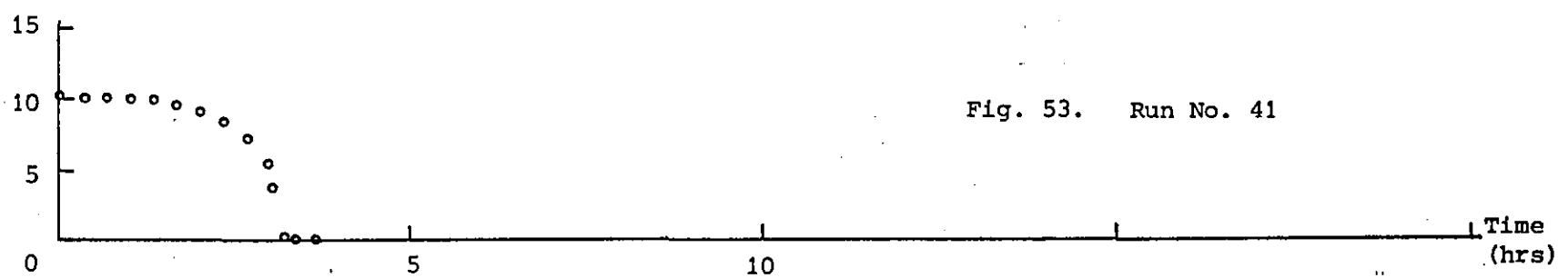

Fig. 53. Run No. 41

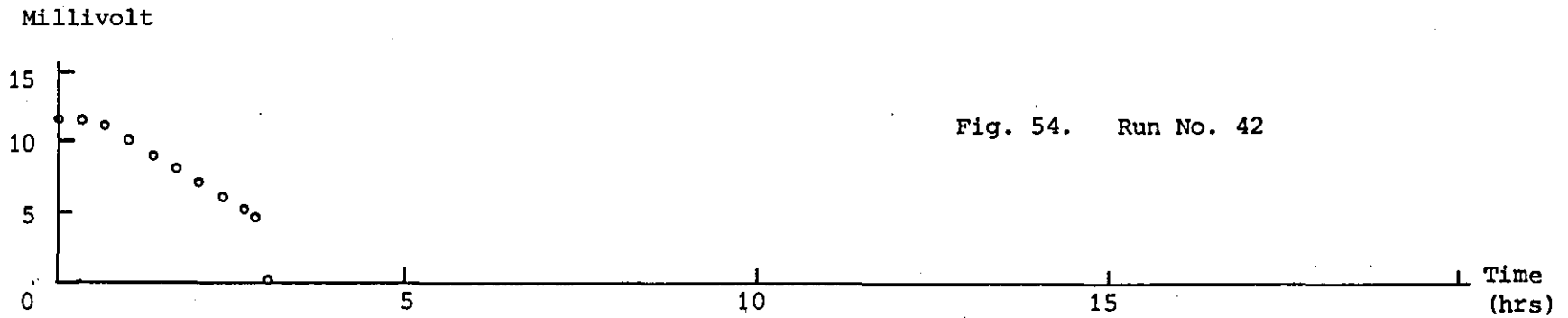

Fig. 54. Run No. 42

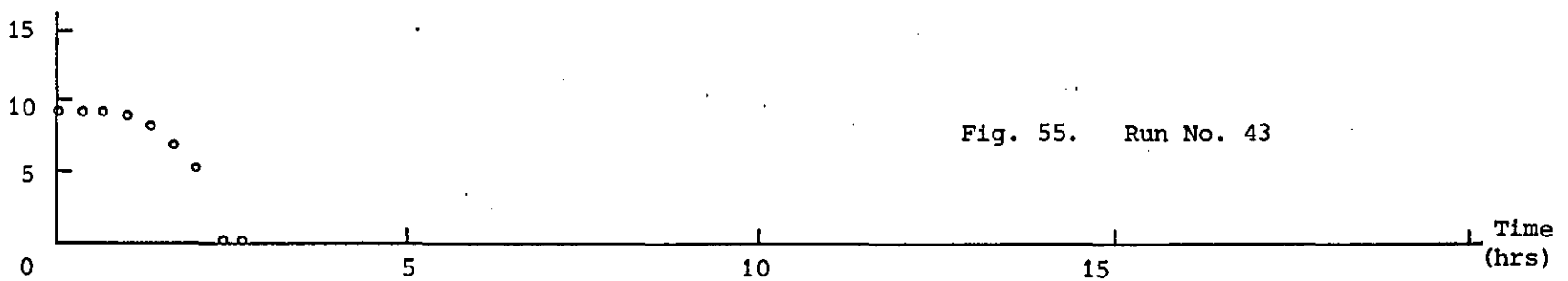

Fig. 55. Run No. 43

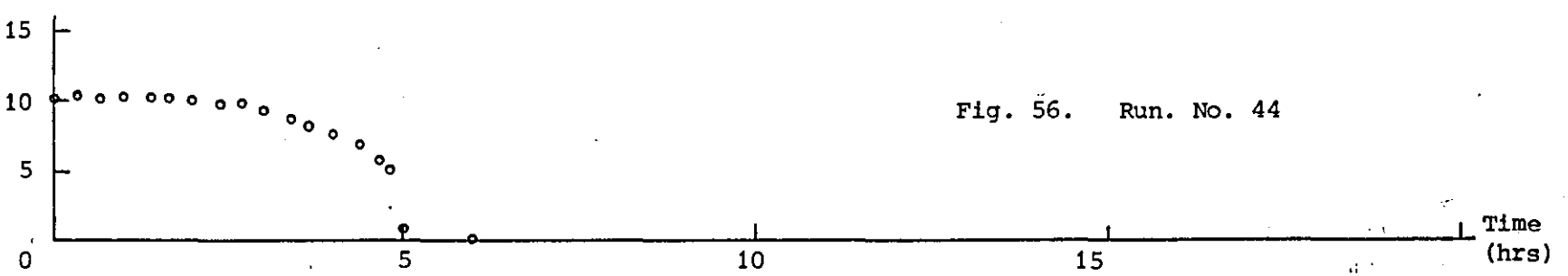

Fig. 56. Run. No. 44

ratio.

The increase of permeability, where calculated, for runs 5-44 all showed increases of more than one order of magnitude except for runs 18 and 21. The rate of change of pressure difference of run 21 was rather slow (c.f. Fig. 33) and the experiment was terminated before "breakthrough" occurred.

More accurate determinations of the final permeability ratio (marked by ' in the appropriate column in Appendix II) showed increases of permeability of over one hundred fold with the exception of runs 27, 28 whose individual values were sixty-five and ninety fold respectively.

It can be safely concluded that for plaster of Paris cores, increases of permeability of fifty fold can easily be attained. However, for sand-plaster of Paris cores, no definite conclusion of the average increase in permeability can be made, although an increase of ten fold appears to be a reasonable estimate, assuming no major disintegration of the core.

Let us now consider the other experimental aim which was to identify, if possible, the mechanism responsible for the increase of permeability.

Progressive leaching of a porous matrix has been compared to the displacement of oil by water (Chapter Six). The portion of the porous matrix containing the water phase was replaced by a region of leached porous material whereas the oil phase was replaced by a region of unleached porous material. The relative movement of the interface was determined by a permeability ratio (leached to unleached) whereas in the oil displacement model the motion of the interface was governed by a viscosity ratio (μ_o/μ_w).

For mobility ratios $(m = (k_1\mu_2)/(k_2\mu_1))$ [7] greater than unity, small outgrowths on an otherwise uniform interface grow rapidly. Eventually the overall flow pattern is governed by the

now enlarged outgrowths (wormholes). A simplified model[8] of the dynamics of a frontal system possessing large wormholes predicted a linear rate of decrease of pressure difference across the porous material, assuming that the injection rate of fluid remained constant. Examination of the results showed that about one half of the experimental runs showed some linear behaviour (see Figs. 8-11 and Figs. 18-56).

Briefly, the traces of runs 2, 3, 5, 6, 10, 15, 16, 18, 26, 27 and 33 are initially curved but the final portion of the trace shows a linear decrease; similarly runs 30, 42, and 44 also exhibit a linear rate of failure at the end of the trace, although the duration of these runs is a little short. The traces of runs 22, 31, 34, 37 and 38 are initially flat, (i.e. Δh_w is constant), the flat portion of the trace is followed directly by a linear rate of decrease. Run 7 was unique because its trace decreased linearly from the outset of the experimental run. Finally, runs 8, 25 also showed a linear failure rate, however in each run there was a short curved section in the middle of the trace separating the linear section. This behaviour is thought to be a result of imperfections (i.e. air bubbles) within the matrix which are encountered by the growing tip of the wormhole.

Traces of runs 9, 10, 18, 33, 34 and 38 exhibit an extra rapid rate of failure immediately prior to "breakthrough". An explanation of this more rapid failure rate is that the permeability may not be sharp but extend over a small distance. A change of failure rate would occur when the leading portion of the interface reached the rear of the core. Complete breakthrough would occur when the latter portion of the interface reached the rear face of the core.

The shape of several wormholes have been photographed and can be found in Figs. 57-67. Their shape is reminiscent of a plant root system, that is a main root and several minor offshoots. A wormhole may be regarded as an enlarged preferential flowpath through an otherwise uniform homogeneous matrix. Visually, the flowpath may have been indistinguishable from the rest of the matrix, at the start of the experiment. However, when fluid is injected, the paths of lower fluid resistance grow at a greater rate than their neighbouring pathways and eventually become distinguishable from them.

For plaster of Paris cores the radii of the wormholes are quite small and exhibit branching, whereas the wormholes of sand-plaster cores are mugh larger and do not exhibit well defined side branches. It should be noted for runs 37-40, 150g of glass beads (in the size range 600-710 μm) were added to the plaster of Paris mix, the ratio of plaster/glass beads/water by weight was 2/3/1. The addition of glass beads was an attempt to simulate the behaviour of the sand-plaster cores. The weight of glass beads added was an arbitrary chosen amount.

A visible wormhole was obtained in run 40 (Fig. 67). The radius of the wormhole is quite narrow, and approximately the same size as those obtained with plaster of Paris. The wormhole of run 40 exhibited very little side branching.

The branching exhibited by plaster of Paris cores indicates that there are several secondary preferential flowpaths emanating from the central wormhole. Each of these secondary pathways are partially developed until they are overtaken by the more rapidly moving tip of the central wormhole. The older pathways become redundant and have little further growth. The older secondary pathways are replaced by new ones uncovered by the movement of the growing tip of the central wormhole.

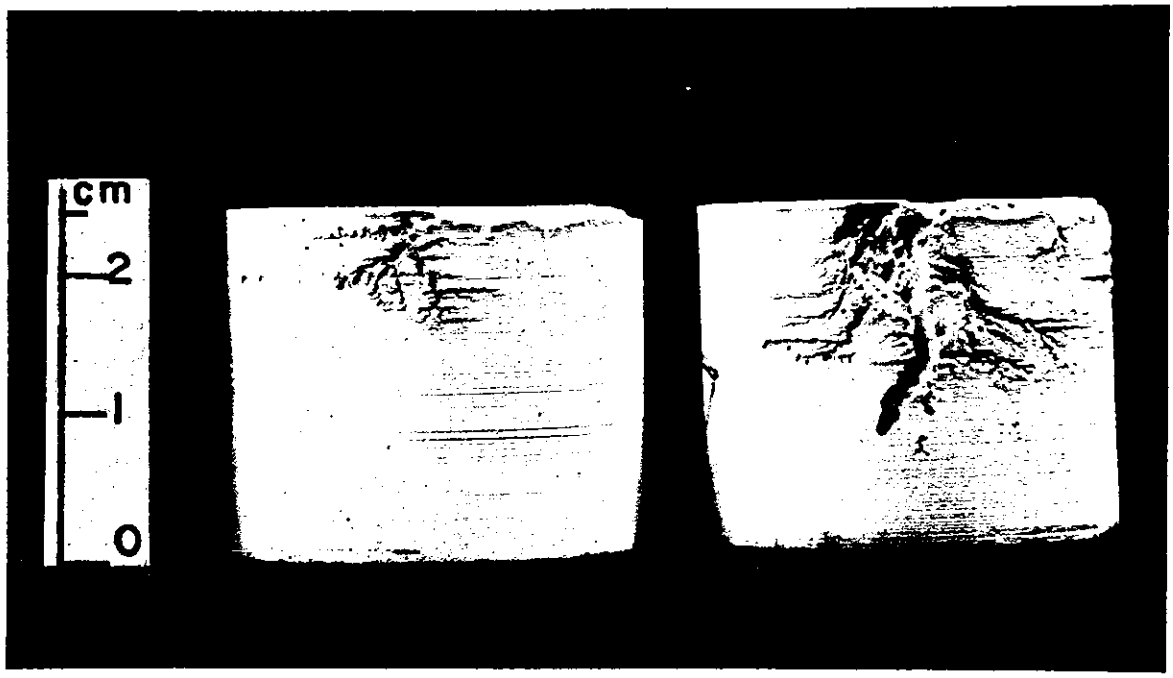

Fig. 57 (left) Fingers developed in sample cores of
Fig. 58 (right) Runs No. 6 and No. 7 respectively.

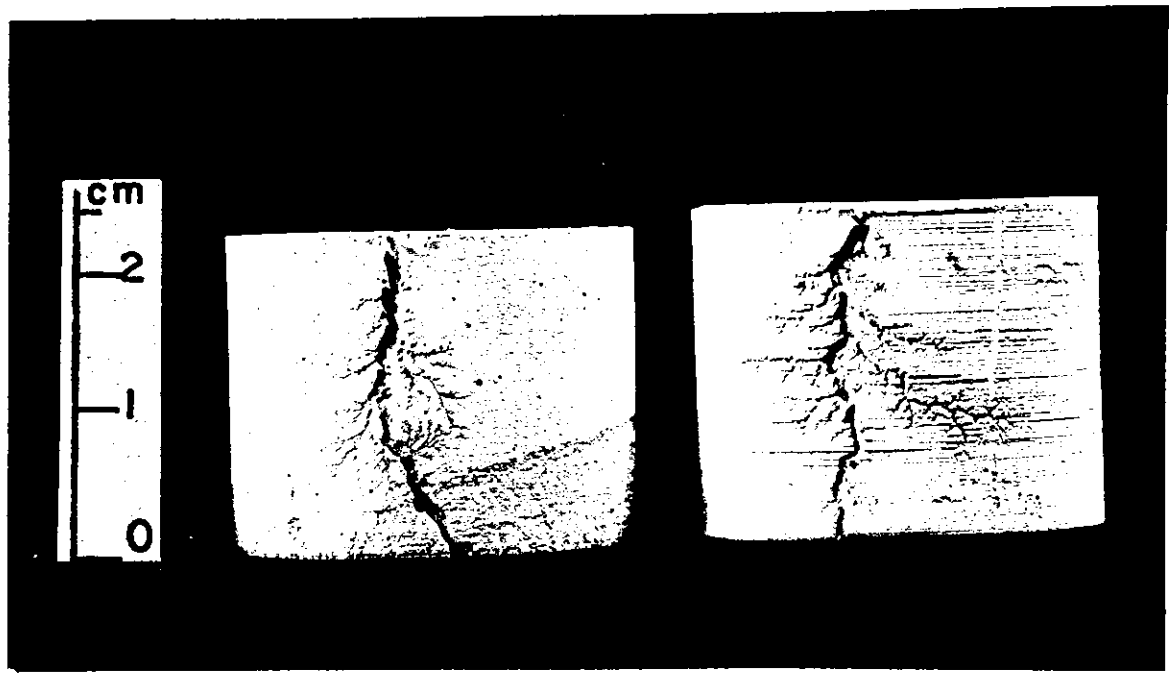

Fig. 59 (left) Fingers developed in sample cores of
Fig. 60 (right) Run No. 9 and No. 11 respectively.

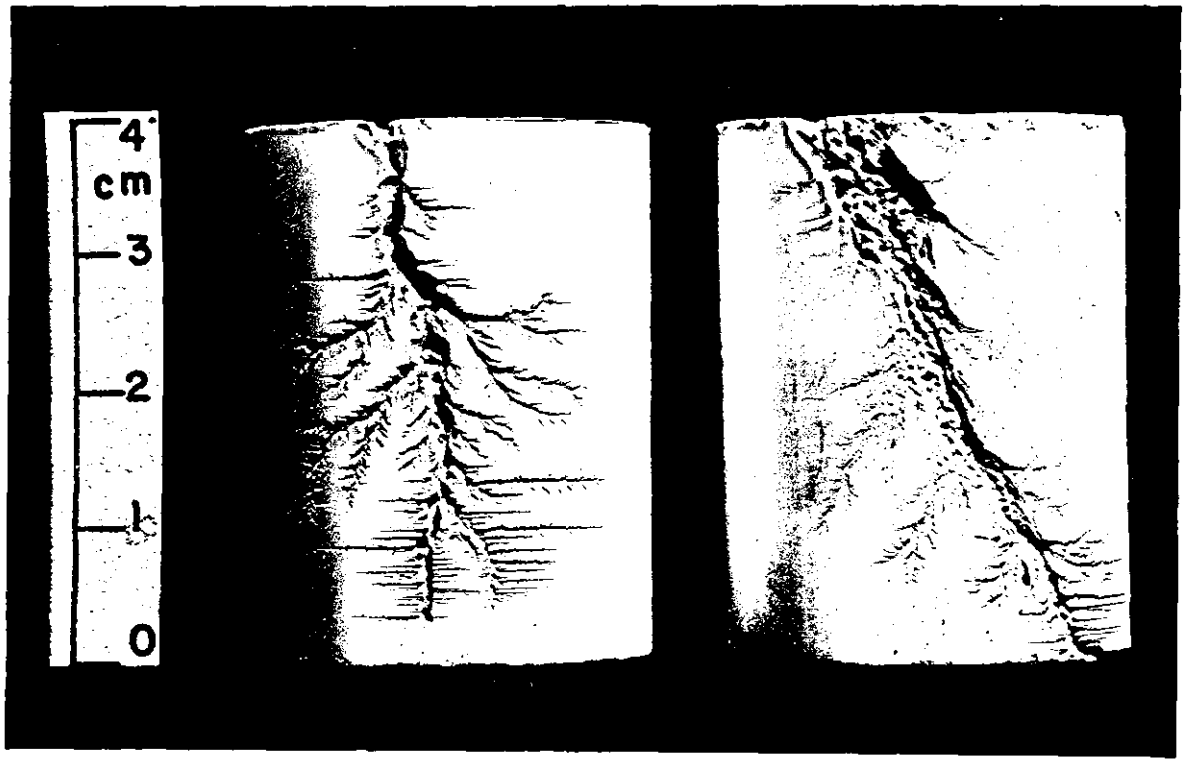

Fig. 64 (left) Fingers developed in sample cores of
Fig. 65 (right) Run No. 26 and No. 29 respectively.

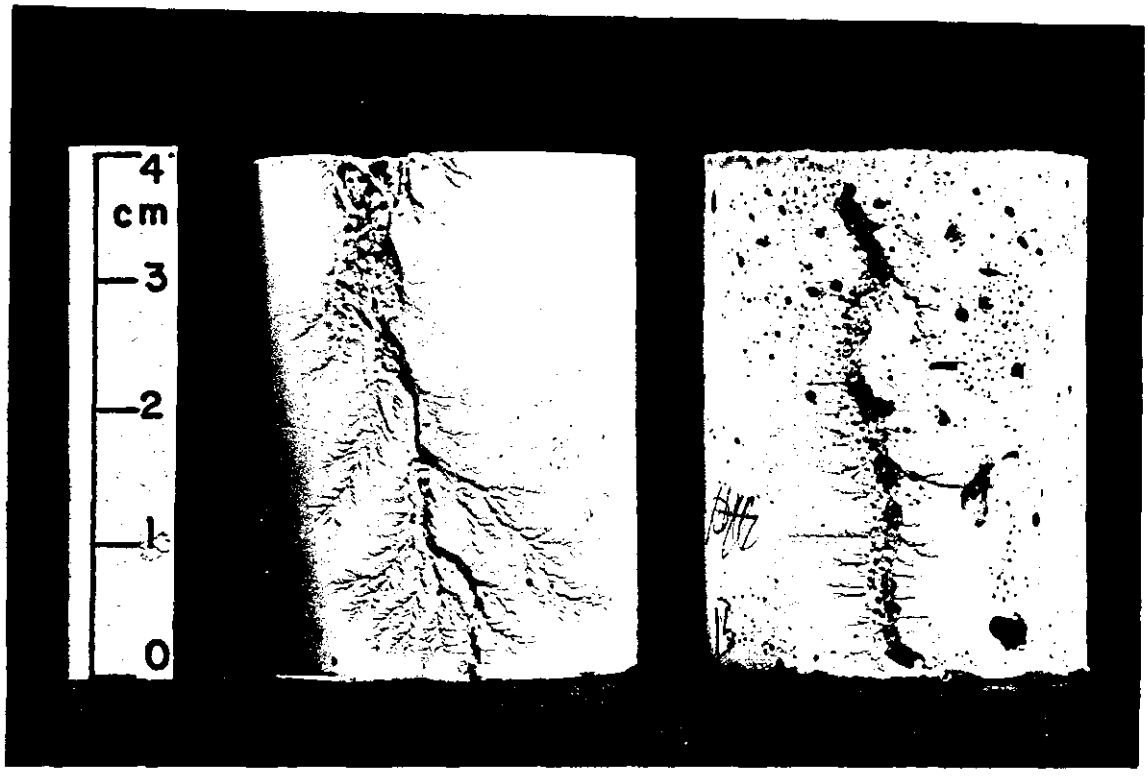

Fig. 66 (left) Fingers developed in sample cores of
Fig. 67 (right) Run No. 30 and No. 40 respectively.

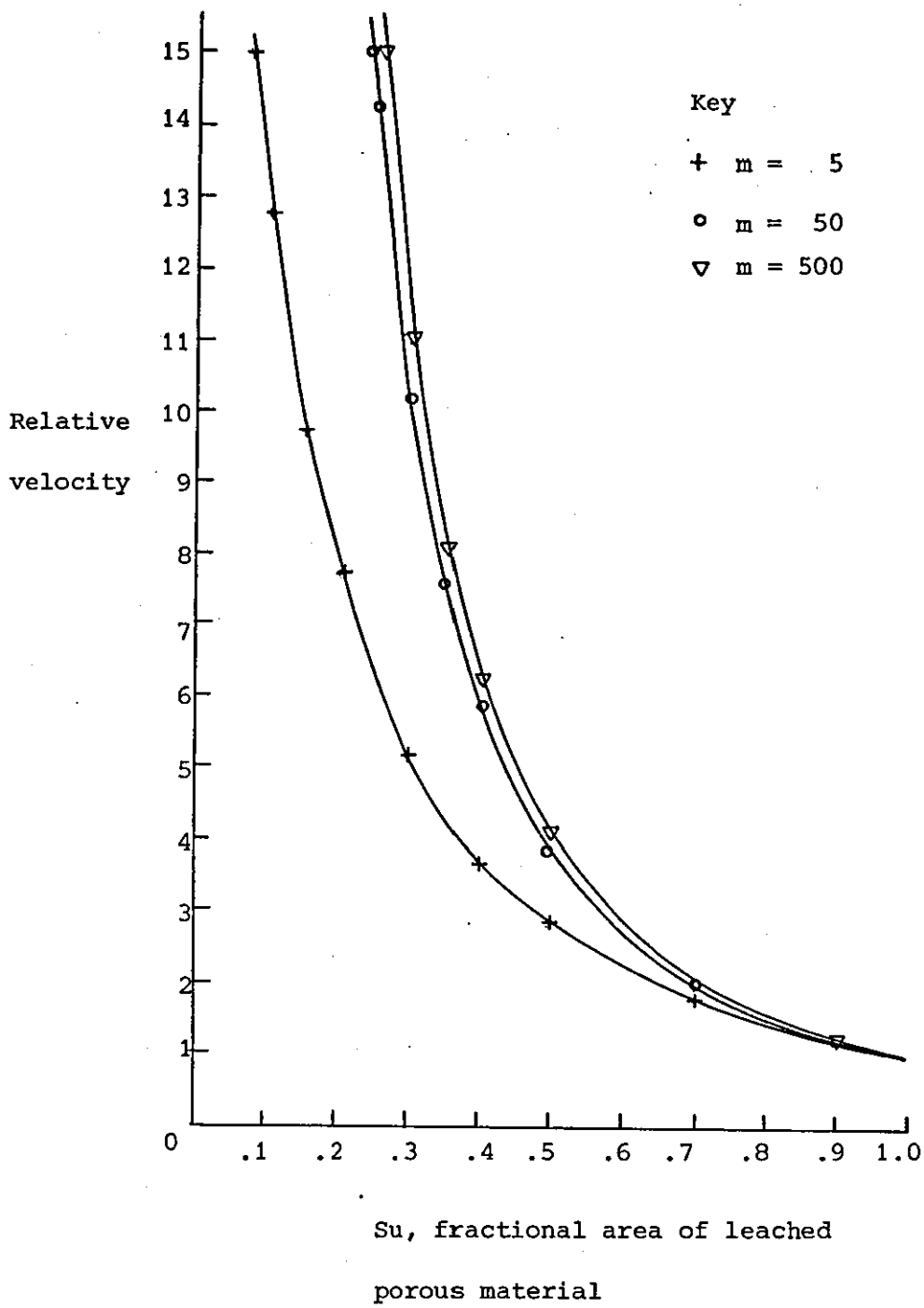

Fig. 68. Ratio of the velocity of the permeability front of a given leached area, Su, with respect to the velocity of the permeability front when the flow area has been fully leached (Su=1)

The lack of branching in the wormhole of the sand-plaster cores would appear to indicate that there are no secondary preferential pathways. However, the presence of inert material (sand) in the core must be considered. Imagine the growing tip of a wormhole encountering the sharp angular contours of sand grains. The central flow path could be deflected sidewards or more likely become split into several minor flowpaths, each of which may likewise become subdivided. This dispersive action of the sand grains would inherently reduce the net forward velocity of the wormhole and increase its radial component thus resulting in broader wormholes.

A similar behaviour can be predicted from the model originally proposed by Scheidegger and Johnson[8] which has been discussed in Chapter Six. The speed of any given fractional area of leached porous material was represented by the expression

$$\left[\frac{d_x}{d_t}\right]_{S_u} = \frac{1}{c'}\,\frac{Q_T}{A}\,\frac{m''}{\left[S_u(m''-1) + 1\right]^2}$$

where $(d_x/d_t)_{S_u}$ is the velocity of a given fractional area, S_u, of leached porous material; Q_T, the overal volumetric fluid injection rate; A, the area for flow; c', a constant; m", the mobility ratio (= k_u/k_s); k_u, the permeability of the matrix containing unsaturated fluid (the leached permeability); k_s, the permeability of the matrix containing saturated fluid (the original permeability).

Curves of relative velocity versus fractional area of leached porous matrix for three mobility ratios (m" = 5, 50, 500) can be found in Fig. 68. It can be observed from the figure that as m" increases the diameter of the wormhole will decrease because the relative velocity of different fractional areas of leached material increases as m" increases. Addition of sand to the plaster of Paris lowers the final permeability of the core and consequently m"

is correspondingly lowered. Similarly one would expect that addition of glass beads to the plaster of Paris would also lower the final permeability of the core; however examination of the permeability values of runs 37-40 (Appendix II) shows that the final permeability is similar to those cores containing only plaster of Paris.

Explanations of these anomolous results are:- (1) the concentration of glass beads was not high enough to significantly affect the growth and development of the wormholes, except to limit the growth of secondary side branches. (2) the smooth spherical shape of the beads would not be expected to produce a large amount of wormhole dispersion when compared with the sharp angular grains of sand.

Thus the development of a wormhole appears to be influenced by both the shape and concentration of inert materials within the matrix. The shape and concentration of inert materials will also influence the initial and final permeabilities of the porous matrix and the motion of an interface.

The modification of including vacuum saturation of the cores was introduced so that the porosity of cores could be calculated. Knowledge of this property was useful since it was used as an indicator of the degree of homogeneity of the casting procedure and a measure of the quality of the cores. The consistency of the casting procedure can be found by inspection of the porosities of cores in Appendix II. For runs 17-44, excluding runs 37-40, the variation of porosity was calculated to be about $\pm$ 5%. The average porosity value was calculated to be 42%.

An additional benefit of vacuum saturation was that the amount of air remaining in the core and subsequently affecting the core response was minimised. The presence of air in the core would restrict fluid movement, and consequently lower values of

permeability would be obtained. The entrapped air could also be liberated during the course of the experiment or interfere with the growth of wormholes both of which affect the permeability response.

Sample calculations of the permeability and porosity can be found in Appendix III, together with error estimation associated with the measurement of the physical properties.

3. Experimental study number two. Investigation of the seasonal variation of suction developed by a wall suffering from Rising Damp

3.1 Introduction

The purpose of this study is to measure the vertical distribution and seasonal variation developed by a wall suffering from Rising Damp.

Determination of the capillary suction is important because it is a measure of the energy condition existing at that point. Capillary suction can be used to correlate the hydraulic properties (moisture content, unsaturated permeability, local evaporation rate) of porous building materials. Moisture content, unsaturated permeability together with the suction gradient and local evaporation rate can be used to estimate the overall rate of moisture movement both spatially and temporally, within the wall.

Capillary suction is measured with a tensiometer[(10)-(13)]. A mercury tensiometer consists of a mercury manometer which is connected hydraulically to a fine-pored porous cup. The cup is inserted into the porous material whose suction is to be determined. Movement of moisture across the porous cup is registered as a difference in height of the mercury levels. At equilibrium the difference in mercury level is used to calculate the capillary suction within the porous material.

One of the uses of tensiometers is following the position of the ground water tables[(14)]. These instruments measure the

pressure difference between the soil water and free water, hence tensiometer readings may be interpreted in terms of the equilibrium height of the instrument above the free water surface. Interpretation of this nature implies that the porous material, at the point of measurement, is in equilibrium with the water table.[10] [12]-[14] However, for wall suffering from Rising Damp, one would expect there to be a net upward movement of moisture to replace that lost by evaporation. The upward flow of moisture would produce an additional energy difference due to frictional forces and hence the suction gradient would be greater than that for equilibrium conditions.

For transient moisture conditions the suction will be governed by the difference between the rate at which moisture can enter or leave the wall. The infiltration rate is dependent on the depth of the water table to a large extent, whilst the evaporation rate is determined by local atmospheric conditions. Both the water table and the evaporation rate exhibit seasonal (and diurnal) variations and consequently the wall suction will reflect these variations.

It is important to remember that both the suction-moisture content and suction-unsaturated permeability relationships exhibit hysteresis (c.f. references (10), (13), (14) and Chapter Two), which would affect the change of suction response in the wall.

The range of suction measured by a mercury-water tensiometer is limited, because of the need to maintain liquid continuity throughout the apparatus. The maximum suction of a mercury-water tensiometer is limited to pressure heads greater than -850 cm of water because of the vapour pressure of water[12]. When aerated water is used in the tensiometer, the maximum usable suction is reduced to -550 cm of water head.

The latter figure was adopted as the maximum suction head that could confidently be maintained by mercury-water tensiometers. A short term increase in "usable" suction could be ontained by replacing the water in the tensiometer with fresh deaerated water, however after a period of time, the problem of dissolved air would recur, because of air diffusing through the porous cup of the tensiometer.

It is essential to maintain good liquid contact between the porous cup and the porous material. For unconsolidated materials (sand, soil) this condition is easily maintained, however for consolidated materials (cement, mortar, stone, bricks), maintenance of good liquid contact is more difficult, because of the rigid structure of both the tensiometer cup and the porous material. In addition, soil tensiometers are designed to be used with horizontal surfaces rather than vertical (wall) surfaces. Because of these difficulties it was decided that tensiometers designed for soil use were unsuitable and that a tensiometer suitable for use with consolidated materials should be developed. The design considerations of the tensiometer are discussed in the next section. A feature of the design is that the porous cup should be of a small size to facilitiate its fixture into the wall and to minimise the damage and disturbance to the wall.

3.2 Experimental procedure

3.2.1 Design of a mercury-water tensiometer

To perform satisfactorily a tensiometer must satisfy certain requirements. Excluding the porous cup, all the other materials used in the construction of the tensiometer should be impermeable to both air and water. The porous wall of the cup, when thoroughly wetted, must withstand an air pressure head in excess of 550cm of water head. It is recommended that the cup conductance to water

should be in excess of $1cm^3$ per minute when one atmosphere of hydraulic pressure is applied across the cup wall. The sensing gauge (mercury manometer) should require only a small volume be displaced. A satisfactory value for most purposes is $1cm^3$ per atmosphere pressure change. A transparent air trap is usually included, so that the volume of air within the tensiometer can be observed and removed. If the volume of air is in excess of 2 to 3 cm^3 the instrument should be vented and refilled with water.

3.2.2 Design of the porous cup

A number 4 porosity, 10mm microfilter was chosen as the porous cup. The dimensions of the microfilter and subsequent modifications to it are shown in Fig. 69. The minimum size range of particles removed by the filter is 5 μm to 15 μm. Assuming the larger figure to represent the maximum pore diameter of the filter and assuming the pores to be circular, the maximum suction that the filter can sustain, at 20°C, is approximately 200cm of water head. The maximum suction developed by six filters can be found in Table I.

Table I. Maximum suction developed by six unmodified microfilters.

microfilter	maximum suction (cm. water head)
1	96.2
2	109.2
3	182.0
4	136.5
5	114.4
6	167.7

None of the microfilters attained a suction of 200cm of water head. The highest suction observed was 182cm, whilst the lowest suction was 96.2cm of water head. In view of these lower than expected suction values, it was decided to include a plug of plaster

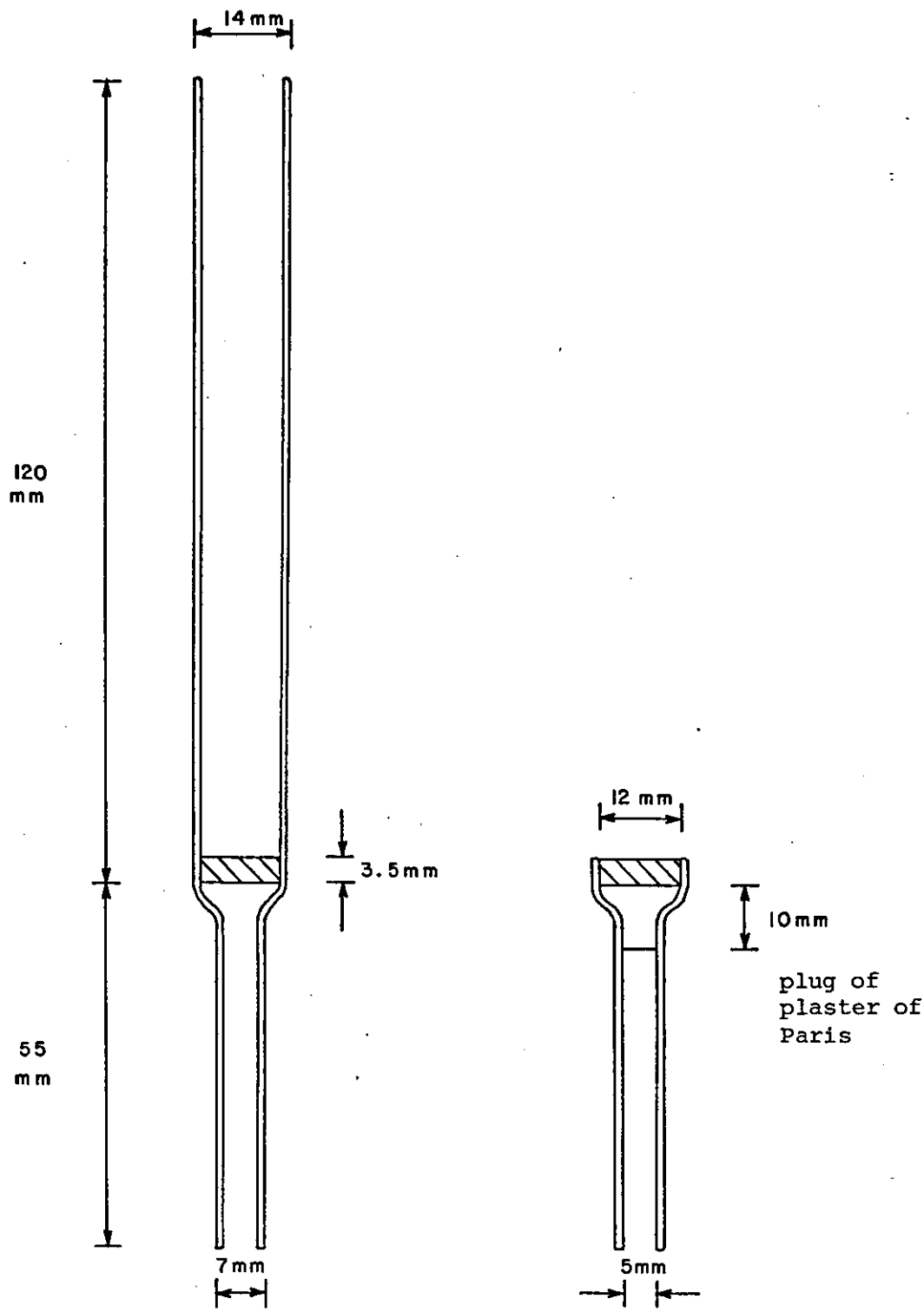

Fig. 69 Schematic representation of the tensiometer cup

of Paris 1cm deep directly behind the sintered disc of the microfilter as shown in Fig. 69.

The permeability of freshly cast plaster of Paris is of the order of 1×10^{-11} cm² (c.f. previous experimental study). The permeability is generally assumed to be a measure of the square of the average pore radius. Thus the average pore radius of fresh plaster of Paris is 3.16×10^{-6} cm. The approximate entry value of pores of this size if 4.7×10^{4} cm of water head. Subsequent tests upon fourteen microfilters containing the plaster of Paris plug showed that they were able to sustain suctions greater than 550cm of water head, and hence satisfied the suction requirement of the porous tensiometer cup.

3.3 Sensitivity of the tensiometer instrument. S_e (ats. cm^{-3})

The sensitivity of a tensiometer is defined as the amount of water displacement required to register a suction of one atmosphere, from an instrument that was at zero suction. The sensitivity is usually expressed as atmospheres per cm³ of displacement, i.e. a typical value is 1 atmosphere per cm³.

Consider the sensitivity of a U-tube mercury manometer containing a water-mercury interface in one arm and a mercury-air interface in the other arm. Assuming the density of mercury and water to be 13.5 and 1 g per cm³, then each centimetre height of mercury difference is equivalent to 13cm of water head. The mercury height difference required to develop a pressure of one atmosphere (1036cm of water head) is 79.69cm. However, the length of water displaced is only half this length, i.e. 39.85cm. Hence the diameter of tube to satisfy the condition of 1cm³ per atmosphere is 0.179cm.

The diameter of tube used in this study was 0.16cm, which has a sensitivity of approximately 1.25 ats cm⁻³. The choice of tube diameter is a compromise between instrument sensitivity and

hysteresis errors associated with surface tension forces. Surface tension forces are proportional to the reciprocal of the tube diameter.

3.4 Cup conductance K (cm^3 min^{-1} ats^{-1})

Cup conductance is defined as the volume of liquid (cm^3) per unit time (min.) that can pass through the walls of the porous cup when one atmosphere of pressure (10^5 N m^{-2}) is applied across the wall of the cup. An acceptable value of cup conductance is 1cm^3 per min. per atmosphere pressure difference across the cup walls,[12] although values of 0.1cm^3 per minute per atmosphere have been used[11].

The cup conductance is usually determined in the following manner. The tensiometer is allowed to develop a known suction, h_{so}. The porous cup is then immersed in a container of (free) water; corresponding measurements of suction, h_s and time, t are than recorded. The relationship between the suction and time, which is derived in Appendix IV, is given by

$$(h_s/h_{so}) = e^{-K S_e t} \qquad (1)$$

where h_s is the suction after time t has elapsed, h_{so} is the original suction; S_e, the sensitivity of the instrument; t, the time that has elapsed since immersion of the tensiometer cup into free water; K, the cup conductance. A graph of ln (h_s/h_{so}) versus time should yield a straight line of slope K S_e, and assuming S_e to be already known then K can be evaluated.

Cup conductances of three modified microfilters has been determined using a slightly different procedure, which is more appropriate to tensiometer studies using consolidated materials. The method is called the "in situ" method since the cup conductances are determined after the porous tensiometer cups have been fitted into the porous sample.

Holes of depth 1 to 2 cm and diameter 15 mm were drilled into three dry house bricks. A modified porous cup (sintered glass and plaster of Paris plug - Fig. 69) was cemented, using plaster of Paris, into each hole. Additional plaster of Paris was attached to the external surface of the porous cup to ensure good contact between it and the brick surface. The plaster was allowed to set overnight, and the porous cups were filled with water and connected to a mercury manometer. Care was taken to remove all air bubbles from the apparatus.

As moisture migrated into the brick, from the instrument, measurements of mercury height difference and time were recorded until the system had attained equilibrium. The mercury height differences were converted to water pressure head differences. The curves of water head (suction) versus time have been reproduced in Fig. 70. The suction-time data together with equation (3) were used to calculate the values of the cup conductances of the three modified, in situ, microfilters.

The relationship describing the suction-time response for the "in-situ" method is

$$h_s = h_{ms} (1 - e^{-K S_e t}) \qquad (2)$$

where h_{ms} is the maximum suction developed by the tensiometer when in contact with the dry house bricks; the other symbols have their usual meaning.

The derivation of eqn. (2) can be found in Appendix IV. The expression was rearranged to yield

$$\ln (1 - (h_s/h_{ms})) = - K S_e t \qquad (3)$$

A graph of $\ln (1 - (h_s/h_{ms}))$ versus t should yield a straight line of slope $K S_e$. If S_e is known then K can be evaluated.

The suction-time measurements for each tensiometer system have been substituted into eqn.(3). The results obtained have

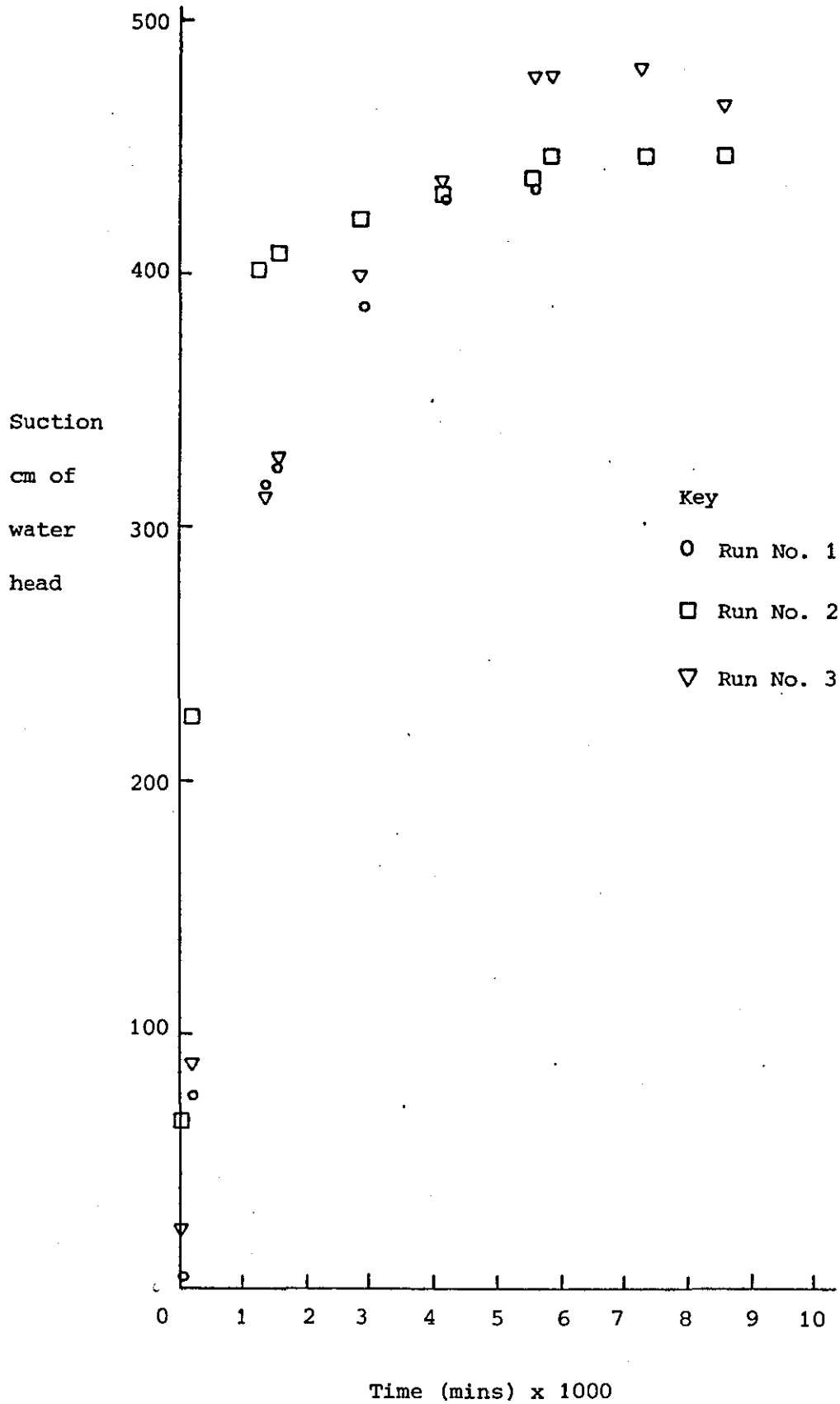

Fig. 70 Suction response times of three tensiometers

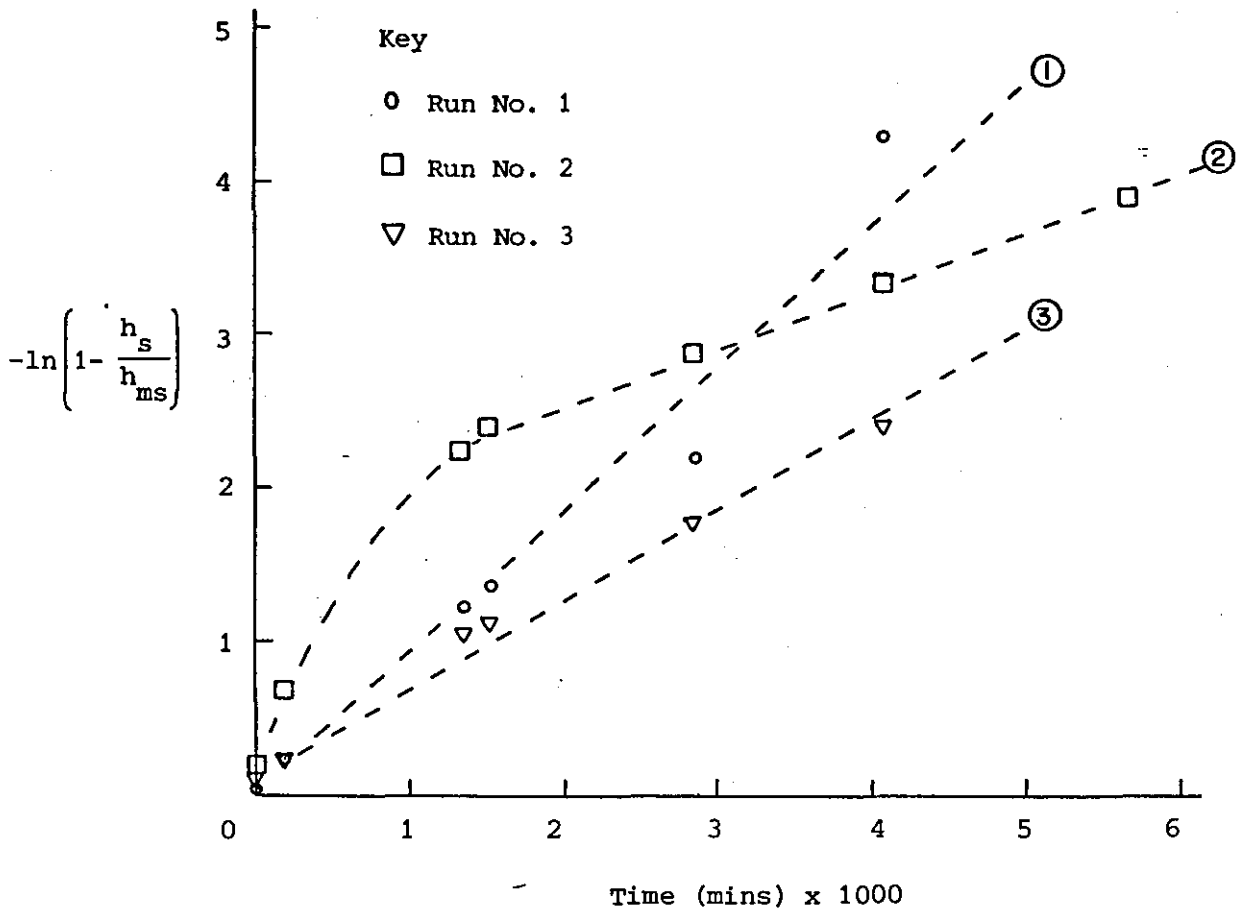

Fig. 71 Logarithmic suction response times of three tensiometers using the "in-situ" method of suction response

been expressed graphically and can be found in Fig. 71. Excluding the two initial measurement of tensiometer no. 2, then all the other measurement fit the expected linear relationship. Straight lines were fitted to each set of points using a least squares regression technique. The diameter of the manometer tube used in this experimental study was 0.35cm which has a sensitivity of approximately o.26 ats cm^{-3}. The conductance values of cups 1, 2, 3 were 3.75×10^{-3}, 1.41×10^{-3} and 2.16×10^{-3} (cm^3 min. ats^{-1}) respectively.

An estimate of the cup conductance prior to cementation in position in the brick can be obtained by applying Darcy's law to the plaster plug of the tensiometer cup. Assuming the plug length to be 1(cm); viscosity of water to be 0.01 (g $cm^{-1}sec^{-1}$) and the permeability of the plaster to be 1×10^{-11}(cm^2), then the flow rate, Q (cm^3 min) can be calculated. The volume flowing through the plug in one minute, when a pressure difference of one atmosphere is applied across the plaster, is a measure of the cup conductance. Using the figure above, the approximate flow rate through the plug is 0.05 ($cm^3 min^{-1}$). This figure indicates that the cup conductance has been reduced by a factor of ten upon cementation into the brick. It is also a justification of using the "in situ" method as a means of determining more realistic values of cup conductance for the experimental arrangement used in this study.

3.5 Time constant

The response time constant of a tensiometer is defined as $(K\ S_e)^{-1}$ and is a measure of the overall responsiveness of the instrument to a change of moisture tension at the porous cup surface. Assuming a minimum value of cup conductance (in situ) of 1×10^{-3} ($cm^3 min^{-1} ats^{-1}$) and a sensitivity, S_e, of 1.25 (ats cm^{-3}), then the time response of the instrument is 800 min (approximately

13.5 hours). The recommended response time constant of tensiometers designed for soil use is about 1 minute.

3.6 Air trap

The air trap of the instrument was created by inserting a glass T-piece in between the mercury manometer and the porous cup (as shown in Fig. 73). Additional P.V.C. tubing was connected to the third arm of the T-piece. The P.V.C. tubing was sealed off, using two thumbscrews which were positioned approximately 10cm apart. Two thumbscrews were used so that air could be vented from the instrument with minimal loss of suction, thus reducing the displacement of the tensiometer reading from its equilibrium value. This modification is particularly useful in view of the relatively slow time response constant.

3.7 Experimental method

The tensiometer survey was conducted from July 1977 to March 1979. The experimental site was in the cellar of a house suffering from Rising Damp. Suctions at three locations in the cellar were recorded. Two of the sites were single leaf internal brick walls whilst the third site was located at an outside wall below soil level. The cellar floor was approximately 1.5 metres below soil level. The walls at the internal sites (1, 2) had been replastered up to a height of 1 metre and the surface then painted with gloss paint. Site 3 had not been replastered; the surface was covered with emulsion paint. All three sites suffered from moisture damage. Surface plaster had become swollen, bubbled and cracked. Salt damage was also visible in areas where faults had occurred in the gloss paint. The location of each site within the house is shown in Fig. 72.

Each site consisted of six tensiometers, spaced about 30cm apart in a vertical direction. The individual heights of each

tensiometer above the cellar floor is given in Table II. Each tensiometer consisted of a porous cup (Fig. 69) connected to a U-tube mercury manometer. The bore of the glass tubing of the manometer was 1.6mm. Each manometer was attached to a wooden panel whose surface was covered with a graduated scale. In between the porous cup and the manometer was a glass T-piece whose third arm comprised the air trap. The air trap was a length of P.V.C. tubing sealed by two thumbscrews. The whole of the apparatus was filled with distilled water, care being taken to exclude all air bubbles. A schematic representation of a tensiometer is shown in Fig. 73.

At the start of the survey daily measurements of mercury heights were recorded, together with wet and dry bulb temperatures of the cellar air. After one month had elapsed it was realised from the response of the tensiometers that the frequency of the measurements could be reduced to one set per week.

Occasionally air was removed from each tensiometer when thought to be necessary. Air was removed in two ways. One method was to open both thumbscrews, consequently losing the suction developed in the instrument. The second method was to release the inner thumbscrew and transfer air into the P.V.C. tubing between the thumbscrews. The inner clip was retightened and the outer one released. The outer portion of the tube was refilled with distilled water and the outer thumbscrew retightened. This method only resulted in a slight loss of suction in the instrument. The latter method of air removal was adopted as normal practice, in view of the slow time response of the tensiometers.

The measurements of mercury height differences were converted into corresponding suction pressure heads of water. These tensions corresponding to suctions at the height of the porous cup were adjusted to the same datum plane, which was taken as the cellar floor. A sample calculation of this procedure can be found in

Appendix V. The suction curves for each of the tensiometers at sites 1, 2, 3 have been reproduced in Figs. 74, 75, 76 respectively. The dry bulb temperatures and corresponding relative humidity (percent) are expressed graphically in Fig. 77.

The opportunity was taken, one week after the start of the survey, to drill an additional set of holes at each site. In addition a set of holes at a new location (site 4) was drilled in an internal wall where the plaster had been removed fron both brick surfaces, at an earlier date. The vertical heights of this new set of holes can be found in Table II. For sites 1, 2, 3 each additional hole corresponded to the height of a tensiometer. The horizontal difference between the holes was about 15cm.

Table II. Tensiometer and moisture content sampling heights above cellar floor

	Height (cm)			
Tapping No. Site	1.	2.	3.	4.
1	10.0	14.5	29.5	10
2	39.5	45.0	60.0	40
3	70.0	75.5	90.0	70
4	99.5	106.5	121.0	100
5	130.0	130.0	151.5	130
6	160.0	167.0	188.0	160

The dust from each hole was collected in a sample jar[15] and taken back to the laboratory where each sample jar was weighed. The samples were oven dried for five days at 100°C, and allowed to cool overnight in a desiccator. The samples were weighed and returned to the oven for one additional day. The samples were again allowed to cool overnight in a desiccator and reweighed. This procedure was continued until the weight of the sample jar remained constant (constancy of 1 milligram). The sample jars

were washed and the dry weight of each jar determined in a similar manner to method described above.

The differences of the three sets of weighings was then used to calculate the moisture content (weight of water per dry weight of brick dust) at each of the points in the wall. The results of sites 1 and 2 together with the results of site 4 can be found in Fig. 78. The results of site 3 together with site 4 can be found in Fig. 79. The results of site 4 were reproduced in both figures for comparative purposes.

3.8 Experimental results

The results of the tensiometer survey have been reproduced graphically in Figs. 74, 75 and 76 respectively. The suctions have been calculated with respect to a common datum, that is the cellar floor. The suction in the wall at the height of the tensiometer cup can be obtained by adding the height of the tensiometer above the cellar floor to the suctions in Figs. 74, 75, 76. The heights of the tensiometers above the cellar floor can be found in Table II. If the wall is in static equilibrium with the water table, then each of the tensiometers should register the same suction when adjusted to the datum level. If there is some net overall flow up the wall then the suctions at the various heights should exhibit some systematic variation of suction.

The moisture contents of house bricks at sites 1 - 4 can be found in Figs. 78 and 79.

The dry bulb temperature of the cellar, measured using a Mason type hygrometer, together with the relative humidity can be found in Fig. 77.

3.9 Experimental errors

3.9.1 Tensiometer errors

The height of each mercury column was read to an accuracy of $\pm$0.05cm, that is a total variation of $\pm$0.1cm. The mercury height

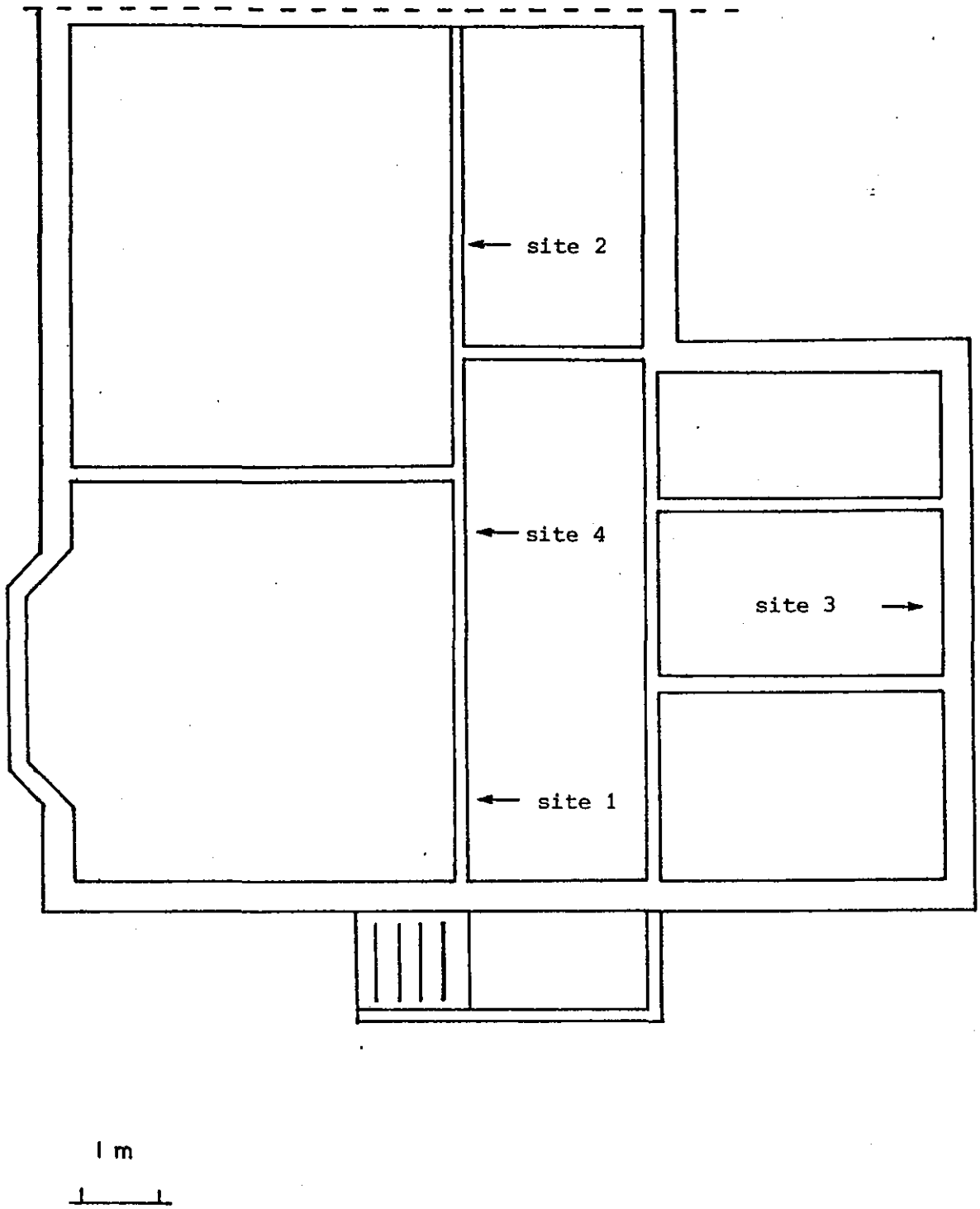

Fig. 72 Schematic representation of the experimental site used for the tensiometric survey

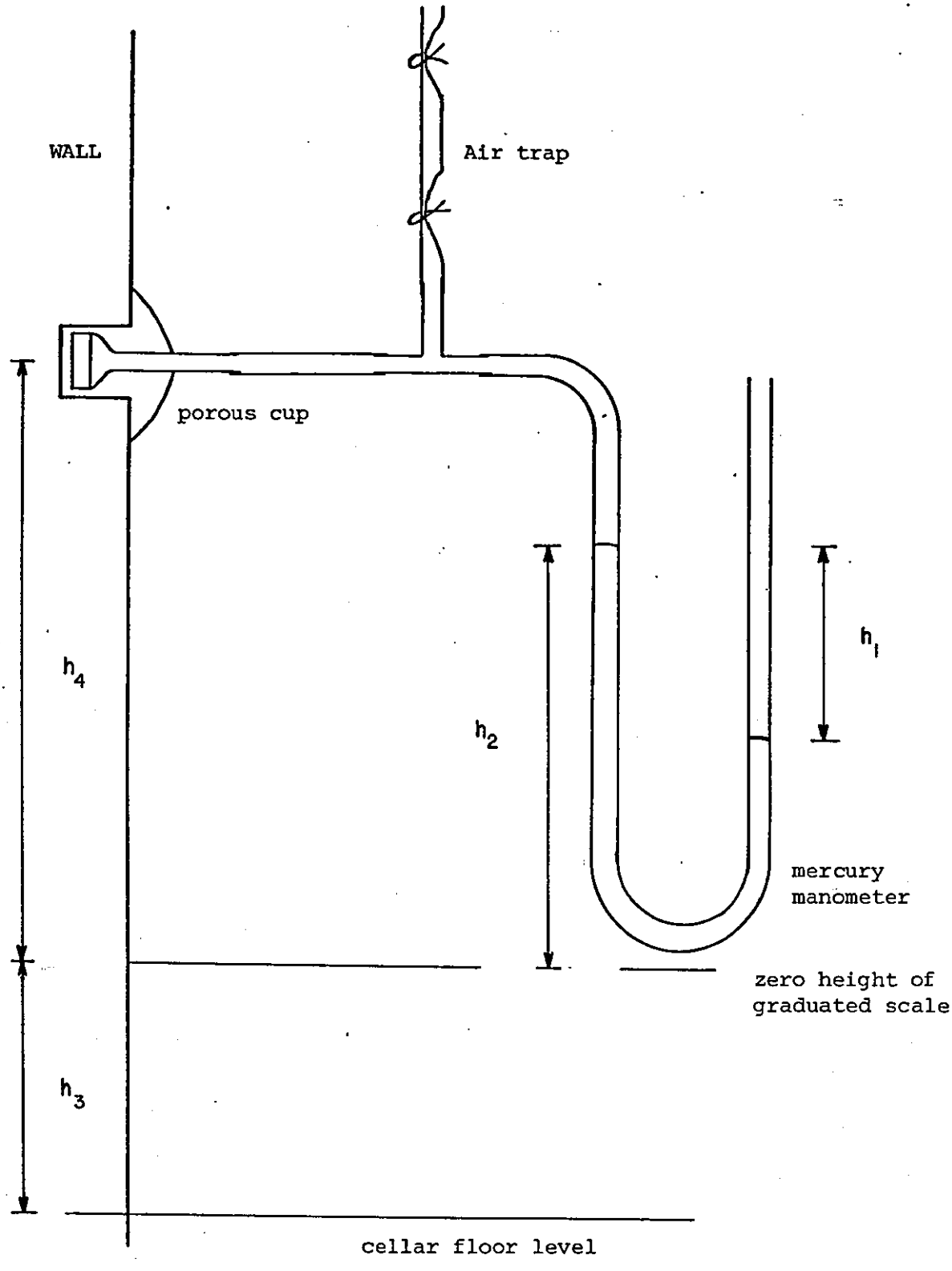

Fig. 73 Schematic representation of tensiometer construction

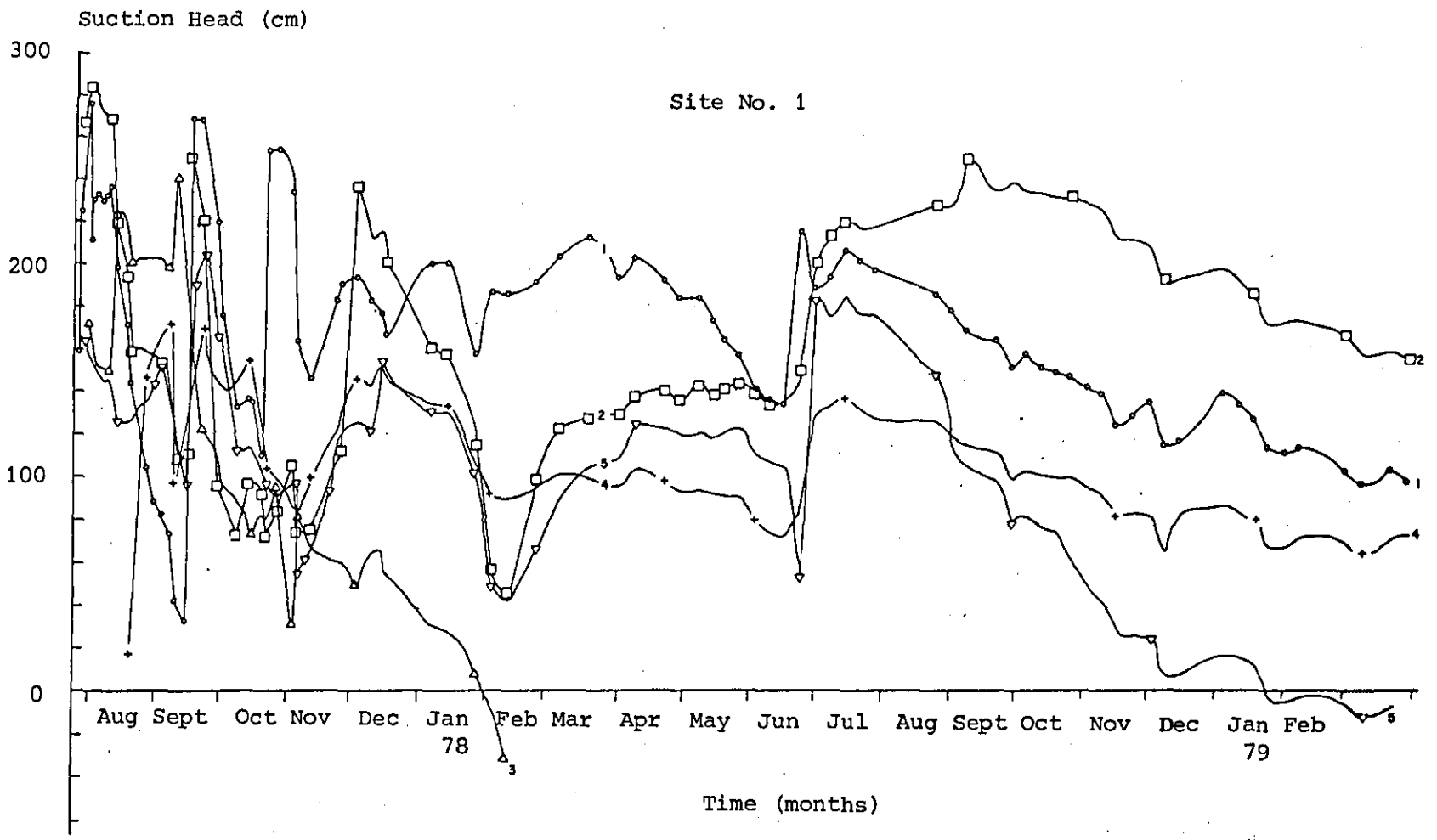

Fig. 74 Suction-time response at site No. 1

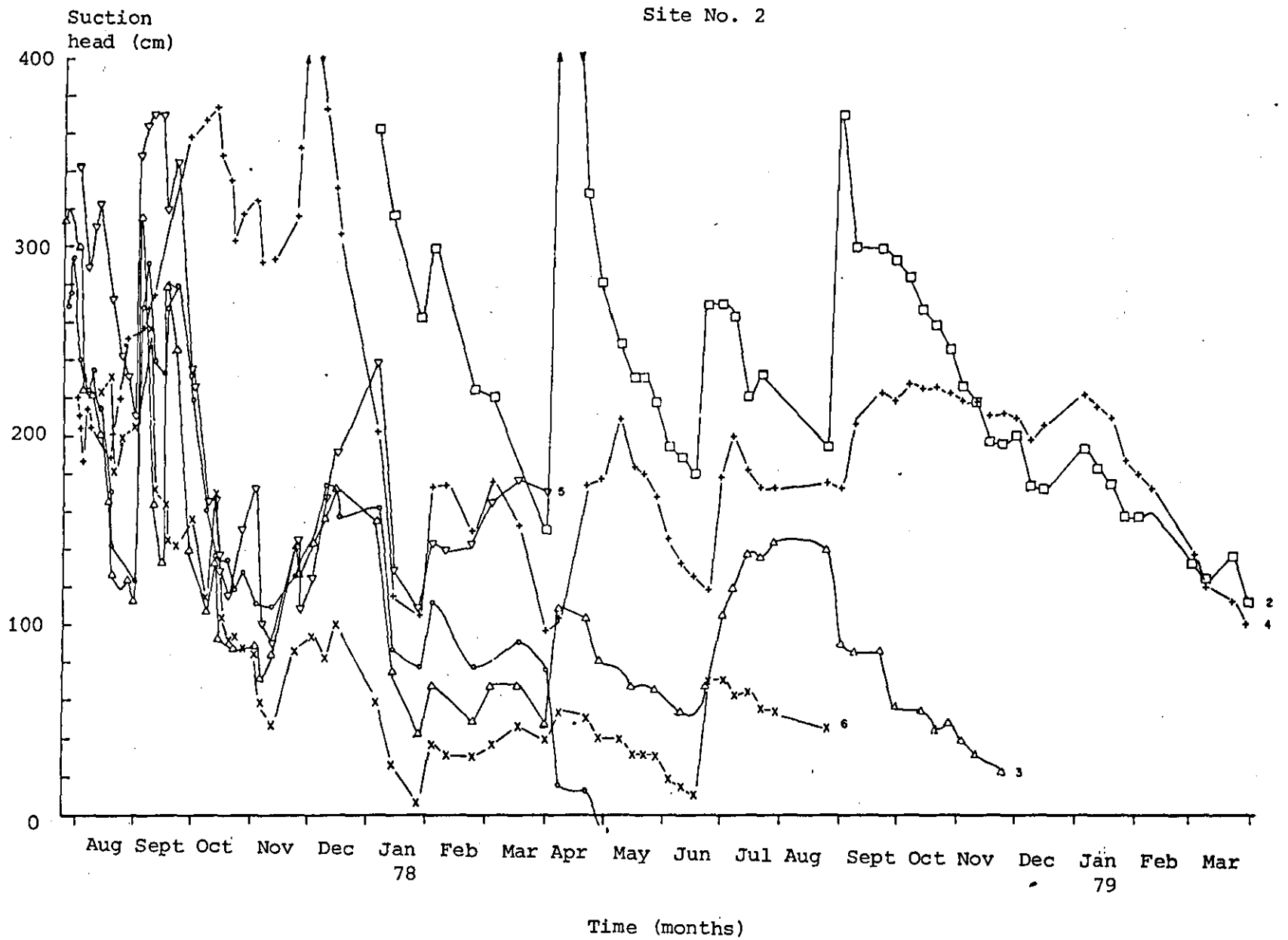

Fig. 75 Suction-time response at site No. 2

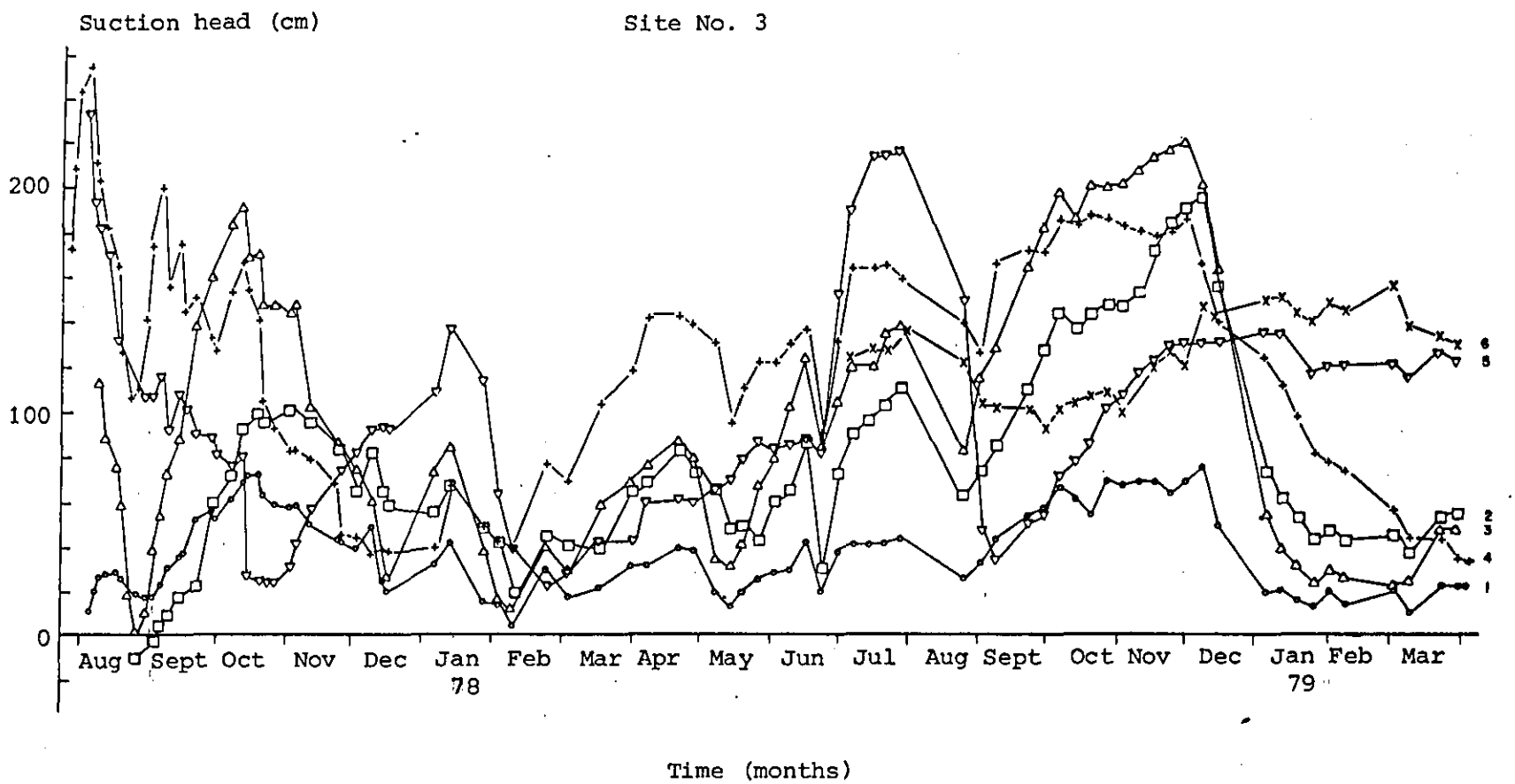

Fig. 76 Suction-time response at site No. 3

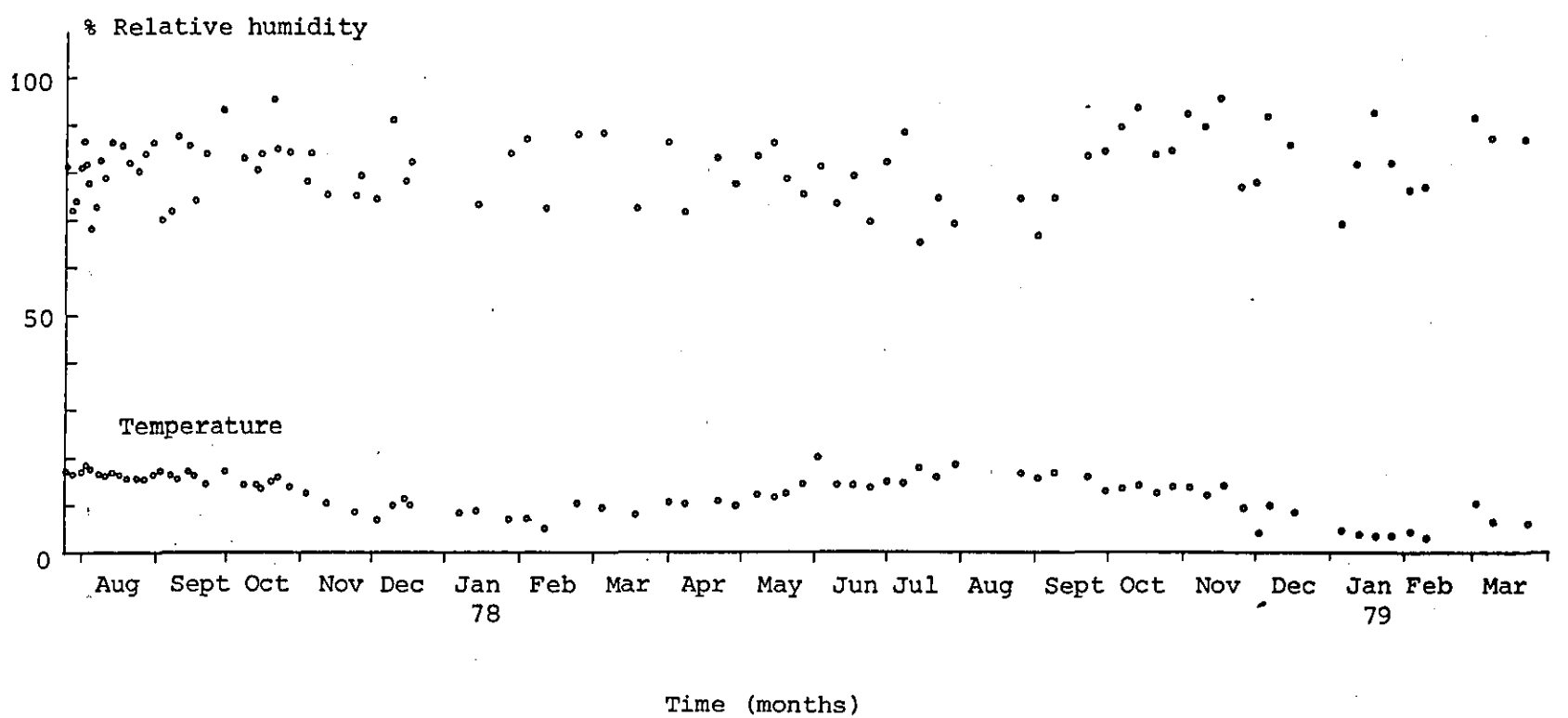

Fig. 77 Cellar temperature and humidity

differences measured at each tensiometer varied considerably. However for experimental purposes an average mercury height difference of 10cm was assumed. The height of the mercury water face was assumed to be 80cm above the floor. Hence the suction at the floor is 55cm of water head. The variation of mercury height of $\pm$0.05 cm produces an equivalent water head variation of $\pm$ 1.3cm. Hence an estimate of the average percentage error associated with measurement of suction to be 2.36%, assuming the densities of mercury and water to be 13.5 and 1 gram per cm^3 respectively.

3.9.2 Moisture content errors

Similarly the calculation of individual experimental errors for each set of weighings is rather tedious. An estimate of the average error involved in the calculation of moisture content was obtained by assuming average values for the quantities measured.

The average weight of moisture in the brick dust was assumed to be 1 gram. The dust was weighed to an accuracy of $\pm$0.002g. Thus the average expected error in the determination of the moisture contents is about 0.20%. However on one occasion the variation of moisture content was of the order of $\pm$0.007g for a net dust weight of 1.68g. This latter figure represents an error of about 0.42%.

The average weight of a dry sample jar was taken as 10g. The sample jars were weighed to an accuracy of $\pm$0.005g, which represents an error of $\pm$0.005%, which compared to the above figure is quite small and may be ignored.

Thus the average error may be taken as 0.20%.

It should be noted that no estimate of the moisture loss by dust during the drilling process can be made. Furthermore no estimate of moisture loss was made whilst the sample jar was being weighed when it contained moist dust.

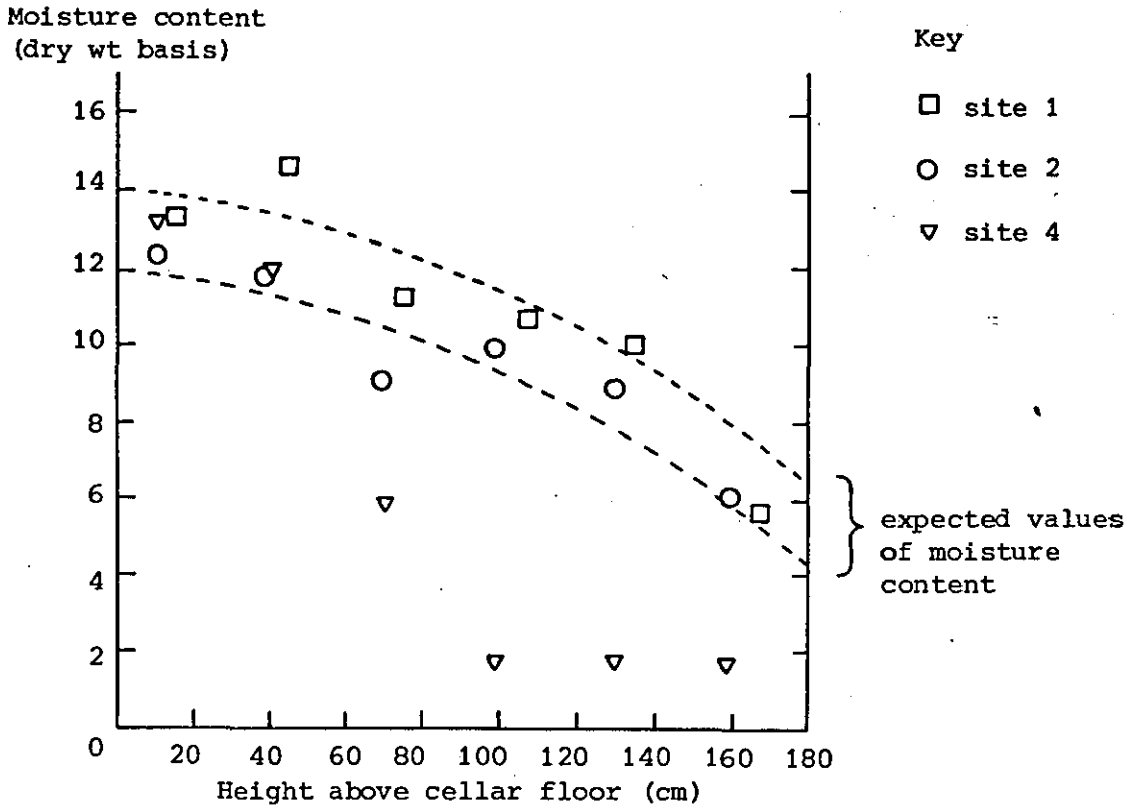

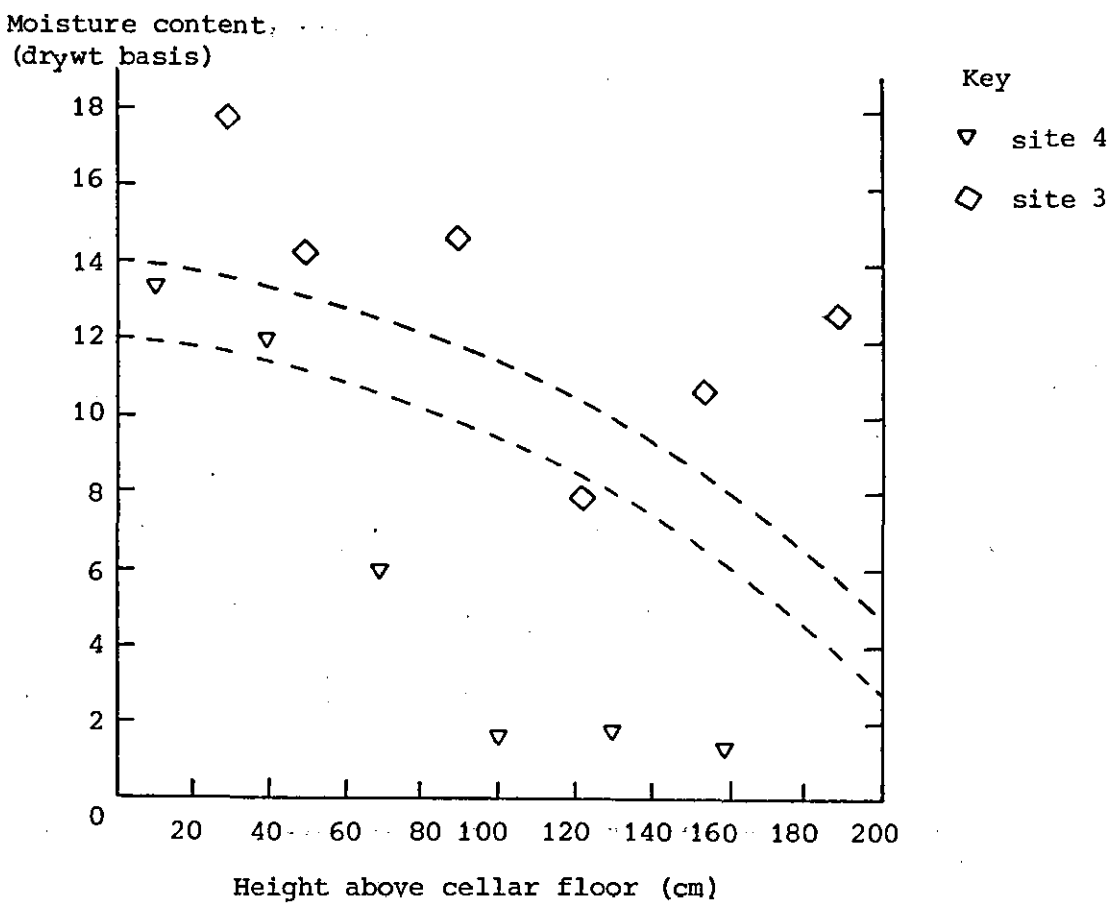

Fig. 78 (upper) Moisture content of damp walls with respect to
Fig. 79 (lower) their height above a datum level (cellar floor)

3.10 Discussion

3.10.1 Tensiometer curves and tensiometer design

No seasonal variation of suction can be observed at sites 1 and 2. However, at site 3, a seasonal variation of suction can be observed. At site 3, during the winter months (December through February), the suctions were low. The suctions rose in spring and continued rising through the summer and into autumn, where the suctions fell rapidly. The rapid fall is particularly apparent during December 1978 and January 1979. During this period the four lowest tensiometers at site 3 fell systematically, whereas the suctions at the higher levels in the wall (heights 5 and 6) remained almost constant. The rapid reduction of suction of tensiometers at heights 1 - 4 indicate that the underlying water table had risen sharply. Note that none of the tensiometers at the other sites responded in a similar fashion. The seasonal variation of the tensiometers of site 3 is similar to the response observed in the soil survey conducted by Croney et al[14].

The large fluctuations of suction values at the start of the survey (August and September 1977) were a consequence of the removal of air from the tensiometers and the need to re-cement several of the tensiometer cups that had become loose. Air was also removed from all the tensiometers at the start of June 1978. The suctions of the instruments were completely released at this time.

The behaviour of the tensiometers at sites 1 and 2 is more difficult to interpret since no underlying trends similar to those of site 3 can be observed. Possible explanations of the behaviour at these sites are loss of liquid continuity in the wall, or loss of liquid continuity within the tensiometer cup.

Liquid continuity is important because liquid phase moisture migration is a major factor affecting the time response of the tensiometer system. Loss of liquid continuity in the wall will result in the isolation of the tensiometer cup from its neighbours or seriously impede the moisture flow in response to pressure potentials between them. Suctions measured by isolated tensiometers will only relate to the region surrounding each tensiometer cup.

Unequal moisture movement will produce misleading suction values if corrected to a common datum level. Moisture movement (and hence suction change) can only occur by vapour diffusion within isolated regions and hence the rate of change of suction with time is slow, whereas for regions in the zone of liquid continuity, suction changes are more rapid. This situation will also contribute to the production of misleading or inconsistent tensiometer behaviour.

An example of uneven localised moisture movement is evaporation from cracks or faults in the gloss paint which increases the liquid suction in these areas. Evaporation from around each tensiometer cup may also lead to inconsistent tensiometer results. In an attempt to reduce the latter evaporation loss, the plaster of Paris which was used to fix the tensiometer into the wall was painted with gloss paint.

Loss of liquid continuity is not thought to be the major cause of the inconsistent results at sites 1 and 2 since the tensiometers at the lower heights at these sites also behaved irregularly. Inspection of their moisture content curves showed that their values were quite high, and were greater than the lowest value that was observed at site 3, which showed no signs of irregular behaviour. It is unlikely therefore that loss of liquid

continuity was the cause of the irregular tensiometer behaviour at sites 1 and 2.

A more likely explanation of the behaviour of the tensiometers at sites 1 and 2 can be obtained by considering the design of the tensiometer cup and the method of fixing it into the wall. The assembly of the tensiometer at the wall resulted in the sintered glass of the microfilter being sandwiched between two layers of more finely pored plaster of Paris. Air bubbles forming in the sintered glass disc of the tensiometer cup would become trapped. Eventually sufficient air may be trapped to prevent or seriously impede liquid phase moisture movement between the plaster of Paris layers.

For sites 1 and 2 moisture may only enter through the ground and it is to be expected that the moisture content would vary much more severely than at site 3. Furthermore during the summer months large suctions could be developed by portions of the wall which would assist the formation of air bubbles that could subsequently become trapped in the tensiometer.

At first glance one would expect this situation to occur at site 3. However, the wall at this location is much damper, since moisture can enter the wall through its entire length rather than just at its base, hence the variation of moisture conditions is much less severe and hence the probability of air becoming trapped much smaller.

Another explanation for the failure of liquid phase moisture movement is that the porous cup may have become loose within the wall. The small gap between the outer surface of the disc and the plaster holding it into the wall being sufficient to prevent moisture movement.

In view of the failure at sites 1 and 2, the design of the tensiometer cup and the method of attaching it into the wall is

unsatisfactory. The problem associated with the design of the tensiometer cup can readily be overcome. However the problem of fixing the tensiometer into the wall to maintain good liquid contact over a long period of time is a more difficult problem to solve. A solution to this problem would be the use of a flexible porous material to act as the tensiometer cup.

Another design fault associated with the porous cups of the tensiometers is their slow time response to a change in suction because of their low values of cup conductance. The low values of these properties make the instruments developed in this experimental study unsuitable for measuring rapidly fluctuating suctions. However, it was decided that the instruments should be used since the rate of change of suction within a damp wall is unknown and hence may be sufficiently slow, that the sluggish response of the instruments is not a major disadvantage.

3.10.2 Cup conductance via the "in situ" method

The determination of cup conductance of three tensiometer cups in the laboratory using the "in situ" method was found to be satisfactory. The validity of this method depends upon the assumption of constant suction within the porous material absorbing the moisture (i.e. dry house bricks). An underlying condition of this assumption is that the moisture content of the brick should not significantly increase during the experiment. The weight of moisture absorbed by a brick, to develop a suction of 500cm water head by the tensiometer, was about 1.75g and assuming the weight of a dry house brick to be 3kg, it is self evident the increase in moisture content is minimal.

Serious problems will be encountered in this method if the flow of moisture from the tensiometer becomes limited by the absorbing porous material. This situation will result in a varying suction at the external surface of the porous wall of the tensio-

meter cup. The increase in suction with respect to time will be controlled by the absorbing porous material and not the tensiometer cup.

Examination of the results of Fig. 71 shows that the measurements of suction and time recorded during the absorption experiment are in agreement with the theoretical expression derived in Appendix IV, and hence the flow of moisture was controlled by the tensiometer cup.

It can be shown by comparison of the average pore sizes of the plaster of Paris and dry house brick, that it was the plaster of Paris in the tensiometer cup that was controlling the migration of moisture through the tensiometer cup. An estimate of the pore size of brick can be obtained by combining the surface tension equation ($2\gamma_{LG}/r = \rho_w g h_w$) together with the fact that the maximum suction developed by the bricks was about 500cm of water head.

Assuming the surface tension of water to be 72.75 (g cm^{-2}) at 20^oC; $g = 981$ (cm sec^{-2}); $\rho_w = 1$ (g cm^{-3}); $h_w = 500$ (cm), then calculation shows the brick radius to be about 3 μm. Estimates of the pore radius of plaster of Paris from permeability data indicate that the average pore radius of plaster to be about 3×10^{-2} μm, i.e. one hundredth that of dry brick. Poiseuille's eqn. (Chapter Three - eqn.(7)) states that the average velocity of fluid with the pores to be proportional to the square of the radius of the pore. Hence, assuming the number of pores in the plaster of Paris to be the same as the number within the brick, then the conductivity of the brick will be 10^4 greater than that of plaster of Paris. It is reasonable to assume that it was the plaster of Paris in the tensiometer cup that was controlling the migration of moisture through the tensiometer cup and that the values of cup conductance obtained were applicable to the tensiometer cup and not the absorbing material.

3.10.3 Moisture content profiles

Comparison of the profiles of moisture content at sites 1, 2 and 4 in Fig. 78 shows the effect of evaporation upon the degree of moisture observed in the internal walls. Sites 1, 2 were single leaf brick walls that had been partially replastered and then painted with gloss paint. The surface layer of paint effectively reduces the evaporation rate from the wall to zero. Site 4 was also a single leaf brick wall, but at this location, paint and plaster had been removed from the wall exposing the brick surfaces. No estimate of the time that had elapsed between removal of the plaster and the moisture content survey was obtained. However, the effect of evaporation upon the moisture profile of a damp wall is plainly visible as can be seen in Fig. 78.

At site 4 the moisture content is effectively constant above a height of 1 metre from the cellar floor. Above this level the wall may be assumed to be dry. The residual moisture content of the dry wall was about 1.5% on a dry weight basis (gram of moisture per gram of dry brick). At the base of the wall at site 4 the moisture content was about 13% which was approximately the same value found at corresponding heights at sites 1 and 2.

The rate of decrease of moisture content at site 4 is greater than at sites 1 and 2, demonstrating the effect of evaporation upon the level of moisture within the wall. The moisture content at site 4 at a height of 70cm corresponds to a moisture level at a height of 170cm for sites 1 and 2, that is evaporation had reduced the height of the given moisture content by 1 metre.

The expected values of moisture content at sites 1 and 2 have been expressed as a band of moisture values in Fig. 78 whilst the values at site 4 have been expressed as a continuous curve. The band and the curve have been drawn for comparative purposes, the upper and lower bounds of the curves are arbitrary and have no

scientific merit. The band for site 1 and 2 and the curve from site 4 have been reproduced in Fig. 79 for comparison with the corresponding height values at site 3.

The moisture contents at site 3 exhibited a much greater scatter, particularly at the lower heights. Explanations of the scatter are attributed to:- (1) faulty sampling of the wall which includes loss of moisture by evaporation during drilling: contaminations of the brick dust during or after drilling, the most likely source being mortar dust especially if a hole was drilled at the edge of a brick. (2) very wet bricks and the assumption that their individual suction-moisture content exhibited a greater variation at higher moisture levels. (3) different types of brick being used during the construction of the wall. (4) the possibility of transient moisture conditions existing in the wall at the time of sampling.

Moisture contents of the three lowest heights were all in excess of 14% at site 3 which places them beyond the upper limit of the moisture band obtained from sites 1 and 2. This observation shows the walls to be very damp. Also at site 4 and at a height 30cm above the cellar floor was found to be about 18% on a dry basis.

The moisture content profile became inverted higher up the wall, that is the moisture content increased with increasing height above the cellar floor. The inversion is attributed to rainfall percolating downwards through the soil and wall. A similar observation has been noted during soil tensiometric studies[10].

The moisture content survey was not repeated because the effects of any possible disturbances to the adjacent tensiometers could not be assessed and that suctions, developed by moist

porous materials, should be used as the fundamental measurements to which other hydraulic functions should be correlated. Consider the example of several different moist porous materials in equilibrium with each other. The suction within each material is the same but their individual moisture contents might very considerably even though they may nominally be the same type of porous material.

4. Experimental study number three. An experimental study to investigate the feasibility of a method to simultaneously measure the hydraulic properties of unsaturated permeability, moisture content and evaporation rate with respect to the capillary suction developed by a moist porous material

4.1 Introduction

The hydraulic properties of unsaturated permeability, moisture content, and evaporation rate, need to be correlated with respect to wall suction before a mathematical analysis of moisture movement in buildings suffering from Rising Damp can be attempted.

The property of unsaturated permeability to moisture relates the amount of water that can be transmitted by the unsaturated porous material in response to an applied pressure potential. The property of moisture content relates the amount of moisture that can be retained (or lost, by the unsaturated porous material in response to a change in suction potential. The relationship between evaporation rate and suction simply relates the amount of moisture that can be lost by the porous material at different suctions within the porous material. Both the evaporation rate and the unsaturated permeability affect the extent and degree of dampness of the wall.

The evaporation rate of a porous material is either energy - limited or flow-limited. For the former situation, the evaporating surface is saturated with moisture and can be regarded as a "free" water surface. Under these conditions the evaporation rate is determined by the supply of energy to the surface.

As expected for flow-limited evaporation, its rate is controlled by the supply of moisture to the surface. The evaporation surface is no longer saturated and as a consequence, more harsh drying conditions are developed, (i.e. partial drying of surface; development of large suctions). Flow limited evaporation rates are always less than their corresponding energy limited evaporation rates.

For engineering purposes the hydraulic functions of most interest are unsaturated permeability, moisture content and evaporation rate, all correlated with respect to capillary suction. The pore structure of each porous material is unique and consequently the hydraulic functions of the material are also unique. This situation would make the prediction of moisture movement very difficult, if not impossible. However, even though the hydraulic functions of individual materials are unique, the hydraulic relations of several similar materials can be averaged to provide a "typical" hydraulic relationship for that material.

Additional series of experiments must be performed when the hydraulic functions exhibit hysteresis (c.f. Section 4, Chapter Two). Hence several series of experiments must be performed to establish the relationships of the hydraulic properties mentioned above.

For unconsolidated materials such as soils, the series of experiments, although tedious, is not too difficult to perform. The porous sample, by definition, is loose and consequently can easily be fitted into a sample holder of almost any shape. Furthermore the sample can be removed from its holder and then replaced; the new configuration of particles can be regarded as a different porous material with its own set of unique hydraulic functions. Several measurements can be obtained in this manner, using only a small amount of unconsolidated porous material. In addition since

the bed of material is loose, good liquid contact can be maintained between the bed and tensiometer cups, and between the bed and the porous membrane through which water is introduced or removed from the bed of particles.

With consolidated materials the porous sample to be examined is by definition rigid. The rigid structure can be destroyed by reducing the sample to a powder, but the powder would not have the same hydraulic properties as the original material had. Since the sample must be used in its natural rigid state, the sample holder must be tailored to fit the sample shape. Furthermore there will also be problems of obtaining and maintaining good liquid contact between the rigid sample and the tensiometer cups, and between the rigid sample and the porous membrane through which water is introduced or removed from the bulk of the sample.

In view of the problems encountered with consolidated porous materials, (i.e. most building materials) and the large number of repetitive experiments required to determine "typical" hydraulic relationships, the aim of this experimental study is to investigate the feasibility of simultaneously measuring the hydraulic properties of unsaturated permeability, moisture content and evaporation rate, all with respect to suction. If successful the method would reduce the number of consolidated porous samples to be prepared and would reduce the amount of experimental time and work involved in determining "typical" hydraulic relationships.

The consolidated material chosen for the study was plaster of Paris. The choice of material avoids and overcomes the problem of fitting the sample holder to the sample or vice versa. Plaster of Paris as a consolidated material also has the advantages of rapid setting; of expansion on setting and negligible shrinkage on drying out, which are not found with other cementing materials. Another advantage of the use of plaster of Paris is that a degree of experi-

mental technique of casting and preparing plaster samples had been obtained previously during the leaching study.

4.2 Experimental procedure

4.2.1 Preparation of samples

Three perspex sample holders were placed upon each other to form a tower. Each sample holder was separated from its neighbours by a layer of perspex about 6mm thick. An additional spacer was included at the base of the tower. The perspex spacers had been cut in half to facilitate their removal from the tower with minimum disturbance to the sample holders. The internal diameter of the sample holders was 3cm. Their length was 4cm. Three 5mm holes were drilled midway along the length of the sample holder, i.e. their centres were 2cm from both end faces of the sample holder. The holes were spaced radially at an angle of 120° from each other. The holes were countersunk to a depth of 2cm and then a 3cm length of glass tubing was cemented into each hole, as shown in Fig. 80. The holes and glass tubing were used as pressure tapping points.

Each of the pressure tapping points of the two lower sample holders in the tower were sealed prior to casting of plaster of Paris to prevent plaster entering into the holes. Plaster of Paris slurry was poured into the hollow centre of the tower and agitated slightly to remove any entrapped air. The slurry was a mixture of two parts plaster of Paris to one part distilled water, by weight.

When the plaster of Paris in the tower had become firm (about ten minutes after casting), the spacing layers of perspex separating the sample holders were removed. The sample holders were separated and the uppermost one discarded. The plaster cores of the two remaining sample holders were allowed to dry, in the open air of the laboratory for about one week. After a week had

elapsed, any plaster projecting beyond the end faces of the sample holder was removed to produce continuous flat surfaces.

The sample holder and dry core was weighed. The core was vacuum saturated with distilled water, the pressure in the vacuum chamber being reduced to 6.5 kN m^{-2}. The core remained in the vacuum chamber for about fifteen minutes. The sample holder and core was removed from the vacuum chamber and wiped to remove excess water, particularly from the bolt holes and pressure tapping tubes.

The sample holder and "saturated" core was reweighed. The difference between the wet and dry cores was used to determine the porosity of the core. The sample holder was then connected to the remainder of the apparatus, as described in the following section.

4.2.2 Experimental apparatus and method

The apparatus consisted of a mercury-water U-tube manometer, a carbon tetrachloride-water U-tube manometer, three glass T-pieces, two thumbscrews, the sample holder plus integral plaster core and base plate, two 1 metre lengths of stainless steel capillary tubing, and several short lengths of P.V.C. tubing which were used to connect the pieces of apparatus together.

A schematic representation of the assembled apparatus can be found in Fig. 81.

One end of the stainless steel capillary tubing, marked D in Fig. 81 was sealed (using "Araldite") into the end plate C such that the capillary tube was level with the upper surface of the end plate. The other end of the capillary tubing was sealed into a short length of glass tubing. The glass tubing was connected to a glass T-piece (L2) by using a short length of P.V.C. tubing. Similarly the ends of the capillary tubing marked by K in Fig. 81, were sealed into short lengths of glass tubing. One end of the capillary tubing was connected to the glass T-piece, L3, whilst the

Side view

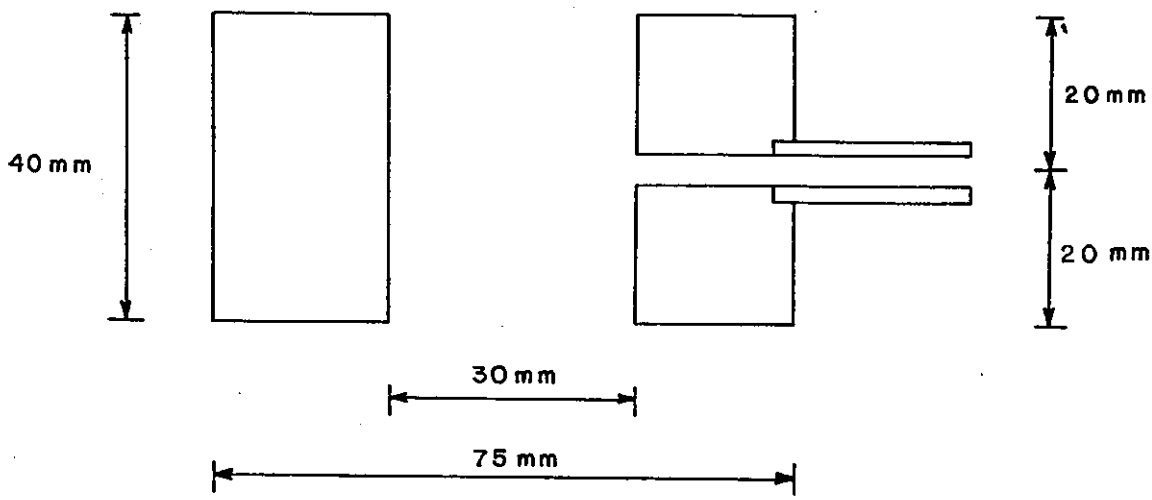

Top view

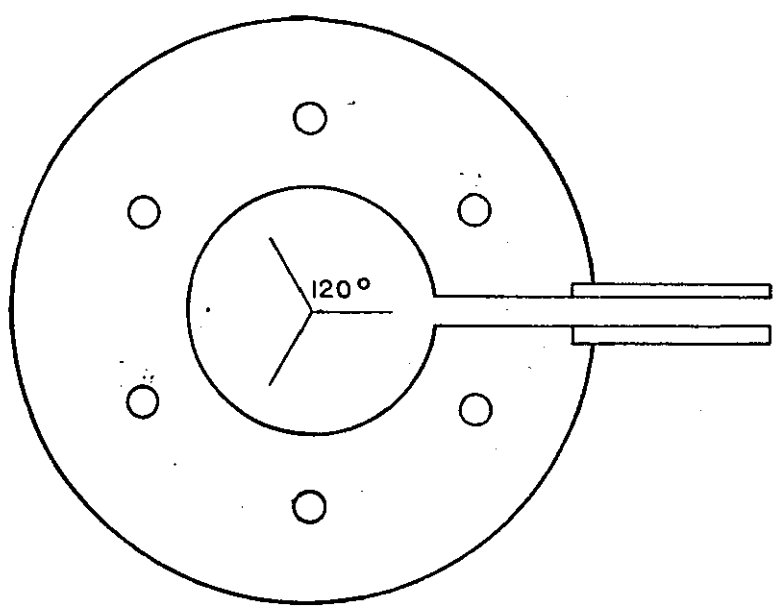

Fig. 80 Top and side views of the sample holder used in the evaporation experiments

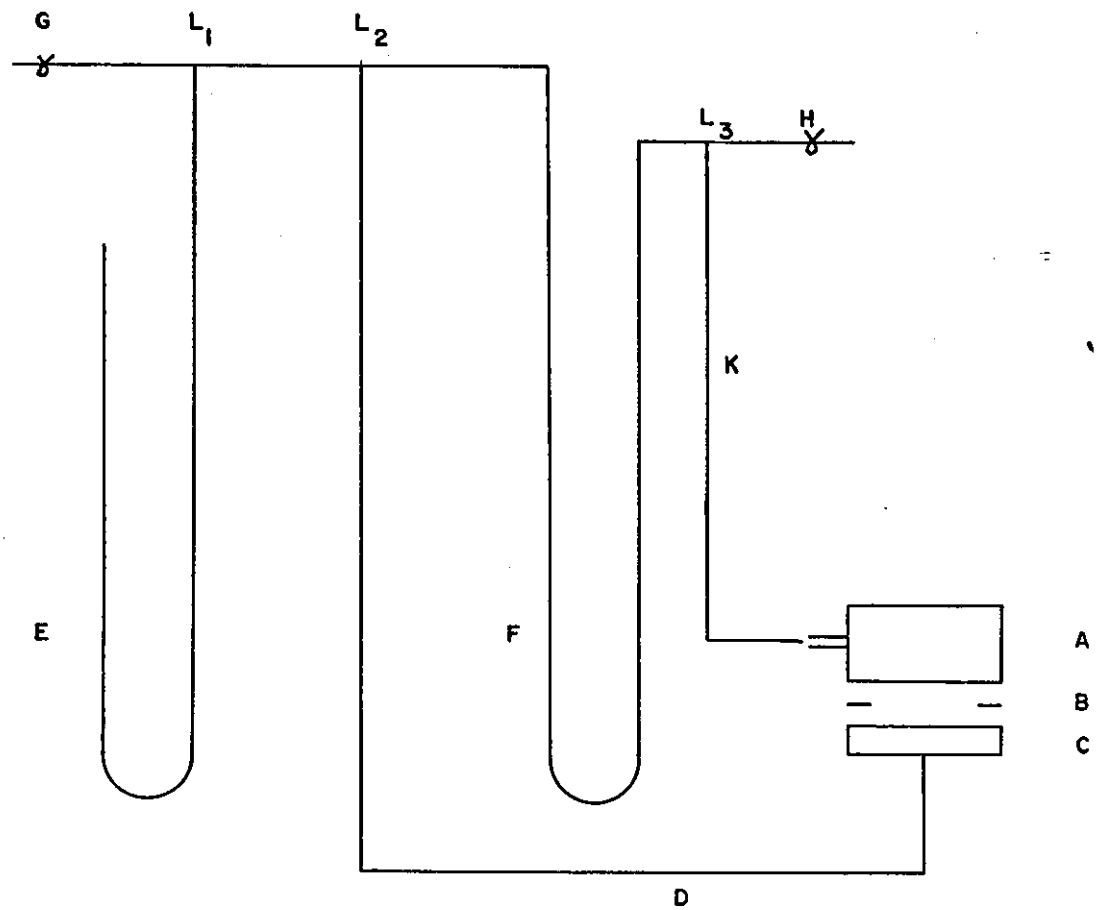

A perspex sample holder and saturated plaster core

B gasket

C end plate

D microbore stainless steel tubing (int. dia. 0.0635 cm)

E mercury/water manometer (int. tub dia. 0.35±0.01 cm)

F carbon tetrachloride/water manometer (int. tube dia. 0.35 ±0.01 cm)

G,H thumbscrews

K microbore stainless steel tubing (int. dia. 0.0635 cm)

L glass T piece

Fig. 81 Schematic representation of the assembled apparatus used in the evaporation experiments

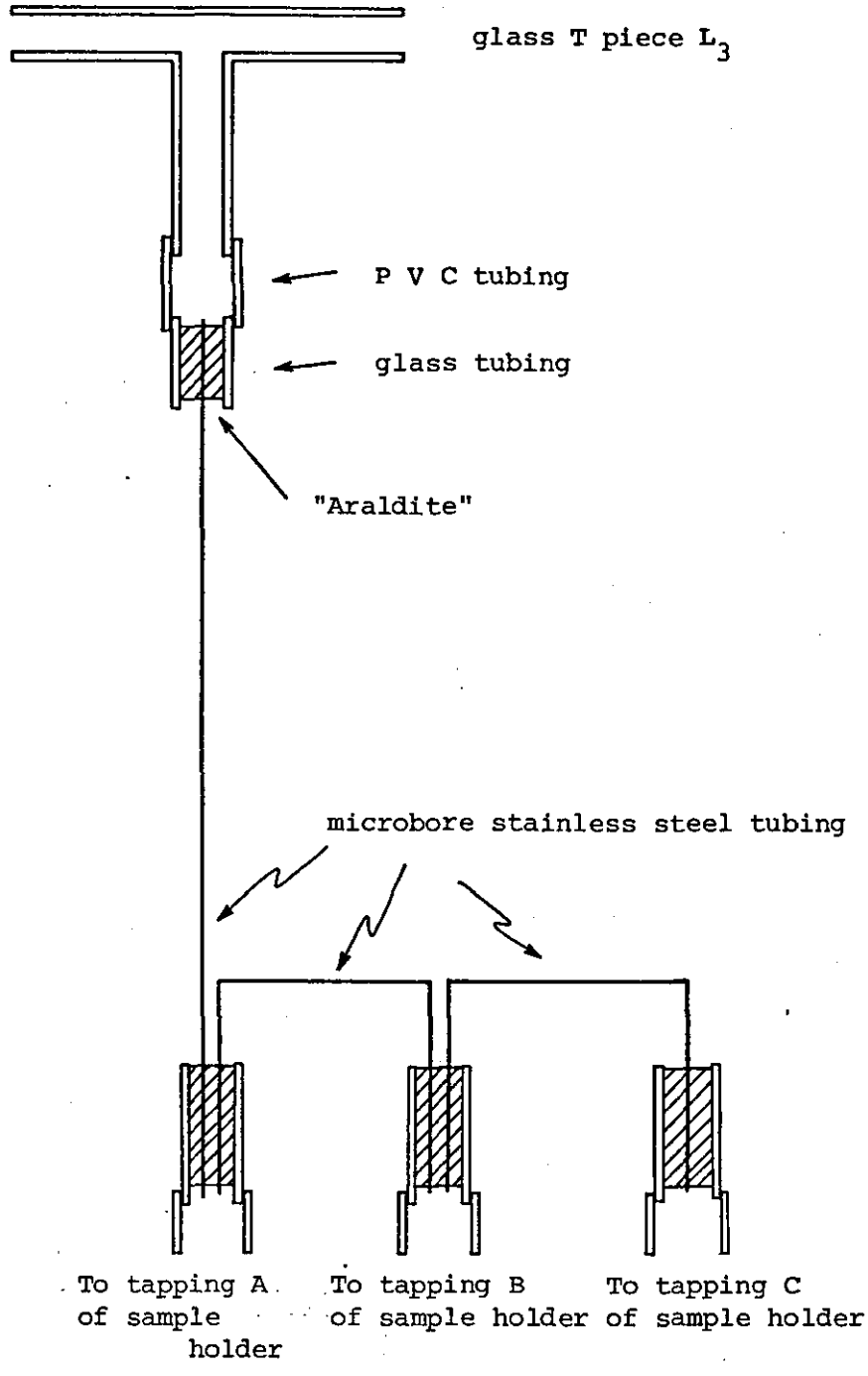

Fig. 82 Schematic representation of pressure tapping connecting tubes

other end was attached to the three pressure tapping points of the sample holder. The detailed arrangement of the capillary tubing can be found in Fig. 82.

The mercury-water manometer carbon tetrachloride-water manometer and capillary tubing, D, were connected together and filled with deaerated distilled water. Thumbscrew G was opened and deaerated distilled water was pumped through this opening until moisture appeared on the upper surface of the end plate C. A further 5 cm^3 of water was pumped through the capillary tubing and was collected on the end plate C. The water was prevented from spreading by the rubber gasket B. The volume of water collected on the end plate ensured that there was no air remaining in the stainless steel capillary tubing D and that no air was trapped between the end plate C and sample holder A when they were bolted together.

After the sample holder and end plate had been bolted together, more distilled water was pumped into the apparatus at the opening G until water exuded from the three pressure tapping tubes of the sample holder. The stainless steel capillary tubing K was then connected to each of the pressure tapping points; once again care was taken to remove all air from the tubing. Tapping point C (Fig. 82) was connected first, point B second and A last. This order of connection facilitated the removal of air from the capillary tubing connecting pressure tappings A to B and B to C (Fig. 82).

Distilled deaerated water was pumped into the apparatus until a continuous flow of water exuded from the unattached end of the capillary tubing K. When enough water had exuded from the capillary tubing to ensure that no air remained in the tubing, it was attached to the glass T-piece L3; care was taken to prevent any air remaining inside the apparatus. The pump was stopped and

thumbscrew G re-tightened.

For runs 4 and 5 an additional refinement was added. Thumbscrew H was opened and distilled deaerated water was pumped into the apparatus from this point. Pumping continued until the pressure difference registered by the carbon tetrachloride-water manometer was about the same as the equilibrium static pressure difference observed between the pressure tapping points and the base of the sample holder. The height difference btween the two levels was 2cm.

After approximate equilibrium was registered by the carbon tetrachloride-water manometer, the pumping was stopped and thumscrew H closed. All excess moisture was removed from the external surfaces of the apparatus and then the apparatus was placed upon a balance which was positioned in a "quieting" chamber. The dimensions of the chamber were 1.5 metres width, 0.55 metres depth and 1.8 metres in height. All the external surfaces of the quieting chamber were insulated using 5cm thick expanded polystyrene sheeting, except for a small window, of height 1.2 metres by 0.3 metres width, through which experimental observations were made.

Measurements of weight lost by the apparatus, mercury height difference, carbon tetrachloride height difference, wet and dry bulb temperature of the chamber (using a Mason Type hygrometer) and time were recorded. Additional measurements of dry bulb temperature and relative humidity were recorded using thermohydrograph (manufactured by C.F. Casella and Co. Ltd. - London. Reference No. T9150-58. Catalogue No. 931). The thermohydrograph was also positioned in the quieting chamber.

Each experimental run was terminated when liquid continuity was lost, usually because of air bubbles appearing in the tubing of the apparatus. After the experiment had been terminated, the apparatus was dismantled. The plaster core was removed from the

sample holder and then the sample holder was cleaned and weighed.

4.3 Experimental computations and results

4.3.1 Calculation of porosity

The weights of the sample holders, the weights of the sample holders and dry plaster cores and the weights of the sample holders and saturated plaster cores, of each run, can be found in Table III. If the density of water is assumed to be 1 (g cm^{-3}) then the weight of water absorbed by the core on vacuum saturation is also numerically equal to the volume absorbed by the core. This volume of water was assumed to be equal to the volume of voids within the core. The volume of the plaster core was calculated directly since its physical dimensions were known. The porosity of the samples was taken as the volume of water absorbed by the core, on vacuum saturation, divided by the net volume of the core. Porosities of each of the samples can be found in Table III.

4.3.2 Calculation of evaporation rate

The cumulative weight lost by evaporation from the cores is shown graphically in Fig. 83 for runs 1, 2, 3 and in Fig. 84 for runs 4, 5. Straight lines were drawn through the points using a least squares linear regression technique and the slope of each line determined. The evaporation flux (evaporation rate per unit area) of each sample was obtained by dividing the (cumulative) weight of water lost per unit time, (i.e. the slopes of Figs. 83 amd 84) by the area of the core, which was 7.069 (cm^2). The evaporation fluxes of each run can be found in Table III.

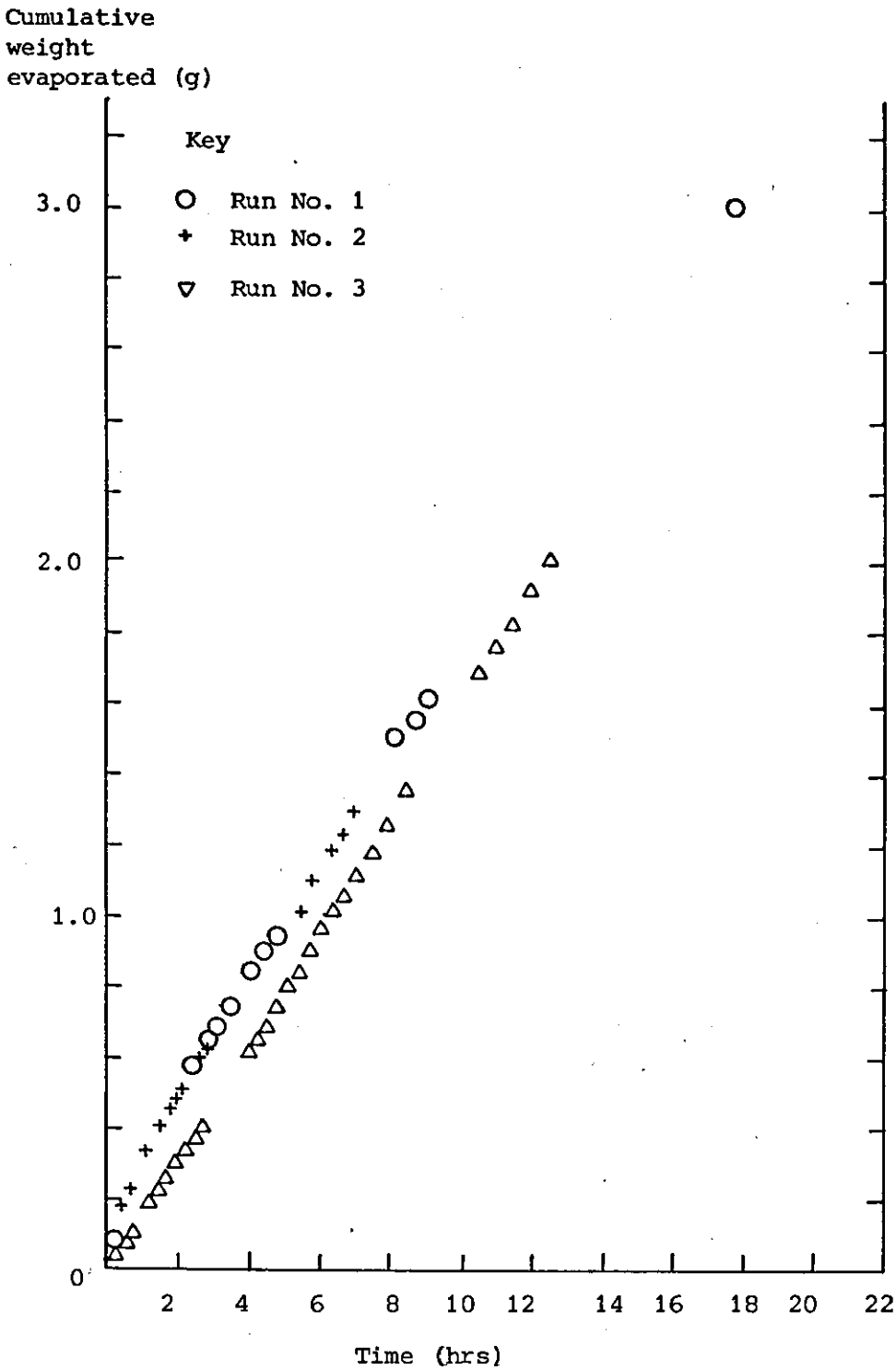

Fig. 83 Cumulative weight evporated versus time of Run No. 1,2,3

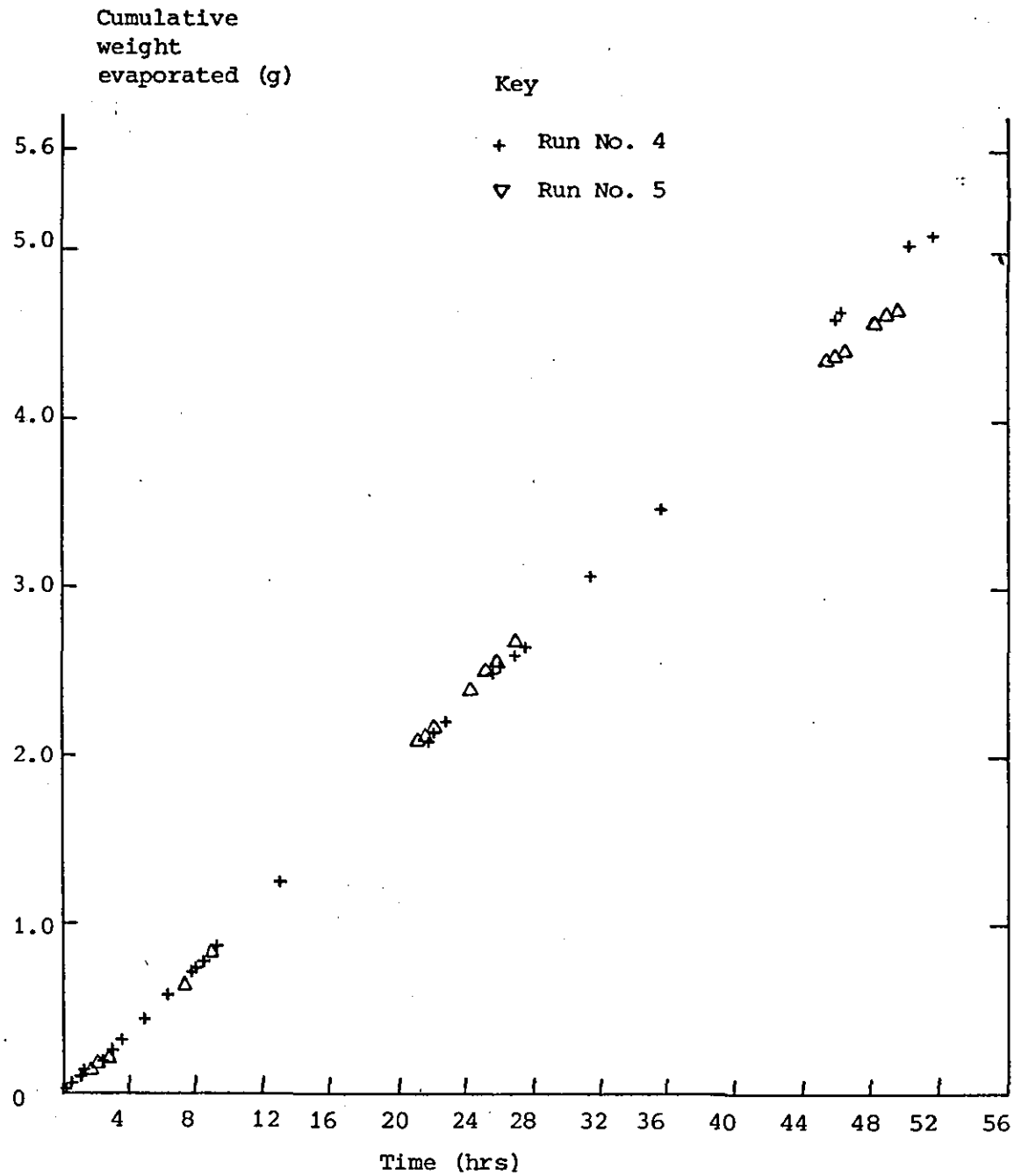

Fig. 84 Cumulative weight evaporated versus time of Run No. 4,5

Table III. Summary of the weighing measurements, evaporation rates and porosities of the plaster of Paris cores used in runs 1 - 5

Run No.	1	2	3	4	5
Weight of sample holder (g)	177.035	177.44	177.055	178.005	178.665
Weight of sample holder and dry core (g)	214.35	216.085	215.848	215.05	214.69
Weight of sample holder and saturated core (g)	226.24	226.98	227.218	226.17	225.86
Percentage porosity	42.1	38.5	38.8	39.3	39.5
Evaporation flux ($g\ cm^{-2}\ day^{-1}$)	0.532	0.554	0.559	0.340	0.323

Notes.

1. The error associated with the calculation of porosity was assumed to be the same at the porosity error calculated in Appendix II, that is, the error is $\pm$ 0.55%.
2. The error associated with the calculation of the evaporation rate is discussed in section 4.4.3 and was taken to be $\pm$ 1.25%.

4.3.3 Calculation of suction developed by the core

The height difference of the mercury U-tube manometer was converted into a suction of water pressure head, the density of water was taken as unity. The suction was calculated with respect to the evaporating surface. A sample calculation can be found in Appendix VI. The density of mercury was assumed to be 13.5 ($g\ cm^{-3}$). The value of 13.5 ($g\ cm^{-3}$) represents a maximum error of $\pm$ 0.5% in the temperature range 15°-$25^{o}C$ [9], which was the approximate range of dry bulb temperatures observed for the experimental runs.

4.3.4 Calculation of the pressure potential between the pressure tapping points and the base of the core

The carbon tetrachloride height difference between the pressure tapping points and the base of the core was converted into a pressure head of water, once again assuming the density of water to be 1 (g cm^{-3}). A sample calculation can be found in Appendix VII. The measurement of pressure potential between these points together with the flow rate of water measured through the base of the core was to be used to calculate the unsaturated permeability of the core.

4.3.5 Calculation of the weight lost by the plaster core

The weight lost by the plaster core was calculated by subtracting the weight of water that had migrated from the mercury manometer from the corresponding cumulative weight of water lost by the sample. The volume of water lost by the mercury manometer was calculated by multiplying the area of the tube by the distance travelled by the mercury-water interface with respect to its original position. The diameter of the tube used in the manometer was 0.35 cm $\pm$ 0.01 cm tolerance.

4.3.6 Calculation of the percent saturation of the core

The percentage loss of saturation of the core was obtained from the weight of water lost by the core divided by the weight of water required to saturate the core, multiplied by 100. The percentage saturation of the core is simply 100 minus this latter value. The percentage saturation of the core with respect to suction for runs 1-5 can be found in Fig. 85. Since the suction was continually increasing during the experiment, the points represent the "drying" moisture content curve.

A problem associated with the calculation of percent saturation with respect to suction is excess surface moisture at the evaporating surface. The presence of excess moisture at the

surface is manifested by a loss in weight from the apparatus without any increase of suction being developed by the porous material.

This type of behaviour was observed in runs 2, 3, 4. Calculations showed that the period of constant suction coincided with a value of zero suction at the evaporating surface. Thus the weight of the apparatus that corresponded to a value of 100% moisture saturation was taken as the weight of the apparatus at the end of the period of constant suction.

4.3.7 Unsaturated permeability of the core

The unsaturated permeability of the core was not calculated due to difficulties associated with the measurement of pressure difference between the pressure tapping points and the base of the core. The difficulties are discussed fully in section 4.5.

4.3.8 Dry bulb temperature and relative humidity

The relative humidity, calculated from the wet and dry bulb temperature of the Mason type hygrometer, and corresponding temperature of runs 1-5 can be found in Fig. 86 through Fig. 90 respectively. Additional measurements of air temperature (dry bulb) and relative humidity recorded by a thermohydrograph (manufactured by C.F. Cassella and Co. Ltd. - London. Catalogue No. 931) have also been reproduced in Fig. 86 - Fig. 90

4.4 Experimental errors

4.4.1 Manometer errors

The difference in height of both manometers was measured to an accuracy of $\pm$ 1mm. This accuracy represents a water pressure head of about $\pm$ 1.3 cm with respect to the mercury manometer. This variation is only significant at the lower values of suction. Furthermore the magnitude of this variation is small in comparison to the spread of experimental results, of each run, that are used to determine the "typical" hydraulic relationship of the porous material (c.f. Fig. 85). In other words the experimental error is

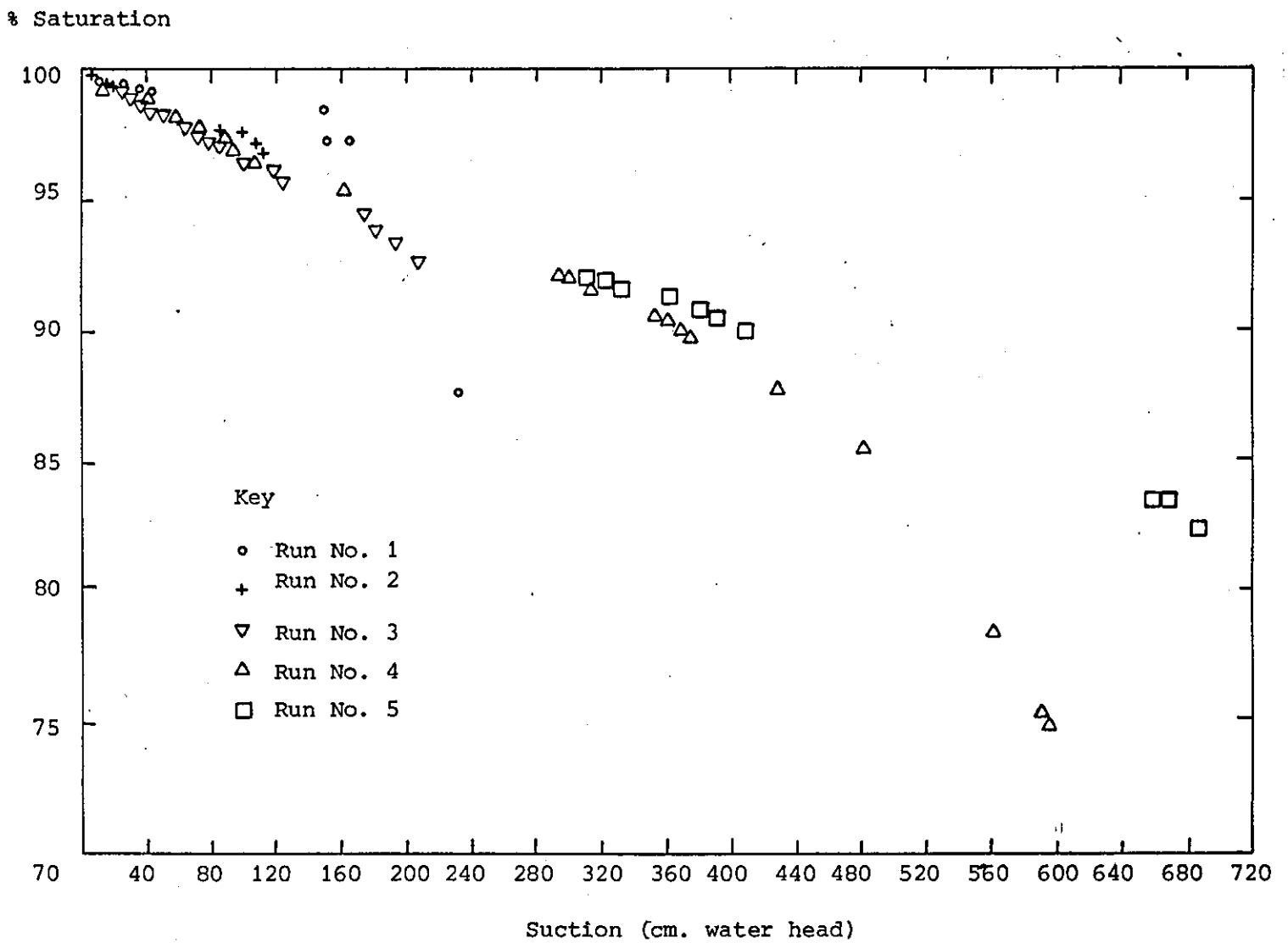

Fig. 85 Percent saturation versus suction (drying curve) of Run No. 1 through 5

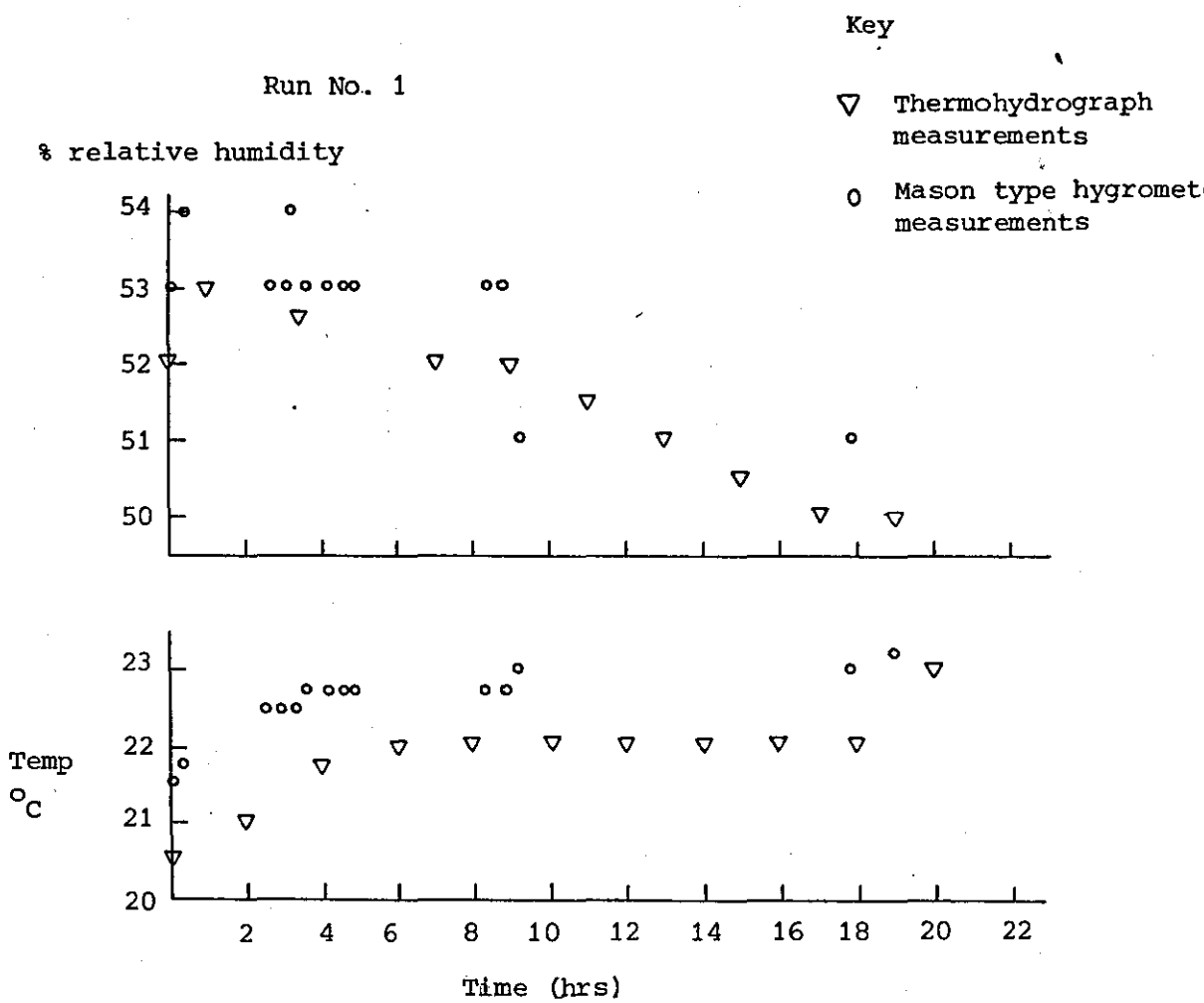

Fig. 86 Measurement of air temperature and humidity within the enclosure, using a Mason type hygrometer and a thermohydrograph

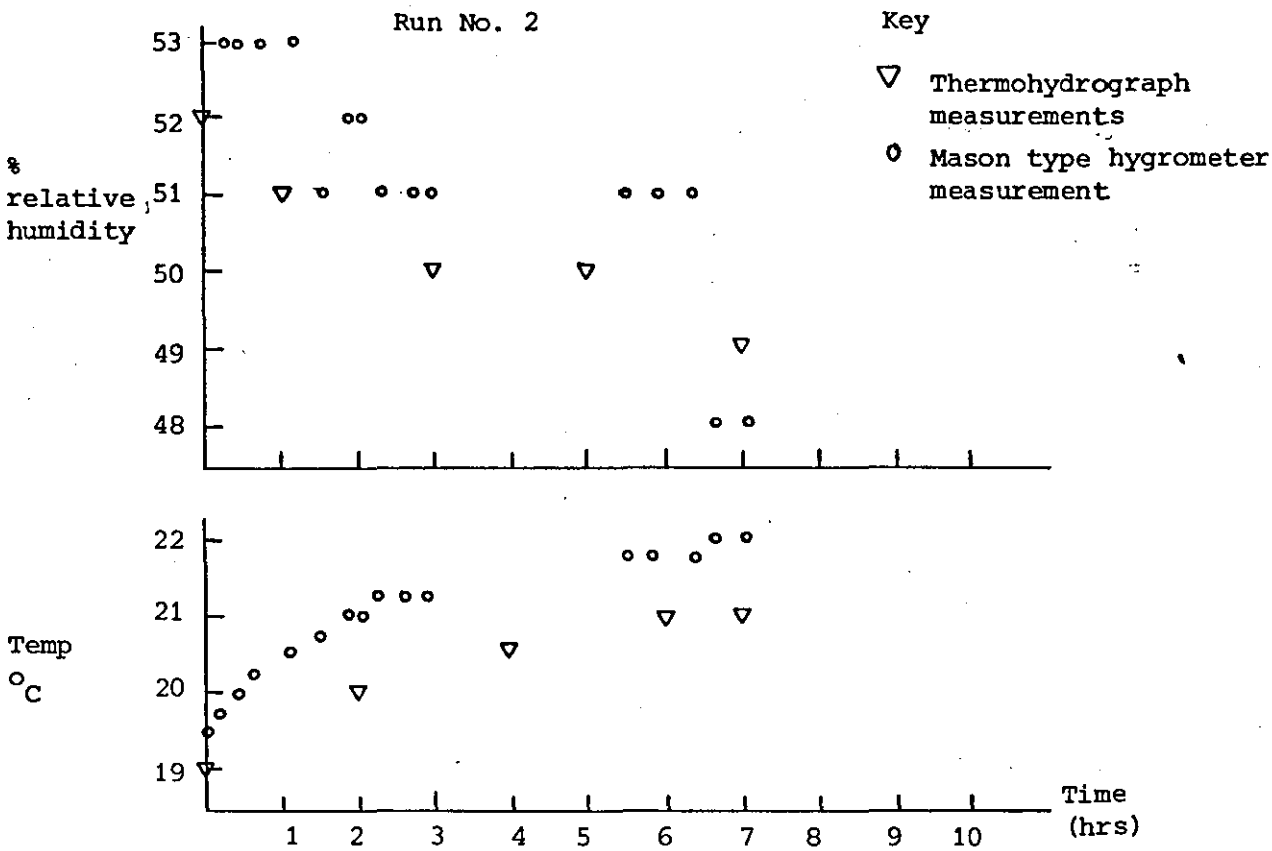

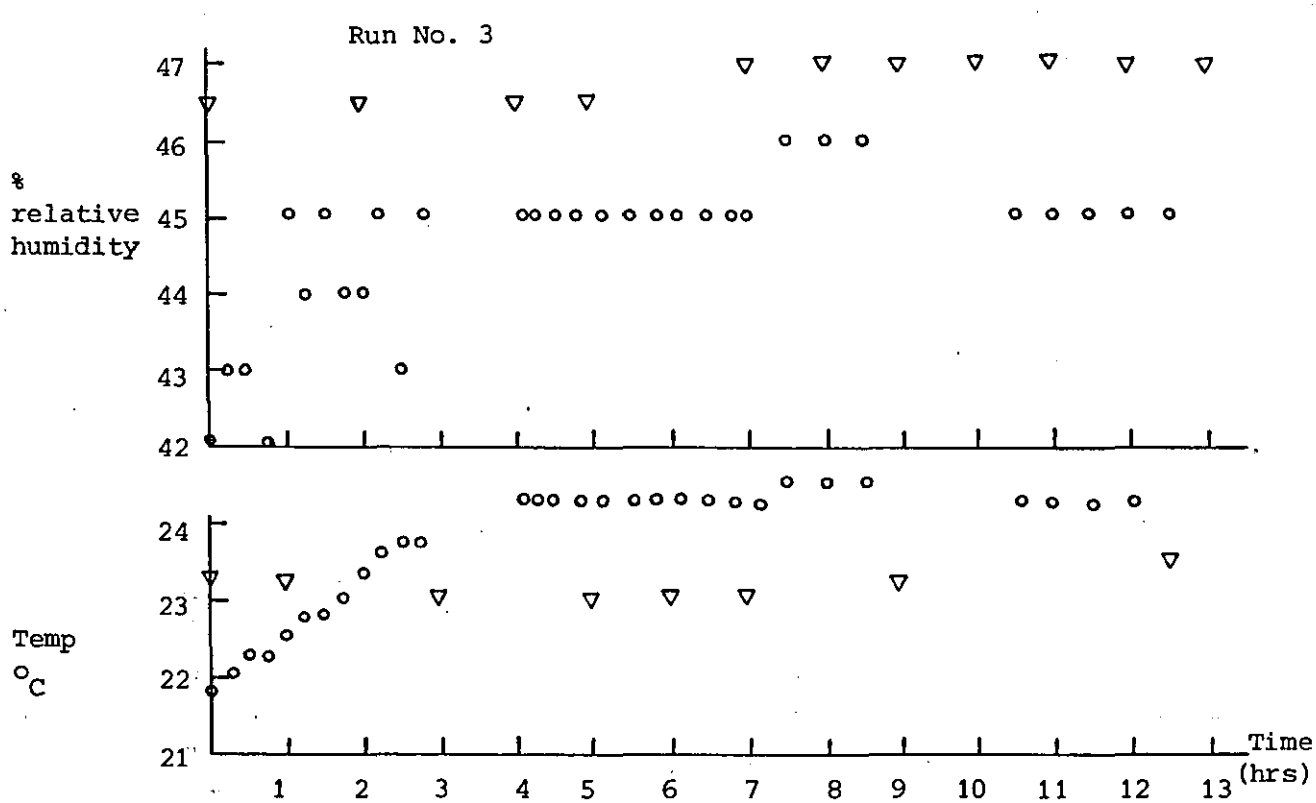

Fig. 87 (upper pair) Measurements of air temperature and humidity
Fig. 88 (lower pair) within the enclosure, using a Mason type hygrometer and a thermohydrograph

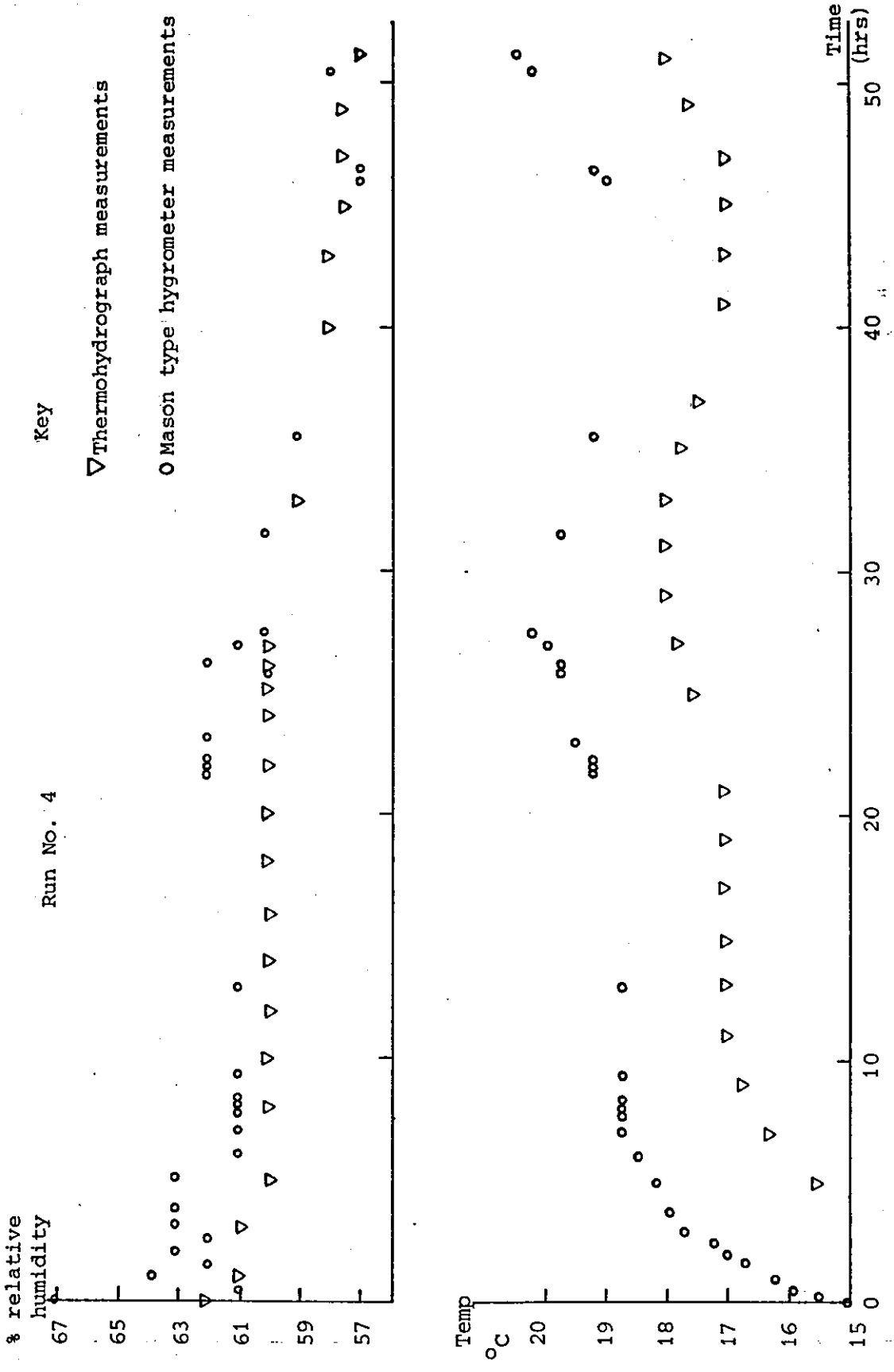

Fig. 89 Measurements of air temperature and humidity within the enclosure, using a Mason type hygrometer and a thermohydrograph

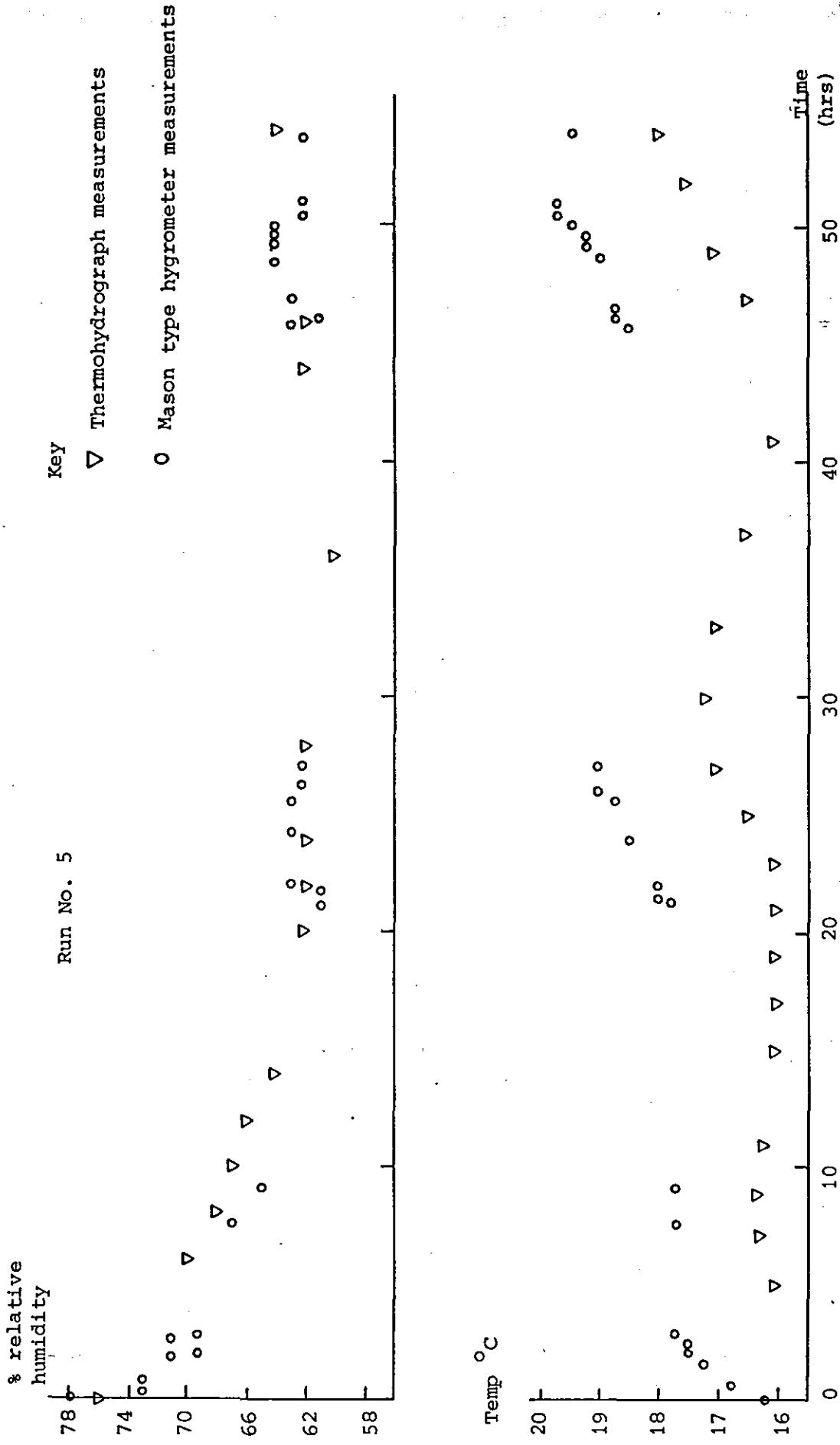

Fig. 90 Measurements of air temperature and humidity within the enclosure, using a Mason type hygrometer and a thermohydrograph

small when compared to the errors that are incurred in the determination of the "typical" moisture content-suction curve.

Discussion of the error associated with the carbon tetrachloride-water manometer has been omitted since no use was made of this experimental height difference. The problems associated with the measurement of this height difference are discussed in Section 4.5.

4.4.2 Temperature errors

The temperatures of the wet and dry bulb thermometers were measured to an accuracy of $\pm$ 0.25°C. This variation of temperature measurement is reflected by an average variation in the actual value of relative humidity of about $\pm$ 4%. The range of relative humidity of the different experimental runs varied between 45% and 61%. Assuming an average value of relative humidity of 50%, then the error associated with the calculation of relative humidity was $\pm$ 8%.

4.4.3 Evaporation rate error

The evaporation rate of each run was obtained by using a least squares regression technique. Calculation of the error of each individual experimental measurement would be tedious. However an estimate of the error was obtained by comparing the evaporation rate calculated from observations recorded at the beginning and end of the experiment to the evaporation rate calculated using the regression technique. The maximum deviation of the evaporation rate, calculated from the two point method compared to that calculated by the regression technique was found to be about $\pm$ 1.25%.

4.4.4 Moisture content (percent saturation) error

The moisture content error is the sum of two errors, one associated with the measurement of the weight of the apparatus and the other, being associated with the volume of water that had migrated from the mercury-water manometer arm into the plaster

core.

The error associated with the former is the same error that has been determined with respect to the calculation of the evaporation rate, i.e. the error is $\pm$ 1.25%. The error associated with the mercury manometer is the error which is related to the measurement of mercury-water interface movement, which was measured to an accuracy of $\pm$ 0.01 (cm). For a tube of 0.35 (cm) diameter, the variation of water volume corresponding to the variation of length is $\pm$ 9.62 x 10^{-4} (cm^3), which is vanishingly small in comparison to the volume of water absorbed by the sample. Note 1% saturation of the core corresponds to a volume of about 1 (cm^3). Hence the error associated with the measurement of moisture content was taken to be $\pm$ 1.25%.

4.4.5 Porosity error

The error associated with the calculation of porosity was assumed to be the same as the porosity error calculated in Appendix II, which was $\pm$ 0.55%.

4.5 Discussion

4.5.1 Unsaturated permeability experiment

1. No calculations of unsaturated permeability of the plaster cores were attempted in any of the experimental runs because of the uncertainty associated with the magnitude of the pressure difference across the fractional length of the core.

The pressure difference was to be determined from the difference in height of the carbon tetrachloride-water interfaces within the U-tube manometer. At static equilibrium, the pressure at the base of the sample, Fig. 81, is greater than the pressure observed at the height of the pressure tapping points. The vertical height from the base of the plaster core to the centre of the pressure tapping tubes was 2 (cm); and assuming the differential

density of carbon tetrachloride and water to be 0.6 (g cm^{-3}), the equilibrium height difference between the manometer arms is 3.33 cm. The equilibrium height differences observed for runs 1, 4 and 5 was 3.85, 2.35 and 2.6 (cm) respectively.

The equilibrium height was calculated, on the assumption that the radii of curvature of both manometer arms was the same. As a "worst" case situation, it was assumed that the advancing contact angle was 0° and the receding contact angle was 90°. It should be noted however, that the curvature of both manometer arms was concave towards the carbon tetrachloride.

The interfacial tension of a carbon tetrachloride-water interface was taken as 45 (dynes cm^{-1})[9]. Calculations indicate that on reversal of the two contact angles, there will be a change in height of the two interfaces of about 1.75 (cm). This height-difference is representative of an inbuilt design error, arising from hysteretic surface tension effects. The deviations of the observed equilibrium heights fall within the range of expected equilibrium height, when surface tension effects are included, and hence the deviations of equilibrium height have been attributed to hysteretic surface tension forces.

The diameter of the manometer tube was 0.35 (cm) $\pm$ 0.01 (cm) tolerance. The tube tolerance would account for a variation of equilibrium height of $\pm$ 0.5 (cm) and hence might also contribute to the variation of equilibrium heights.

2. Further difficulties associated with the calculation of unsaturated permeability were encountered in determining the actual flow rate of water between the base of the core and the pressure sampling points. If the "exit" surface is assumed to be the horizontal plane passing through the centres of the three pressure tapping tubes, then moisture passing across this surface is com-

posed of moisture entering at the base of the core, together with moisture that has been lost from the core itself, on desaturation.

As an approximation, the contribution of the latter to the overall flowrate calculated with respect to the "exit" surface has been ignored. Moisture entering at the base of the core was moisture that had migrated from the mercury manometer. Movement of moisture from the mercury manometer varied almost linearly with time, except towards the end of the experimental runs. The non linearity coincided with the appearance of air within the apparatus.

The flow rate from the mercury manometer for runs 1, 4 and 5 was calculated to be 0.084, 0.057 and 0.06 (cm^3 hr^{-1}). Substitution of the lowest value (0.057) as the flow rate into Darcy's law; and assuming the permeability of fresh plaster to be 1 x 10^{-10} (cm^2 - from leaching experiment); the viscosity of water to be 0.01 (g cm^{-1} sec^{-1}); the differential density between carbon tetrachloride and water to be 0.6 (g cm^{-3}); the length and area of the core to be 2 (cm) and 7.068 (cm^2); the gravitational constant, 980.7 (cm sec^{-2}); and including the static water pressure head of 2 (cm) then the carbon tetrachloride height difference between the pressure tapping points and the base of the core was calculated to be 4.09 (cm). This pressure difference is only about twice the value of the expected surface tension variation. The differential head attributed to moisture flow was calculated to be about 0.7 (cm). This pressure difference is inadequate for the determination of accurate values of unsaturated permeability.

3. The major fault of the experiment was the oversight of not including porous membranes at the base of the core and at the three pressure tapping points to prevent air from entering into the manometers. It was fortuitous that the experimental runs were

terminated because of dissolved air appearing in the manometers before air had had chance to penetrate through to the pressure tapping points or through to the base of the core.

For coarser pored materials, (i.e. house bricks), penetration of the air-water interface through the sample would have occurred at lower suctions and hence the absence of membranes would have resulted in the termination of the experiment.

Installation of a membrane at the base of the core can easily be accomplished. However, for the pressure tapping points, the problem is more difficult to overcome particularly for consolidated porous materials.

4. Since the suction was continually increasing throughout the duration of the experiments, the unsaturated permeability, if calculated, would have corresponded to its value along the "drying" curve. However, for the method to be useful, it should be capable of also measuring the "wetting" curve or subsequent "scanning" curves within the hysteretic envelope. Difficulties are envisaged with respect to the measurement and supply of moisture to and within the porous material.

5. In view of the problems encountered with the carbon tetrachloride-water manometer; the (natural) low flow rates within the apparatus leading to the measurement of low pressure differences; the need to modify the apparatus by inclusion of membranes; it is concluded that the present method is unsuitable for the measurement of unsaturated permeability of porous materials. Unsaturated permeability of consolidated porous materials should be measured in a similar fashion to the experimental method developed for unconsolidated porous materials[10][12][14].

4.5.2 Moisture content experiment

1. The saturation-suction curve for all five experimental runs can be found in Fig. 85. Since the suction increased progress-

ively throughout the duration of the experiment and since the core was initially saturated, the saturation-suction curve is the primary desaturation curve.

The relationship between saturation and suction was substantially linear within the range of suction (0 - 680 cm water head) measured. Deviations from the linear relationship, for all runs, occurred in the latter stages of the experiment. The deviations coincided with the appearance of air bubbles within the glass tubes of the manometers. The slope of the desaturation curve was approximately 2.7 percent desaturation per 100 (cm) suction of water head.

2. The results of the tensiometer survey of the previous experimental study showed that the suction developed by dry house bricks to be about 500 (cm) of water head. Thus the upper working limit of the present apparatus should be at least as high as the value above.

The maximum suctions developed in runs 1-3 were all less than 500 (cm) of water head. In run 4, the suction of 500 (cm) of water head marked the onset of non linearity between saturation and suction. However, in run 5 the linear relationship between saturation and suction was still evident at a suction of about 680 (cm) of water head. From this latter result, it can be concluded that the present apparatus is capable of achieving the required maximum "working" suction of 500 (cm) of water head.

In addition, since the suction developed by dry house bricks was only 500 (cm) of water head, there is little point in determining the hydraulic properties of building beyond this suction value.

3. A problem that arose during the calculation of percent saturation was the determination of the weight of assembled

apparatus that corresponded to a fully saturated core. Excess moisture on the external surfaces of the apparatus, particularly on top of the plaster core surface, if ignored, would appear in the calculations as moisture lost from the core, and hence result in saturation values that were too low.

The problem was overcome by examination of the corresponding suction values, with respect to the evaporating surface, developed by the core. At the start of the experimental observations the suction developed by the plaster core was zero (or slightly positive). The suction remained constant until all excess moisture had evaporated from the surface of the core. Further loss of moisture resulted in the formation of menisci at the surface and as a consequence suctions are developed by the core. Hence the suction curve is characterised by a period of constant suction, (i.e. zero or almost zero with respect to the evaporating surface) followed by a period of continually increasing suction. It was assumed that the weight of apparatus that corresponded to a completely saturated core was the weight at the end of the period of constant suction.

4. The suction-saturation results expressed in Fig. 85 are only representative of the "drying" curve of plaster of Paris and as such the results were obtained relatively easily using the present apparatus. However, the determination of the "wetting" curve using the apparatus appears to be more difficult.

The porous material on resaturation can be wetted in two different ways, indirectly through the vapour phase by condensation or directly through the liquid phase by addition of water to the porous surface. For water vapour to be absorbed at the surface, the water vapour pressure of bulk air must be greater than that at the moist porous surface. The expression relating the reduction

of vapour pressure due to suctions within the liquid phase is

$$h = \frac{p}{p_o} = \exp\left[\frac{g(-h_w)M}{R_m T}\right]$$

where h is the relative humidity due to the applied suction; p_o, the vapour pressure of a "free" moisture surface at the absolute temperature T; p, the vapour pressure of the moisture when subject to an applied suction $(-h_w)$; g, the gravitational acceleration; M, the molecular weight of the moisture; R_m, the Universal gas constant per mole.

For water at 20°C, and a suction of 700 (cm) of water head, the percentage relative humidity is about 99.9%, i.e. there is very little reduction of vapour pressure at this suction. If the core was resaturated via the bulk air at this high humidity, then there is a considerable possibility of moisture condensing on the apparatus as well as the plaster core, which would consequently lead to incorrect suction-saturation results.

Addition of moisture directly to the saturated core via the evaporating surface is also unsatisfactory because some of the moisture added at the surface must travel through the core and into the mercury manometer, in order for the suction to be reduced. No difficulties arise whilst there is "free" moisture at the surface. However, consider the situation when the availability of free moisture at the surface has just ceased. The suction at the surface whilst the pressure in the mercury manometer is negative with respect to the surface. Moisture from the porous material will be still withdrawn by the mercury manometer until the imbalance of suction is neutralised.

Withdrawal of moisture from the material (suction increasing) leads to "drying" conditions being established. Even though the water saturation has been increased the plaster core, at equilibrium has been left in the "drying" condition, which is unsatisfactory

with respect to the measurement of "wetting" properties.

5. In view of the difficulties envisaged in the experimental determination of "wetting" suction-saturation relationships with the present apparatus, it was concluded that the moisture content-suction relationships of porous building materials should be measured using conventional techniques and apparatus[12].

4.5.3 Evaporation experiment

1. The evaporation results for the five runs have been expressed graphically in Fig. 83 (runs 1-3) and Fig. 84 (runs 4,5). Evaporation has been expressed as cumulative weight lost by the apparatus versus time. For the range of suctions covered by the experiment (0 - 760 cm of water head, the evaporation rate was found to be substantially constant ($\pm$ 1% for each run), the average evaporation rates can be found in Table III.

2. It has been shown, in the previous section, that a suction of 700 cm of water head reduces the relative humidity by only 0.1%. in other words, at 20°C the saturated vapour pressure of water is reduced by 0.0234 millibars (mb) of pressure. Assuming a driving force of 2 mb to exist between the saturated surface and bulk air, the reduction of evaporation rate when a suction of 700 (cm) water head is applied is about 1%. Hence for the suction range 0 - 700 (cm), the evaporation rate will be substantially constant, unless the driving force is significantly reduced. For runs 1-3 the driving force was about 5 mb and for runs 4-5 it was 3.5 mb.

3. The correlation between the concentration difference of water vapour and evaporation rate has been expressed graphically in Fig. 91. With mass transfer processes, the concentration difference is usually expressed as (g cm^{-3}), however for meteorological studies the concentration difference is often expressed as (mm) of mercury or more correctly as millibars. The latter unit is

more correct since it is an "absolute" unit and 1 bar is defined as being equal to 10^6 (dynes cm^{-2}), whereas the former unit is dependent upon the density of mercury.

The relationship between the vapour pressure of water, p, (millibars) and the density of water, ρ_v, (g cm^{-3}) is

$$p = \frac{10^3 \rho_v R_m T}{M}$$

where M is the molecular weight of water (g $mole^{-1}$); R_m, Universal gas constant (8.31×10^7 ergs $mole^{-1}$ $^oK^{-1}$); T, the absolute temperature (^oK).

For small variations in temperature between the evaporating surface and bulk air, the concentration difference of water vapour is proportional to the water vapour pressure difference of the two gaseous mixtures.

To perform the calculation of concentration difference, it was assumed that the temperature of the evaporating surface was equal to the wet bulb temperature and that the water vapour pressure at the evaporating surface was equal to the saturation vapour pressure at the wet bulb temperature.

The water vapour pressure of bulk air was obtained using hygrometric tables. Note tables suitable for a Mason (screen) hygrometer were used. Average temperatures of wet and dry bulb measurements of each experimental run can be found in Table IV.

Table IV. Average wet and dry bulb temperatures of runs 1-5. The values were obtained from Figs.86-90 respectively.

Run No.	Wet bulb (^oC)	Dry bulb (^oC)	Relative humidity (%)
1	17	22.75	53
2	15.75	21.75	51
3	17.25	24.25	45
4	14.5	18.75	61
5	13.5	17.75	61

The temperatures of the wet and dry bulbs were measured to an accuracy of $\pm$ 0.25°C. Owing to this temperature variation, it was necessary to express the driving force (millibar) in terms of a maximum and minimum value. The extreme values of driving force were chosen from the range of values calculated, when the wet and dry bulb temperatures were allowed to vary by $\pm$ 0.25°C from their average values. As an example, in run 1 the dry bulb temperature was taken to vary between 22.5 and 23°C and the wet bulb from 16.75 to 17.25°C. The relationship between the evaporation rates and corresponding range of driving force can be found in Fig. 91.

Maximum and minimum straight lines were drawn which intersected the bands of pressure of each of five runs. An average value of the relationship between the evaporation rate and the vapour pressure difference was taken as the mean value between the two extremes, which was 0.106 $\pm$ 10% (g cm^{-2} day^{-1} per mb).

4. Evaporation of water into quiet air from a "free" horizontal water surface has been studied by several workers[(16)-(20)]. The earliest empirical relation between unit evaporation rate, E_v, and vapour pressure difference, $p_{es} - p_a$, was expressed in the form[(16)-(18)]

$$E_v = a\,(p_{es} - p_a)^{1.2 - 1.25} \qquad (1)$$

where a is a constant; p_{es}, the saturated vapour pressure at the evaporating surface; p_a, the vapour pressure of bulk air.

If 760 mm of mercury is assumed to be equal to 1 bar of pressure then Hinchley's[(17)] empirical expression may be expressed as

$$E_v = 0.0158\,(\Delta mb)^{1.2} \qquad (2)$$

Similarly, Wade[(18)] investigated forced and natural evaporation of several liquids and obtained the relationship

$$E_v = 6.0 \times 10^{-2} \times M^{0.71}\,(\Delta mb)^{1.25} \qquad (3)$$

where M is the molecular weight of liquid. Wade stated that the

expression was accurate to $\pm 15\%$. For water the relationship reduces to

$$E_v = 0.467\ (\Delta mb)^{1.25} \tag{4}$$

Wade did not state whether the evaporation rate was based upon unit area or total evaporative area of the surface (i.e. 79.21 cm^2). However, comparison of evaporation rates calculated from eqn. (4) with evaporation rates using other empirical relationships indicate that eqn. (4) corresponds to evaporation from the total surface. Hence Wade's empirical relationship, for water, per unit area is taken to be

$$E_v = 5.9 \times 10^{-3}\ (\Delta mb)^{1.25} \tag{5}$$

A more systematic study of evaporation of water into still air from a free liquid surface has been conducted by Boelter et al[19][20]. Boelter correlated the evaporation rate with respect to vapour buoyancy. For heated evaporating surfaces Boelter stated that water vapour would rise vertically from the surface (Fig. 92a). Air would be induced into the vapour stream by virtue of the momentum of the latter. Lowering the surface temperature would lead to a reduction in the buoyancy of the air-water vapour mixture at the evaporating surface. Eventually a point would be reached where the density of the mixture far away was equal to that at the evaporating surface. The corresponding mixture flow system is indifferent and the surface temperature is at its "critical" value.

For still lower surface temperatures the mixture at the evaporating surface is denser than the mixture far away. The air-water vapour mixture slips outward, dragging air with it, Fig. 92b.

The evaporation process was characterised using the following dimensionless groups,[21]

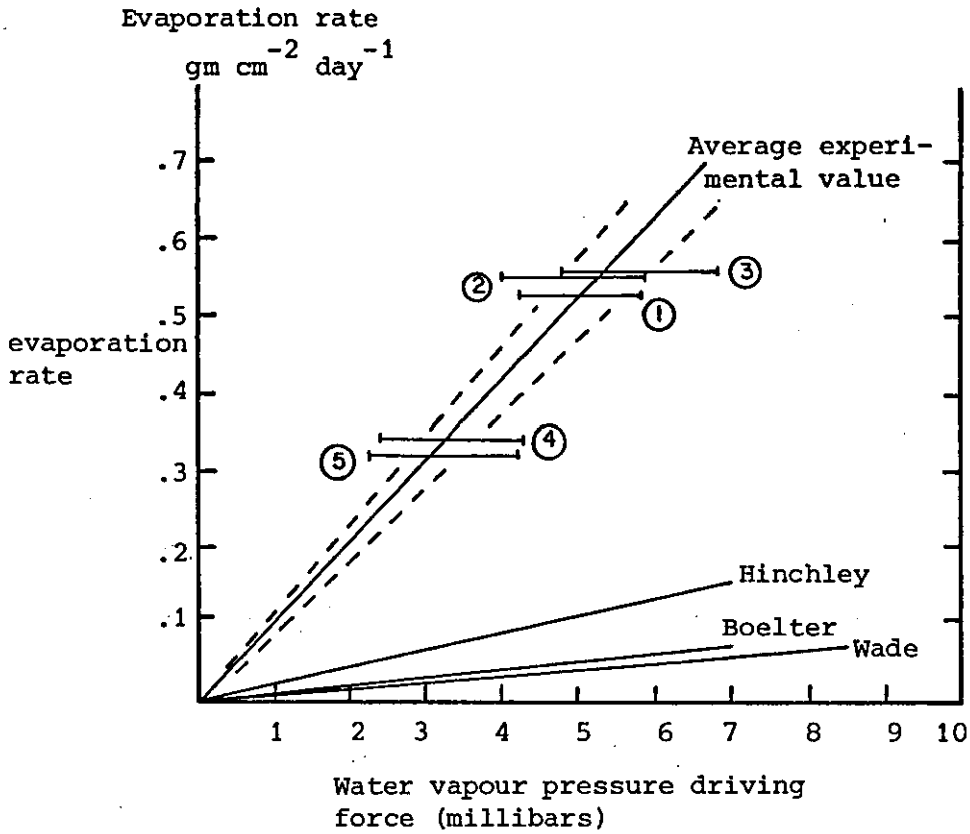

Fig. 91 Correlation of evaporation of water from a free water surface into still air

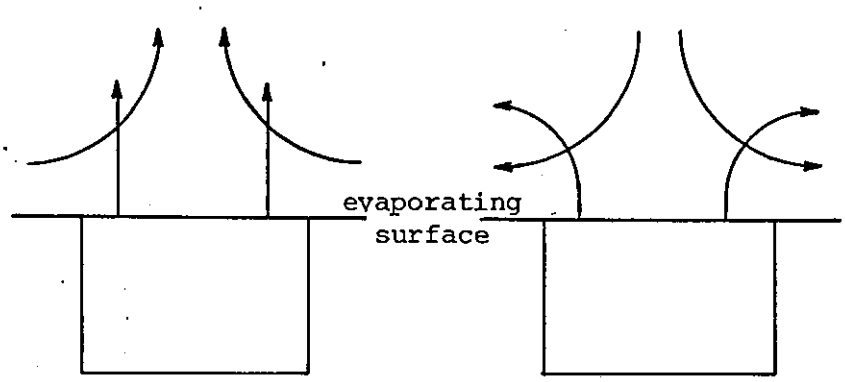

(a) High surface temperature (b) Low surface temperature

Fig. 92 Mixture flow diagram above a horizontal damp surface

$$N_{Sh} = \frac{h_D \ell}{D_{atm}} \; ; \; N_{Gr} = \frac{\ell^3 \rho g \Delta\rho}{\mu^2} \; ; \; N_{Sc} = \frac{\mu}{D_{atm} \rho}$$

where h_D, unit conductance for mass transfer ($= E_v'/\Delta\rho$) $(g\ cm^{-2}\ sec^{-1})/(g\ cm^{-3})$; ℓ, the diameter of the evaporating surface (cm); D_{atm}, diffusion coefficient of water vapour in air ($cm^2\ sec^{-1}$); ρ, density of the mixture ($g\ cm^{-3}$); g, gravitational acceleration ($cm\ sec^{-2}$); $\Delta\rho$, density difference of the mixture at the evaporating surface and the mixture far away ($g\ cm^{-3}$); μ, coefficient of viscosity of the mixture ($g\ cm^{-1}\ sec^{-1}$).

The critical point is characterised by the product $N_{Gr} \times N_{Sc} = 0$. A detailed calculation of the product $N_{Gr} \times N_{Sc}$ for the maximum water vapour pressure difference of runs 1-5 can be found in Appendix VII. The value obtained for $N_{Gr} \times N_{Sc}$ was approximately -1.6×10^3. Hence the air flow system is below the critical point (Fig. 92b). For flow systems below the critical point Boelter[19][20] stated that the evaporation rate was a linear function of vapour concentration difference and for water the relationship was

$$E_v = 0.01\ (\Delta mb) \qquad (5)$$

Where E_v, unit evaporation rate ($g\ cm^{-2}\ day^{-1}$); Δmb, water vapour concentration difference expressed in millibars of pressure.

The empirical relationships of Hinchley et al,[17] Wade,[18] Boelter et al[19] have been reproduced in Fig. 91. The values of Wade ($\pm$15%) and Boelter are in close agreement, whilst Hinchley's value is about twice that of Boelter. The present experimental results are about a factor of ten greater than those of Boelter.

5. The present, higher than expected evaporation rate is attributed to random air currents within the quieting chamber. Powell[16], Wade[18] and Boelter et al[19][20] have all commented about the problem of random air movement within the quieting chamber.

In addition to the air currents generated and already existing in the chamber when it was closed, further air currents could be generated because of heat exchanges through the unlagged window of the quieting chamber and because of heat originating from the electrically operated balance whose scale was illuminated internally by an electric bulb.

6. Inspection of Figs. 86-90 show that the temperature of the chamber increased when it was sealed and that for run 5 (Fig. 90) diurnal variations of temperature could be observed. The amplitude of the variation was $\pm 0.6^{\circ}C$. The temperature differences between the wet and dry bulb thermometer remained constant though, the difference was about $4^{\circ}C$.

Assuming peak dry bulb temperature to be $19.25^{\circ}C$ and the minimum to be $18^{\circ}C$, the vapour concentration difference corresponding to both sets of temperature differences was found to be the same, i.e. 3 mb. This result is rather fortunate.

A greater confidence in the actual value of the water vapour pressure difference would be achieved if the temperature variations within the chamber were controlled to an accuracy of $\pm 0.1^{\circ}C$.

7. In view of the unsuitability of the apparatus to measure the other hydraulic functions, it was concluded that the evaporation experiment should also be performed separately; using more stringent methods of temperature control and measurement. The evaporating surface should be orientated in a vertical plane to more closely simulate evaporative conditions associated with damp walls. The method of determining the evaporation rate by weighing should be changed. An independent method of determining the actual temperature of the evaporating surface should be included, rather than the assumption that the surface is at the wet bulb temperature.

4.6 Summary of the feasibility investigation

The apparatus has been found to be inadequate to simulatan-eously measure the hydraulic properties of unsaturated permeability, moisture content and evaporation rate with respect to capillary suction.

It is recommended that the relationship between each hydraulic property and suction be determined separately. The evaporation experiment should be re-designed with particular attention being paid to the accuracy of measurement of the wet and dry bulb temperatures and inclusion of an independent measurement of the temperature of the evaporating surface.

List of symbols and units of Chapter Seven

A	area available for fluid flow (cm^2)
E_v'	mass evaporation rate per unit area ($g\ cm^{-2}\ day^{-1}$)
g	gravitational acceleration ($cm\ sec^{-2}$)
h_w	pressure head of water (cm)
h_s	suction pressure head of water (cm)
h_{ms}	maximum suction pressure head of water (cm)
K	tensiometer cup conductance ($cm^3\ min^{-1}\ ats^{-1}$)
k	permeability to fluid of the porous material (cm^2)
k_f	final permeability to fluid of the porous material (cm^2)
k_i	initial permeability to fluid of the porous material (cm^2)
ℓ	length of porous material (cm)
m''	permeability ratio (k_f/k_i)
ΔP	pressure difference ($g\ cm^{-1}\ sec^{-2}$)
p_a	water vapour pressure in bulk air ($g\ cm^{-1}\ sec^{-2}$)
p_{es}	saturated water vapour pressure of air at the surface temperature, T_{es} ($g\ cm^{-1}\ sec^{-2}$)
Q	volumetric flowrate of fluid ($cm^3\ sec^{-1}$)
Q_T	overall volumetric flowrate of fluids ($cm^3\ sec^{-1}$)
r	capillary pore radius (cm)
S_c	tensiometer sensitivity ($ats\ cm^{-3}$)
t	time (mins)
γ_{LG}	surface tension between the liquid and gaseous phase ($g\ sec^{-2}$)
μ	viscosity of a fluid ($g\ cm^{-1}\ sec^{-1}$)
ρ	density of a fluid ($g\ cm^{-3}$)
ρ_m	density of mercury ($g\ cm^{-3}$)
ρ_w	density of water ($g\ cm^{-3}$)
ϕ	porosity of a porous material

References Chapter Seven

1. Rising Damp, G. Mason. Building Sci., 9, pp.227-231, 1974

2. Brickwork, S. Smith. The Macmillan Press Ltd., 1972

3. The chemistry of building materials, R.M.E. Diamant. Business Books Ltd., London, 1970

4. Building materials: science and practise, C.C. Handisyde. The Architectural Press, London, 1961

5. Mortars for bricklaying, Building Research Establishment Digest, No. 160, 4 pages, 1973

6. Permeability of Portland cement paste, T.C. Powers, L.E. Copeland, J.C. Hayes, H.M. Mann. Proc. Amer. Concrete Isnt. 51, pp.285-298, 1954.

7. Flow of fluids through porous materials, R. Collins. Rheinhold Chemical Engineering Series, Rheinhold Publ. Corp. New York, 1961

8. The statistical behaviour of instabilities in displacement processes in porous media, A.E. Scheidegger, E.F. Johnson. Canad Jnl. of Phys., 39, pp.326-334, 1961

9. C.R.C. Handbook of Physics and Chemistry. 46 Ed., 1965-1966

10. The energy concept of soil moisture and mechanics of unsaturated flow, M.B. Russell, M.G. Spangler. Proc. 21st Ann. Meeting Highway Research Board, pp.435-450, 1941

11. Methods of measuring soil moisture tension, L.A. Richards. Soil Sci., 68, pp.95-112, 1949

12. Methods of soil analysis, Part 1. C.A. Black, D.D. Evans, J.L. White, L.E. Ensminger, F.E. Clark. Agronomy Series No. 9 American Soc. of Agronomy, Inc., Publ., 1965

13. Advanced soil physics, D. Kirkham, W.L. Powers. Wiley-Interscience Inc., 1972

14. Movement and distribution of water in soil in relation to highway design and performance, D. Croney, J.D. Soleman, W.P.M. Black. Highway Research Board, Special Report No. 14, pp.225-252, 1958

15. Improvement of the drilling method for the determination of moisture content in building materials. A.J. Newman. Building Research Establishment paper No. 4/75, 7 pages 1953

16. Further experiments on the evaporation of water from saturated surfaces. R.W. Powell. Trans. Inst. Chem. Eng., 18, pp.36-55, 1940

17. Evaporation in currents of air. J.W. Hinchley, G.W. Himus. Trans. Inst. Chem. Eng., 2, pp.57-64, 1924

18. Evaporation of liquids in currents of air. S.H. Wade. Trans. Inst. Chem. Eng., 20, pp.1-13, 1942

19. Evaporation of water into quiet air. B.F. Sharpley, L.M.K. Boelter. Ind. Eng. Chem., 30, No. 10, pp.1125-1131, 1938

20. Free evaporation into air of water from a free horizontal quiet surface. L.M.K. Boelter, H.S. Gordon, J.R. Griffin. Ind. Eng. Chem., 38, No. 5, pp.596-600, 1946

21. Momentum heat and mass transfer. C.O. Bennet, J. Myers. 2nd Ed., McGraw Hill Book Co., 1974

APPENDIX I

Miniature Pressure Transducer

Type AE 830

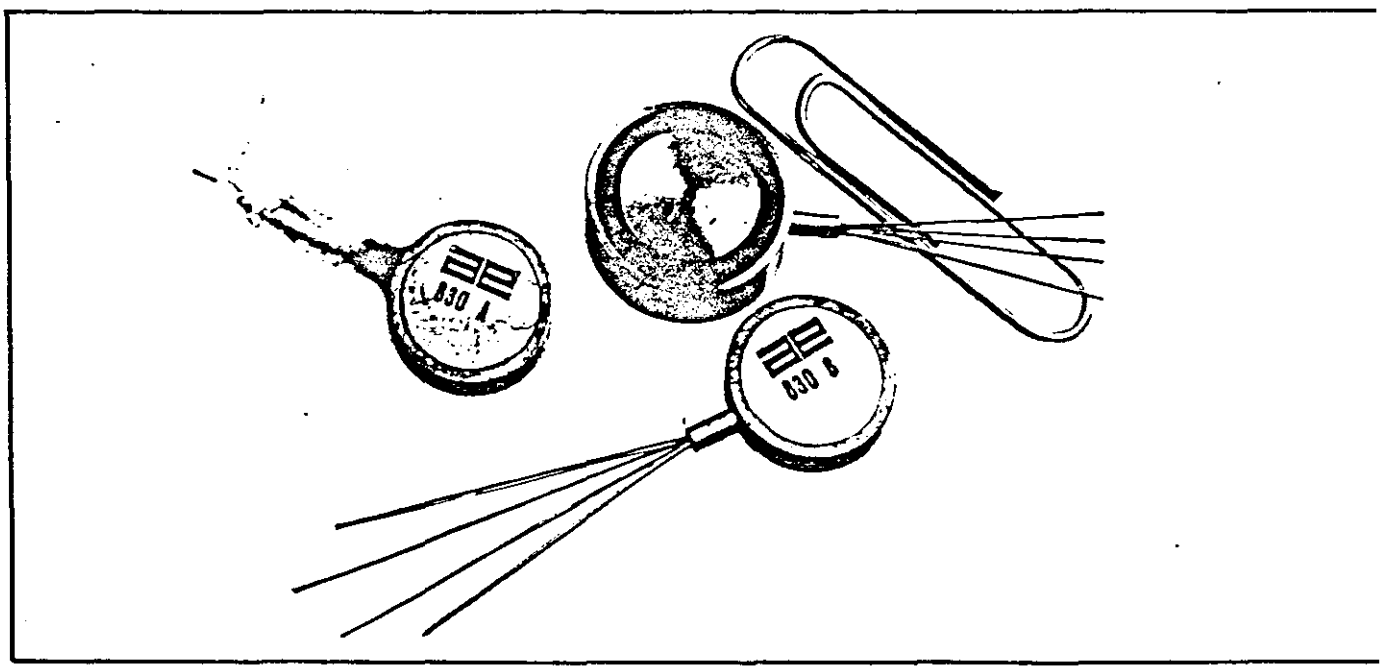

DESCRIPTION

The AE 830 series of miniature pressure transducers are designed for medium accuracy and small size requiremen

The heart of the transducer is a silicon beam on each side of which is a diffused planar resistor. The pressure sensiti membrane converts the applied pressure into a proportional deflection of the beam element. This deflection produces linear change in the two diffused resistors and by applying a DC voltage, the pressure gauge will be converted into electrical signal.

The standard transducer housing is brass. The membrane and the housing are made in one piece to prevent unwant relative movement between the transducer element and the membrane. Normally the AE 830 is hermetically sealed, but f special applications, vented versions can be delivered. On request, the transducer can be silver or gold plated. When requir the transducer housing can be made from titanium.

SPECIFICATIONS FOR STANDARD TYPES AVAILABLE:

Type	Range Kp/cm^2	Range p.s.i.	Sensitivity mV/V full scale ± 25%	Linearity & Hystersis % FS	Zero Shift % FS/°C	Load (gm)
AE 830 A	0 – 0.4	0 – 6	10	± 1	± 0.85	90

SPECIFICATIONS FOR STANDARD TYPES AVAILABLE

Transducer impedance	: 2 x 1000 ohm	Sensitivity shift	: -0.2 %/°C
Excitation	: Max. 6 V DC	Acceleration sensitivity	: 0.02 %/g
Zero shift, vented type	: ± 0.01 to ± 0.10 % FS/°C	Temperature range	: -30 to +55°C : -30 to +100°C on request
Over pressure	: 100 % FS	Dimensions	: 12° x 2.5mm + 38mm lead

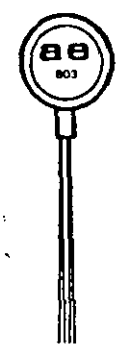

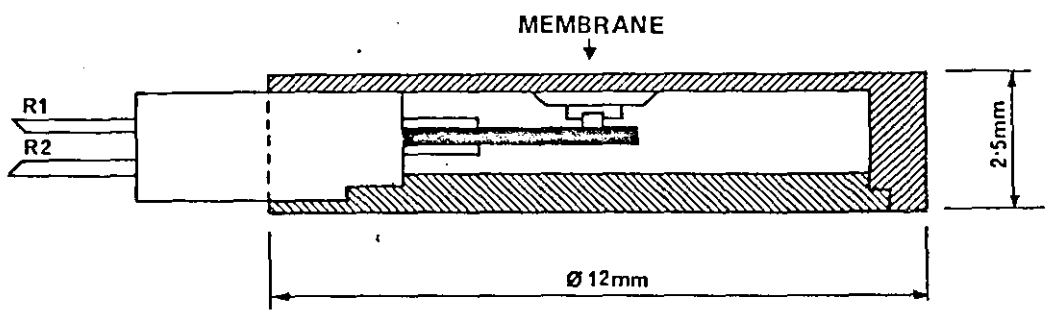

ELECTRICAL CONNECTION DIAGRAM

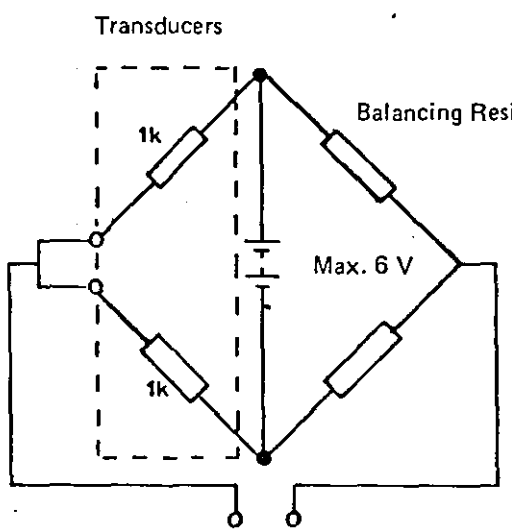

Fig. 1

VENTED TRANSDUCER

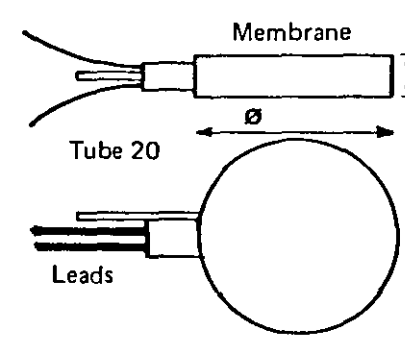

Fig. 2

The figure shows the complete circuit diagram necessary for applying the AE 830 miniature transducer. As indicating instrument a millivoltmeter or a chart recorder can be used.

For special applications the internal pressure can b vented to the atmosphere. This measure cancels ou changes in the atmospheric pressure and also reduces th zero-shift. Fig. 2 shows one method of venting th interior. This type can be delivered with water tigh silicone tubing around the leads and the venting tub (length up to 2 meters).

Run No.	Permeability $(cm)^2 \times 10^{-11}$ Initial	Permeability $(cm)^2 \times 10^{-11}$ Final	Permeability ratio (k_f/k_i)	Porosity	Flow Rate $(cm^3\ min^{-1})$	Core length (cm)
1	1.02 ± 18.35%	177 ± 30%	172	-	0.0083	2.54
2	1.75 ± 18.35%	10 ± 18.35%	5.8	-	0.0071	2.54
3	1.4 ± 18.35%	5.7 ± 18.35%	4.1	-	0.0062	2.54
4	1.2 ± 18.35%	9.5 ± 18.35%	8.1	-	0.0082	2.54
5	3.0 ± 8.25%	560 ± 14.25%	186'	-	0.083	2.5
6	2.6 ± 8.25%	420 ± 107.25%	160	-	0.088	2.5
7	2.5 ± 8.25%	400 ± 107.25%	160	-	0.084	2.5
8	1.6 ± 8.25%	47 ± 107.25%	30	-	0.073	2.5
9	2.3 ± 8.25%	29 ± 107.25%	12.5	-	0.05	2.5
10	1.15 ± 8.25%	100 ± 107.25%	85	44.7	0.16	2.4
11	3.1 ± 8.25%	220 ± 107.25%	70	36.1	0.068	2.45
12	4.9 ± 8.25%	520 ± 107.25%	105	42.8	0.12	2.425
13	-	-	-	46.0	-	2.35
14	3.4 ± 8.25%	500 ± 32.25%	145'	20.3	0.082	2.4
15	1.45 ± 8.0%	60 ± 107.25%	45	37.0	0.04	2.4
16	0.87 ± 8.0%	150 ± 107.25%	170	34.5	0.055	2.5
17	7.0 ± 8.0%	280 ± 107.25%	40	43.7	0.145	2.4

Run No.	Permeability $(cm)^2 \times 10^{-11}$ Initial	Permeability $(cm)^2 \times 10^{-11}$ Final	Permeability ratio (k_f/k_i)	Porosity	Flow Rate $(cm^3\ min^{-1})$	Core length (cm)
18	7.2 ± 8.0%	28 ± 107.25%	4	43.4	0.16	2.4
19	9.7 ± 8.0%	850 ± 107.25%	90	39.9	0.14	2.4
20	8.8 ± 8.0%	4.2 ± 107.25%	45	37.0	0.15	2.325
21	2.4 ± 8.0%	10.5 ± 107.25%	4	42.7	0.06	2.4
22	3.0 ± 8.0%	1600 ± 107.25%	530'	43.2	0.06	2.4
23	4.3 ± 6.3%	-	-	44.0	0.11	2.35
24	2.0 ± 6.3%	230 ± 105.3%	115	43.5	0.057	2.332
25	7.25 ± 6.3%	425 ± 9.2%	60	42.5	0.12	4.005
26	7.2 ± 6.3%	6000 ± 55.3%	835'	42.3	0.12	3.995
27	5.7 ± 6.3%	375 ± 8.9%	65'	41.4	0.15	2.496
28	4.5 ± 5.8%	400 ± 9.8%	90'	43.0	0.13	2.405
29	1.2 ± 5.8%	530 ± 104.8%	45	42.4	0.18	3.995
30	11.0 ± 5.8%	580 ± 104.8%	55	41.6	0.17	4.006
31	3.1 ± 5.8%	370 ± 104.8%	120	42.8	0.088	2.48
32	4.0 ± 5.8%	3100 ± 54.8%	770'	43.1	0.10	2.332
33	5.8 ± 5.8%	3300 ± 38.1%	560'	38.7	0.09	3.995
34	5.8 ± 5.8%	1400 ± 19.8%	240'	42.7	0.095	4.003
35	5.5 ± 5.8%	8500 ± 104.8%	1550'	42.4	0.14	2.415

Run No.	Permeability $(cm)^2 \times 10^{-11}$ Initial	Permeability $(cm)^2 \times 10^{-11}$ Final	Permeability ratio (k_f/k_i)	Porosity	Flow Rate $(cm^3\ min^{-1})$	Core length (cm)
36	5.9 ± 5.8%	2100 ± 29.8%	360'	42.0	0.14	2.445
37	1.4 ± 5.8%	-	-	22.0	0.025	3.995
38	2.1 ± 5.8%	590 ± 22.5%	270'	23.4	0.037	3.995
39	2.0 ± 5.8%	325 ± 104.8%	170	28.1	0.033	3.995
40	3.0 ± 5.8%	1000 ± 104.8%	370	23.0	0.053	4.006
41	8.6 ± 5.8%	2900 ± 38.1%	340'	44.0	0.16	2.328
42	10.0 ± 5.8%	2500 ± 104.8%	250	43.5	0.20	2.247
43	9.2 ± 5.8%	850 ± 104.8%	90	43.5	0.15	2.395
44	7.8 ± 5.8%	1600 ± 104.8%	200	41.5	0.13	2.50

Notes.

1. Average errors

	length	flow rate	porosity
Run No. 1 - 22	± 2%	± 3%	± 2.35%
Run No. 23 - 44	± 0.2%	± 3%	± 0.55%

APPENDIX III

Estimation of errors of leaching experiment

Calculation of the permeability (from Darcy's law) and the porosity of the porous cores involved the measurement of the following variables:- flow rate, Q; viscosity of the fluid, μ; length of the core, ℓ; fluid density, ρ; differential head of fluid across the plaster core, Δh_w. The diameter of the core, although involved in the calculation of permeability and porosity was not measured; and it was assumed that the value was constant for all the sample holders. Although as an estimate of the error of the diameter, it may be assumed that the error is the same as the error associated with the measurement of the length of the core.

Flow rate Q(cm^3 sec^{-1}) The flowrate was calculated from corresponding measurements of volume of water pumped through the core and measurements of time. Volume differences were measured using a burette. Examination of Figs. 4-7 shows that the maximum error associated with the measurement of flow rate to be $\pm$ 3%. This result was confirmed when the flow rate of run 21 was calculated.

Fluid viscosity μ(g cm^{-1} sec^{-1}) The temperature variation occurring during runs 1-4 was not measured and hence no accurate assessment of the temperature error can be made. It was assumed however, that the temperature variation was $\pm$ 2.5°C which corresponds to a variation of viscosity of $\pm$ 12%. Examination of the temperature variation of the water bath for runs 5-14 to be $\pm$ 0.5°C. The corresponding viscosity variation is $\pm$ 1.25%. Similarly for runs 15-27 the temperature variation was $\pm$ 0.25°C and for runs 28-44 the temperature variation was reduced to $\pm$ 0.1°C. The corresponding viscosity changes are $\pm$ 1% and $\pm$ 0.5% respectively.

Fluid density ρ (g cm^{-3}) The change of fluid density because of leaching was not measured, and has been assumed to be negligible. The temperature dependence of the fluid was assumed to be the same as pure water which for the range 15°C to 25°C is only $\pm$ 0.1%,[9] assuming that an average density at 20°C was used as a datum. Hence the temperature dependence of density can be ignored.

Length of core ℓ (cm) For runs 1 - 22 the core length was measured using a metal rule. Measurements to the nearest 0.5 mm were obtained, which for an average core length of 2.5 cm is an error of $\pm$2%. For runs 23 - 44, the length of the core was taken as the average of six measurements, using a micrometer. The variation of length was reduced to $\pm$0.05mm which for an average core length of 2.5cm represents an error of $\pm$0.2%.

Differential pressure head Δh_w (cm) For runs 1 - 4 the differential pressure head was read directly from a calibrated scale. To estimate an average error in the measurement of Δh_w at the start of the experimental run, it was assumed that the pressure head difference of 40cm existed across the core. Pressure head measurements were determined to an accuracy of $\pm$0.5mm, and the average error was taken as $\pm$1.25%. The pressure head difference at the end of the experiments was much reduced and hence the magnitude of the pressure error correspondingly increased. Since the pressure head differences at the end of each run were different individual errors in Δh_w have been calculated for each run.

The error calculation in Δh_w for runs 5 - 44 is different since Δh_w was obtained indirectly from the chart recorder as a difference in millivolt readings. Examination of the third calibration curve showed that the largest calibration error, (i.e. difference between the experimental value and the optimised value using the regression technique) was $\pm$1%. A further error is intro-

duced due to inaccuracies in the measurement of the millivolt chart recorder values. At the start of the experiment, an average millivolt difference of 10 mv (= 50 divisions) was assumed. Millivolt readings were determined to an accuracy of 0.5 divisions and hence the initial average error was conservatively estimated to be $\pm 1\%$.

After failure, the pressure difference across the core was much reduced. The magnitude of the final pressure difference was often of the order of half a division (same value as the experimental accuracy). Hence at the end of an experimental run the error associated with the measurement of Δh_w was taken as $\pm 100\%$. However, for runs 5, 14, 22, 26, 27, 28, 32-36, 38 and 41, the final millivolt difference was determined by using a more sensitive but uncalibrated scale, i.e. full scale readings of 2 mv, 5 mv rather than 20 mv. For each of the above named experimental runs the error in Δh_w at the end of the experiment was individually determined.

Sample calculation

(1) Determination of permeability, k. The permeability was calculated using Darcy's law,

$$k = \frac{Q \mu \ell}{A \Delta P} = \frac{4 Q \mu \ell}{d^2 \pi \rho g \Delta h_w}$$

where the symbols have their usual meaning. As an example, consider the initial pressure difference across the sand-plaster core of run no. 1; $Q = 1.39 \times 10^{-4} \pm 3\%$; $\mu = 0.01 \pm 12\%$; $\ell = 2.54 \pm 0.1\%$; $g = 980.7$; $\Delta h_w = 68.84 \pm 1.25\%$; $d = 2.54$.

$$k = \frac{4 \times 1.39 \times 10^{-4} \times 0.01 \times 2.54}{(2.54)^2 \times \pi \times 1. \times 980.7 \times 68.5}$$

$$= 1.037 \times 10^{-11} \pm 18.35\%$$

i.e. $k = 1 \times 10^{-11} \pm 18.35\%$ (cm²)

(2) Calculation of porosity, ϕ. The weight of water absorbed by the core after vacuum saturation was converted to a volume of water,

which was taken as the volume of voids within the sample. As an example consider the data for run 39.

Perspex sample holder and saturated core	229.03 (g)	$\pm$0.01 (g)
Perspex sample holder and dry core	221.11 (g)	$\pm$0.01 (g)
Weight of water absorbed	7.92 (g)	$\pm$0.02 (g)

Volume of water at 22°C = (7.92/0.998) = 7.9359 (cm^3)

Net volume of core = ($\pi x 3^2 x 3.995$)/4 = 28.2389 (cm^3)

Percentage porosity of the core =

(100 x 7.9359)/28.2389 = 28.1 $\pm$0.55%

The error associated with the weighings of the wet and dry cores is $\pm$0.25%; the error associated with the measurement of water density is $\pm$0.1%; the error associated with the measurement of length is $\pm$0.2%. Hence the net error is $\pm$0.55%. Note, the average error associated with the measurement of length for runs 1 - 22 was taken as $\pm$2% whereas for runs 23 - 44 the average error was $\pm$0.2%. The error associated with the measurement of flow area A has been neglected.

APPENDIX IV

1. Determination of the cup conductance, when employing the established method.

In this method the tensiometer is allowed to develop its maximum suction, h_{so}, usually by allowing moisture from the tensiometer cup to evaporate into the air. The porous cup is then immersed in "free" water and corresponding measurements of time and suction are recorded.

The flow rate of water into the tensiometer is given by

$$(d_V/d_t) = -K\ (h_s - h_{fs}) \qquad \text{(a)}$$

where d_V is the volume of fluid passing into the tensiometer in time d_t; K, the cup conductance; h_s, the suction in the tensiometer at time t; h_{fs}, the suction of a free water surface, which is taken as equal to zero.

The sensitivity, S_e, of the tensiometer can also be expressed in differential form,

$$(d_{h_s}/d_V) = S_e \qquad \text{(b)}$$

Combining eqns. (a) and (b) to eliminate d_V, and re-arranging

$$(d_{h_s}/h_s) = -K\ S_e\ d_t \qquad \text{(c)}$$

which on integration between the limits t = 0, $h_s = h_{so}$ and t = t, $h_s = h_s$ yields

$$\ln\ (h_s/h_{so}) = -K\ S_e\ t \qquad \text{(d)}$$

Equation (d) is the same as eqn. (1) in the text (c.f. section 3.4).

2. Determination of the cup conductance, when employing the "in situ" method.

In this method, the tensiometer is initially at equilibrium with the free water surface. The porous cup is then brought into contact with a large amount of dry porous material. Measurements

of increasing suction versus time are recorded. It is assumed that the volume of fluid absorbed by the porous material is small and is insufficient to alter the suction developed by the dry porous material during the absorption process.

The flow of water out of the tensiometer is

$$(d_v/d_t) = K\ (h_s - h_{ms}) \qquad \text{(e)}$$

where h_{ms} is the suction developed by the dry porous material, and is assumed to remain constant. The other symbols have their usual notation.

Combining eqns. (c) and (e) to eliminate d_v and re-arranging

$$d_{h_s}/(h_{ms} - h_s) = -K\ S_e\ d_t \qquad \text{(f)}$$

which on integration between the limits $t = 0$, $h_s = 0$ and $t = t$, $h_s = h_s$ yields

$$h_s = h_{ms}(1 - e^{-K\ S_e\ t} \qquad \text{(g)}$$

Equation (g) is the same as eqn. (2) in the text (c.f. 3.4)

APPENDIX V

Sample calculation showing the conversion of mercury-water height differences of the tensiometer instrument into suction pressure head of water with respect to the position of the tensiometer cup and at the cellar floor. The heights used in the calculation are shown in Fig. 73, and are all measured in centimetres. The four heights of interest are

h_1, the mercury height difference of the tensiometer

h_2, the height of the mercury-water interface of the manmeter above the zero level of graduated scale.

h_3, the height of the zero level of the graduated scale above the cellar floor, which was constant for all three sites,

h_4, the height of the tensiometer cup above the zero level of the graduated scale.

The suction observed at the tensiometer cup is given by the expression

$$h_1 \rho_m + \rho_w (h_4 - h_2)$$

The suction observed at the cellar floor is given by the expression

$$h_1 \rho_m - \rho_w (h_2 + h_3)$$

where ρ_m is the density of mercury which was assumed to be 13.5 (g cm^{-3}) and ρ_w, the density of water which was assumed to be 1 (g cm^{-3}). Thus as an example if $h_1 = 7.55$; $h_2 = 45.4$; $h_3 = 40$; $h_4 = -10.5$ then the suction at the tensiometer cup is

$$7.55 \times 13.5 + 1 \times (-10.5 - 45.5) = 45.9 \text{ (cm of water head)}$$

The suction at the tensiometer cup when corrected to the datum plane (cellar floor) is given by

$$7.55 \times 13.5 - 1 \times (45.5 + 40) = 16.4 \text{ (cm of water head)}$$

APPENDIX VI

Calculation of the suction developed with respect to the evaporating surface.

Height of the evaporating measured upon the graduated scale, h_1 (cm)

Height of the air-mercury interface measured upon the graduated scale, h_2 (cm)

Height of the water-mercury interface measured upon the graduated scale, h_3 (cm)

Assumed density of water, ρ_w, 1 (g cm^{-3})

Assumed density of mercury, ρ_m, 13.55 (g cm^{-3})

The suction with respect to the evaporating surface (cm of water head) is given by $(h_2 - h_1)\ \rho_m - (h_2 - h_3)\ \rho_w$.

Example. Run 1 (after 4.5 hrs) $h_1 = 31.0$, $h_2 = 36.2$, $h_3 = 3$.

Note h_3 was the same for all the experimental runs.

Suction with respect to the evaporating surface, (5.2 x 13.55) - (33.2 x 1) = 37.26 cm of water head.

APPENDIX VII

Calculation of the Grashof and Schmidt numbers

1. Assumptions, values of constants and experimental values.

wall temperature	$17.5^{o}C$
Air temperature	$24.5^{o}C$
relative humidity	43%
Average molecular weight of air	28.95 (g $mole^{-1}$)
Molecular weight of water	18.02 (g $mole^{-1}$)
Molecular weight of mixture	$28.95 - (28.95-18.02)p_v/P$

p_v, vapour pressure of water

P, the total pressure (assumed to be 1.01325 bar).

Diffusion coefficient of water vapour in air, D_{atm}, 0.239 (cm^2 sec^{-1}) at $8^{o}C$.

Diameter of the evaporating surface 3 (cm)

gravitational acceleration	980.7 (cm sec^{-2})
Universal gas constant, R_m	8.31×10^7 (erg g $mole^{-1}$ $^{o}K^{-1}$)

The properties of viscosity of the mixture, and diffusion coefficient were evaluated at the arithmetic mean temperature, $21^{o}C$ ($294^{o}K$). The viscosity of mixture was taken as that of pure air.

2. Calculation of the density difference $\Delta\rho$.

Below the critical region, Boelter[19] stated that the product of the Schmidt and Grashof numbers was less than zero ($N_{Gr} \times N_{Sc} < 0$). The density at the evaporating surface was greater than the bulk air. For $N_{Gr} \times N_{Sc} < 0$, the density difference, $\Delta\rho$ is $\rho_a - \rho_w$. Note, the subscripts a, w, T refer to properties of the bulk air, the wall and total respectively.

The pressure of the gas (dynes cm^{-2}) is given by the expression

$$P_T = (\rho R_m T)/(M)$$

where P_T is the total pressure; ρ, the density; R_m, the Universal gas constant per mole; M, the molecular weight of the gas; T, the absolute temperature.

The density difference $\Delta\rho$ is given by

$$\Delta\rho = \frac{P_T}{R_m}\left[\frac{M_a}{T_a} - \frac{M_w}{T_w}\right]$$

It is assumed that the pressure at the wall surface and in the bulk air is the same.

$$\Delta\rho = \frac{P_T}{R_m}\left[\left(\frac{28.05 - \frac{10.93\ p_a}{P_T}}{T_a}\right) - \left(\frac{28.95 - \frac{10.93\ p_w}{P_T}}{T_w}\right)\right]$$

which on substitution of the values

$$\Delta\rho = \frac{1.01325 \times 10^6}{8.31 \times 10^7}\left[28.95\left(\frac{1}{297.5} - \frac{1}{290.5}\right) - \frac{10.93\times10^3}{1.01325\times10^6}\left(\frac{20}{290.5} - \frac{13.2}{297.5}\right)\right]$$

$$\nabla\rho = -\ 0.00002537\ (g\ cm^{-3})$$

3. Calculation of $N_{Gr} \times N_{Sc}$.

$$N_{Gr} \times N_{Sc} = \frac{\ell^3\ g\ \Delta\rho}{\mu\ D_{atm}}$$

Note $D_{atm\ 21^oC} = 0.329\ (294/281)^{1.5} = 0.256\ (cm^2\ sec^{-1})$

$\mu_{air\ 21^oC} = 1.6 \times 10^{-4}\ (g\ cm^{-1}\ sec^{-1})$

$$N_{Gr} \times N_{Sc} = -\left(\frac{27 \times 980.7 \times 2.537 \times 10^{-5}}{1.6 \times 10^{-4} \times 0.256}\right)$$

$$= -\ 1640$$

CHAPTER EIGHT

DISCUSSION OF THE PHENOMENON OF RISING DAMP

1. Introduction

This chapter is divided into four parts. The first part (Section 2) is a theoretical section in which the equation of motion is redeveloped in terms of "free energy" type expressions rather than their equivalent "diffusivity" type expressions. "Diffusivity" type expressions were initially proposed by Philip[1] and have been discussed in Chapter Three.

The advantage of "free energy" expressions over the "diffusivity" expressions is that the potential gradients of the former are expressed in consistent units (ergs g^{-1} cm^{-1}) whilst the units of the "diffusivity" potentials are related to the particular potential, e.g. for thermally driven flow, the potential gradient has units of degrees centigrade per centimetre. Because the "free energy" potential gradients are expressed in consistent units, it is easy to compare the relative efficiency of each mode of moisture transport when unit potential gradients are applied.

A consequence of this superficial comparison is that inefficient modes of moisture transport can be identified, and can subsequently be omitted from the equation of motion without any significant loss of accuracy in predicting the overall net moisture flux, thus simplifying the equation of motion of moisture within porous building materials.

The second part of the chapter is an examination of the relative magnitude of each mode of moisture movement in soils or under naturally occurring potential gradients. Originally it was hoped to perform the examination upon porous building materials, but a shortage of experimental data prevented the analysis from being performed at the present time. In fact the data used for the soil analysis was not consistent, i.e. not obtained from one type of soil but from several different types of soil. Hence the conclusions of the analysis should be regarded as guidelines

rather than accurate results.

The analysis does not simply represent an example of how to identify the important modes of moisture movement, with soil as the porous material, because water must move through the soil prior to it rising up the wall; thus soil moisture movement is an integral part of Rising Damp.

Several cures and various treatment of Rising Damp are discussed in the third part of the chapter. The cures include active and passive electro-osmosis, injection methods and installation of new damp proof courses. Methods of alleviating and hiding dampness are also examined.

The chapter is concluded by an assessment of the whole phenomenon of Rising Damp with regard to the theoretical and experimental work that has been covered previously. Included in the assessment are suggestions for further work.

2. Equation of motion. Free energy expressions.

The diffusivity type equation representing each mode of water transport can be written in the following general form

$$J_\alpha = - D_\alpha \nabla \alpha \qquad (1)$$

where the subscript α refers to pressure, temperature, solute concentration and electrical potential; J_α, the velocity of fluid associated with the gradient of α; D_α, the diffusivity (associated with either the liquid or vapour phase) related to the gradient of α.

The diffusivity expressions have been discussed in detail in Chapter Three.

In terms of free energy, the equation corresponding to equation (1) may be written as

$$J_\alpha = - K_\alpha (\nabla_f)_\alpha \qquad (2)$$

where $(\nabla_f)_\alpha$ is the free energy gradient associated with the

gradient of α; K_α, the coefficient that relates the liquid velocity, J_α, to the free energy gradient associated with α.

In Chapter Two it was stated that free energy gradient can be expressed as energy per unit volume, unit mass or unit weight. In the subsequent expressions the free energy gradient will be consistently expressed as energy per unit mass per cm (ergs $g^{-1}cm^{-1}$).

2.1 Moisture liquid diffusivity

Liquid flow induced by pressure gradients is commonly expressed in two forms. It can be expressed as a diffusivity type equation where a difference in volumetric moisture content corresponds to the pressure gradient, or liquid flow can be expressed directly in terms of pressure gradient. The latter form is known as Darcy's law. The two forms are given by the expressions

$$J_{\theta L} = - D_{\theta L} \nabla\theta \tag{3}$$

$$J_{PL} = - (k/\mu) \nabla P \tag{4}$$

where the subscripts, θ, P, L refer to volumetric moisture content, pressure, liquid phase respectively; $D_{\theta L}$, the moisture liquid diffusivity; J, the velocity of liquid water; k, the permeability of the porous material to water; μ, the viscosity of water.

Expanding the pressure gradient term, ∇P, in eqn.(4) yields

$$J_{PL} = - (k/\mu) \rho_w g \nabla h_w = -K \nabla h_w \tag{5}$$

where ρ_w is the density of water; g, gravitational acceleration; h_w, the pressure head of eater; K (= $(k \rho_w g/\mu)$), the hydraulic conductivity.

The free energy gradient, $(\nabla_f)_\theta$, and free energy coefficient, $K_{\theta L}$, can be expressed in terms of the diffusivity equation thus

$$(\nabla_f)_\theta = \partial h_w/\partial\theta \; \nabla(g\theta) \tag{6}$$

$$K_{\theta L} = \frac{D_{\theta L}}{g} \left(\frac{\partial h_w}{\partial\theta}\right)^{-1} \tag{7}$$

where the symbols have their usual meanings.

Similarly, in terms of Darcy's law, the free energy gradient, $(\nabla_f)_p$ and corresponding flow coefficient, K_{PL}, can be expressed as

$$(\nabla_f)_p = \nabla(P/\rho_w) = \nabla(g\ h_w) \tag{8}$$

and

$$K_{PL} = (k\ \rho_w)/\mu \tag{9}$$

2.2 Thermal liquid diffusivity

It has been assumed in the previous derivation of the thermal liquid diffusivity, that the moisture was solute free. The assumption was introduced to simplify the derivation of the diffusivity coefficient, in that osmotic changes due to temperature dependent dissociation or temperature dependent solubilities can be neglected. In addition it was assumed that liquid phase movement was a result of temperature effects upon the surface forces at the gas-liquid interfaces. The effect of temperature upon contact angle was not considered.

The thermal free energy coefficient, associated with Darcy's law is the same as that of pressure induced flow:-

$$K_{TL} = (k\ \rho_w)/\mu \tag{10}$$

It should be noted that both ρ_w and μ are temperature dependent. The thermal free energy gradient is expressed as

$$(\nabla_f)_T = g \left(\frac{\partial h_w}{\partial \gamma_{LG}}\right)\left(\frac{\partial \gamma_{LG}}{\partial T}\right) \nabla T \tag{11}$$

where γ_{LG}, the interfacial tension between water and air ; T, the temperature. For circular capillaries and zero contact angle, the partial differential $(\partial h_w/\partial \gamma_{LG})$ is equal to $2/(r\ \rho_w\ g)$, where r is the radius of the capillary. With porous materials, r corresponds to the radius of a circular capillary that will just support a water meniscus at the same water suction under the same conditions existing within the porous material

Substitution for $(\partial h_w/\partial \gamma_{LG})$ in eqn. (11) yields

$$(\nabla_f)_T = \left(\frac{2}{r\ \rho_w}\right)\left(\frac{\partial \gamma_{LG}}{\partial T}\right) \nabla T \tag{12}$$

The free energy gradient is a function of r, (i.e. capillary suction or moisture content), ρ_w and $(\partial \gamma_{LG}/\partial T)$. The variation of interfacial tension of pure water as a function of temperature was expressed as[2]

$$\gamma_{LG} = 117.1 - 0.1516\ T \tag{13}$$

where γ_{LG} is the interfacial tension (dynes cm^{-1}) and T, the absolute temperature (^{o}K). The partial differential $(\partial \gamma_{LG}/\partial T)$ is thus equal to - 0.1516. The variation of water density (pure) with respect to temperature is small (approximately 2×10^{-4} g cm^{-3} $^{o}C^{-1}$)[3], and hence can be neglected. Substitution of the values above in equation (12) gives

$$(\nabla_f)_T = (0.3032/r)\ \nabla T \tag{14}$$

Equation (14) shows that for a fixed temperature gradient, the corresponding free energy gradient varies inversely with r, (i.e. capillary suction). For dry porous materials (r small), the corresponding free energy will be relatively large, whilst for wetter porous materials (r large), the free energy gradient will be relatively small.

The flow coefficient expressed in terms of the thermal liquid diffusivity D_{TL} is

$$K_{TL} = D_{TL}\ \frac{r\ \rho_w}{2}\left(\frac{\partial \gamma_{LG}}{\partial T}\right)^{-1} \tag{15}$$

It should be noted that the free energy gradient associated with equation (15) is the same as the free energy gradient as defined in equations (11), (12) and (14).

2.3 Solute liquid diffusivity

An osmotic pressure difference across a semi-permeable membrane induces moisture flow in a similar but opposite manner to

that of an applied mechanical pressure difference. By opposite manner it is understood that osmotic flow is in the direction of increasing solute concentration, whilst mechanical pressure flow is in the direction of decreasing pressure. In addition, Kemper et al[4] have stated that the type of flow of moisture within the pores of a porous material was largely viscous rather than diffusive in character. In view of the two previous statements, it is expected that the flow coefficient for solute and pressure induced flows to be same provided the porous material is unaffected by the solute.

Porous materials do not always behave as semi-permeable membranes but often they act as "leaky" membranes in that the solute is partially restricted from moving within the porous material.

Assuming the concentration gradient to remain constant then the flux of moisture through a leaky membrane would be less than that for a semi-permeable membrane provided the pore structure of the two materials was the same. The flow is less through the leaky membrane because moisture movement is impeded by solute diffusing in the opposite direction. Solute induced flow for a leaky membrane may also be regarded as the fraction of moisture flow that would correspondingly be obtained upon the application of a mechanical pressure gradient of equal magnitude to the osmotic pressure gradient, i.e.

$$J_{CL} = K_C \nabla \pi = - K_p \sigma \nabla P \qquad (16)$$

where J_{CL} is the osmotic flux of moisture in the liquid phase; K_C, the osmotic coefficient (solute liquid diffusivity); K_p, the flow coefficient associated with pressure induced flow. $\nabla \pi$ and ∇P are the osmotic and mechanically applied pressure gradients, and are of equal magnitude; σ, the osmotic efficiency coefficient.[4] [5] [6]

With porous materials classed as semi-permeable membrane, σ will be equal to unity since osmotic pressure differences are as

efficient as mechanical pressure differences in producing moisture movement. However for "leaky" porous materials σ will be less than unity. Kemper et al discussed the effect of solute size[14], film thickness and solute concentration[5] upon σ. It should be noted that σ is the ratio K_C/K_p, and that either K_p or K_C can be independently changed. In other words K_p may remain constant whilst σ is changed because of variations of K_C and vice versa.

The osmotic free energy coefficient, in terms of the Darcy coefficient may be written as

$$K_{CL} = \frac{k \rho_w \sigma}{\mu} \tag{17}$$

Similarly the free energy gradient may be written as

$$(\nabla_f)_c = \nabla\pi/\rho_w \tag{18}$$

However for dilute solutions, and assuming Raoult's law to be applicable (Section 8, Chapter Three), the free energy gradient can be expressed in terms of solute concentration

$$(\nabla_f)_c = (R\ T\ \nabla\ x_s)/x_L \tag{19}$$

where R is the Universal gas constant per gram of solvent (water); T, the absolute temperature; x_s, the mole fraction of ionic species; x_L, the mole fraction of solvent which for dilute solutions may be taken as equal to unity.

2.4 Electro osmotic diffusivity

The electro osmotic diffusivity is more commonly known as the electro osmotic coefficient. The electro osmotic diffusivity is the coefficient that relates the flux of moisture to the applied potential difference,

$$J_{EL} = k_e \nabla E \tag{20}$$

The flow coefficient, k_e, is discussed in greater detail in Chapter Four. The free energy flow coefficient related to k_e can be defined as

$$K_{EL} = k_e/(\sigma)^+ \quad (21)$$

where $(\sigma)^+$ is the net charge density per unit mass of liquid. The free energy gradient can be expressed as

$$(\nabla_f)_E = (\sigma)^+ \nabla E \quad (22)$$

A net charge arises within the fluid since ions of a particular charge, (i.e. positive charge) or even particular ions (Ca^{2+}, Na^+) which are preferentially absorbed or desorbed at the solid surface. An equal but opposite charge remains in the bulk liquid, which is affected by the applied electrical potential gradient. The ions remaining in the bulk are induced to move to a particular electrode, and in doing so, impart a drag upon the surrounding water molecules hence moisture migrates to a particular electrode. Note that the ions themselves may be hydrated, which may also assist the movement of ions to a particular electrode. $(\sigma)^+$ is affected by the ionic species, ionic charge, concentration of the ionic species, an the ion adsorption properties of the solid surface.

2.5 Vapour moisture diffusion

Since it has been assumed that moisture movement in the adsorbed phase is negligible, then the term 'liquid phase' moisture transfer is used to denote transfer which occurs exclusively within the liquid phase. Moisture movement that occurs partly in the liquid and partly in the vapour phase, together with that which occurs exclusively in vapour phase is deemed to be "vapour phase" moisture movement.

Philip et al[7] developed a "simple" theory of isothermal vapour moisture flow within porous materials when subjected to moisture gradients. The theory was an extension of water vapour diffusion in free air. The flow area was modified to allow for the presence of solid and liquid in the diffusion space. A

tortuosity factor was introduced to account for variations of path length.

Philip[8] stated that the "simple" theory was in general agreement with moisture fluxes observed in both the field in the laboratory. Hence the simple theory of isothermal flow, proposed by Philip, can be used to predict isothermal water vapour flow within porous materials when subject to moisture content (pressure) potentials.

However, for water vapour transfer under temperature gradients, Philip[8] stated that the "simple" theory of thermally driven moisture flow was inadequate because observed moisture fluxes were five to ten times greater than that predicted by the "simple" theory. The non-isothermal flow theory was modified by Philip et al[7]. The "simple" theory has been developed in Chapter Three. The subsequent modifications to this theory will be developed in the present chapter in Section 2.7.

2.6 Moisture vapour diffusivity

The vapour flux of moisture in terms of diffusivity coefficient is described by

$$J_{\theta V} = -D_{\theta V} \nabla\theta \tag{23}$$

The free energy gradient associated with the volumetric moisture content is the same as that defined for liquid phase moisture movement when subject to gradients of moisture content.

$$(\nabla_f)_\theta = (\partial h_w/\partial\theta) \quad \nabla(g\theta) \tag{24}$$

The corresponding free energy flow coefficient, $K_{\theta V}$, is defined as

$$K_{\theta V} = \frac{D_{\theta V}}{g} \left(\frac{\partial h_w}{\partial\theta} \right)^{-1} \tag{25}$$

The coefficient $D_{\theta V}$, from the "simple" vapour theory (described in Chapter Three) can be expanded which when substituted into eqn.

(25) yields

$$K_{\theta V} = -\alpha \frac{P}{P-p} (\phi-\theta) D_{atm} \frac{\rho_{SV}}{\rho_w} \frac{1}{RT} \exp\left(\frac{-h_w g}{RT}\right) \tag{26}$$

where α, tortuosity coefficient; P, the total pressure; p, the vapour pressure of water; ϕ, the porosity of the porous material; θ, the volumetric moisture content; D_{atm}, molecular diffusivity of water vapour in air at the absolute temperature T; ρ_{SV}, the density of saturated water vapour at temperature T; ρ_w, density of water; R, the Universal gas constant per gram of water; h_w, the suction pressure head of water; g, the gravitational acceleration.

2.7 Thermal vapour diffusivity

The expression representing the thermal vapour diffusivity derived from the "simple" theory, (c.f. Chapter Three) is given by

$$J_{TV} = -D_{TV} \nabla T \tag{27}$$

D_{TV} can be expanded to yield

$$J_{TV} = -\left[\alpha \frac{P}{P-p} \frac{(\phi-\theta)}{\rho_w} D_{atm} \frac{\rho_V}{\rho_{SV}} \frac{\partial \rho_{SV}}{\partial T} \right] \nabla T \tag{28}$$

where the symbols have their usual meaning.

The observed fluxes of moisture flow have been found to be five to ten times the theoretical fluxes predicted by eqn.(28). Philip et al[7] stated that the greater than predicted moisture flux was a consequence of the interaction between the vapour phase and liquid islands along the flow path. Philip re-examined the diffusional process with respect to a single air filled pore and introduced the concept of a temperature gradient $(\nabla T)_a$ associated with the gaseous phase. The moisture flux associated with a single pore, J_p, was given by

$$J_p = \frac{-P}{P-p} \frac{1}{\rho_w} D_{atm} \frac{\rho_V}{\rho_{SV}} \frac{\partial \rho_{SV}}{\partial T} (\nabla T)_a \tag{29}$$

Note that factors $\alpha(\phi-\theta)$ were taken as unity.

Philip also stated that the water islands were also capable of transmitting moisture, and hence the flow area for vapour transfer is increased from $(\phi-\theta)$ to ϕ.

Summing the diffusional process for each pore yields

$$J_{TV} = \frac{-P}{P-p} \frac{\phi}{\rho_w} D_{atm} \frac{\rho_V}{\rho_{SV}} \frac{\partial \rho_{SV}}{\partial T} (\nabla T)_a \tag{30}$$

No tortuosity factor, α, was introduced because it has already been accounted for in $(\nabla T)_a$.

The ratio η_V $\left(= \frac{\phi(\nabla T)_a}{\alpha(\phi-\theta)\nabla T}\right)$ was introduced. (31)

The first factor, comprising η_V, $(\phi/\alpha(\phi-\theta))$ can be simply evaluated. ∇T is the observed overall temperature gradient, whilst $(\nabla T)_a$ is the temperature gradient in the air filled pores. The method of calculating $(\nabla T)_a$ was derived via an analogous electrical example[9].

Equation (31) is applicable until the onset of liquid continuity. Philip[7] suggested that at the onset of liquid continuity a further slight modification to eqn. (31) was required

$$\eta_V = \frac{(a + f(a)\theta)(\nabla T)_a}{\alpha(\phi-\theta) \quad \nabla T} \tag{32}$$

where a, θ are the volumetric air and volumetric moisture contents respectively; f(a) is a function of the volumetric air content. Before the onset of liquid continuity f(a) was equal to unity. Note ϕ, the porosity is approximately equal to $a+\theta$.

When liquid continuity had been established, as a first approximation, $f(a) = a/a_{cr}$, where a_{cr} is the volumetric air content at the onset of liquid continuity. Philip[7] stated that the agreement between the theoretical estimation of η_V above and

the experimental determination of η_V was satisfactory. In view of the statements above, the revised theory of vapour transfer will be used as a basis to predict thermally induced moisture fluxes.

Inspection of eqns. (27),(28),(30) and (31) show that the vapour flux predicted by the "revised" theory can be simply expressed in terms of the vapour diffusivity predicted from the "simple" theory, together with the factor η_V

$$J_{TV} = -\eta_V \; D_{TV} \; \nabla T \tag{33}$$

where D_{TV} is the "simple" thermal vapour diffusivity and ∇T, the average observed temperature gradient.

The flow mechanism in the vapour phase for moisture and temperature induced moisture flow is the same, that is diffusion. Although it must be remembered that in the latter case (thermal vapour flow) it was necessary to introduce an additional coefficient η_V. Hence the average free energy flow coefficient for thermally induced flow is

$$K_{TV} = \eta_V \; K_{\theta V}$$

$$= -\eta_V \; \alpha \frac{P}{P-p} (\phi-\theta) \; D_{atm} \frac{\rho_{SV}}{\rho_w} \frac{1}{RT} \exp\left(\frac{-h_w \; g}{RT}\right) \tag{34}$$

The corresponding thermal free energy coefficient is (c.f. eqn. (28))

$$(\nabla f)_T = \frac{1}{\rho_{SV}} \frac{\partial \rho_{SV}}{\partial T} RT \quad \nabla T \tag{35}$$

ρ_{SV} and $(\partial \rho_{SV}/\partial T)$ are evaluated at the absolute temperature T. Philip[7] has stated that although $(\partial \rho_{SV}/\partial T)$ is temperature dependent, it is possible to adopt a constant value for the partial differential of 1.05×10^{-6} (g cm^{-3} ^{o}C^{-1}), in the temperature range 10°C to 30°C.

2.8 Osmotic vapour diffusivity

Because of the similarities between osmotic pressure gradients and mechanical pressure gradients, it is reasonable to assume that their free energy flow coefficients are the same

$$K_{CV} = -\alpha \frac{P}{P-p} \frac{(\phi-\theta)}{\rho_w} \frac{D_{atm}}{RT} \rho_{SV} \exp\left[\frac{-h_w g}{RT}\right] \tag{36}$$

For dilute solutions and assuming Raoult's law to be applicable, the free energy expressed in terms of solute concentration gradient

$$(\nabla f)_c = \frac{RT \nabla(x_S)}{x_L} \tag{37}$$

The symbols in eqn. (36), (37) have their usual meaning. Note that moisture flow in the vapour phase for an osmotic pressure gradient is as efficient as flow under a mechanical pressure gradient. Hence the osmotic efficiency coefficient, σ, is not required.

In terms of a diffusivity expression the moisture flux is expressed as

$$J_{CV} = D_{CV} \nabla(x_S) \tag{38}$$

and the free energy flow coefficient can similarly be expressed by

$$K_{CV} = \frac{D_{CV} x_L}{RT} \tag{39}$$

2.9 Vapour diffusion supplement

1. Movement of moisture in the vapour phase by an electrical potential difference has not been considered, since it was assumed that there were no charged particles in the vapour phase.
2. Currie[10a][10b] has shown that the simple tortuosity relationship $\alpha(\phi-\theta)$, proposed by Philip is only of limited applicability and that in general a more complex expression is needed. Rose[11a][11b] expressed Currie's tortuosity function in terms of relative diffusion coefficients. The group $\alpha(\phi-\theta)$ was replaced by the group D_T/D_O multiplied by D/D_T. D is the gaseous diffusion

coefficient through the porous material; D_T, the gaseous diffusion coefficient through the porous material when the pore space is full of the gaseous mixture; D_O, the diffusion coefficient in free air.

The function D/D_T was determined experimentally for a range of water saturations using an inert gas (hydrogen). It was assumed that the functional relationship D/D_T was still the same for water vapour as for hydrogen. Furthermore the problem of thermal vapour transfer was not discussed. In view of the two previous statements, only the vapour diffusion theories of Philip et al. will be used in the following analysis of soil moisture fluxes.

3. Moisture fluxes in soils under natural conditions

In damp walls it is important to identify which are the major modes of moisture transport since this information has considerable bearing upon the optimum treatment of the damp problem. At the present time a full analysis of moisture movement within building materials cannot be attempted due to lack of data. There is however, sufficient data available to be able to perform this analysis upon soils, albeit a very tentative one.

To perform the analysis it is necessary to determine an overall net moisture flux, the moisture conditions and the naturally occurring potentials gradients. The rate of potential evaporation from a free water surface was chosen as the overall moisture flux.[12] The next step in the analysis is to determine the moisture conditions of the soil. This decision is quite important since some of the flow coefficients can change by a factor of one million ($\times 10^6$) over the range of moisture conditions.

It has been stated in Chapter Seven that the suction developed by dry house bricks was found to be about 550 cm of

water head. It was decided to use this information as a guide to the choice of moisture conditions and to limit the analysis to moisture conditions occurring at suctions less than one thousand centimetres of water head. A higher suction than five hundred centimetres of water head was chosen so that a margin of error could be included in the estimations. However some of the flow coefficients exhibit maximum values at a particular moisture content or range of moisture conents; hence the analysis was simplified by using the peak values to determine the maximum flux of moisture that could be obtained from the corresponding modes of moisture transport.

To complete the analysis, it is necessary to determine or estimate the potential gradients that occur naturally in soils. Moisture content gradients and temperature gradients were obtained from a study conducted by Jackson et al.[13][14] Additional estimates of evaporation rate were also obtained from this study.

The measurements presented in the study were recorded during the months of March and April 1971; and are assumed to be representative of conditions occurring in Phoenix, Arizona, America. However, for the purposes of the analysis, it was assumed the potential gradients are similar to gradients developed in this country, at the same time of the year.

Additional moisture fluxes were also calculated from diffusivity coefficients presented by Philip[15] using the potential gradients presented by Jackson et al.[13][14]

The flow arising from electrical potential gradients is different, in that usually the electrical potential is applied externally. Hence the procedure is reversed such that an electrical potential gradient will be determined for a given moisture flux and, varying, electro osmotic coefficients.

Moisture movement due to concentration gradients will be discussed in terms of the osmotic efficiency coefficient (or reflection coefficient), σ.

3.1 Net moisture flux

The net moisture flux was assumed to be equal to the potential evapotranspiration rates of Bedfordshire in England[12] This area was chosen as a typical example of the evaporation rates that are likely to be encountered in this country. The potential evapotranspiration rates are listed as monthly averages, however for convenience the values have been smoothed and have been reproduced as a continuous curve in Fig. 1.

The soil data recorded by Jackson et al[13][14] was obtained during the months of March and early April, hence the potential evaporation for the month of March (Fig. 1) was taken as the "overall" moisture flux to be used in the moisture movement analysis.

3.2 Thermal and moisture gradients

An investigation of the moisture fluxes in soils induced by naturally occurring gradients of temperature and moisture content has been conducted by Jackson et al.[13][14] Ground water liquid and vapour fluxes and corresponding potential gradients were determined at soil depths of 0.5 and 1 cm, on several days in March and April 1971 near Phoenix, Arizona, America. From their measurements, an average temperature gradient within the soil was estimated to be 1.5^{o}C per cm. Similarly, the moisture gradient was estimated to vary in the range 0.025 to 0.075 (cm^3 per cm^4).

3.3 Thermal moisture fluxes

Thermal vapour diffusivity is an example of a flow coefficient which exhibits a maximum value at a particular moisture content. The maximum value presented by Jackson[14] was about 3×10^{-7} (cm^2 sec^{-1} $^{o}C^{-1}$). At low moisture contents the thermal liquid

was so small that it was assumed to be zero. However for higher moisture contents the liquid diffusivity was found to be of the same order of magnitude as the vapour diffusivity. In addition, over a large portion of the moisture content range, the sum of the thermal diffusivites was found to be approximately constant and equal to 3×10^{-7} (cm^2 sec^{-1} $^oC^{-1}$).

The magnitudes of both thermal diffusivities are comparable to the values calculated by Philip.[15] Similarly, the sum of the diffusivities of Philip was found to be approximately constant over a wide range of moisture contents; the peak value of the sum was approximately 2.5×10^{-7} (cm^2 sec^{-1} $^oC^{-1}$).

An alternative estimate of the vapour thermal diffusivity was estimated from the site data of Jackson et al.[14] The average moisture flux was estimated to be 1.67×10^{-7} (g cm^{-2} sec^{-1}), which for the average temperature gradient 1.5 (^oC cm^{-1}) yields a value of 1.1×10^{-7} (cm^2 sec^{-1} $^oC^{-1}$) for the thermal vapour diffusivity. This value is about half the maximum value of Philip and one third that of Jackson. However, it appears that the value of the thermal vapour diffusivity can be assumed to be of the order of 10^{-7} (cm^2 sec^{-1} $^oC^{-1}$).

The site data of Jackson[14] showed that the thermal liquid moisture fluxes (and hence liquid diffusivities) were so small as to be negligible. However, it should be noted that the observations were recorded for low moisture contents where liquid continuity is expected to be low and hence liquid diffusivity is correspondingly low.

Using the joint thermal diffusivity presented by Philip (i.e. 2.5×10^{-7} (cm^2 sec^{-1} $^oC^{-1}$)) and assuming a temperature gradient of 1.5 (^oC cm^{-1}) then the thermal moisture flux was calculated to be 3.75×10^{-7} (cm sec^{-1}), which is about one third of the March evapotranspiration rate shown in Fig. 1.

Letey[16] suggested that the sum of the thermal diffusivities was generally of the order of 8.33×10^{-7} (cm^2 sec^{-1} $^oC^{-1}$). Using this value and a temperature gradient of 1.5 (^oC cm^{-1}), the moisture flux was calculated to be 1.25×10^{-6} (cm sec^{-1}) which is slightly larger than the March potential evapotranspiration rate. From these calculations, it may be concluded that the thermal moisture flux appears to be of sufficient magnitude to significantly contribute to the overall moisture flux.

3.4 Moisture fluxes induced by moisture content gradients

Estimation of the moisture liquid and moisture vapour diffusivities was more difficult since their magnitudes are much more sensitive to moisture conditions existing within the soil. The difficulty was further complicated since for the moisture conditions observed by Jackson et al,[13][14] there was an overlap of values of the liquid and vapour moisture diffusivities.

At low moisture contents, the vapour moisture diffusivity rises rapidly to a maximum value and thereafter declines slowly. The peak vapour diffusivity roughly coincides with the onset of liquid continuity (and liquid diffusivity). Liquid moisture diffusivity increases steadily as the moisture content increases and, over the remaining moisture content range, can change by a factor of one million.

Liquid moisture diffusivities, estimated from the data of Jackson, were of the order of 0.5×10^{-5} and 2.5×10^{-5} (cm^2 sec^{-1}). Similarly, values of vapour moisture diffusivity were estimated to be in the range 0.5×10^{-5} to 3.5×10^{-5} (cm^2 sec^{-1}). The higher values of liquid and vapour diffusivity were observed at the higher soil moisture levels.

The sum of the higher diffusivity values is 6×10^{-5} (cm^{-2} sec^{-1}) and assuming the average moisture content gradient to be 0.05 (cm^3 of moisture per cm^3 of porous material per cm length),

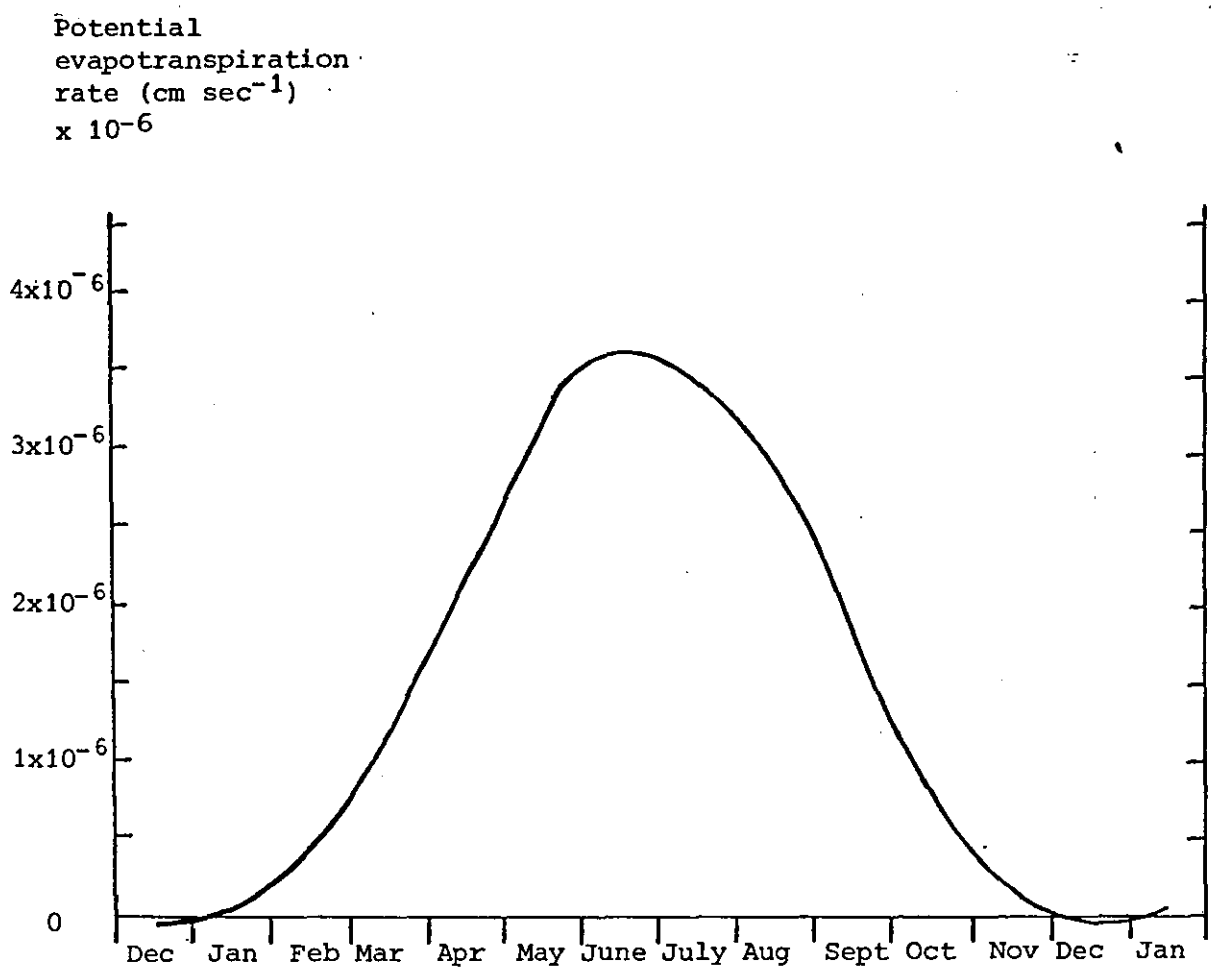

Fig. 1. Monthly potential evapotranspiration rates in England.[12]

then the corresponding moisture flux was calculated to be 3×10^{-6} (cm sec^{-1}). This value is about three times the potential evapotranspiration rate for March or April in this country (Fig. 1). Thus at high moisture contents, it appears that both the liquid and vapour moisture diffusivities are sufficiently large to produce the expected evaporation rate.

Alternatively the potential evapotranspiration rate for March corresponds to a water velocity of 1.2×10^{-6} (cm sec^{-1}); which, assuming an average moisture gradient of 0.05 (cm^3 cm^{-4}) to exist, requires the joint moisture diffusivity to have a value of 2.4×10^{-5} (cm^2 sec^{-1}) to satisfy the evaporation flux. The vapour and liquid moisture diffusivity data calculated by Philip[15] has been reproduced in Fig. 2. It can be observed that the value of the diffusivity (i.e. 2.4×10^{-5} (cm^2 sec^{-1})) falls within a region where the joint diffusivity curve is multivalued.

The bulk of moisture movement can either occur in the liquid phase (low suction) or in the vapour phase (high suction) or in a region where there is approximately equal contributions from both phases (intermediate suctions). However, it should be noted that although the moisture content may remain constant at the three suction levels, the corresponding free energy gradient is dependent upon the moisture conditions and in particular upon the rate of change of suction with respect to moisture content, ($\partial h_w / \partial \theta$). Generally at high moisture contents ($\partial h_w / \partial \theta$) is greater than at low suctions and hence the same moisture gradient at high suctions corresponds to a larger free energy gradient.

Inspection of Fig. 2 shows that the diffusivity value 2.4×10^{-5} (cm^2 sec^{-1}) is satisfied at suctions of approximately 4×10^6, 6.3×10^5 and 6.3×10^3 centimetres of water head. Assuming the temperature to be 20^oC these suctions correspond to 'suction'

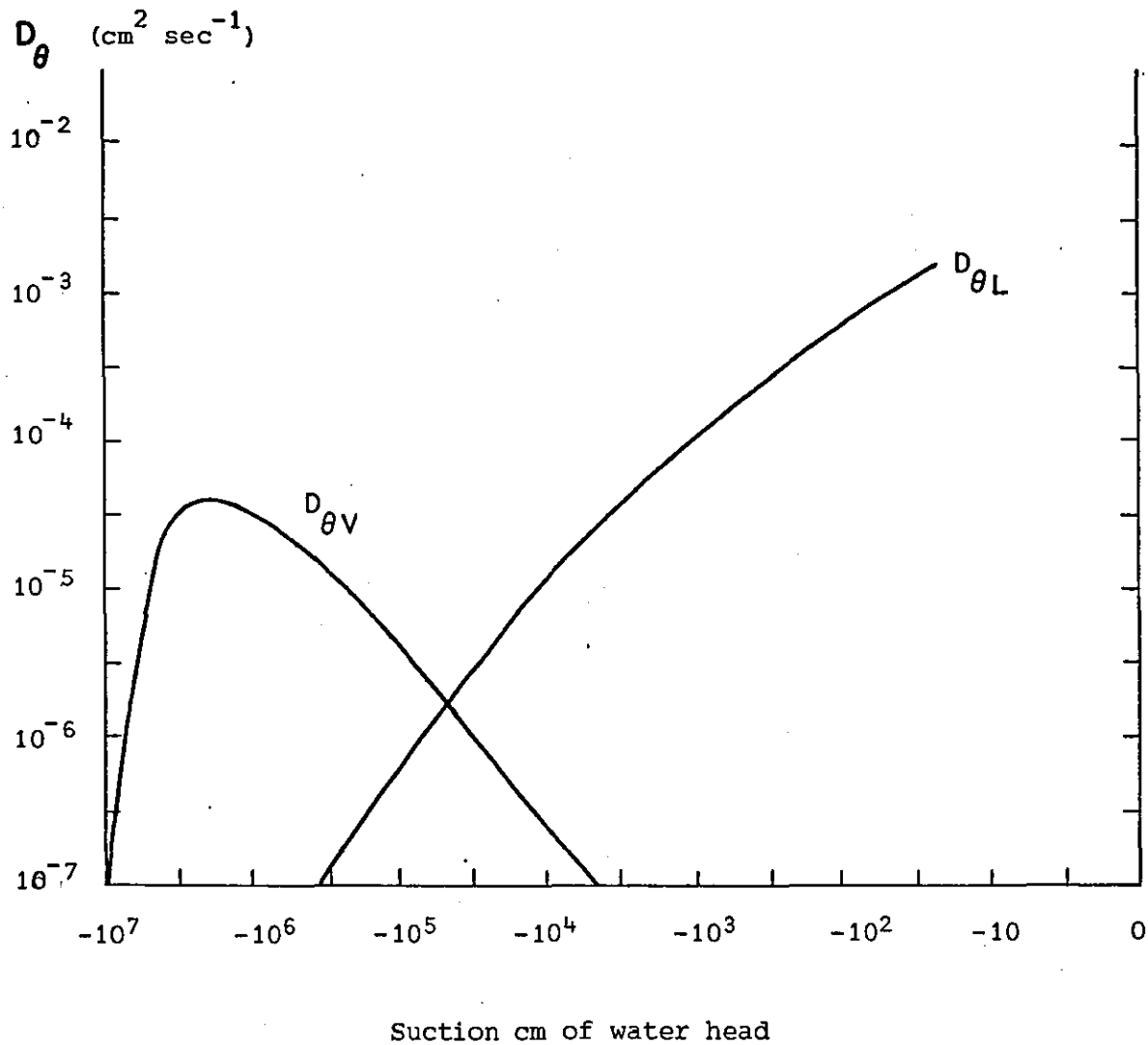

Fig. 2. Liquid and vapour soil moisture diffusivities.[15]

relative humidities of 5.5, 63 and 99 percent. Relative humidity observations at the field site of a cellar suffering from Rising Damp were found to be in the region of 70 to 80 percent (Fig. 77, Chapter Seven).

The diffusivity associated with the higher suctions represents moisture conditions that can be considered as being too dry for Rising Damp to occur, whilst the diffusivity at the lowest suction is more likely to be the controlling factor of dampness in walls. With respect to the diffusivities calculated by Philip[15] it can be concluded that only the liquid phase moisture diffusivity, and not the vapour diffusivity, is the major contributor to the moisture flux, under moisture conditions associated with Rising Damp.

3.5 Solute-induced moisture flow

The effectiveness of concentration potentials in producing moisture flow has been expressed previously using the osmotic efficiency coefficient (or reflection coefficient) σ. This coefficient is generally defined as the ratio of the moisture flux produced by an osmotic concentration gradient, $(\nabla\pi)$, to the moisture flux produced by a mechanical pressure gradient, (∇P), of equal magnitude. Because of the condition $(\nabla\pi)$ equal to (∇P), σ is also defined by the ratio of their corresponding flow coefficients.

Factors which affect the coefficient σ have been discussed in Chapter Three and are not discussed here. In addition, for present purposes, it is only the value of σ at different suctions that is important.

Kemper[17] stated that at suctions less than one bar (10^6 dyne cm^{-2}) soil film thicknesses were so large that salt concentration gradients could be neglected as a factor producing

moisture movement. Similar results were obtained from further experimental studies.[5][6]

Letey[16] concluded that under most conditions, for soil suctions less than 0.25 bar (2.5×10^5 (dynes cm^{-2})), the osmotic flow coefficient can be assumed to be zero. At suctions between 0.25 bar and 1 bar, the value of the osmotic flow coefficient was unlikely to be greater than ten percent of the Darcy flow coefficient. In fact the most likely value was only three percent of the Darcy coefficient.

Rising Damp conditions are unlikely to be found at suctions greater than 1 bar. Hence assuming Letey's lower value for the osmotic flow coefficient ($\sigma = 0.03$), then osmotic pressure gradients thirty times greater than the pressure gradient are required to induce comparable amounts of moisture flow between these two modes of moisture movement.

In order to be able to examine the moisture flux produced by osmotic pressure gradients, it is necessary to express the diffusivity equation in terms of its equivalent Darcy type expression, and noting that the analysis has been limited to moisture fluxes occurring at 1 bar of suction. The hydraulic conductivity of the soil, examined by Philip,[15] at 1 bar suction was estimated to be 5.0×10^{-9} (cm sec^{-1}). The difference in water head to produce the potential evapotranspiration flux of 1.195×10^{-6} (cm sec^{-1}) was calculated to be 2.37×10^2 (cm), which is equivalent to a pressure of 2.32×10^5 (dynes cm^{-2}).

Assuming Raoult's law to be applicable, and for dilute solutions, the osmotic pressure difference between the two solutions can be expressed as

$$\Delta\pi = \frac{RT\ \Delta x_S}{v_L\ x_L} \tag{40}$$

where R, the gas constant per gram of water (i.e. 4.165×10^6 (ergs g^{-1} $^oK^{-1}$)); x_L, the mole fraction of water; Δx_S, the difference in mole fraction of ionic species in the solutions. For the present example the absolute temperature was assumed to be 283^oK, in addition the specific volume of water, ν_L, and the mole fraction of water, x_L, were both assumed to be unity. Furthermore, for dilute solutions, the mole fraction of ionic species can be approximated to the number of moles of solute divided by the number of moles of water.

Hence the difference in moles of solute to produce an osmotic pressure difference of 2.32×10^5 (dynes cm^{-2}), at 10^oC is approximately 1.95×10^{-4} moles of solute per mole of water, or more usefully, 1.0×10^{-2} moles of ionic species per 1000 cm^3 of water. If, in addition the recommendation of Letey is introduced, (i.e. σ is 0.03), then a concentration difference of approximately 3×10^{-1} moles of ionic species per 1000 cm^3 of water will be required to produce the March potential evaporation flux (Fig. 1). The solubility of most common ground water salts exceeds this figure, hence there is no restriction of the development of the osmotic pressure from solubility limitations.

It should be noted that the calculations refer to ionic species in solution, i.e. with sodium sulphate, which assumed to be fully dissociated; one mole of sodium sulphate will produce three moles of ionic species ($2 \times Na^+$ and $1 \times SO_4^{2-}$) in solution. Thus for the above example, the concentration difference of sodium sulphate salt will be one third of the calculated figure, i.e. 1×10^{-1} moles of solid salt per 1000 cm^3 of water. For sodium chloride which is fully dissociated in solution, the required solute concentration difference is 1.5×10^{-1} moles per 1000 cm^3 of water.

Let us now consider whether a concentration gradient can be generated or sustained for a given moisture (evaporation) flux. It is assumed that the flow area for moisture and salts is the same, and that as a simplifying approximation the concentration of salts, the velocity of salts and velocity of water within the pores is constant.

The convective flux of salt carried by the moisture is $V \times A \times \nabla C$ where V is the velocity of moisture within the pore; A, the area for flow and ∇C, the concentration difference of the salt. The back diffusive flow of salt is given by $D \times A \times \nabla C$ where D is the molecular diffusion coefficient of the salt in water. The value of D for a wide variety of solutes and solvents falls within the range 0.5×10^{-5} to 4×10^{-5} ($cm^2\ sec^{-1}$).[18]

Assuming an average value of 1×10^{-5} ($cm^2\ sec^{-1}$) and an evaporative flux of 1.185×10^{-6} ($cm\ sec^{-1}$) together with the assumptions stated above, then the ratio of the diffusive flux to the convective flux of salt is approximately eight. This result means that any solute concentration gradient established across the porous material will steadily diffuse away until the solute concentration gradient becomes uniform.

Even using the value of 0.5×10^{-5} ($cm^2\ sec^{-1}$) for the diffusion coefficient and a peak summer evaporation rate of 3.6×10^{-6} ($cm\ sec^{-1}$) (Fig. 2) as a worst case estimate, then the ratio of the diffusive flux to the convective flux is 1.38; and hence it appears that salt concentration gradients cannot become established. However the difference between the two fluxes is quite small and any interference with either flux could lead to the development of salt concentration gradients.

3.6 Electrically induced moisture flow

This section is only concerned with externally applied potential gradients rather than those developed by uneven movement of ions

due to fluid movement. The theory of electro omosis and electro osmotic coefficient are discussed in Chapter Three and Chapter 4. Furthermore, for present needs, it is only the magnitude of the electro osmotic coefficient that is of interest.

The electro osmotic coefficient has been found to depend on temperature[(19)-(20)] and moisture content[(21)-(23)] and in a more complex fashion upon solute concentration and the ion absorbtion (or desorption) capacity of the porous material (c.f. section 19, Chapter Three). Fortunately, the variation of electro osmotic coefficient of soils, in response to the variables above, appears to be limited to one or two orders of magnitude that is 1×10^6 to 50×10^6 ($cm^2\ sec^{-1}\ volt^{-1}$).[(19)(20)(22-26)]

If the lowest value of the electro osmotic coefficient is used, as a worst case to estimate the electrical potential gradient required to satisfy the potential evaporation flux of 1.185×10^6 ($cm\ sec^{-1}$), then the voltage gradient required is approximately 1 volt per centimetre. However, to satisfy the peak summer potential evaporation rate, an electrical potential gradient of about 4 volts per centimetre is required.

3.7 Summary of natural moisture fluxes

It must be stated that the analysis of soil moisture flow is tentative since no extensive experimental data for a particular soil is available; and that the analysis represents a first order approximation of the moisture fluxes arising from naturally occurring potential gradients in soils.

It was assumed that the upward moisture flux was, at least, equal to the potential evaporation rate. The potential evaporation for March was chosen so as to coincide with thermal and moisture gradients available for that particular month, even

though the measurements may not be typical of this country.

For the assumed moisture conditions, the thermal flux was predicted to be one third the expected potential evaporation flux[13] [14] [15] although a general estimate[16] predicted that the thermal flux was sufficiently large to equal the expected potential evaporation flux.

The moisture flux was of sufficient magnitude to satisfy the potential evaporation flux. However the diffusivity was found to be multivalued, in that the flux could either occur primarily in the liquid phase or in the vapour phase or in a region where the vapour flux and liquid flux were of equal magnitude. However, moisture suction limitations favoured liquid phase flow.

Solute concentration gradients necessary, to satisfy the evaporation flux, were calculated to be relatively small in that solute solubility was not a limitation in the establishment of the concentration gradient required. A simple approximation of the relative movement of salt predicted that development of solute gradients was unlikely to occur and consequently no osmotic flow could be generated. However the two salt fluxes (convective and diffusive) were calculated to be of almost equal magnitude and hence this result should be used with caution.

The position regarding electrically induced moisture flow is slightly different in that the flow is induced externally rather than it occurring naturally. Consequently the analysis was directed towards the determination of the size of the electric potential gradient to satisfy the potential evaporation flux. The potential gradient required to satisfy the potential evaporation rate, as a worst case, was estimated to be of the order of 1 volt per centimetre.

4. Cures and cures of the symptoms of dampness

Treatments of Rising Damp may be classified into two groups:- (i) genuine cures, that is cures which prevent ground water from rising up or entering into the wall; and (ii) treatment or alleviation of the damp symptoms, where the emphasis is not directed towards preventing upward moisture movement but to minimise the effects of dampness.

The more common treatments of damp, classified under group (i) are active and passive electro osmosis, chemical injection, and insertion of a damp proof course. Common treatments classified under group (ii) are cement rendering, painting the surface with specially prepared waterproof paints, covering the damp surface with waterproof materials. Another common form of treatment is methods to improve the evaporation rate, either by removal of low permeability barriers or by increasing the evaporation area.

4.1 Cures of Rising Damp

4.1.1 Electro osmotic methods

Rising dampness within the walls of buildings is often accompanied by an uneven charge distribution, observed in the direction of moisture flow. It is important to determine whether the charge distribution is a cause of moisture movement or a consequence of it. For the former case, removal of the distribution will alleviate the damp problem whereas for the latter case, removal of the charge distribution will accelerate moisture movement within the walls.

Electro osmotic cures can be charaterised as belonging to either 'active' or 'passive' treatments. With 'passive' electro osmotic treatments, no external energy is supplied to the system whereas with the 'active' system, an external direct current is applied to the wall.

Passive electro osmotic damp proofing

The passive electro osmotic system consists of a copper band or series of electrodes fixed into the wall, usually at the height of a conventional damp proof course.[27] The copper band (or electrodes) is earthed to the ground via a metal spike (or spikes). The aim of the system is to provide a path of low resistance such that the unevenly charged state of the wall can be dissipated.

Several theories have been proposed to explain the action of this system as a cure of Rising Damp. It was proposed[27] that the charged state of the wall is somehow associated with the property of surface tension of the ground water. That surface tension is responsible for rising moisture (capillarity). It was argued that removal of the uneven charge distribution via the low resistance path would rob the moisture of its property of surface tension and hence prevent moisture rising within the wall.

The property of surface tension is associated with Van der Waals forces.[28] [29] These forces originate from the electrostatic (charged) interactions of atoms, or molecules, or even particles, of an electrically neutral system. The charges may originate from ions or dipoles (permanent or induced) in the atoms or molecules. It is the sum of these interactions at the phase interface that results in the property of surface tension.

Water is an example of a polar fluid (i.e. a permanent dipole),[30] and that the dipoles of water molecules can be affected by external electric fields, which in turn affect the property of surface tension. Schmid et al[31] investigated the effect of electric fields, of either polarity, upon the surface tension of salt solutions. Schmid found that applied fields of up to 6700 volts per centimetre reduced the surface tension by

about one percent of its normal value. Since the surface tension was reduced for applied fields of either polarity (the reduction is a result of increasing dipole alighment), Schmid concluded that the orientation of the water dipoles was usually only very slight. Pronounced orientation of the dipoles in one direction would lead, on application of an electric field, to a lowering of the surface tension with one polarity and a raising of the surface tension with the reverse polarity. This may be followed by a lowering of the surface tension in the case where the applied field is strong enough to reverse the dipole orientation.

The almost random orientation of water molecules (and associated ions) is not a condition which would be affected by removal of excess local ionic charge. Hence it is concluded that the earthed copper band cannot significantly affect the property of surface tension of moisture, and hence prevent its subsequent movement up the wall. A simple repudiation of this theory would be to test whether a liquid meniscus could be observed when a copper plate is dipped in water, or whether water could be observed to rise up a copper capillary.

A general comparison between active and passive damp treatments has been discussed, in a later paper by Holmes.[32] In the later paper, the wall was likened to that of a battery on permanent trickle charge. It was argued that the charged state of the 'battery' was responsible for Rising Damp and that by discharging the battery, the problem of dampness could be cured. A simplified diagram of the wall moisture system presented by Holmes can be found in Fig. 3.

In the passive system it is argued that the copper band provides a low resistance path such that the excess charges can neutralise each other. Alternatively the excess charges can be actively destroyed using an external D.C. generator G.2.

It is interesting to note that Reuss demonstrated that for powdered silica water moved from the anode to the cathode.[33] Building materials are commonly composed of silaceous materials, and it is to be expected that moisture would migrate from the anode to the cathode. Inspection of Fig. 3 shows that the polarisation of the generator G.2 would in fact accelerate the upward movement of moisture.

From this it may be inferred that removal of the positive charge from the wall would exacerbate the dampness, a point which was noted by Richardson.[34]

A more scientific explanation of how the passive system of electro osmosis might cure Rising Damp was proposed by Gray[35] who discussed the problem in terms of thermodynamics of irreversible processes. Gray proposed that ground water, containing dissolved salts, was drawn up the wall by the normal capillary potential of the wall. The concentration of dissolved salts increases with height because of evaporation. Subsequently the differential concentration of salts produces an osmotic pressure head in addition to the capillary head, which would enhance moisture flow up the wall. The process would continue until a maximum osmotic pressure difference was developed.

A maximum solute pressure would be established when back diffusion of salt down the wall becomes equal to the upward migration of salt associated with the ground water flow or when the concentration of salt in solution becomes limited by the solubility of the salt. If the solubility product is exceeded then localised efflorescence would appear as a salt band, high up the wall. Its upper limit may be taken as the boundary between the wet and dry portions of the wall. A schematic diagram of the above process can be found in Fig. 4.

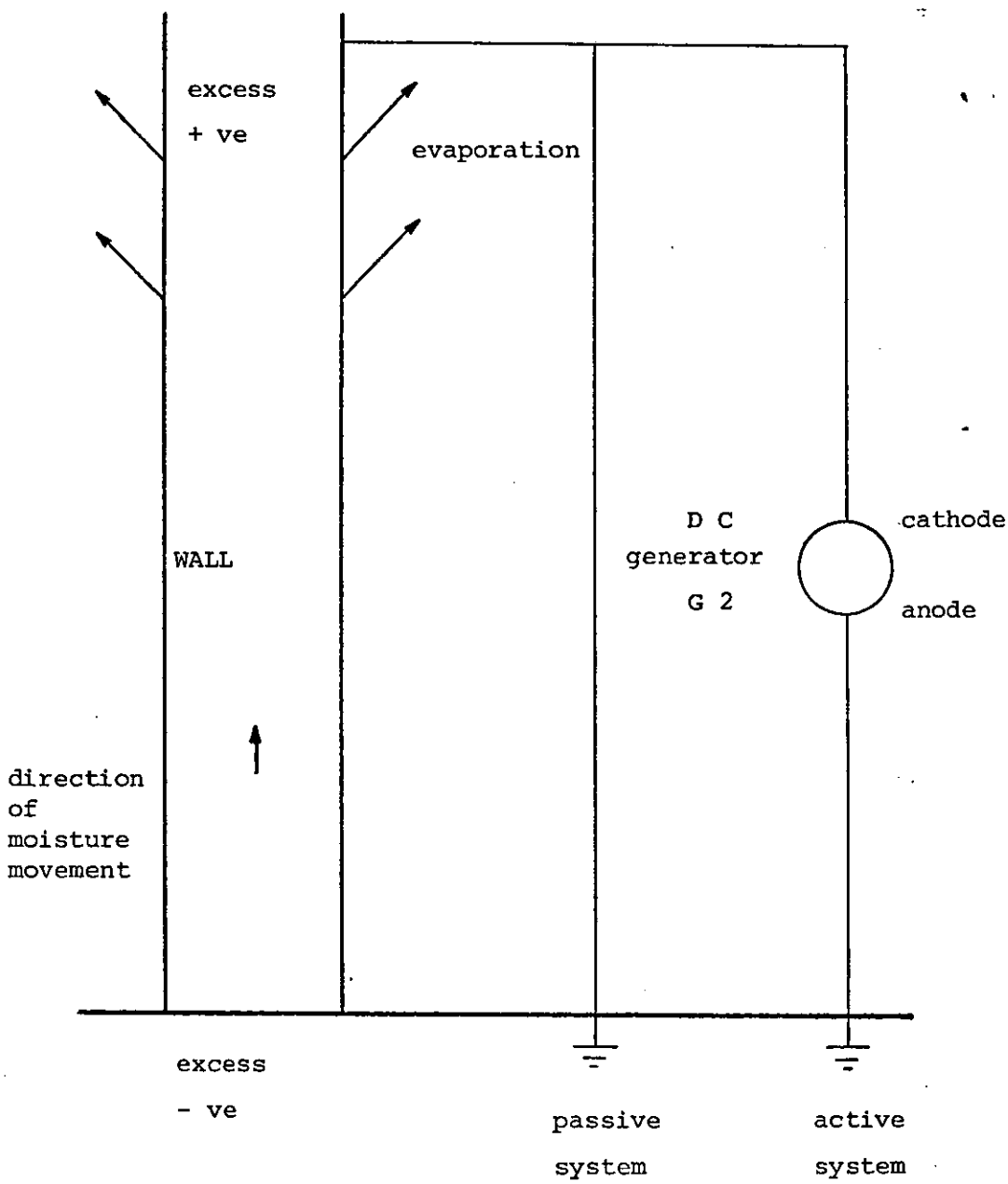

Fig. 3. A schematic circuit diagram showing alternative methods of preventing rising damp by electro osmotic damp-proofing.

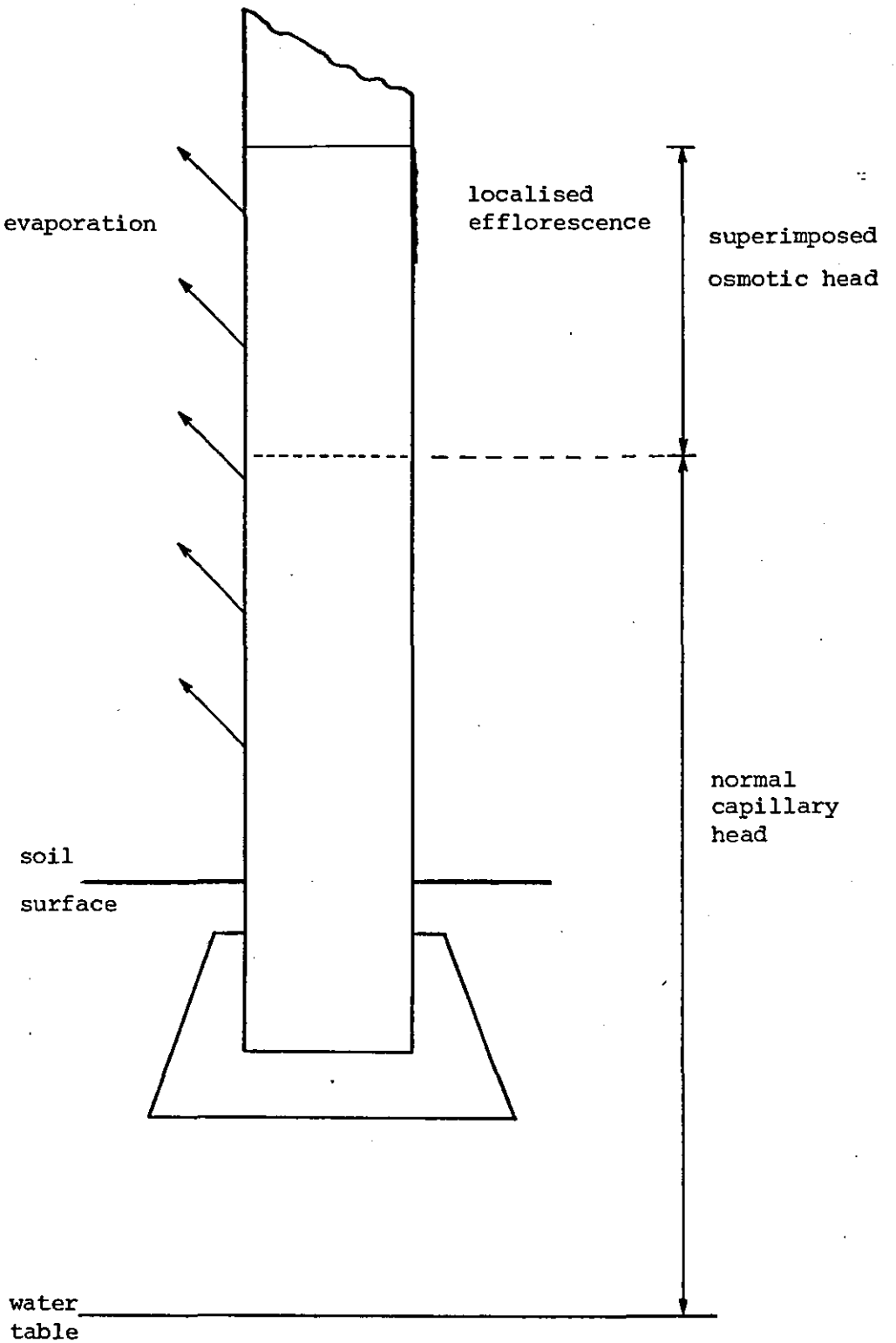

Fig. 4. Schematic illustration of a capillary rise - evaporation cycle producing an osmotic head which is superimposed on the normal capillary head in a masonry wall.

The surfaces of porous building materials normally acquire a negative charge, either by absorption of anions (-ve) or more likely by desorption of cations (+ve). In either case the bulk liquid is left with a net positive charge. Upward movement of the bulk liquid may lead to an accumulation of cations higher up the wall. This effect is enhanced by the negatively charged surface since it would repel anions and attract cations.

Upward anion movement can be restricted or even prevented when thin films of moisture or small pores are encountered. The restriction of ions by charged surfaces has been used to explain the temporary blocking of membranes.[36] In addition negatively charged ions tend to be larger than cations and hence anions might be physically impeded or completely restricted from entering certain pores or films, as noted by Richardson[34] and experimentally demonstrated by Kemper and Evans.[4]

For the system described above, the mobility of cations is greater than that of the anions and it is expected that a positive charge would accumulate higher up the wall, and a net negative charge would accumulate at the base of the wall. In addition, the volume flow of solution is accompanied by the simultaneous movement of salt and electricity.

The theory of non equilibrium thermodynamics offers a possible description of the flow processes. For systems not far from equilibrium the fluxes are linearly related to their respective driving forces (c.f. Darcy's law). For combined flow systems, an allowance must be made for the coupling of the forces (i.e. salt concentration differences can produce volume (liquid) flow and an electrical current as well as the primary salt flow.

For isothermal conditions, the simultaneous fluxes of volume, salt and electricity can be represented by a 3 x 3 matrix of

driving forces and associated coefficients. If a proper choice of forces and fluxes has been made, then the following identity will hold $L_{ik} = L_{ki}$, which is Onsager's well known reciprocity relationship.[37] The letter L is the flow coefficient associated with a particular driving force. The coefficients L_{ii} are the primary conductivity coefficients whereas L_{ik} $(i \neq k)$ are the coupling, or interaction coefficients. The flow matrix can be characterised by six flow coefficients. Kedem and Katchalsky[38] have shown that the flow matrix can be written in terms of so-called "practical" transport coefficients,

$$J_V = L_p (\Delta P - \Delta\pi_i) - \sigma L_p \Delta\pi_S + \beta I \tag{41}$$

$$J_S = C_S (1-\sigma) J_V + \omega \Delta\pi_S + (\tau_1/(\gamma_1 Z_1 F) I \tag{42}$$

$$I = (\kappa\beta/L_p) J_V + (\kappa\tau_1/(C_S \gamma_1 Z_1 F) \Delta\pi_S + \kappa E \tag{43}$$

Equation (41) may also be expressed in the equivalent form,

$$J_V = L_p (\Delta P - \Delta\pi) + L_p (1-\sigma) \Delta\pi_S + \beta I \tag{41a}$$

Further variations can be generated by substitution of the following relationships

$$\beta = (- P_E L_p/\kappa) \tag{44}$$

$$\Delta\pi = \Delta\pi_i + \Delta\pi_S \tag{45}$$

J_V, J_S, I are flows of volume (liquid), salt (species S) and current, all with respect to unit flow area of porous material. The 'practical' transport coefficients introduced are L_p, the filtration coefficient; σ, the reflection (or osmotic efficiency coefficient); β, the electro osmotic peremeability; ω, solute permeability; τ_1, transference number; κ, the electrical conductance. The additional parameter P_E is called the electro osmotic pressure. The driving forces are ΔP, the mechanical pressure difference; $\Delta\pi$, the net osmotic pressure difference;

$\Delta\pi_i$, net difference in the osmotic pressure arising from all impermeable solutes; $\Delta\pi_S$, the difference in osmotic pressure of the permeable solute. Note that $\Delta\pi = \Delta\pi_i + \Delta\pi_S$; E, the electromotive force measured between reversible electrodes. The other variables are C_S, the mean concentration of permeable solute, defined as $C_S = \Delta\pi_S/(R_n T \Delta \ln a_s)$ where a_s is the activity of the solute; γ_1, a stoichiometric number, that is number of moles of type 1 ion per mole of salt; Z_1, the valency of the type 1 ion not involved in the electrode process; F, Faraday constant; R_m, the universal gas constant per mole; T, the absolute temperature.

Gray[35], using equations (41)-(43) together with the following assumptions:-

(i) For short circuiting, E = 0

(ii) Open circuit, I = 0

(iii) For quasi steady state, $J_V = 0$

(iv) A leaky membrane, $\Delta\pi_i = 0$,

developed the following expression

$$\frac{(\Delta P)_E}{(\Delta P)_I} = \left\{ 1 - \frac{\beta \kappa \tau_1}{C_S \gamma_1 Z_1 F L_p \sigma} \right\} \tag{46}$$

where the subscripts E, I refer to open circuit and closed circuit respectively. The other symbols have their usual meaning. Gray stated that for electrical short circuiting to be successful in suppressing the osmotic component of moisture rise then

$$(\Delta P)_E / (\Delta P)_I \rightarrow 0 \tag{47}$$

Gray however appears to have confused the osmotic component of the pressure head ($\Delta\pi_i$ or $\Delta\pi$) with the 'mechanical' pressure head (ΔP). Inspection of Fig. 4 shows that the assumption $J_V \rightarrow 0$ is not valid.

Let us now reconsider the effect of short circuiting, and concentrate upon its effect upon the moisture flow into the wall. Note, in the present examination, eqn.(41) is replaced by its

equivalent expressiong eqn. (41a), and the group $(\kappa\beta)/L_p$ is replaced by the variable $-P_E$. Assumptions (i), (ii) above are taken to be valid and assuming the wall to be in steady state, then for open circuit J_S, I are both equal to zero. The fluxes and forces associated with short circuiting will be marked by a dash (') whilst for open circuit the fluxes and forces will be unmarked. It is assumed that the transport coefficients remain the same for both open and closed circuit.

Eqn. (41a) for short circuiting yields

$$J_V' = L_p\ (\Delta P-\Delta\pi') + L_p\ (1-\sigma)\ \Delta\pi_S' + \beta I' \tag{48}$$

The current density I' can be obtained from eqn. (43), which when substituted into eqn. (48) yields

$$J_V' = L_p(\Delta P-\Delta\pi') + L_p(1-\sigma)\Delta\pi_S' + \beta\left|-P_E\ J_V' + \kappa(\tau_1/(\gamma_1 Z_1 F)\ )\ (\Delta\pi_S'/C_S')\right| \tag{49}$$

The groups $\kappa(\tau_1/(\gamma_1 Z_1 F\ \ )\ )$ and $L_p(1-\sigma)$ can be eliminated, using equations (43), (41a) for the open circuit to yield

$$(1+\beta P_E)J_V' - L_p(\Delta P-\Delta\pi') = \frac{\Delta\pi_S'}{\Delta\pi_S}\left[J_V\left(1+\beta P_E\left(\frac{C_S}{C_S'}\right)\right) - L_p(\Delta P-\Delta\pi) + P_E\ L_p\ E\left(\frac{C_S}{C_S'}\right)\right] \tag{50}$$

Note that in eqn. (50) for the last term on the right hand side, $P_E\ L_p$ is equal to $-\beta\kappa$.

It is assumed that the mechanical pressure (ΔP) is the matrix (or capillary) suction, and it remains constant irrespective of short circuiting or not. For short circuiting to work J_V' should tend to zero. Furthermore J_V(open circuit) may be eliminated, using eqn. (41a). Hence eqn. (50) may be expressed as

$$-(\Delta P-\Delta\pi') = \frac{\Delta\pi_S'}{\Delta\pi_S}\left[(1-\sigma)\Delta\pi_S\left|1+\beta P_E\ \frac{C_S}{C_S'}\right| + (\Delta P-\Delta\pi)\ (\beta P_E\ \frac{C_S}{C_S'}) + P_E\ E\ \frac{C_S}{C_S'}\right] \tag{51}$$

Both eqns. (50), (51) are characterised by only three transport coefficients (β, P_E, L_p or β, P_E, σ) together with the concentrations C_S, C_S' and permeable solute osmotic pressures (π_S, π_S'), and net osmotic pressure of all dissolved materials ($\Delta\pi$, $\Delta\pi'$). Eqn. (50) predicts the effect of short circuiting whilst eqn. (51) describes the expected effect of short circuiting ($J_V' \to 0$).

It has been stated that the electrical potential differences observed in damp walls were solely a result of the differential mobility between the cations (+ve) and the anions (-ve). The potential difference generated by this uneven movement is called the streaming potential and has been defined by Kedem and Katchalsky[38] as

$$\text{streaming potential} = -\left(\frac{\Delta E}{\Delta P - \Delta\pi}\right)_{\pi_S', I} \tag{52}$$

where the subscripts refer to flows or forces which are held at zero. Eqn. (52) can be obtained by substitution for J_V, from eqn. (41a), into eqn. (43).

Another potential difference (membrane potential) has also been defined by Kedem and Katchalsky[38] in terms of the transference number

$$\text{membrane potential } (=\tau_1) = -\gamma_1 Z_1 F\left(\frac{E}{(\Delta\pi_S/C_S)}\right)_{J_V', I} \tag{53}$$

This potential is related to the concentration difference of the permeable solute across the porous material, and as such, may be likened to the effect of concentration difference upon electrode potential.[28] The dependence of electrode potential upon concentration difference can be expressed by

$$E = \frac{R_m T}{Z F} \ln\left(\frac{a_{i2}}{a_{i1}}\right) \tag{54}$$

where Z is the valency of the species i; R_m, the Universal gas constant per mole; T, the absolute temperature; F, Faraday's constant; a_i, the activity of permeable species i at the two concentration levels 1, 2.

For dilute solutions, the activity (a) can be replaced by concentration, hence eqn. (54) may be written as

$$E = \frac{R_m T}{Z F} \ln\left(\frac{C_{i2}}{C_{i1}}\right)$$

$$= \frac{R_m T}{Z F} 2.303 \log_{10}\left(\frac{C_{i2}}{C_{i1}}\right) \tag{55}$$

For a univalent ion at 25°C, the group 2.303 $R_m T/F$ approximately equal to 0.059 and hence a tenfold difference in concentration would produce an electrical potential difference of 0.059 (volts). Voltage differences in damp walls are generally in the range 0.2 to 0.4 (volts), although readings as high as 0.6 to 0.8 (volts) have been observed.[27] It is apparent from the calculations above that concentration (and temperature) differences in damp walls might account for a large fraction of the observed potential differences, particularly for salts with a high solubility in water.

However, it is immaterial whether the observed voltage differences are a result of either streaming potential or membrane potential since both phenomena are accounted for in the formulation of eqns. (41)-(43) and hence the effect of short circuiting upon the flow of moisture as described by eqn. (50) is unaffected.

The discussion of passive electro osmosis so far has been limited to an investigation of the theoretical principles of how the system affects dampness within a wall. Let us now consider

whether there is any experimental evidence to determine whether the passive system does or does not work. Once again, there appears to be little published data pertaining to the effects produced on installation of a passive electro-osmotic system.

The passive system was observed at two locations in Australia.[39] At the first location, the damp problem was investigated for a period of nine months after the system had been installed. The authors[39] found no evidence that the installation was having any worthwhile effect, and that a later consultation with the owner four years after installation, also confirmed that there had been no apparent reduction in the dampness of the walls. After such a long period it was concluded that it was unlikely that any change in the damp condition of the wall was to be expected.

Observation at the second location commenced about three months after installation of the passive system. Resistance (electrical) measurements by the installers had already shown that there had been a considerable degree of drying out. However, further investigation revealed that the installation of the electrodes had been accompanied by the removal of several layers of oil based paint, up to a height of 1.2 metres above the floor. Paint was subsequently removed from an untreated section of wall, and measurements of moisture content of both treated and untreated wall were recorded, for a further period of ten months. The drying curves of the two walls were found to be almost coincident. From this it was concluded that the passive system did not influence the results, or that there was no evidence, at either site, to suggest that the passive electro-osmotic system facilitated the drying of damp walls.

It is difficult to determine whether the two sites were typical examples of damp walls or whether they were examples of

exceptional conditions where the passive system would produce no desired effects. However, Benster[33], Holmes[27][32] and Wieden[40] all quoted cases where the passive system had been successful in curing wall dampness, but provided no factual evidence to support these claims.

It appears that, as a cure of dampness, passive electro-osmosis is highly controversial. Even if the system does work, it cannot yet be satisfactorily labelled as a 'good' cure, since installation of the system does not always provide a cure of dampness, and furthermore no explanations for the failures have been correlated. This means that there are no guide lines availables to assess whether this type of installation should be used at a given location.

Active electro osmotic damp proofing

The theory of active electro osmosis is much less controversial. The movement of water is a result of the interaction between an applied electrical potential and the electric (Gouy) double layer at the solid surface. The more common (silaceous) building materials acquire a net negative charge at the solid surface either by absorption of anions (-ve) or more likely by desorption of cations.

The negatively charged state of the wall results in a greater concentration of cations near to the solid surface. On application of an external potential difference (D.C.), the cations are induced to flow towards the cathode. However, not all the cations are free to move; general movement of cations is assumed to occur at a given distance from the solid surface. The electrical potential of this shear plane, determined by its proximity to the charged solid surface is called the zeta potential. The drag from the cations as they move towards the

cathode induces moisture to move towards the cathode. Furthermore the cations may be hydrated which may also assist the movement of moisture towards the cathode.

If the solids surface acquired a positive charge then it is to be expected that build-up of moisture would occur at the anode on application of a direct current electrical potential.

The theory of 'active' electro osmosis is discussed more fully in Chapter Four.

Active electro osmosis may be regarded as a peculiar example of electrolysis. The difference between it and ordinary electrolysis arises solely from the presence of the porous material. The action of the porous material is that of a buffer or resistance which enables moisture to build up at one of the elctrodes, a situation that cannot be observed in ordinary electrolysis. The porous material also enhances the movement of water in a particular direction; which is a consequence of the double layer, the ionic concentration associated with the double layer, and the applied electrical potential difference.

Because of the simularity of electro osmosis with electrolysis, it is expected that factors which tend to restore the system to one of ordinary electrolysis are the ones which will reduce the efficiency of the electro-osmotic process. The most obvious factor which affects the electro osmotic coefficient is moisture content (i.e. film thickness). For thin films and assuming a negatively charged solid surface, bulk liquid movement is towards the cathode when a potential difference is applied.

Anions may be partially restricted from entering the thin films because of their similar polarity to that of the solid surface. However, as the film thickness is increased, more and more anions will be able to traverse the porous material in the outer regions of the film away from the surface. However, because

of their charge, anion motion is opposite to the direction of bulk moisture flow. Not only does this reduce the net ionic drag upon the moisture (towards the cathode), but a fraction of the electricity is now conducted by the anions. This action reduces the electrical efficiency of the process.

For large films a situation may be reached where the inner regions of moisture near to the solid surface are moving towards the cathode whilst the outer regions (under the influence of anions) are moving towards the anode. This is an example of a situation where a portion of the electrical energy is merely used to circulate moisture rather than transport it in a given direction. This circulating motion can also occur between pores of dissimilar sizes.[36]

The action of solute concentration is more complex. In dilute solutions the electro osmotic coefficient increases with solute concentration (the increasing ionic concentration in the double layer increases the osmotic effect, until a maximum is reached).

Further increases in solute concentration reduces the effective double layer thickness which in turn reduces the degree of restriction of anions. Greater anion mobility lowers the electrical efficiency of the pores which is reflected by the value of the electro osmotic coefficient (c.f. Chapter Three, sections 18, 19).

The thickness of the double layer is also diminished by the replacement of monovalent ions by divalent ions (or ions of greater valency). The effect of reducing the thickness of the double layer is equivalent to increasing the thickness of the moisture film. In addition the fraction of electricity associated with the electro osmotic pumping action decreases as the concentration of the electrolyte is increased. In other

words as the concentration of electrolyte is increased more energy is wasted on electrolysing the solution rather than transporting water towards the cathode.

From the discussion above, the use of active electro osmosis cannot be recommended for very wet walls containing large pores (greater than 2×10^{-6} (cm)) or for highly saline ground waters, and particularly not in the situation where both are combined.

The action of active electro osmosis may not be limited to the electro osmotic pumping action but may yield the additional benefit of a reduction in permeability of the wall to moisture. The reduction of permeability may be a consequence of salts precipitating at the cathode and/or by entrainment of relatively large charged particles, which have been induced to move by the action of the applied potential difference but have subsequently become trapped within the porous material itself (electrophoretic blocking). With the former method of pore blocking, no lasting reduction of permeability can be obtained since removal of the applied potential difference will allow moisture to re-invade the wall and consequently the precipitated salt barrier will slowly be dissolved away.

Where the blocking is effected by insoluble charged particles the pore blocking may be more permanent since the particles may remain in position after the electrical potential has been removed,[40] i.e. a damp proof course has been established 'electro-phoretically'.

A disadvantage, in the past, of active electro osmosis was corrosion of the anode, a phenomenon which is also frequently associated with electrolysis. Anodic corrosion can lead to failure of the system (reduced effectiveness) and increased costs

(replacement and maintenance of the anodes). However, the problem has been overcome by the introduction of a corrosion-free carbon anode.[34]

Even so the major disadvantage still remains, which is the continual use of electricity by the system. The cost of running the system may become prohibitively expensive especially where highly saline wall moisture is encountered and particularly where the walls are rather damp.

However, it should be noted that as the electrical efficiency decreases, more energy appears as heat in the wall, which may in turn considerably affect evaporation from the wall, thus enabling it to dry out.

4.1.2 Chemical injection

With this method damp proofing is affected by injection of water repellent chemicals into holes spaced at intervals, along the bottom of the wall. The aim of the system is to allow the chemicals to spread out from their injection points until they meet up to form a continuous water proofing band.

Early types of water repellents used were solutions or emulsions of waxes, oils, resins, fats and metallic soaps. A typical example of the latter is aluminium stearate. More recently developed water repellents are silicone based, either as silicones in organic solvents or as silicone emulsions, or as aqueous solutions of siliconates.[41]-[43]

One of the problems associated with chemical injection is that different formulations of chemicals are required for different building materials. An example is the recommendations relating to the silicone treatments of various building materials.[43]

Other problems with chemical injection is the 'useful' life of the barrier; and the effectiveness with which the barrier can

be installed. At present neither the life of the barrier nor the rate of degradation of the barrier by chemical attack can be predicted. Problems associated with the actual injection of the chemicals with respect to the effectiveness of establishing a barrier have been examined at the Building Research Establishment at Watford.[44]

Three areas of difficulty were identified, 'frontal instability', 'residual water saturation' and 'recovery at breakthrough'.

A consequence of frontal instability (fingering, wormholing) is that a complete water proofing barrier might never be formed. The appearance of injected fluid at the outer faces of the damp porous material might be mistakenly associated with complete replacement of wall moisture by water repellent chemical solution.

Similarly recovery at breakthrough, which is defined as the amount of resident fluid displaced before appearance of injected fluid is observed at the outlet surfaces of the porous material, might also be mistakenly associated with complete replacement of the original fluid by the injected fluid.

Residual saturations of water and air, after injection, are important since they can provide continuous moisture pathways across the water repellent barrier and hence reduce the effectiveness of the barrier.

Frontal instability associated with chemical injection is very similar to the instability encountered with oil-water displacement, which has been discussed in Chapter Six. A difference that exists between the two examples of displacement is that for the oil-water example it was assumed that the pore space was either full of oil or water. With chemical injection, the pore

space may initially contain air and water, and after injection, the pore space may contain air, water, and injected water repellent. In other words oil-water displacement was taken as a two phase displacement problem whilst chemical injection represents a three phase (or multiphase) displacement problem. Hence the two phase criterion of frontal stability, defined as the mobility ration η (= $(k_w\mu_o/k_o\mu_w)$ must be extended to allow for the presence of the gaseous phase. Note that k is the permeability to a given phase; μ, the viscosity of a given fluid phase; the subscripts w,o refer to water phase and oil phase respectively.

Although the theory of multiphase displacement is required to describe the process of chemical injection, and in particular the topics of residual saturation and recovery at breakthrough, complete discussion of the theory is deemed to be beyond the scope of present needs and hence it has been omitted. However the effectiveness of chemical injection as a damp proofing has been examined at the Building Research Establishment, Watford.[44]

Investigations at the Building Research Establishment showed that if recovery at breakthrough was adopted as the main criterion for displacement efficiency, the optimum results could be obtained by using slow rates of chemical injection and by increasing the viscosity ratio of the injected fluid to that of the resident fluid. The viscosity effect could have been tentatively predicted from consideration of the mobility ratio η.

Increasing the viscosity of the injected fluid above that of the resident fluid leads to the development of stable fronts (reduced fingering) and ultimately a more effective moisture barrier. Lowering the injection rate allows more time for the development of stable fronts.

The various types of chemical injection methods and the two electro osmotic methods of treating dampness are examples of non-traditional or more modern solutions of the problem of Rising Damp. They are characterised by their ease of installation and almost universal application at most damp locations. These factors contribute to their relative cheapness when compared to the cost of installing more traditional damp proof barriers. However, their effectiveness and success rate in curing dampness is lower than the more conventional treatments of damp.

4.1.3 Traditional methods of treating dampness

Replacement or installation of an accepted damp proof course[45] is the only reliable, and traditional, method of treating Rising Damp. The installation of an established damp proof course is slow, dirty and relatively expensive compared to other treatments of dampness.[46] One method involves the removal of short lengths of house bricks (about 0.6 metres at a time) which are replaced by a course of Engineering Blue bricks.

An alternative method to that of replacing a course of ordinary house bricks is to cut away the mortar binding two courses of bricks together. The mortar may be removed by a hand saw or a specially designed power saw.[46][47] The damp proof course is again inserted in 0.6 metre lengths. This method is less costly than the insertion of a blue brick damp proof course.

A disadvantage of both methods is subsequent settlement of the building, which may cause other structural damage. The amount of settlement is estimated to be about 1.5 millimetres.

With respect to the removal of mortar, two thicknesses of slot may be cut. For the narrower slot half-hard copper sheet is hammered into position, which then acts as the damp proof course. An alternative is to use zinc sheet which is cheaper,

but only has an estimated life of ten to fifteen years. For wide slots the damp proofing materials recommended are two layers of bitumen felt which when in position are ovelapped slightly to provide a more continuous barrier. Soft copper sheet or polythene sheet (0.5 cm thick) may also be used. The latter is impregnated with carbon black to prevent deterioration by sunlight.

Estimated rates of installation of the damp proof course are 3.3 metres for a nine inch wall (22.5 cm). However where obstructions are encountered the rate may decrease to 0.6 metres per hour. For older houses, rates of 1.3 metres per hour for a nine inch wall or 2 metres per hour for a four and half inch wall are common.

The advantage of these methods is that they provide a definite cure for dampness; unfortunately however this type of treatment cannot be used at every location. In addition, as stated earlier, these treatments are relatively more expensive than less traditional treatments.

4.2 Alleviating or hiding dampness

The remaining methods of treating dampness are not strictly classified as cures since moisture is not prevented from entering into the wall but is either assisted in evaporating from the wall or where convenient, the damp area is covered over with a waterproof material.

4.2.1 Methods of increasing the evaporation flux

One of the methods of improving the evaporation rate is removal of impermeable or only slightly permeable layers such as oil based paint, cement, vinyl wallpaper, and plaster. Another method of increasing the evaporation rate is increasing the ventilation rate around the damp wall and/or increasing the

evaporation area. Examples of this type of method is the insertion of air bricks or specially designed tubes (Knapen tubes) or, more simply, by drilling holes through the house bricks or into the building materials. Removal of items from the base of the walls will also assist the drying of the damp areas.

The effectiveness of Knapen tubes has been investigated by Heiman et al[39] who found that the most efficient type of tube was merely a hole drilled into the wall. The authors summarised the conditions which were favourable or unfavourable for the installation of Knapen tubes.

The major problem associated with this method of treating damp is that moisture is encouraged to evaporate. With internal rooms, this would result in cold damp conditions or for inhabited rooms it would require extra energy to keep the rooms warm. This latter situation is also favourable to formation of dew within the room and secondary moisture problems such as growth of moulds or fungi. Hence this method cannot be recommended for internal rooms although it may be suitable for external locations.

4.2.2 Wall linings

Wall linings represent methods of hiding dampness. Types of lining used are cement rendering, oil-based paints, waterproof wallpaper and polythene sheeting. Cement rendering requires the removal of plaster from the wall. The recommended height to which cement should be applied is 0.5 metres above the highest level of dampness. The cement surface may then either be painted or covered in waterproof wallpaper.

Alternatively[46] the plaster may be removed and the wall coated with corrugated pitch or bitumen lathing or to simply coat the wall with bitumen or a rubber tar preparation. Note when rubber tar or bitumen is applied directly to the wall, a special

plaster mix is required which does not shrink on drying. In addition, these materials tend to lose their adhesion from the walls after about 10 years.

A good cheap method which does not necessitate the removal of plaster and which also provides a degree of thermal insulation is the use of plasterboard and timber battens. The wooden battens should be treated with wood preservative and the gap should be treated with fungicide to prevent mould growth.

For damp areas where the plaster has not been damaged, pitch paper may be fixed to the wall with bitumen. Alternatively lead foil together with red lead and gold size, as an adhesive, can be used or even aluminium foil backed by a thermosetting glue, which can simply be ironed onto the wall.

General recommendations relating to the use of wall linings are that the wall should be treated up to a height 0.5 metres beyond the damp area. Where plaster has been removed from the wall, it should be allowed to dry out so that salts which subsequently become precipitated can be removed. It should be noted that where wall linings are used, evaporation is reduced or prevented, and consequently dampness in the wall becomes more severe. The method should be used with caution where there is a danger of moisture reaching structural woodwork.

4.3 Summary of treatments of Rising Damp

Traditional methods of treating wall dampness are the only sure method of curing damp. They are relatively expensive to install because replacement or installation may involve large amounts of structural work. The methods are applicable to most locations where dampness is prevalent. However, the method is not suitable for solid walls and walls constructed of irregular sized building materials. Problems occur where obstructions such

as pipes, are located close to the wall. Settling of the building after installation of the damp proof course may also cause structural problems.

Less traditional methods of treating dampness such as active and passive electro osmosis, and chemical injection suffer the disadvantage that their installation does not necessarily lead to a cure of the damp problem. The action of passive electro osmosis is still controversial. The theory of active electro osmosis is better understood, however the high cost of running the system and its effectiveness in very wet salty areas may prohibit its general use.

Chemical injection suffers from the problem of establishing an effective waterproof barrier, and the length of the useful life of the barrier. However, it is almost impossible to distinguish whether dampness is a result of erosion of the injected barrier or due to its initial leaky installation. Chemical injection is an example of a multiphase displacement problem, which for the sake of brevity has not been covered in the present work.

Wall linings are merely methods of hiding dampness, and cannot strictly be called cures of damp. Care must be taken with their installation, since the method leads to increased wall dampness.

Methods of increasing the net evaporation rate from the wall are examples of attempts to alleviate the damp problem and again cannot be regarded as cures of damp. These methods might be useful for external walls but their use with internal walls leads to cold damp rooms which, if heated, require extra energy to maintain them at a comfortable temperature. Problems of condensation particularly overnight, are also more probable when this system is used. In addition the damp, warm conditions will

favour the growth of moulds, fungi and insects, which cause structural damage particularly to woodwork.

5. Review of the phenomenon of Rising Damp

Rising Damp is usually regarded as the continual upward movement of moisture from the ground into the walls of buildings and then into the atmosphere. The moisture migration process is in fact much more complicated since moisture movement is accompanied by movement of heat energy, solutes and electric charge (current flow).

Additional factors which add to the complexity are:- (i) the considerable variability of the values of the flow coefficients over the full range of moisture conditions, and that these same coefficients exhibit hysteresis when subject to diurnal and seasonal changes in moisture levels. (ii) The spatial and temporal changes of the porous matrix system which permanently alters the values of one or more of the flow coefficients. Typical examples are dissolution of the matrix by rising ground water (leaching) and precipitation of salts at the evaporating surface (pore clogging, efflorescence). (iii) The interaction or coupling between the flows and potentials, i.e. a temperature gradient can induce the flow of moisture (mass) as well as the obvious flow of heat.

The upward flow of moisture is essentially classed as either a flow-limited or an energy-limited process. For the flow-limited process, moisture conditions within the wall are largely determined by the flow of moisture into the wall.

Alternatively with energy-limited moisture motion, moisture movement within the wall is governed by the supply of energy, which is consumed by moisture evaporating at the surface of the porous material.

Energy-limited moisture movement is normally associated with walls that were constructed without a damp proof course or where the damp proof course has failed. The process is characterised by excessive moisture levels within the walls, which can subsequently result in structural damage.

Since moisture is in excess, then evaporation conditions within the damp area of the wall tend to behave as though the wall was a free liquid surface where the surface temperature is equal to or very close to the wet bulb temperature. Also the suction developed by the damp wall will be relatively low.

It should be noted that moisture movement within a wall constructed without a damp proof course, may initially behave as a flow-limited process, however over the years, as a consequence of leaching, the moisture migration process may change into an energy-limited process. The change over may be hastened by the fact that the leached salts may precipitate out at the evaporating surface thus reducing the evaporative area.

Flow limited moisture movement is usually found in walls with a functioning damp proof course. The walls develop higher suctions when compared to energy-limited walls. The level of dampness within the wall is primarily controlled by atmospheric moisture conditions; or in other words, the water vapour pressure of bulk air determines the radii of curvature of the liquid-vapour interface and hence indirectly determines the corresponding moisture content level.

The relatively high suctions (and corresponding low moisture contents) tend to restrict moisture movement solely to the vapour phase or to vapour phase movement with some liquid movement in thin films. Under these conditions solute mobility is seriously

impeded and hence it is unlikely that large amounts of salt could accumulate at the evaporating surface causing damage or efflorescence.

However, where the ground water is very saline and, in addition, the potential evapotranspiration rate is high then solute damage and/or effloresence might be developed by the wall even though the moisture migration process is described as flow-limiting.

In the United Kingdom the most likely type of moisture migration process thought to be responsible for Rising Damp is the energy-limited process. As stated earlier the extent and movement of moisture within the wall under these conditions is primarily affected by the rate of supply of energy to the evaporating surface. In addition moisture conditions within the wall can also be affected by transient moisture conditions within the ground, since the wall offers little resistance to the inflow or outflow of moisture.

Hence the wall would tend to dry out during the summer months when water tables are low, and evaporation is high, and soils relatively dry. The speed and extent of drying of the wall may determine whether extensive efflorescence occurred during this period, however the probability of efflorescence appearing may be offset to some extent by the increasing solubility of the salts during the warm summer months.

During the winter months, the evaporation rate is low, the water tables are high and the soil wetter and colder than in summer all of which contribute to higher moisture levels becoming established within the wall. Similar moisture changes would also be produced as a result of diurnal variations of temperature. The wall would tend to dry out during the daytime and become wetter during the night time.

The prediction of moisture movement during these cyclical atmospheric conditions is complicated by the fact that the hydraulic flow properties exhibit hysteresis during wetting and drying periods within the wall.

Thus to summarise, Rising Damp, in this country is characterised by excessively damp walls where the degree and extent of damp is controlled by energy-limited evaporation and underlying soil moisture conditions. Both of these controlling factors exhibit annual and diurnal variations which leads to complications when analysing the moisture migration process owing to the fact that the hydraulic functions of the porous material exhibit hysteresis on wetting and drying.

The degree and extent of dampness within a wall is also affected by leaching of mortar at the base of the wall, and the amount of pore clogging by precipitated salts at the evaporating surface and, possibly, within the porous material.

It has been reported that salt concentration gradients exist at the surface of walls suffering from Rising Damp[46] but it has not been shown whether these salts do in fact reduce the permeability of the porous material.

The presence of salts within the wall moisture will reduce the water vapour pressure and hence the actual evaporation rate will be less than the potential evapotranspiration rate of pure water under the same atmospheric conditions.

The reduction of evaporation rate owing to the presence of salts within the wall moisture will in fact tend to move the moisture migration process in favour of an energy-limited type rather than a flow-limited type.

Progressive leaching of wall mortar is also a factor which will also tend to shift the balance of moisture migration in

favour of an energy-limited kind. Its action is twofold. Dissolution of the porous matrix by ground water normally results in an increased permeability of the matrix, allowing greater penetration of ground water (and dissolved salts) into the wall. Further dissolved salts within the wall moisture reduces the evaporation rate, as described above.

From the discussion above it will be observed that 'leaching' is peculiar since it is both a consequence of the upward flow of moisture and it is also a controlling factor of the degree and extent of dampness within the wall. In other words it is both a consequence of and a cause of rising dampness.

So far the present description of Rising Damp has been limited to a general discussion of the flow processes and moisture conditions which characterise the phenomenon. Let us now consider particular aspects of the phenomenon. These topics include the interaction of solutes and the wall; the maximum height of the wet line; and the progressive increased height of the wet line.

The most important solute-wall interaction is the generation or maintenance of an osmotic pressure difference within the wall and the corresponding value of the osmotic efficiency coefficient, σ. Osmotic pressure differences are important since they can potentially greatly exceed the normal capillary potential developed by the porous system. In other words, osmotic gradients can suck water up a wall to a far greater height than capillary forces. The osmotic efficiency coefficient is important since it relates the efficiency of the osmotic pressure to transport moisture within the porous material when compared to the amount of moisture transported by mechanically applied pressure gradients of equal magnitude.

Evidence to support the existence of solute gradients within damp walls is that efflorescence can be observed high up a wall where none exists at lower levels; and that experimental analysis, conducted by the Building Research Establishment,[46] of salts within a damp wall, has shown that the concentration of salts high up the wall was greater than salt concentrations at the base of the wall.

However calculations in section 3.5 of this chapter indicated that it was unlikely that concentration gradients could be maintained within walls under normal evapotranspiration rates that exist in this country.

The results of the Building Research Establishment salt analysis refer only to the concentrations of chlorides and nitrates, which are both anions. No corresponding cation concentrations were reported. Hence their results may not be representative of osmotic potentials but merely as overall differential anion concentration differences. However for present purposes, it is assumed that an osmotic potential gradient does exist within the wall and hence its effectiveness in causing moisture movement is determined by the osmotic efficiency coefficient whose value is a function of the moisture conditions existing within the wall.

Unfortunately osmotic efficiency coefficients for partially saturated porous building materials have not been measured, and hence accurate analysis of solute-wall interactions cannot be computed. However the effects and implications upon moisture levels will be considered when the wall is assumed to act as a semi-permeable membrane (worst case estimate) and when the wall acts as a selective semi-permeable membrane or alternatively as a leaky membrane.

If the wall does act as a semi-permeable membrane, then there can be no salt movement from the ground into the wall. For the wall to develop an osmotic gradient it means that salt must already be present in the building materials when the wall was constructed. Fresh supplies of salt to the wall moisture can only occur if the wall moisture encountered solid salts within the wall. In addition as moisture is drawn into the wall, the wall moisture would become more dilute and hence it would be unlikely that efflorescence would occur.

If the osmotic potential is large then considerable amounts of moisture could be sucked into the wall causing the wet line to rise to a much greater height than would have occurred if the moisture was only sucked into the wall by surface tension forces. However, it should be noted that the practical maximum height of the wet line to which moisture can rise is determined by the larger pores of the building material, rather than the height corresponding to the suction head of the finer pores (capillary forces), or the height corresponding to the osmotic suction head (solute forces).

The cases where the wall is regarded as though it was a selective semi-permeable membrane (the wall is permeable to a particular ion or solute species) and as though it was a leaky membrane (the wall is permeable to most ions or solutes, although the ions and solute species have different mobilities within the porous material) are very similar.

Both membrane types will result in regions becoming charged because of selective ion migration, as a result of osmotically induced moisture flow and as a result of ionic diffusion of the selected ion through the material. For a leaky membrane, the charged state is attributed to preferential cation or anion mobility. Further electrical potential differences may be

developed in either type of membrane because of thermal-solute interactions.

The migration of moisture into the wall is determined by surface tension forces and by osmotic forces. The maximum height of the wet line is still determined by the coarser pores of the building materials.

Efflorescence could occur with either type of membrane. With the permiselective membrane diffusion of the selected ion could result in the solubility product of an associated salt being exceeded. With the leaky membrane the production of efflorescence could be caused by the daily wetting and drying cycle. During wetting, when moisture films are thicker, concentrated or almost concentrated solution could be transferred up the wall. On drying, the moisture films would become thinner and as a consequence the mobility of ions or solute moving back down the wall would be restricted or impeded. Salts would be trapped in the wider moisture films existing at the contact points between the solid material. Removal of moisture by drainage or evaporation could cause the solubility products of salts in these films to be exceeded, thus resulting in precipitation of salts.

Since this process is restricted to a particular band of film thicknesses, efflorescence would tend to appear as a white fringe at some point on the wall surface, a phenomenon which can commonly be observed with walls suffering from damp. Note that if the wall dried out rapidly during the summer months a much wider and more extensive zone affected by efflorescence could be developed.

Let us now consider the role of the porous material in determining the maximum height of the wet line in response to

capillary and osmotic suctions.

The height of the wet line is usually taken to represent the boundary between wet and dry sections of the wall, using the floor as a datum level. However for present purposes the height of the wet line will be measured with respect to the free water surface.

In the dry section of the wall moisture movement within the porous material is assumed to occur solely in the vapour phase, that is in a zone where liquid continuity does not exist. Whereas in the wet section of the wall liquid continuity is assumed to exist.

The point at which liquid continuity ceases within the wall is difficult to determine, however it has been found experimentally (Chapter Seven, Fig. 70) that the equilibrium suction developed by dry house bricks was about 550 (cm) of water head. As an approximation this value will be used to represent the equilibrium height to which moisture would rise up a wall, in the absence of evaporation, from a free water surface. If the foundation of the wall was stood in free water, then moisture would rise up the wall to a height of 5.5 (m) and furthermore the pressures measured within the liquid phase in the wall would be less than or equal to atmospheric pressure.

Consider now the effect of an additional osmotic suction gradient within the wall and its effect upon the height of the wet line. As a worst case the foundations of the wall are assumed to act as a perfect semi-permeable membrane.

In addition to moisture sucked into the wall as a consequence of capillary forces, further moisture will be sucked into the wall in response to the osmotic potential.

The height of the wet line corresponding to the combined potentials will be greater than the height reached when only the capillary forces were acting.

The menisci at the base of the wall will be convex towards the vapour phase, and as the pressure at the base of the wall increases, drops of moisture will tend to form at the surface of the wall. Eventually the convex meniscii, within the pores, will no longer be able to support the column of moisture higher up the wall, the meniscii will rupture allowing moisture to drain away down the outer surface of the wall, thus preventing further moisture rise, and in addition, nullifying the osmotic pressure difference at the base of the wall.

Since the rupture pressure, at the base of the wall, decreases as the radius of the capillaries increases, then the rupture pressure will be determined by the larger pores within the building materials. Examination of the pore size distribution of several types of house bricks shows that their larger pores to be in excess of 1000 (μm) (equivalent pore diameter).[48] [49]

Assuming that the moisture fully wets the brick surface ($\theta=0$) and that the surface tension of the ground water is about 75 ($g\ cm^2\ sec^{-2}$) then the rupture pressure of the pores is approximately 3 (cm) of water head. This means that the maximum height of the wet line can only increase by an additional 3 (cm) irrespective of the size of the osmotic pressure (assuming it to be greater than 3 (cm) of water head) and for any type of assumed wall membrane (semi-permeable, selective semi-permeable or leaky).

Although it has been shown that the osmotic head has very little effect upon the maximum height of the wet line compared to the capillary head, the presence of salt may significantly affect the level of moisture within the wall. The presence of salts will reduce the evaporation rate from the wall owing to their effect upon the vapour pressure. Liquid infiltration into the wall will be increased, as a consequence of the moisture flux

generated by the osmotic pressure gradient.

The action of dissolved salts in reducing the evaporation rate and simultaneously increasing the infiltration rate into the wall also provides an explanation of the slow steady increase in height of the wet line, with time. The slow rate of increase in concentration of salts would, consequently, account for the steady rise of the wet line.

Another explanation of the steady rise of the wet line could be attributed to leaching of the building mortar and plaster upon the walls. Dissolution of the soluble constituents from these materials will increase their permeability to moisture which obviously will result in damper walls. The dissolved salts from the mortar or plaster will also contribute to the development of an osmotic head within the wall, to efflorescence and to the reduction of water vapour pressure of wall moisture.

It is of interest to note that if a damp porous material is wetted and then dried to its original suction value, the final moisture content of the material is generally larger than its initial value. Thus the annual wetting and drying cycle within a damp wall may also contribute to the steady rise of the wet line.

6. Suggestions for further work

The major deficiency with respect to the problem of describing Rising Damp is the shortage of experimental data both from the laboratory and from on site locations. Until this data is obtained a complete description of the phenomenon or a moisture balance of the soil-wall system cannot be presented.

Areas that require further investigation are the measurement of evaporation rates from the internal and external walls of buildings suffering from damp; the variation of the flow coefficients with respect to moisture conditions; the magnitude

of naturally occurring potential gradients; and the source of moisture fuelling the damp area (i.e. proximity of the water table).

The data should be correlated on a long term basis (at least two years) and at several locations. A minimum survey time of two years duration is desired so that the reproducibility of the annual cycle of moisture changes within the wall and the neighbouring soil can be examined.

The importance of collecting data from different sites is that the range of variation of each of the naturally occurring moisture flow potentials can be ascertained. The data can also be used to determine whether Rising Damp is characterised by a set of widely differing moisture flow potentials and moisture conditions or whether it is characterised by a limited range of flow potentials and moisture conditions.

Knowledge of naturally occurring wall and soil moisture conditions and corresponding flow coefficients is essential if moisture movement within the wall is to be accurately predicted. The knowledge may be used to simplify the moisture flow equation in that particular modes of moisture movement may be found to be comparatively insignificant and hence may be neglected. However care must be taken not to automatically discount particular modes of moisture transport as always being insignificant.

The knowledge is also useful in that damp problems could be diagnosed more effectively; existing damp treatment could be made more efficient; novel treatment of damp could be developed. The effectiveness of existing damp treatments could be assessed, and the occurrence of future damp problems could be minimised.

Specific topics that require further investigation are active and passive electro-osmosis in building materials,

chemical injection methods and leaching of porous materials. Two items to be investigated with respect to active electro osmosis are the heating effect within the wall, due to the passage of an electrical current, upon the evaporation rate from the wall; and secondly the effectiveness of the pore blocking mechanism, as a consequence of electro-phoresis, with a view to making the effect a permanent feature. The heating effect should be investigated since this may represent a major portion of the moisture lost by the wall during the 'drying out' period on application of the electric potential difference.

Passive electro osmosis requires investigation since its action as a cure of Rising Damp is highly controversial. The theoretical change within a wall as a result of passive electro-osmosis has been predicted by eqn. (50) of this chapter. Experiments are required to test the validity of this expression and to assess the effectiveness of passive electro osmosis as a method of treating dampness. Secondary aspects associated with this topic are determination of the source and cause of the potential difference observed in damp walls, and the magnitude, if any, of the electrical current passing to earth through the copper loop system.

The growing popularity of chemical injection methods as a treatment of dampness requires that this type of method should be investigated both theoretically and experimentally, with a view to improving the installation efficiency and useful life of the chemical treatment.

Experimental investigation is required to test whether leaching of building mortar is a major cause of Rising Damp and that on leaching, increases of moisture permeability of fifty fold can be attained. Further work is required to confirm that the leaching theory presented in Chapter Six predicting a linear

rate of decrease of pressure difference with time, provided the fluid injection rate remains constant, is correct and that this theory can be successfully applied to predict the rate of failure of building mortar as a moisture barrier.

The theory and experimental work associated with leaching, together with that of chemical injection is closely allied to the more economically important field of reservoir engineering, particularly with respect to the improvement of the rate of oil extraction through acidisation, and the consequences of such rates of extraction as reflected by residual oil and gas saturations and the amount of oil recovered before water breakthrough occurs.

7. Conclusions

1. At present there is no theoretical model which fully describes the rate of change of fluid permeability of a porous material when leached by penetrating fluid, injected at constant flow rate.

2. The theory of Scheidegger and Johnson,[50] describing the macroscopic movement of a viscosity front between two fluids, can be modified to partly describe the pressure difference response (or permeability change), caused by a moving permeability front within a plaster of Paris core.

3. Leaching of fresh plaster of Paris cores can result in permeability increases of over one hundred fold.

4. The rate of change of permeability of a porous matrix, caused by leaching of the matrix by penetrating fluid, is governed by the sequential arrangement of interconnecting pores in the matrix.

5. Suction experiments upon dry house bricks showed that their equilibrium suctions to be in the range 500-550 (cm) of water head. At this suction level, the house bricks were still quite

dry, and hence it is concluded that walls suffering from excess dampness should be characterised by capillary suctions of less than 550 (cm) of water head.

6. Where moisture tensiometers are cemented into a wall, the values of cup conductance and time constant of the instrument should be determined using the 'in-situ' method (Appendix IV, Chapter Seven).

7. Osmotic potential differences, within a wall, have very little effect upon the maximum height of the wet line, calculated solely from surface tension forces, that moisture might attain within a wall.

8. Passive electro osmosis as a cure of Rising Damp is highly controversial.

List of Symbols and units of Chapter Eight

A	area for flow (cm^2)
a	volumetric air content
a_{cr}	volumetric air content at the onset of liquid continuity
a_s	activity of solute species s
C	concentration of salt solution (g mole cm^{-3})
C_s	mean concentration of permeable salt species s (g mole cm^{-3})
$D_{\theta L}$	the moisture liquid diffusivity ($cm^2 sec^{-1}$)
$D_{\theta V}$	the moisture vapour diffusivity ($cm^2 sec^{-1}$)
D_{TL}	the thermal liquid diffusivity ($cm^2 sec^{-1}$)
D_{TV}	the thermal vapour diffusivity ($cm^2 sec^{-1}$)
D_{CL}	the solute liquid diffusivity ($cm^2 sec^{-1}$)
D_{CV}	the solute vapour diffusivity ($cm^2 sec^{-1}$)
D_{atm}	molecular diffusion coefficient of water vapour in air ($cm^2 sec^{-1}$)
D	gaseous diffusion coefficient through the porous material ($cm^2 sec^{-1}$)
D_O	gaseous diffusion coefficient in free air ($cm^2 sec^{-1}$)
D_T	gaseous diffusion coefficient through the porous material when the pore space is full of gaseous mixture ($cm^2 sec^{-1}$)
E	applied voltage (stat volt)
F	Faradays constant (stat coulomb)
$(\nabla_f)_\alpha$	free energy gradient associated with the gradient of α
g	gravitational acceleration (cm sec^{-2})
h_w	pressure head of water (cm)
I	current flux density (stat amp cm^{-2})
$J_{\theta L}$	velocity of moisture in the liquid phase produced by a volumetric moisture gradient (cm sec^{-1})

$J_{\theta V}$	velocity of moisture in the vapour phase produced by a volumetric moisture gradient (cm sec^{-1})
J_{TL}	velocity of moisture in the liquid phase produced by a temperature gradient (cm sec^{-1})
J_{TV}	velocity of moisture in the vapour phase produced by a temperature gradient (cm sec^{-1})
J_{CL}	velocity of moisture in the liquid phase produced by a solute concentration gradient (cm sec^{-1})
J_{CV}	velocity of moisture in the vapour phase produced by a solute concentration gradient (cm sec^{-1})
J_{PL}	velocity of moisture in the liquid phase produced by a pressure gradient (cm sec^{-1})
J_{PV}	velocity of moisture in the vapour phase produced by a pressure gradient (cm sec^{-1})
J_{EL}	velocity of moisture in the liquid phase produced by an applied voltage gradient (cm sec^{-1})
J_S	flux of salt (species S) (g mole $cm^{-2} sec^{-1}$)
J_V	net volume flux of moisture (cm sec^{-1})
J_p	moisture flow associated with a single pore (cm sec^{-1})
K	Hydraulic Conductivity (cm sec^{-1})
$K_{\theta L}$	moisture liquid phase free energy coefficient (sec)
$K_{\theta V}$	moisture vapour phase free energy coefficient (sec)
K_{TL}	thermal liquid phase free energy coefficient (sec)
K_{TV}	thermal vapour phase free energy coefficient (sec)
K_{CL}	solute liquid phase free energy coefficient (sec)
K_{CV}	solute vapour phase free energy coefficient (sec)
K_{PL}	pressure liquid phase free energy coefficient (sec)
K_{PV}	pressure vapour phase free energy coefficient (sec)
K_{EL}	electrical liquid phase free energy coefficient (sec)
k	permeability of the porous material to moisture (cm^2)
k_e	electro osmotic coefficient ($cm^2 sec^{-1}$ stat $volt^{-1}$)

L_p	filtration coefficient (cm^2 sec g^{-1})
P	pressure (g cm^{-1} sec^{-2})
P_E	electro osmotic pressure (g $cm^{-1}sec^{-2}$ stat $volt^{-1}$)
p	vapour pressure of water (g $cm^{-1}sec^{-2}$)
R	Universal gas constant per gram of fluid (cm^2sec^{-2} $^oK^{-1}$)
R_m	Universal gas constant per mole of fluid (g cm^2 sec^{-2} $mole^{-1}$ $^oK^{-1}$)
r	capillary radius (cm)
T	temperature (^oK, ^oC)
$(\nabla T)_a$	temperature gradient within a porous material associated with the gaseous phase (^oC cm^{-1})
x_L	mole fraction of solvent
x_S	mole fraction of ionic species in solution
Z_1	valency of type 1 ion
α	tortuosity coefficient
γ_1	stoichiometric coefficient of type 1 ion
γ_{LG}	interfacial tension between the liquid and gaseous phases (g sec^{-2})
η_V	a group defined by $(a + f(a)\theta(\nabla T)_a)/(\alpha(\phi-\theta)\nabla T)$
η	mobility ratio ($= k_1\mu_2/k_2\mu_1$)
θ	volumetric moisture content
κ	electric conductance (stat ohm^{-1} cm^{-2})
μ	viscosity of moisture within the porous material (g cm^{-1} sec^{-1})
π	osmotic pressure (g cm^{-1} sec^{-1})
π_i	osmotic pressure arising from impermeable solutes (g cm^{-1} sec^{-2})
π_s	osmotic pressure arising from permeable solute (g cm^{-1} sec^{-2})
ρ_w	density of water (g cm^{-3})
ρ_{SV}	density of saturated water vapour in air (g cm^{-3})

ρ_V	density of water vapour in air (g cm^{-3})
σ	osmotic efficiency coefficient
$(\sigma)^+$	net charge density per unit mass of fluid (stat coulomb g^{-1})
ν_L	specific volume of water (cm^3 g^{-1})
ϕ	porosity of a porous material
ω	solute permeability (mole sec g^{-1} cm^{-1})
τ_1	transference number of type 1 ion

References Chapter Eight

1. "The concept of diffusion applied to soil water" J.R. Philip. Proc. Nat. Acad. Sci., India, No. 24A, pp.93-104, 1955

2. "Thermodynamics of soil moisture" N.E. Edlefsen, A.B.C. Anderson. Hilgardia, 15, No. 2, Feb. 1943, 298 pages

3. "C.R.C. Handbook of physics and chemistry" 55th Edition 1974-75

4. "Movement of water as affected by free energy and pressure gradients" W.D. Kemper, N.A. Evans. Soil. Sci., Soc. Amer. Proc., 27, No. 5, pp.485-490, 1963

5. "Osmotic efficiency coefficients across compacted clays" W.D. Kemper, J.B. Rollins. Soil Sci. Soc. Amer. Proc., 30, No. 5, pp.529-534, 1966

6. "The effect of osmotic pressure gradients of water movement in unsaturated soils" J. Letey, W.D. Kemper, L. Noonan. Soil Sci. Soc. Amer. Proc., 33, pp.15-18, 1969

7. "Moisture movement in porous materials under temperature gradients" J.R. Philip, D.A. de Vries. Trans. Am. Geophys. Union, 38, No. 2, pp.222-232, 1957

8. "Physics of water movement in porous solids" J.R. Philip. Highway Research Board, Special Report No. 40, pp.147-163, 1958

9. "The thermal conductivity of granular materials" D.A. de Vries. Bull. Inst. Int. du Froid (Annexe), pp.115-131, 1952

10a "Gaseous diffusion in porous media. Part 1 A non-steady state method" J.A. Currie. Brit. Jnl. Applied Phys., 11, pp.314-317, 1960

10b "Gaseous diffusion in porous media. Part 2 Dry granular materials" J.A. Currie. Brit. Jnl. Applied Phys., 11, pp.318-324, 1960

10c "Gaseous diffusion in porous media. Part 3 Wet granular materials" J.A. Currie. Brit. Jnl. Applied Phys., 12, pp.275-281, 1961

11a "Water movement in porous materials: part 1 Isothermal vapour transfer" D.A. Rose. Brit. Jnl. Applied Phys., 14 pp.256-262, 1963

11b "Water movement in porous materials: part 2 The separation of the components in water movement" D.A. Rose. Brit. Jnl. Applied Phys., 14, pp.491-496, 1963

12. "Potential evapotranspiration: for use in irrigation in the U.K. and Republic of Ireland". Ministry of Agriculture, Fisheries and Food, Technical Bulletin No. 16, H.M.S.O., London, 1967

13. "Diurnal soil-water evaporation: Time-depth-flux patterns" R.D. Jackson, B.A. Kimball, R.J. Reginato, F.S. Nakayama. Soil Sci. Soc. Amer. Proc., 37, pp.505-509, 1973

14. "Diurnal soil-water evaporation: Comparison of measured and calculated soil-water fluxes" R.D. Jackson, R.J. Reginato, B.A. Kimball, F.S. Nakayama. Soil Sci. Soc. Amer. Proc., 38 No. 6, pp.861-866, 1974

15. "Evaporation, and moisture and heat fields in the soil" J.R. Philip. Jnl. Meteorology, 14, pp.354-366, 1957

16. "Movement of water through soils as influenced by osmotic pressure and temperature gradients" J. Letey. Hilgardia, 39, No. 14, pp.405-418, 1968

17. "Movement of water as affected by free energy and pressure gradients" W.D. Kemper. Soil Sci. Soc. Amer. Proc., 25, No. 4, pp.260-265, 1961

18. "The properties of gases and liquids. Their estimation and correlation" R.C. Reid, T.K. Sherwood. McGraw Hill Book Co. Inc., (page 283), 1958

19. "Surface chemical properties of clay minerals and soils from theoretical and experimental developments in electro-osmosis" H.F. Winterkorn. Symposium on exchange phenomena in soils,

Am. Soc. Testing Matls., Spec. Publ. paper No. 142, pp.44-52, 1952

20. "Mass transport phenomena in moist porous systems as viewed from the thermodynamics of irreversible processes" H.F. Winterkorn. Highway Research Board, Special Report No. 40, pp.324-338, 1958

21. "Fundamental similarities between electro-osmotic and thermo-osmotic phenomena" H.F. Winterkorn. Proc. Highway Research Board, 27, No. 1, pp.443-355, 1947

22. "Electro-osmotic and hydraulic flow in soils with a varying porosity" N.A. Golenko. Soil Mech. Found. Eng., 14, No. 1, pp.42-46, 1977

23. "Electro-osmotic processes in clayey soils and dewatering during excavations" G.M. Lomize, A.V. Netushil, B.A. Rzhanitzin. Proc. of 4th Int. Conf. on Soil Mech. and Foundn. Eng. (London), 1, pp.62-67, 1957

24. "Investigations on electro-osmotic flow in soils in relation to different characteristics" A. Piaskowski. Proc. of 4th Int. Conf. on Soil Mech. and Foundn. Eng. (London), 1, pp.89-92, 1957

25. "Stabilization of fine-grained soils by electro-osmotic and electro-chemical methods" K.P. Karpoff. Conf. New horizons in Constn. Matls. Int. Symp., Lehigh Univ. Bethlehem, Pa., pp.265-272, 1977

26. "Review of some studies of electro-kinetic phenomena" D. Zaslavsky, I. Ravina. Sympn. Moisture equilibria and moisture changes in soils beneath covered areas, Australia, Butterworth, No. 4, pp.55-69, 1965

27. "Electro-osmotic damp proofing" W.J. Holmes. The Architect and Building News, Nov. 21, pp.767-770, 1962

28. "Treatise on electro-chemistry" G. Kortum. Elsevier Publ. Co. Ltd., 2nd Ed., 1965

29. "Molecular physics of boundary friction" A.S. Akhmatov. Israel program for scientific translations, Jerusalem, 1966 Distributed by Oldbourne Press, London

30. "Propeties of water substance" W.H. Rodebush, A.M. Buswell. Highway Research Board, Special Report No. 40, pp.5-13, 1958

31. "Effects of electrostatic fields on the surface tension of salt solutions" G.M. Schmid, R.M. Hurd, E.S. Snavely. Jnl. of Electro Chem. Soc., 109, No. 9, pp.852-858, 1962

32. "Electro-osmotic damp-proofing - 'active' or 'passive'? W.J. Holmes. The Architect and Building News, 6 March, pp.378-379, 1968

33. "Scientific treatment of Rising Damp" N.A. Benster. Building Technology and Management, 8, No. 5, pp.4-5, 1970

34. "Dampness. Recent developments in electro-osmosis" B.A. Richardson. The Architect and Building News, 20/27 December, pp.1007-1009, 1967

35. "Prevention of moisture rise in capillary systems by electricl short circuiting" D.H. Gray. Nature, 223, pp.371-374, 1969

36. "A study of the blocking effect of membranes" G.H. Bishop, F. Urban, H.L. White. Jnl. of Physical Chemistry, 35, pp.137-143, 1931

37. "Reciprocal relations in irreversible processes, II" L. Onsager. Physical Review, 38, pp.2265-2279, 1931

38. "Permeability of composite membranes" O. Kedem, A. Katchalsky Trans. of Faraday Soc., 59, Part I pp.1918-1930, Part II pp.1931-1940, Part III pp.1941-1953, 1963

39. "The treatment of Rising Damp" J.L. Heiman, E.H. Waters, R.C. McTaggart. Architectoral Sci. Review, pp.170-177, Dec. 1973

40. "Experience of wall drying by means of electro-osmose" P. Wieden. Int. Council of Monuments and Sites Convention (Rome) 1967(b), pp.271-280

41. "Colourless treatments for masonry" Building Research Establishment Digest, No. 125, 2nd Series, 1971

42. " Decay and conservation of stone masonry" Building Research Establishment Digest, No. 177, 2nd Series, 1975

43. "Silicone based water repellents for masonry" British Standards Inst., B.S. No. 3826, 1969

44. "Injection systems for damp-proofing" R.W. Sharpe. Building and Environment, 12, pp.191-197, 1977

45. "Materials for damp proof courses" British Standards Inst. B.S. 743, 1970

46. "Rising Damp in walls" Building Research Establishment Digest No. 27, second series, (2nd publication) 1969

47. "Damp proof course insertion" Building Research Establishment Digest, No. 107, 1st series

48. "Studies of pore size distribution II Apparatus for the measurement of coarse pores" A. Watson, J.O. May, B. Butterworth. Science of ceramics, 1, pp.187-199, 1962

49. "A comparison of methods of measuring pore-size distribution in refractories" J.F. Clements, J. Vyse. Trans. Brit. Ceramic Soc., 67, pp.285-317, 1968

50. "The statistical behaviour of instabilities in displacement processes in porous media" A.E. Scheidegger, E.F. Johnson. Canad. Jnl. of Phys., 39, pp.326-334, 1961